Histone deacetylase inhibitors as novel neuroprotective agents in in vitro and in vivo models of Parkinson's disease

Page, Cecilia

Awarding institution:
King's College London

Title: Histone deacetylase inhibitors as novel neuroprotective agents in in vitro and in vivo models of Parkinson's disease

Author: Cecilia Page

Histone deacetylase inhibitors as novel neuroprotective agents in *in vitro* and *in vivo* models of Parkinson's disease

Cecilia Amma Page

March 2014

A thesis submitted to King's College London for the degree of Doctor of Philosophy

Neurodegenerative Diseases Research Group, Institute of Pharmaceutical Sciences, School of Biomedical Sciences, King's College London, London SE1 1UL

To my mother

Certificate

This is to certify that the research work embodied in this thesis has been carried out by me under the supervision and guidance of Dr Sarah Salvage and Professor Peter Jenner.

Cecilia Amma Page

Abstract

Histone deacetylases (HDAC) shift the balance towards chromatin condensation and silence gene expression. Aberrant recruitment of HDACs to alter transcription suggests the use of HDAC inhibitors (HDAC-Is) as potential therapeutic candidates for neurodegenerative disorders such as Parkinson's disease (PD). Post mortem studies of PD, characterised by progressive loss of dopaminergic neurones in the substantia nigra, have linked α-synuclein toxicity and oxidative stress to the pathogenesis of the disorder. Interestingly HDAC-Is have been shown to prevent α-synuclein and 1-methyl-4-phenylpyridinium (MPP^+)-induced cellular toxicity *in vitro*, but there is limited reports on the inhibition HDACs in *in vitro* and *in vivo* models of PD.

For this reason, the effects of the HDAC-Is, suberoylanilide hydroxamic acid (SAHA) and valproic acid (VPA) were investigated in *in vitro* and *in vivo* models of PD. Neither inhibitors protected dopaminergic cell lines, SH-SY5Y and N1E-115, against hydrogen-peroxide (H_2O_2) and MPP^+-induced toxicity. Except, at the highest concentrations (10^{-3}M), where SAHA tended to decrease cell death. However, in the more complex rat ventral mesencephalic cultures, although HDAC-Is did not protect dopaminergic neurones against MPP^+- or Lipopolysaccharide (LPS)-induced toxicity, interestingly, they reduced the number of astrocytes and activated microglia suggesting a positive anti-inflammatory effect. The effects of the HDAC-Is were then assessed in the 6-hydroxydopamine- and LPS-lesioned mouse models of PD. Both SAHA and VPA protected dopaminergic neurones and decreased the number of astrocytes in substantia nigra pars compacta (SNpc), although the number of active microglial cells were not reduced except at the highest dose of VPA.

The results suggest that although the HDAC-Is, SAHA and VPA, are toxic to the immortalised dopaminergic cells *in vitro*, they protect nigral dopamine cells from toxin-induced cell loss *in vivo*. The reduction in astrocyte and microglia activation induced by the HDAC-Is suggest they may exert their protective effects by reducing inflammation associated with PD.

Table of Contents

Table of Figures

Table of Tables

List of abbreviations

3-MT	3-methoxytyramine
3-NT	3-nitrotyrosine
3-OMD	3-O-methyldopa
4-HNE	4-hydroxynonenal
6-OHDA	6-hydroxydopamine
ABC	Avidin-biotin complex
AD	Alzheimer's disease
ALS	Amyotrophic lateral Sclerosis
ANOVA	Analysis of variance
APAF-1	Apoptotic protease activating factor 1
APC	Antigen-presenting cells
ATP	Adenine triphosphate
β-OHB	β-hydroxybutyrate
Bax	Bcl-2 associated x protein
BBB	Blood brain barrier
Bcl-2	B-cell lymphoma-2
BDNF	Brain-derived neurotrophic factor
BSA	Bovine serum albumin
CBP	CREB-binding protein
CMA	Chaperone mediated autophagy
CNS	Central nervous system
CO_2	Carbon dioxide
COMT	Catechol-O-methyl transferase
COX	Cyclooxygenase
CREB	cAMP response element-binding
CSF	Cerebrospinal fluid
DA	Dopamine
DAB	3,3'-Diaminobenzidine
DAPI	4'6-diamino-2-phenylindole
DAT	Dopamine transporter
DIV	Day *in vitro*
DMEM	Dulbecco's modified eagle's medium
DMNV	Dorsal motor nucleus of the vagus
DNA	Deoxyribonucleic acid
DOPAC	3,4-dihydroxyphenylacetic acid

E3	Ubiquitin-protein ligase
E14	Embryonic day 14
EC_{50}	Median effective concentration
ECL	Enhanced chemiluminescence
ED-1	Ectodermal dysplasia 1
EDTA	Ethylenediaminetetraacetic acid
FBS	Foetal bovine serum
GABA	Gamma-amino butyric acid
GAD	Glutamate decarboxylase
GBA	Glucocerebrosidase
GD	Gaucher's disease
GDNF	Glial cell line-derived neurotrophic factor
GFAP	Glial fibrillary acidic protein
GIS	Gastrointestinal symptoms
GSH	glutathione
H_2O_2	Hydrogen peroxide
HAT	Histone acetylase
HD	Huntington's disease
HDAC	Histone deacetylase
HDAC-I	Histone deacetylase inhibitor
HSC	Heat shock cognate
HSP	Heat shock protein
HVA	Homovanilic acid
IBD	Inflammatory bowel disease
IFN-γ	Interferon gamma
IgG	Immunoglobulin G
IgM	Immunoglobulin M
IL	Interleukin
ILBD	Incidental lewy body disease
iNOS	Inducible nitric oxide synthase
IP	Intraperitoneal
LB	Lewy body
LC	Locus coeruleus
LDH	Lactate dehydrogenase
L-DOPA	L-3,4-dihydroxyphenylalanine
LN	Lewy neurites

LPS	Lipopolysaccharide
LRRK2	Leucine-rich-repeat kinase-2
LTM	Long term memory
MANF	Mesencephalic astrocyte derived neurotrophic factor
MAO	Monoamine oxidase
MDA	Malondialdehyde
MEF-2	Myocyte enhancer factor-2
MHCII	Major histocompatibility complex II
MnSOD	Mitochondrial superoxide dismutase
MPP^+	1-methyl-4-phenylpyridium
MPTP	1-methyl-4-phenyl-1,2,3,6-tetrahydropyridine
mRNA	Messenger ribonucleic acid
MS-275	N-(2-aminophenyl)-4-[N-(pyridin-3-yl-Methoxycarbonyl)aminomethyl]
MT2	Metallothionein
mtDNA	Mitochondrial DNA
Nab	Sodium butyrate
NAc	Nucleus accumbens
NADPH	Nicotinamide adenine dinucleotide phosphate
NBM	Nucleus basalis of Meynert
NF-κB	Nuclear factor-κB
NGS	Normal goat serum
NO	Nitric oxide
NSAIDs	Non-steroidal anti-inflammatory drugs
OD	Optical density
O_2^-	Superoxide
$ONOO^-$	Peroxynitrite
p53	Tumour suppressor protein
PAGE	polyacrylamide gel electrophoresis
PARP	Poly (ADP-ribose) polymerase
PBS	Phosphate buffered saline
PD	Parkinson's disease
PFA	Paraformaldehyde
PGE	Prostaglandin
PINK1	PTEN-induced kinase-1
PO	*Per os* (Oral administration)
PNS	Peripheral nervous system

PSI	Proteasome inhibitor I
PSN	Penicillin, streptomycin and neomycin
PTEN	Phosphatase and tensin homologue
PUMA	p53 up-regulated modulator of apoptosis
rAAV	Recombinant adeno-associated virus
RN	Raphe nucleus
RNS	Reactive nitrogen species
ROS	Reactive oxygen species
SAHA	Suberoylanilide hydroxamic acid
SC	Subcutaneous
SDS	Sodium dodecyl sulphate
SEM	Standard error of the mean
SMA	Spinal muscular atrophy
SMN	Survival motor neurones
SN	Substantia nigra
SNpc	Substantia nigra pars compacta
SOD	Superoxide dismutase
Sp-1	Specific protein-1
STN	Sunthalamic nucleus
TBS-T	Tris buffered saline-Triton-X 100
TEMED	N,N,N',N'-Tetramethylethylenediamine
TH	Tyrosine hydroxylase
TLR	Toll-like receptor
TNFα	Tumour necrosis factor alpha
TPX	Trapoxin A
TSA	Trichostatin A
TUNEL	Transferase-mediated Dutp nick end-labelling
UCHL-1	C-terminal hydroxylase-L1
UPDRS	Unified Parkinson's disease rating scale
UPS	Ubiquitin proteasome system
VM	Ventral mesencephalic
VMAT	Vesicular monoamine transporter
VPA	Valproic acid
VTA	Ventral tegmental area

Publications

Posters

Page, C., Rose, S., Jenner, P. (2010) Histone deacetylase inhibitor exacerbates hydrogen peroxide-induced cell death in neuroblastoma cell lines. Poster communication at World Parkinson's Congress II, Glasgow, Scotland, UK

Page, C., Rose, S., Jenner, P. (2011) Histone deacetylase inhibitors inhibit survival of dopaminergic neuronal cells against toxin-induced cytotoxicity. Poster communication at the 40th Society for Neuroscience annual meeting, San Diego, California, USA

Acknowledgements

First and foremost, I am sincerely thankful to my supervisors, Dr. Sarah Salvage and Professor Peter Jenner for the opportunity and their continuous guidance, support and advice throughout this PhD. Without their patience and help in organising and planning the lab work, this project would not have been accomplished.

My deepest gratitude to past and present colleagues, namely Dr. Monika Brzozowski, Dr. Maria Papathanou, Dr. Tamara Hirsch, Dr. Lauren Broom, Dr. Sara Ailane, Dr. Abdu Soltani, Dr. Atsuko Hikima, Dr. Philip Long, Dr. Mahmoud Iravani, Dr. Bai-Yun Zeng, Mike Jackson, Ria Fisher, and Susana Lopez Alcantara for their invaluable support, discussions, advice and friendship during the difficult times.

My utmost gratitude to my family for their continuous moral, physical and emotional support throughout this PhD. George Appiah II and III, you guys have been my rock, especially in the last year. I offer my heartfelt appreciation for your support, love, encouragement and most of all patience despite the distance.

Lastly, I offer my regards and blessings to all of those who supported me in any aspect during the completion of this project.

Chapter 1 General Introduction

1.1 Parkinson's disease

Parkinson's disease (PD) is a chronic progressive neurological movement disorder affecting approximately 1 % of the population older than 65 years (Bossy-Wetzel *et al.*, 2004) and raising to approximately 4 % of the population over 80 years. However, 10 % of cases classified as young onset, occurs between 20 and 50 years (Dexter & Jenner, 2013). It is the second most prevalent neurodegenerative disorder after Alzheimer's disease (AD). The motor symptoms are clinically characterised by four cardinal features: resting tremor, rigidity, bradykinesia and postural instability (Carlsson, 1959; Lang & Lozano, 1998). Non-motor symptoms are also exhibited and these include depression, anxiety, cognitive impairment, constipation, pain, genitourinary problems, sexual dysfunction and sleep disorders (Chaudhuri *et al.*, 2006; Jankovic, 2008; Schapira, 2008; Bandopadhyay & de Belleroche J., 2010).

1.1.1 Pathology

The motor symptoms of PD results primarily from the death of dopaminergic neurones in the substantia nigra pars compacta (SNpc), and the resultant depletion of terminal dopamine (DA) in the caudate putamen (Hornykiewicz, 2008). The onset of the motor symptoms of PD occur after about 50 – 60 % of dopaminergic neurones have degenerated in the substantia nigra, and approximately 70 – 80 % of striatal DA is depleted (McGeer *et al.*, 1988a; Agid, 1991; Fearnley & Lees, 1991). This is due to the compensatory mechanisms of the basal ganglia, where DA turnover is increased and post-synaptic DA D_2-type receptor sensitivity is increased in the striatum to maintain normal function in the early stages of neuronal loss (Bezard & Gross, 1998; Bezard *et al.*, 2003).

In addition to nigral dopaminergic neuronal degeneration, there is also loss of noradrenaline neurones of the locus coeruleus (LC), cholinergic neurones of the nucleus basalis of Meynert (NBM), serotonin neurones of the dorsal raphe nuclei (RN), as well as degeneration of neurones in the olfactory system, the dorsal motor nucleus of the vagus (DMNV) and the peripheral nervous system (PNS) (Javoy-Agid *et al.*, 1984; Lang & Lozano, 1998; Olanow *et al.*, 2004). Degeneration of these neurones in other brain regions has been suggested to underlie the prevalence of non-motor symptoms of PD. For example, non-motor symptom such as depression in PD has been implicated to relate to the loss of noradrenergic transmission in the limbic system, whereas dementia has been linked to the destruction of the cholinergic system (Remy *et al.*, 2005; Langston, 2006).

PD is also defined pathologically by the presence of Lewy bodies (LB) and Lewy neurites (LN). LBs are intracytoplasmic proteinaceous aggregates, consisting of spherical bodies and dense cores

whereas LNs display thread-like structures found in neuronal processes (Forno, 1996). They contain a wide variety of proteins including ubiquitin and neurofilaments with α-synuclein being the major component (Spillantini *et al.*, 1997). They are typically found in the SNpc, but also seen in brain areas that experience degeneration (Olanow *et al.*, 2004). The mechanism by which LBs and LNs are formed or their contribution to disease progression is unknown. However, by staining for α-synuclein immunoreactive aggregates through the brain at different stages of the disease, Braak and colleagues (2003) hypothesised a topographical and chronological spread of the disease through the brain. They concluded that the pathological process in PD occurs in 6 stages. Lewy bodies are initially confined to the medulla oblongata in the dorsal glossopharyngeal-vagus complex before progressing to other parts of the brain in an ascending manner (Braak *et al.*, 2003) (Figure 1-1). According to the Braak's hypothesis, SNpc degeneration occurs at stage 3 but motor symptoms are not evident until stage 4 (Braak *et al.*, 2004).

Even though there is evidence in support of Braak's hypothesis, the use of α-synuclein as a pathological marker to mark disease progression has criticised the validity of the hypothesis (Lang, 2007; Burke *et al.*, 2008a). This is because Braak's hypothesis assumes that patients with α-synuclein immunoreactive inclusions in any part of the central nervous system (CNS) have PD, but it is unclear whether the α-synuclein pathological changes correlate with neuronal dysfunction or loss. In addition, α-synuclein is not the only protein found in LBs, and he failed to consider other LB-associated proteins. Furthermore, clinico-pathological studies showed that α-synuclein inclusions, even though were present in the SN and cortical regions, were not present in the LC and DMNV of some PD cases (Parkkinen *et al.*, 2005; Kalaitzakis *et al.*, 2008).

Recently, an alternative hypothesis has emerged that PD starts in the intestinal nerve cells prior to brain stem pathology. Initial evidence from investigations on 5 autopsies with Parkinson-associated synucleinopathy, found α-synuclein immunoreactive inclusions in the neurones of the gastrointestinal submucosa (Braak *et al.*, 2006). This has been confirmed recently by immunohistochemistry studies for α-synuclein on biopsy specimens of untreated PD patients. Positive staining of α-synuclein in nerve fibres in the colonic submucosa was found to be dissimilar to the pattern in control samples and patients with inflammatory bowel disease (IBD) (Shannon *et al.*, 2012). In addition, questionnaires completed by 129 PD patients to determine the onset of gastrointestinal symptoms (GIS) with respect to motor symptoms, showed that gastrointestinal dysfunction preceded motor symptoms (Cersosimo *et al.*, 2012). Despite these evidences, whether the pathological process begins in the brain or elsewhere in the nervous system is still unknown and remains under investigation.

However, Braak's staging concept has gained support from recent findings, as it has been demonstrated that α-synuclein transfers from cell-to-cell in a prion-like manner in cell culture, animal models and embryonic brain tissue transplanted into PD patients (Dunning *et al.*, 2012). Exactly how this occurs is unknown, but it does suggest that mutated α-synuclein proteins released by affected neurones could be taken up by healthy neurones to spread the α-synuclein pathology and continue the cycle of protein misfolding and lewy body formation (Dunning *et al.*, 2012). Nevertheless, this theory requires further investigation to clarify the molecular understanding of the pathogenesis of PD.

Although there is progressive neurodegeneration in various parts of the brain, pathological findings show cell loss in the SNpc to be undoubtedly the main contributor of the onset of motor symptoms. Whether this cell loss is primarily due to the presence of LBs is yet to be determined, as they are also present in the brainstem of the elderly, and the link between LBs and PD is yet to be fully elucidated. At present, the factors that cause dopaminergic neuronal demise still remains elusive.

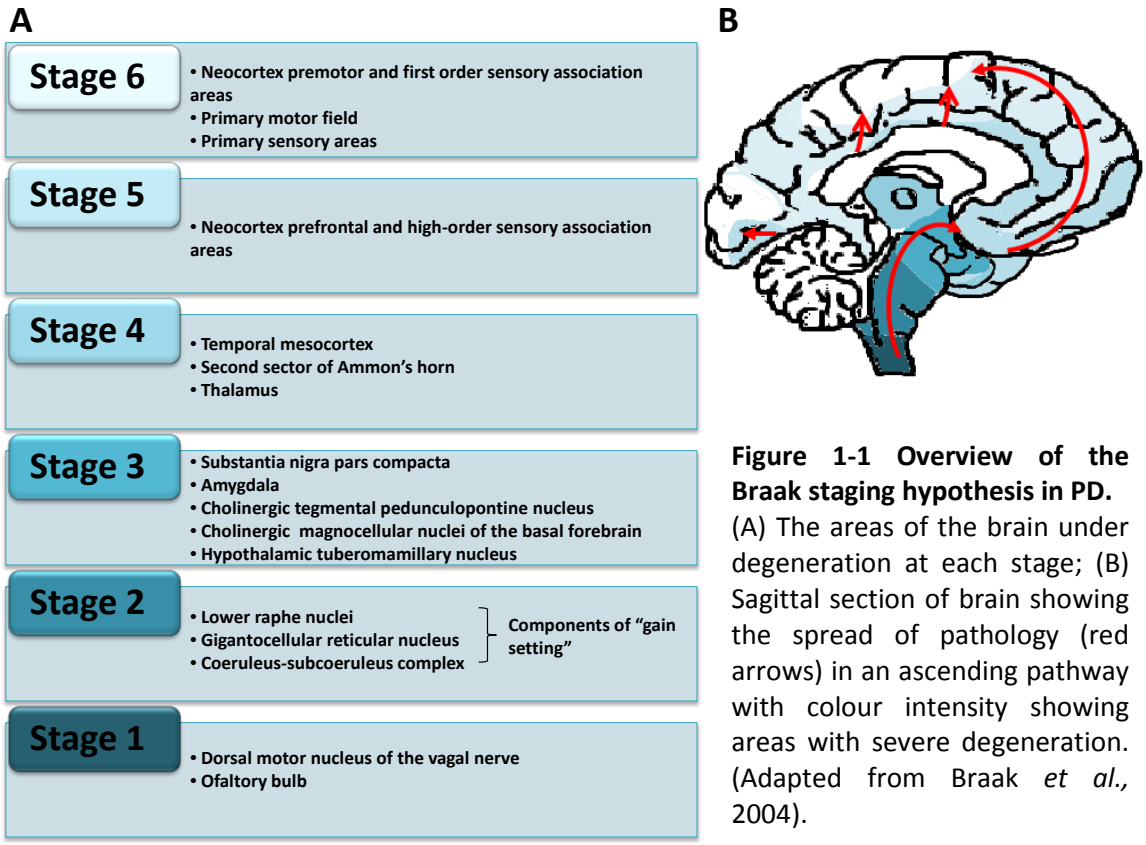

Figure 1-1 Overview of the Braak staging hypothesis in PD. (A) The areas of the brain under degeneration at each stage; (B) Sagittal section of brain showing the spread of pathology (red arrows) in an ascending pathway with colour intensity showing areas with severe degeneration. (Adapted from Braak *et al.*, 2004).

1.1.2 Treatments of PD

The current and most effective treatment for PD tackles the motor deficits of the disease whereas management of the non-motor symptoms are limited. Current treatment involves dopamine replacement therapy using levodopa (L-DOPA; L-3,4-dihydroxyphenylalanine), a precursor of dopamine (Jenner, 2002; Schapira *et al.*, 2006). This is administered in conjunction with the dopa-decarboxylase inhibitor, carbidopa or benserazide, which inhibits the peripheral dopamine production from L-DOPA (Celesia & Wanamaker, 1976; Hornykiewicz, 2002). This makes L-DOPA more readily and rapidly available for brain metabolism and allows a reduction in L-DOPA dose, in addition to limiting its side effects such as nausea, hypotension and vomiting (Cedarbaum, 1987; Hauser, 2009). This drug combination effectively improves motor disability in PD, resulting in a reduction in morbidity and mortality, and overall improvement in the quality of life (Olanow, 2004). Despite the therapeutic benefits of L-DOPA, chronic administration is associated with motor complications or fluctuations, such as 'wearing off' effect, 'ON-OFF' periods and dyskinesia. These develop in 40 – 60 % of patients after 4 – 6 years of L-DOPA therapy, and 70 - 80 % of patients after 10 years of usage experience significant social and functional disability (Marsden & Parkes, 1977).

Dopamine agonists (pergolide, pramipexole, ropinirole, rotigotine, apomorphine, cabergoline and bromocriptine) are used as monotherapy or in combination with L-DOPA and can delay the onset of motor fluctuations. Monotherapy is used in early stages of the disorder and can delay the need for L-DOPA for up to 5 years (Lees, 2005). They act on dopamine receptors located on the striatal cholinergic interneurones and GABAergic efferent neurones, but can enhance the non-motor symptoms such as confusion, depression and hallucinations via activation of non-striatal dopamine receptors (Rascol *et al.*, 2000). Monoamine oxidase-B (MAO-B) inhibitors such as rasagiline and selegiline reduce endogenous dopamine breakdown. In early disease, they provide only mild improvement of the motor symptoms (Ives *et al.*, 2004; Goetz *et al.*, 2005), but are used in late stage disease, as they enhance the effects of L-DOPA (Rascol *et al.*, 2000; Schapira, 2009). Catechol-O-methyl transferase (COMT) inhibitors such as entacapone and tolcapone are also co-administered with L-DOPA. They inhibit the metabolism of L-DOPA and dopamine into 3-O-methyldopa (3-OMD) and 3-methoxytyramine (3-MT), respectively (Thanvi & Lo, 2004). Similar to decarboxylase inhibitors, COMT inhibitors also extend the plasma half-life of L-DOPA, thereby prolonging the duration of action of each L-DOPA dose (Rinne *et al.*, 1998). This reduces the L-DOPA requirement in patients (Kurth *et al.*, 1997).

At present, as these treatments only alleviate the motor symptoms and remain symptomatic in nature, there is an urgent need for a neuroprotective agent that can prevent further loss of

dopaminergic neurones in the SNpc and eventually halt disease progression. In order to find neuroprotective strategies, it is important to understand the aetiology of PD and the processes involved in neuronal degeneration.

1.1.3 Aetiology of PD

The aetiology of PD is unknown, however numerous studies have shown genetics and environmental factors are both involved. In most cases, PD appears to be sporadic, but the discovery of an increase in the incidence of PD in rare families have identified a number of cases to be genetically related and have thus been termed as familial PD (Polymeropoulos *et al.*, 1997; Gasser, 1998; Kitada *et al.*, 1998). Using genetic linkage analysis in large families and genome-wide association studies, 18 autosomal dominant and autosomal recessive gene mutations responsible for variants of the disease have been identified (Klein & Westenberger, 2012). The chromosomal loci are given the nomenclature 'PARK' and include α-synclein (SNCA) (PARK 1 & 4), parkin (PARK 2), ubiquitin-C-terminal hydroxylase-L1 (UCH-L1) (PARK 5), PTEN (Phosphatase and tensin homologue)-induced kinase 1 (PINK1) (PARK 6), DJ-1 (PARK 7), Leucine-rich repeat kinase 2 (LRRK2) (PARK 8), ATP13A2 (PARK 9) (Wirdefeldt *et al.*, 2011; Klein & Westenberger, 2012) (Table 1-1).

These 8 genes have been extensively validated and they express proteins that are involved in one or more pathological pathway of PD, such as the impairment of the protein degradation system, mitochondrial dysfunction and oxidative stress (Figure 1-2). In summary:

- SNCA codes for the protein *α-synuclein*, which forms fibril-like aggregates found in LBs and LNs. It is a feature of both familial and sporadic PD (Spillantini *et al.*, 1997). Point mutations in this gene, have been shown to increase protein expression (Polymeropoulos *et al.*, 1997; Farrer *et al.*, 2004) which is associated with enhanced protofibril formation (Miller *et al.*, 2004). Triplication of the locus has also been identified (Singleton *et al.*, 2003) and shown to result in the development of PD (Devine *et al.*, 2011b).
- *Parkin*, an E3 ubiquitin ligase (Kitada et al., 1998) and *UCH-L1*, a deubiquitinating enzyme (Leroy *et al.*, 1998), are both involved in the ubiquitin-proteasome system (UPS) which degrades unwanted proteins. Investigations in parkin-null mice resulted in mitochondrial dysfunction and oxidative stress (Palacino *et al.*, 2004). UCH-L1 inhibition reduced the availability of free monomeric ubiquitin molecules and contributed to the impaired clearance of unwanted proteins by the UPS (Cartier *et al.*, 2009). This resulted in accumulation of abnormal proteins in the brain of knock-out mice (Saigoh *et al.*, 1999).
- *PINK1*, is a mitochondrial membrane anchored-kinase protein (Valente *et al.*, 2004). Overexpression and loss of function investigations implicate PINK1 in apoptosis, impaired

dopamine release, motor deficits and decreased complex I activity (Kitada *et al.*, 2007; Morais *et al.*, 2009). It also plays a role in the survival of neurones, especially against MPTP-induced toxicity (Haque *et al.*, 2008).

- *DJ-1* acts as an anti-oxidant and protects cells from oxidative stress (Nagakubo *et al.*, 1997; Bonifati *et al.*, 2003). Overexpression of DJ-1 results in mice being resistant to MPTP. Mutations in DJ-1 are associated with increased oxidative stress (Takahashi-Niki *et al.*, 2004) and impaired mitochondrial dynamics and function (Wang *et al.*, 2012).
- *LRRK2*, is a tyrosine kinase-like protein (Zimprich *et al.*, 2004). It is localised in membrane microdomains, multivesicular bodies and autophagic vesicles (Lynch-Day *et al.*, 2012). Its function is unknown and its contribution to PD pathology is also unclear, but there is evidence that the mutation I2020T causes an increase in LRRK-2 kinase activity (Gloeckner *et al.*, 2006).
- *ATP13A2* gene encodes a transmembrane lysosomal P5-type ATPase (ATP13A2) (Dehay *et al.*, 2012a). Mutations in ATP13A2 gene results in several lysosomal defects such as impaired lysosomal acidification, decreased proteolytic processing of lysosomal enzymes, reduced degradation of lysosomal substrates, and diminished lysosomal-mediated clearance of autophagosomes (Dehay *et al.*, 2012b). These result in dysfunction of the autophagy degradation system and contributes to the accumulation of unwanted proteins.

Table 1-1 Genes underlying monogenic parkinsonism
AD, autosomal dominant; AR, autosomal recessive. (Adapted and modified from Klein & Westenberger, 2012).

PARK locus	Gene	Gene locus	Inheritance
PARK1	*SNCA*	4q21-22	AD
PARK2	*Parkin*	6q25.2–q27	AR
PARK3	Unknown	2p13	AD
PARK4	*SNCA*	4q21–q23	AD
PARK5	*UCHL1*	4p13	AD
PARK6	*PINK1*	1p35-p36	AR
PARK7	*DJ-1*	1p36	AR
PARK8	*LRRK2*	12q12	AD
PARK9	*ATP13A2*	1p36	AR
PARK10	Unknown	1p32	Not clear
PARK11	*GIGYF2*	2q36-27	AD
PARK12	Unknown	Xq21-q25	Not clear
PARK13	*HTRA2*	2p12	Not clear
PARK14	*PLA2G6*	22q13.1	AR
PARK15	*FBXO7*	22q12-q13	AR
PARK16	Unknown	1q32	Not clear
PARK17	*VPS35*	16q11.2	AD
PARK18	*EIF5G1*	3q27.1	AD

Genetic mutations accounts for 5 – 10 % of PD cases, therefore the disease is commonly sporadic accounting for approximately 90 % of cases (Lesage & Brice, 2009). But as the search for genetic links to PD continues, there are approximately 40 % of the population at risk (Hardy, 2010). This is due to the autosomal dominant and recessive genes, as well as susceptibility genes which have recently been discovered by genome-wide association studies in idiopathic PD, including α-synuclein and LRRK2 (Nalls *et al.*, 2011; International Parkinson's Disease Genomic Consortium, 2011) (Table 1-2). This indicates that even though familial and sporadic forms of PD are clinically and pathologically distinct from each other, they do overlap, and this has enabled genetic mutations to provide insights into the molecular mechanisms underlying the disease process. Such as mitochondrial dysfunction, oxidative stress and impairment in protein handling processes (Houlden & Singleton, 2012). Nevertheless, they do not explain the cause or mechanistic of the sporadic cases (Hardy *et al.*, 2006), but they do imply that environmental factors and genetics can result in PD.

Accumulating evidence from epidemiological studies found increased exposure to the pesticide rotenone, and the weed killer paraquat induces loss of nigral dopaminergic neurones (Priyadarshi *et al.*, 2000; Tanner *et al.*, 2011). In addition, other factors such as well water consumption (Gatto *et al.*, 2009), residing in close proximity to agricultural industries (Priyadarshi *et al.*, 2001), chronic exposure to welding fumes with high manganese levels (Jankovic, 2005), carbon monoxide poisoning and hydrogen sulphide intoxication (Dexter & Jenner, 2013) have been associated with increased risk of PD. Despite the evidence, environmental factors tend to increase the risk of PD but are not the cause of all cases.

The heterogeneous nature of PD causes patients to exhibit differences in the severity of their clinical features. One thing all PD patients have in common is the demise of the dopaminergic neurones in the SNpc. Even though a combination of genetic and environmental factors can be attributed to the cause of PD, the exact cause is unknown, and the molecular mechanisms underlying the neuronal loss await to be fully elucidated.

Table 1-2 Susceptibility genes for PD.
(Adapted and modified from Nalls *et al.*, 2011; International Parkinson's Disease Genomic Consortium, 2011).

Gene	Protein
ACMSD	Aminocarboxymuconate semialdehyde decarboxylase
BST1	Bone marrow stromal cell antigen 1
FGF20	Fibroblast growth factor 20
GAK	Cyclin G-associated kinase
GPNMB	Glycoprotein NMB
HIP1R	Huntingtin-interacting protein 1-related
HLA-DRB5	Major histocompatibility complex class II, DR β5
LRRK2	Leucine-rich repeat kinase 2
LAMP3	Lysosomal-associated membrane protein 3
MAPT	Microtubule-associated protein tau
SNCA	a-synuclein
STK39	Serine threonine kinase 39
STX1B	Syntaxin 1B
SYT11	Synaptotagmin-11

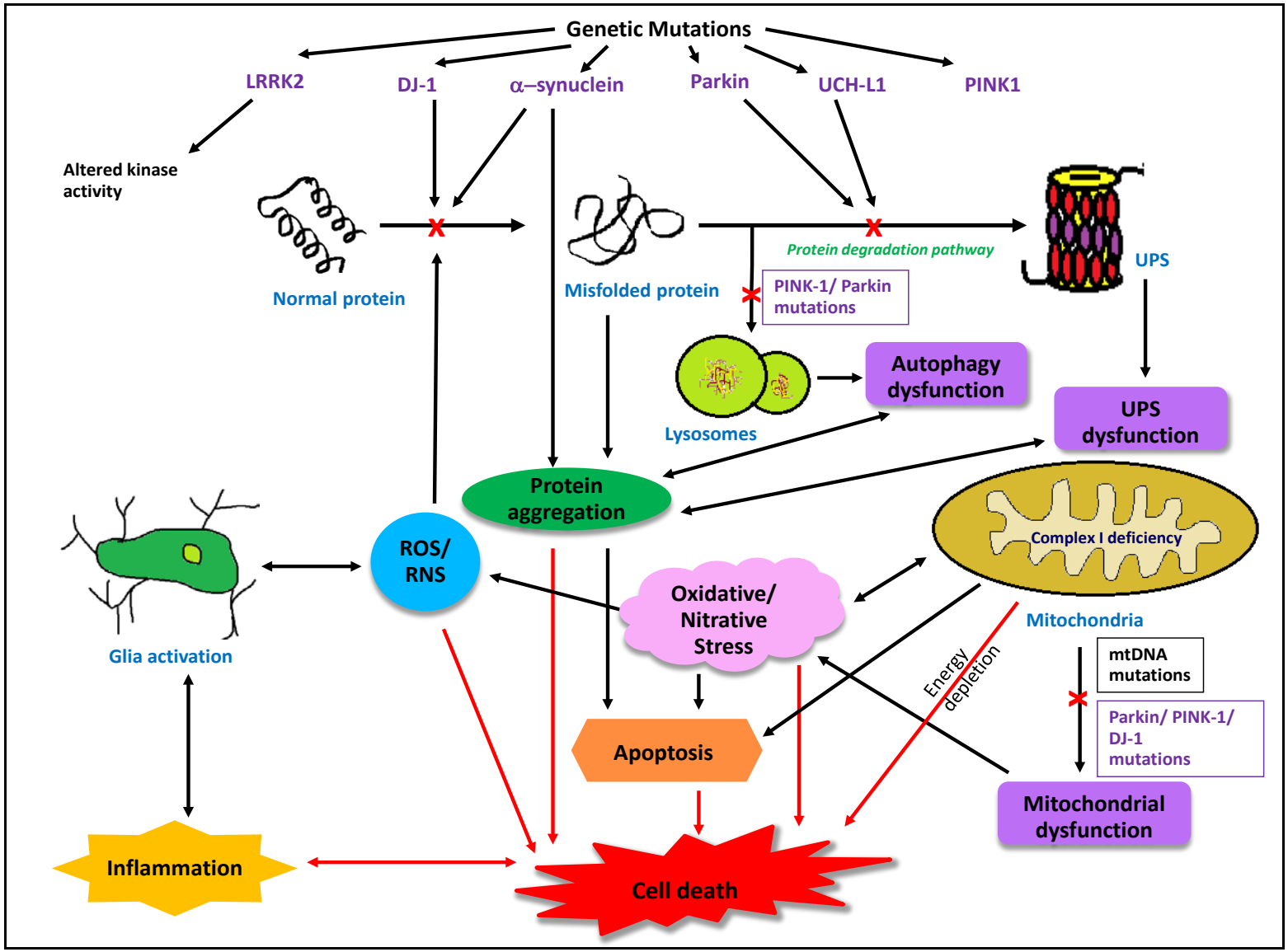

Figure 1-2 Genetics and aetiology of PD.
Diagram links common gene mutations in familial PD to key molecular mechanisms that contribute to neuronal loss in the SN**.** (Adapted and modified from Vila & Przedborski, 2004; Schapira, 2008; Bandopadhyay & de Belleroche J., 2010; Shadrina *et al.*, 2010).

1.1.4 Pathogenesis of PD

Many factors are implicated in the neuronal cell death cascade observed in PD. The initiator of the cascade is unknown, but they are deleterious and potential targets for disease-modifying agents. For this reason, it is essential to fully understand the mechanisms associated with cell death. These mechanisms described in detail below include the dysfunctions in the protein degradation systems: ubiquitin-preoteasome system (UPS) and autophagy, mitochondrial dysfunction, oxidative and nitrative stress and inflammation.

1.1.4.1 Ubiquitin-proteasome dysunction

Dysfunction of the UPS has been implicated in the nigrostriatal neuronal loss. It is a non-lysosomal protein degradation pathway for unwanted intracellular proteins, including misfolded, mutated, mislocated or damaged proteins, and is therefore important in maintaining cell homeostasis (Wang & Maldonado, 2006). It is involved in the regulation of many cellular processes such as cell cycle and division, development and differentiation, apoptosis, cell trafficking and morphogenesis of neuronal networks (Ciechanover, 1998).

The degradation pathway involves "tagging" the protein by covalent attachment to multiple ubiquitin molecules forming polyubiquitin-protein conjugates through a series of enzyme-mediated reactions by ubiquitin ligases (Glickman & Ciechanover, 2002). This marks it for degradation by the 26S proteasome complex, which consists of a proteolytic core complex (20S proteasome) capped at one or both ends with 19S regulatory complexes (Voges *et al.*, 1999), for non-lysosomal protein degradation (Ciechanover, 1998). Once the tagged proteins attach to the ubiquitin receptors in the proteasome, deubiquitinating enzymes recycle the ubiquitin molecules prior to protein degradation (Ciechanover, 1998). A defect in this system results in an accumulation of unwanted proteins (tagged and untagged) which form aggregates in the cells and become toxic to neurones. This was confirmed by *in vitro* studies which showed that proteasomal inhibition in neuronal cells resulted in an accumulation of ubiquitinated proteins, in addition to a pro-inflammatory response, with an increase in inflammatory markers cyclooxygenase-2 (COX-2) and prostaglandin PGE(2) (Rockwell *et al.*, 2000), and subsequently neurodegeneration (McNaught *et al.*, 2002a).

Studies on post mortem brain have observed structural and functional deficits of the proteasome by 33 – 42 % in the SN of idiopathic PD patients (McNaught & Jenner, 2001; McNaught *et al.*, 2003). Particularly, the α-subunits of the 20/26S proteasomes are lost within dopaminergic neurones and the enzymatic activities of the 20S are reduced in the SN (McNaught *et al.*, 2003; Bukhatwa *et al.*, 2010). Additionally, administration of the proteasomal inhibitors N-

benzyloxy-carbonyl-Ile-Glu(*O*-t-butyl)-Ala-leucinal (PSI) and epoxomicin to rodents caused nigrostriatal degeneration and the formation of LB inclusions consisting of ubiquitin and α-synuclein (McNaught *et al.*, 2004; Zeng *et al.*, 2006; Bukhatwa *et al.*, 2009).

Failure of the UPS has been supported by the identification of ubiquitinated proteins in Lewy bodies. These include oxidised (Dexter *et al.*, 1989a; Castellani *et al.*, 2002), nitrated (Good *et al.*, 1998), and phosphorylated proteins (Fujiwara *et al.*, 2002). Additionally, ubiquitin associated with protein processing, and mutated proteins such as parkin, α-synuclein and UCH-L1, linked with the degradation system (Section 1.1.3) (McNaught *et al.*, 2002b; Olanow *et al.*, 2004) are also present.

In conclusion, supporting evidence, such as the discovery of mutated parkin and UCH-L1 proteins, suggests that the impairment of the UPS plays a critical role in the pathogenesis of PD. This impairment promotes the accumulation of misfolded or damaged proteins and the formation of LBs, which may be the initiator or result of a cascade of events such as oxidative stress, nitrative stress and/ or inflammation.

1.1.4.1 Autophagy

Similar to the UPS system, autophagy is also a protein degradation mechanism but involves degradation by lysosomes. These include aggregate-prone proteins, damaged organelles as well as invasive pathogens (Clarke, 1990). Increasing evidence suggests dysregulation of this process results in the accumulation of these proteins in PD, especially as autophagosomal proteins are present in LBs (Banerjee *et al.*, 2010; Tanji *et al.*, 2011). There are three types of autophagy, namely, macroautophagy, where proteins are sequestered into autophagosome which fuses with the lysosomal membrane; microautophagy, where proteins are taken directly into lysosomes; and chaperone-mediated autophagy (CMA), which involves the binding of proteins to chaperone proteins, for example heat-shock cognate 70 (HSC70), to translocate proteins across the lysosomal membrane (Yang & Klionsky, 2010). The expression of CMA proteins, Lysosomal-associated membrane protein 2A (LAMP2A) and HSC70, were reported to be significantly reduced in the SNpc and amygdala of PD brains (Alvarez-Erviti *et al.*, 2010). This evidence confirms the involvement of autophagy impairment in the pathogenesis of PD.

Numerous studies have shown that native α-synuclein is degraded by CMA, and inhibition of autophagy has resulted in accumulation and aggregtion of mono-ubiquitinated α-synuclein (Cuervo *et al.*, 2004; Rott *et al.*, 2008). Cell culture studies have also shown that A53T and A30P mutant α-synuclein, inhibit autophagy and fail to translocate across the lysosomal membrane

for degradation (Martinez-Vicente *et al.*, 2008). In addition, two PD-associated proteins, PINK1 and Parkin have been shown to mediate autophagy. PINK1, which is a mitochondrially targeted serine/threonine kinase, accumulates on the outer membrane of the mitochondrion when there is a loss of membrane potential (Vincow *et al.*, 2013). This triggers the recruitment of Parkin, a cytosolic E3 ubiquitin ligase, to the impaired mitochondria to ubiquitinate the proteins on the outer membrane and facilitate their degradation by autophagy (Narendra *et al.*, 2008; Poole *et al.*, 2010). Mutations in PINK1 as in PD patients and inhibition of PINK1 kinase activity, fails to recruit Parkin to the mitochondria resulting in accumulation of damaged mitochondria (Geisler *et al.*, 2010). Interestingly, deletion of PINK1 gene induces autophagy of the mitochondria through elevation of mitochondrial superoxide; and Parkin overexpression rescues the PINK1-deficient phenotype, by translocating to the depolarized mitochondria to also induce autophagy (Narendra *et al.*, 2008; Dagda *et al.*, 2009). This suggests that the 2 genes may work via different mechanisms to maintain mitochondrial homeostasis. Furthermore, loss of either LRRK2 or DJ-1 also results in impairment of autophagy (Alegre-Abarrategui *et al.*, 2009; Tong *et al.*, 2010; Hao *et al.*, 2010). This indicates that the PD-associated proteins function together, and mutations in one protein can result in an impairment of the lysosomal degradation system which contributes to cell death via accumulation of unwanted protein and mitochondria. They also provide a link between familial PD and autophagy.

More recently, mutations in the gene encoding for glucocerebrosidase (GBA), a lysososmal enzyme that catalyses the hydrolysis of the membrane glycolipid, glucocerebroside to ceramide and glucose, has been linked to increase the risk of PD (Velayati *et al.*, 2010). Deficient glucocerebrosidase activity is implicated in the lysosomal storage disorder, Gaucher's disease (GD). Investigations on the mutations of GBA has been linked to PD through lysososmal insufficiency and autophagic dysfunction, which reduces α-synuclein degradation and contributes to the accumulation of unwanted proteins, resulting in further disruption of the autophagic system (Velayati *et al.*, 2010). Interestingly, heterozygous GBA mutations lead to Gaucher's disease, but both homozygous and heterozygous mutations lead to an increased risk of PD, and the severity of PD is linked to the degree of GBA activity. GBA mutations increase the risk of developing PD by 20- to 30- fold and about 5 – 10 % of PD patients have a GBA mutation (Velayati *et al.*, 2010; Dexter & Jenner, 2013).

Similar to the UPS, autophagy plays a significant role in the clearance of damaged, mutated, misfolded or unwanted proteins. Disruption of this system contributes significantly to the progression of dopaminergic cell loss through the accumulation of proteins and LB formation.

1.1.4.2 Mitochondrial dysfunction

Several reports have documented abnormalities of the mitochondrial respiratory chain in PD. Mitochondria are the primary energy producers of the cells, which regulate cell survival through the production of ATP. This involves the transport of electrons via complexes I-IV in the inner mitochondrial membrane through a series of oxidative phosphorylation reactions. Impairment in this system results in energy deficiency and oxidative stress (Figure 1-2), and renders cells more susceptible to toxins and eventually cell death (Keane *et al.*, 2011).

The most direct evidence for mitochondrial dysfunction comes from studies on autopsy tissue of PD patients, where complex I activity was reported to be decreased in the SN (Schapira *et al.*, 1990) and frontal cortex (Parker, Jr. *et al.*, 2008). However, impairment of complex I is not confined to the brain as platelet mitochondria purified from PD patients also showed a reduction in activity (Parker, Jr. *et al.*, 1989). This is supported by *in vitro* investigations on cybrid cell lines, which contain mitochondria from the platelets of PD patients. It was found that they are more sensitive to MPP^+-induced cell loss than control, and produce an increase in reactive oxygen species (Swerdlow *et al.*, 1996; Gu *et al.*, 1998). This suggests that mitochondrial deficiency may be widespread in PD and is probably due to genetic factors. Indeed, increased levels of mitochondrial DNA (mtDNA) deletions in the striatum of PD patients have been reported (Ikebe *et al.*, 1990). But, there is limited evidence of mtDNA defects in PD, and the link needs to be further investigated.

However, increasing evidence for mitochondrial dysfunction comes from genetic mutations. Particularly the PINK1 gene, which encodes for the mitochondrial membrane kinase and its mutation, is associated with autosomal recessive forms of PD (Gandhi *et al.*, 2006). Preliminary studies in G309D PINK1 transfected neuroblastoma SH-SY5Y cell lines, reported wild-type PINK1 to protect neurones from stress-induced mitochondrial dysfunction and apoptosis, following proteasome inhibitor exposure (Valente *et al.*, 2004). Functionally, PINK1 knock-out mice exhibit dopamine release impairment (Kitada *et al.*, 2007), and impaired mitochondrial respiration, as well as increased sensitivity to oxidative stress (Gautier *et al.*, 2008). Similarly, PINK1 mutant flies showed increased sensitivity to apoptotic stimuli and loss of synaptic function (Morais *et al.*, 2009). Furthermore, mutations in other genes responsible for familial forms of PD such as parkin, DJ-1 and LRRK2 have also been associated with altered mitochondrial function (Yao & Wood, 2009). In particular, loss of function of DJ-1, parkin and PINK1 decreased mitochondrial protection against oxidative stress and subsequently increased its disruption (Dexter & Jenner, 2013). The evidence of mutated proteins linked to the impaired mitochondrial function confirms the genetic links of mitochondrial deficiency in PD pathogenesis.

Environmental factors associated with sporadic PD are also linked to mitochondrial inhibitors and pesticides. In fact, initial evidence for mitochondrial defects comes from investigations of four young drug-users who developed parkinsonism after unintentional exposure to mitochondrial inhibitor MPTP (Langston *et al.*, 1983a). Once this lipophilic toxin crosses the blood brain barrier, it is oxidised to its metabolite MPP^+ in glial cells. MPP^+ has a high affinity for dopamine transporters (DAT) and enters dopaminergic neurones to cause selective degeneration by inhibiting complex I of the mitochondrial respiratory chain and/ or interacting with cytosolic enzymes (Dauer & Przedborski, 2003). In addition, evidence have been obtained from studies where exposure to the pesticide rotenone, a complex I inhibitior (Betarbet *et al.*, 2000), and paraquat, an indirect mitochondrial inhibitor through redox cycling (Richardson *et al.*, 2005; Miller, 2007); and the fungicide maneb, a complex III inhibitor (Meco *et al.*, 1994) induced parkinsonism.

There is no doubt that mitochondrial dysfunction and its association with oxidative stress plays an important role in both familial and sporadic PD progression. However, whether this impairment is a primary or secondary event is still unknown and requires further investigation.

1.1.4.3 Oxidative stress

Oxidative stress, a major implicator of nigral degeneration, is defined as the imbalance between reactive oxygen species (ROS) production and antioxidant defence system (Betteridge, 2000). It is linked to other components of the degenerative process including, UPS dysfunction and inflammation (Jenner, 2003a), but is particularly linked to mitochondrial dysfunction (Figure 1-2).

ROS are produced in the mitochondria as by-products of the electron-transport chain, in the form of superoxide anion (O_2^-) and hydrogen peroxide (H_2O_2) (Pitkanen & Robinson, 1996). A defence mechanism consisting of enzymes such as superoxide dismutase (SOD), catalase, glutathione (GSH) and ascorbate convert these radicals into harmless molecules (Turrens, 2003). Oxidative stress occurs when the radicals are generated at increased levels which overwhelm the antioxidant capacity (Giasson *et al.*, 2002). Post mortem studies have shown that there are increased levels of SOD in the SN which protects against the production of superoxide (Marttila *et al.*, 1988; Saggu *et al.*, 1989). By contrast, reduced levels of GSH are found specifically in the SNpc (Perry & Yong, 1986; Sofic *et al.*, 1992; Sian *et al.*, 1994), resulting in reduced clearance of H_2O_2 (Jenner & Olanow, 1996). Studies in incidental Lewy body disease (ILBD: considered to be pre-clinical PD (DelleDonne *et al.*, 2008)) observed decreased GSH levels, similar to those seen in advanced PD, thus suggesting oxidative stress is an early event in PD pathogenesis (Dexter *et al.*,

1994). This reduction in GSH levels is linked to increased ROS production, which inhibits complex I leading to subsequent mitochondrial dysfunction resulting in neuronal death (Jha *et al.*, 2000).

Furthermore, in dopaminergic neurones, dopamine metabolism also yields oxidative by-products by auto-oxidation, such as superoxide ion ($^{\cdot}O_2^-$), hydrogen peroxide (H_2O_2) and reactive quinones. Enzymatic metabolism of dopamine by monoamine-oxidase B (MAO-B) not only generates deaminated, metabolites homovanilic acid (HVA) and 3,4-dihydroxyphenylacetic acid (DOPAC), but also H_2O_2, which is converted to the highly reactive form hydroxyl radical ($OH^{\cdot}$) by the Fenton reaction in the presence of iron (Olanow, 1990; Jenner & Olanow, 1996). Increased levels of free iron have been reported to be found in the SN, which probably drives the generation of ROS (Dexter *et al.*, 1989b; Sofic *et al.*, 1991), as well as low levels of ferritin, the protein that stores iron in the brain (Dexter *et al.*, 1991). Thus, the environment in the PD brain is pro-oxidant.

ROS readily oxidises cellular macromolecules such as proteins, DNA and lipids, thereby resulting in their damage and eventually their clearance mechanisms. ROS are normally generated, and generally increases with age, as there is evidence of marked increases of oxidised proteins and DNA in ageing brains (Mariani *et al.*, 2005). Direct evidence from post-mortem PD brain tissue revealed elevated levels of lipid peroxidation markers 4-hydroxynonenal (4-HNE) and malondialdehyde (MDA) in dopaminergic cells in the substantia nigra (Dexter *et al.*, 1989a; Dexter *et al.*, 1994; Yoritaka *et al.*, 1996). Moreover, a marked increase in 8-Hydroxy-2-guanosine (8-OHG), an oxidative DNA damage product, is increased in the SN (Sanchez-Ramos *et al.*, 1994; Alam *et al.*, 1997b). Increases of protein carbonyls, indicative of oxidative protein damage has been found in the SN, caudate nucleus and putamen of PD brain tissue, and even in other areas not affected in PD, but may be contributors to the non-motor symptoms of the disorder (Alam *et al.*, 1997a). Therfore indicating that oxidative damage is widespread and not specifically restricted to the nigrostriatal pathway.

1.1.4.4 Nitrative stress

Similarly to oxidative stress, nitrative stress is the imbalance between the reactive nitrogen species (RNS) and the antioxidant defence system, involving nitric oxide (NO), an important signalling molecule in many biological processes (Mayer & Hemmens, 1997). In response to cellular damage, including oxidative stress, there is an increase in the expression of the gene involved in NO production, called nitric oxide synthase (NOS), which exists in 3 major isoforms; endothelial NOS (eNOS), inducible NOS (iNOS) and neuronal NOS (nNOS) (Marletta *et al.*, 1998; McNaught & Jenner, 1999). Excessive production of NO interacts with superoxide anion ($^{\cdot}O_2^-$) to form an unstable reactive free radical species peroxynitrite ($ONOO^-$), which forms nitrogen

dioxide, carbonate and hydroxyl radicals, as by-products (Szabo *et al.*, 2007). These peroxynitrate radicals result in nitration of tyrosine and nitrosylation of cysteine molecules within both proteins and enzymes leading to a loss of function (Jenner, 2003a). For example, nitration of striatal tyrosine hydroxylase (TH), the enzyme involved in dopamine synthesis, resulted in loss of enzyme activity and subsequent decrease in dopamine synthesis (Ara *et al.*, 1998).

Evidence from post-mortem PD patients showed increased levels of 3-nitrotyrosine (3-NT), which is used as a biological marker of $ONOO^-$ formation, in Lewy bodies (Gatto *et al.*, 2000; Greenacre & Ischiropoulos, 2001). Similarly, the increase in 3-NT was also detected in the SN of primates (Ferrante et al., 1999) and in the SN and striatum of mice following MPTP treatment (Pennathur *et al.*, 1999; Riobo *et al.*, 2001). Additional studies found 3-NT-positive α-synuclein in Lewy bodies in post mortem tissue (Giasson *et al.*, 2000), and in the SN and ventral midbrain of MPTP-treated mice (Ferrante *et al.*, 1999), implicating that α-synuclein is a target for nitration.

Some evidence have shown that tyrosine nitration of mitochondrial complex I contributes to its inhibition (Bolanos *et al.*, 1996; Heales & Bolanos, 2002). But it is not clear if this nitration of complex I is related to the mitochondrial dysfunction observed in PD pathology. However, reduced levels of GSH observed following NO-mediated mitochondrial damage (Bolanos *et al.*, 1996) is presumed to be due to the direct nitration of GSH reductase resulting in its inhibition (Ara *et al.*, 1998) and increased oxidative stress.

Moreover, numerous proteins in PD have been found to be modified by the nitrosylation of cysteine residues. This includes enzymes involved in gene transcription, receptor mediated signal transduction, apoptosis (Tsang & Chung, 2009) and importantly, dopamine synthesis (Chung *et al.*, 2004). In addition, genes implicated in familial PD, like Parkin, were detected to be nitrosylated in post mortem PD brain tissue and in mice following MPTP treatment, resulting in loss of activity and subsequently contributing to proteasomal inhibition (Moncada & Bolanos, 2006).

The evidence depicts oxidative and nitrative stress to be involved in neuronal degeneration. They seem to contribute to the cascade resulting in dopaminergic neuronal death through their close associations to other mechanisms of the degenerative process, such as mitochondria dysfunction, protein clearance impairment and inflammation (Figure 1-2). But it is unclear whether they are initiators of these mechanisms or consequences.

1.1.4.5 Inflammation

There is a number of evidence supporting the role of inflammatory changes in the pathogenesis of PD. This is primarily due to the effects of active microglia and to a lesser extent, active astrocytes. Initial evidence comes from post mortem studies on PD patients showing active microglia and T-lymphocytes in the SNpc (McGeer *et al.*, 1988b). In addition, there is an increased number of active microglia in other regions such as the hippocampus, entorhinal cortex, cingulated and temporal cortex (Sawada *et al.*, 2006; Imamura *et al.*, 2003). Moreover, pro-inflammatory cytokines, tumour necrosis factor-α (TNF-α), interleukin 1β (IL-1β), IL-2 and IL-6 have been found to be expressed at high levels in the SN as well as cerebrospinal fluid (CSF) of PD patients (Mogi *et al.*, 1994a; Mogi *et al.*, 1994b; Dobbs *et al.*, 1999; Nagatsu *et al.*, 2000). Furthermore, RANTES, a chemokine produced by activated microglia, is significantly increased in PD patients compared to control, and significantly correlated with Unified Parkinson's Disease Rating Scale scores (UPDRS) (Rentzos *et al.*, 2007).

Glia cell populations in the CNS are composed of macroglia that includes astrocytes and oligodendrocytes (Teismann *et al.*, 2003a), and microglia which constitutes approximately 20% of the glia population (Tremblay *et al.*, 2011). These microglia are regarded as typical resident immune-competent cells of the CNS and key players in fighting disease and neuronal stress (Tremblay *et al.*, 2011). In the 'resting' state, they are characterised by a ramified morphology with small bodies, long slender processes with secondary branching and lamellipodia (Kreutzberg, 1996; Xiang *et al.*, 2006). In response to CNS tissue damage or pathogen insult, the processes of the microglia retract and become amoeboid-like to form the 'active' phenotype (Aloisi, 2001). There is an up-regulation of MHC antigens and their complementary receptors (such as macrophage antigen-complex I (MAC-I)) on the surface of microglia to enable them to act by phagocytosing debris, and promote tissue repair through the secretion of neurotrophic factors, such as brain-derived neurotrophic factors (BDNF) (Graeber & Kreutzberg, 1994; Nakamura, 2002; Banati, 2003). However, if injury is sustained, microglia become cytotoxic and secrete immunomodulatory molecules such as pro-inflammatory cytokines (TNF-α, IL-1β, IL-2 and IL-6), proteinases, eicosanoids and NO to the site of infection to promote persistent degeneration (Knott *et al.*, 2000; Czlonkowska *et al.*, 2002; Beal, 2003; Zhang *et al.*, 2005; Long-Smith *et al.*, 2009). A vast array of evidence supports the toxic role of microglia over their protective role in PD. However, the exact mechanism by which microglia promote dopaminergic cell death via an inflammatory response in PD is unknown, but it is assumed to be linked to the generation of pro-inflammatory factors, ROS and RNS which are deleterious to oxidatively damaged-nigral neurones (Dutta *et al.*, 2008).

Studies in *in vivo* models of PD, have also confirmed inflammation-mediated neuronal degeneration. Elevated levels of active microglia has been reported in the SN of MPTP-treated mice (Breidert *et al.*, 2002), primates (McGeer *et al.*, 2003), and 6-OHDA-treated rodents (Crotty *et al.*, 2008; He *et al.*, 2001; Akiyama & McGeer, 1989). Particularly, studies with lipopolysaccharide (LPS) in animal models of PD, has provided further supporting evidence for inflammation-mediated neurodegeneration. LPS, an endotoxin found on the outside of gram negative bacteria, is a potent stimulator of peripheral immune cells and CNS microglia and astrocytes (Lehnardt *et al.*, 2003; Dutta *et al.*, 2008). LPS acts via the transmembrane protein Toll-like receptor-4 (TLR-4) on glial cells to upregulate gene transcription for a variety of pro-inflammatory factors and free-radical generating enzymes (Lu *et al.*, 2008). Additionally, post mortem studies also reported elevated levels of inflammatory mediators', iNOS and cyclooxygenase-2 (COX-2) in PD patients (Knott *et al.*, 2000), and this was confirmed *in vivo* following LPS treatment (Hunter *et al.*, 2007). Injection of LPS into the SNpc induced a loss of dopaminergic cells (Castano et al., 1998; Herrera et al., 2000), but as neurones lack TLR-4 proteins, LPS does not act directly on dopaminergic neurones but via glial cells involving NO-mediated toxicity, which can be attenuated by iNOS inhibitors (Iravani *et al.*, 2002; Arimoto & Bing, 2003; Iravani *et al.*, 2005; Dutta *et al.*, 2008). Despite the extensive evidence, it is unknown whether inflammation occurs as a primary event or secondary event in PD pathogenesis. However, the presence of microglia activation detected in PD patients and primates years after MPTP exposure (Langston *et al.*, 1999; Barcia *et al.*, 2004) suggest it may be a secondary event and a consequence of dopaminergic neuronal loss.

In conjunction with active microglia, astrocytes are activated and implicated in the inflammatory response observed in PD. Not surprisingly, the density of astrocytes is also elevated in the SN of PD post mortem tissue (Damier *et al.*, 1993) as well as individuals exposed to MPTP (Langston *et al.*, 1999). This is confirmed by reports of increased astrocytic activation in the striatum and SN of 6-OHDA-treated rodents (He *et al.*, 2001), MPTP-treated mice (Breidert *et al.*, 2002; Liberatore *et al.*, 1999) and LPS injected rats (Castano *et al.*, 1998; Herrera *et al.*, 2000).

Typically, astrocytes protect neurones from cell death by releasing neurotrophic factors, namely, glial cell line-derived neurotrophic factor (GDNF) and BDNF, and/ or increasing the activity of glutathione reductase (GSH) (Knott *et al.*, 2002; Chen *et al.*, 2006; Ishida *et al.*, 2006). However, once active, they contribute to neuronal death by releasing neurotoxic factors NO, glutamate and H_2O_2 in primary mesencephalic cultures (McNaught & Jenner, 1999), which promote oxidative and nitrative stress.

In summary, a bulk of post mortem and animal studies support the detrimental role of glial cell-mediated inflammation in PD pathology, and anti-inflammatory therapies could be sought to prevent or halt further degeneration. Pre-clinical data of anti-inflammatory agents have shown them to be protective, however, long-term use of non-steroidal anti-inflammatory drugs (NSAIDs) have been associated with adverse side-effects such as gastrointestinal lesions, and this limits their use in clinic (Hirsch & Hunot, 2009). From the evidence listed here, it can therefore be concluded that inflammation is a mechanism that needs to be closely regulated as it has beneficial components such as, releasing neurotrophic factors and clearing debris which promotes cell survival, but can also be very detrimental resulting in neuronal death.

1.1.4.6 Mode of cell death

Neurones undergo two cell death mechanisms when under stress, namely apoptosis and necrosis. Apoptosis is a genetically regulated cell death mode by which cells undergo self-destruction once apoptotic genes are activated (Hacker, 2000). Morphologically cells undergo shrinkage, chromatin and cytoplasmic condensation, nuclear fragmentation and blebbing of the plasma membrane, and there is no accompanying inflammatory reaction (Majno & Joris, 1995). Conversely, necrosis is a passive form of cell death and occurs in response to toxic insults or spontaneous insults such as stroke or trauma, and results in loss of ATP, cytoplasmic vacuolation and eventually cell bursting triggering an inflammatory response and damage to surrounding tissue (Ziegler & Groscurth, 2004).

Evidence supporting apoptosis come from *in vitro* studies, where neurotoxins selective for dopaminergic neurones, 6-Hydroxydopamine (6-OHDA) and 1-methyl-4-phenyl-pyridinium (MPP^+) were found to induce morphological and biochemical hallmarks of apoptosis in rat phaeochromocytoma PC-12 cell lines and primary dopaminergic cells (Walkinshaw & Waters, 1994; Blum *et al.*, 1997; Lotharius *et al.*, 1999; Viswanath *et al.*, 2001). Overexpressing anti-apoptotic protein Bcl-2 and pre-treatment with caspase inhibitors protected PC-12 cells from 6-OHDA-induced apoptosis (Offen *et al.*, 1997; Takai *et al.*, 1998). Even though there is evidence to support the contribution of apoptosis in PD, necrosis is suggested as a possible mechanism of cell death, although there has not been sufficient supporting evidence (Jellinger, 2000).

Evidence from post-mortem studies on Parkinsonian brain tissue, have reported apoptotic morphological characteristics including chromatin condensation, cell shrinkage and DNA fragmentation in dying neurones (Mochizuki *et al.*, 1996; Anglade *et al.*, 1997; Tatton *et al.*, 1998). Increased expression of pro-apoptotic markers Bax and caspase-3 have been reported

(Anglade *et al.*, 1997; Hartmann *et al.*, 2000; Tatton, 2000), in addition to an increased expression of anti-apoptotic marker Bcl-2 (Mogi *et al.*, 1996). Despite these findings, some investigations have failed to show evidence of apoptotic cell death in the SN of post mortem PD brain tissue, and this may be due to the sensitivity and specificity of the techniques used (Jellinger, 2000).

Finally, data from *in vivo* studies also support the involvement of apoptosis in dopaminergic cell death. In particular, mice treated with 1-methyl-4-phenyl-1,2,3,6-tetrahydropyidine (MPTP), showed DNA fragmentation in the SN (Tatton & Kish, 1997) and neuroprotection of dopaminergic cells was achieved following the inhibiton of Poly (ADP-ribose) polymerase (PARP) (Cosi *et al.*, 1996), or ablation of the pro-apoptotic Bax gene as well as overexpression of Bcl-2 protein (Offen *et al.*, 1997; Yang *et al.*, 1998; Vila *et al.*, 2001). Moreover, cell shrinkage and nuclear chromatin condensation of apoptotic cells in the SN were identified as dopaminergic using terminal deoxynucleotidyl transferase-mediated dUTP nick-end labelling (TUNEL) staining and silver staining in 6-OHDA lesioned rats (He *et al.*, 2000; Marti *et al.*, 2002).

In conclusion, these *in vitro* and *in vivo* evidences support programmed cell death to be involved in neuronal degeneration of PD, despite the limited evidence of necrosis. However, the cause of apoptosis still remains uncertain, but it seems to be the consequence of the other events of the degenerative process, such as mitochondrial and UPS dysfunction, inflammation and oxidative and nitrative stress (Figure 1-2). If this is true, then neuroprotective therapies that prevent these degenerating mechanisms are urgently needed to halt or slow down neuronal demise and subsequent disease progression.

1.1.5 Neuroprotective therapies

As discussed in the previous sections, in order to prevent or reduce the onset of motor symptoms of PD, drugs which prevent neuronal degeneration needs to be sought. With this in mind, many pharmacological compounds have been and are still being investigated for their neuroprotective properties. This includes anti-apoptotic agents, antioxidants, dopamine agonists, MAO-B inhibitors and neurotrophic factors (Table 1-3). Once promising results have been achieved *in vitro*, the neuroprotective effects of the compounds are measured in humans. Clinical trials employ surrogate outcome measures including the time needed for dopaminergic therapy, changes over time in the Unified Parkinson's Disease Rating Scale (UPDRS) clinical score, mortality rates and radio-ligand binding in neuroimaging studies (Lohle & Reichmann, 2010; Lang *et al.*, 2013).

There have been many ambitious efforts in the search for disease-modifying therapies in PD, but many clinical trials have so far failed to identify any compound with neuroprotective properties (Lohle & Reichmann, 2010). This is due to inconsistencies between pre-clinical data in animal models and clinical trials, which questions the validity of the animal models as reflecting the true underlying neurodegenerative processes of PD. As of yet, there is currently no neuroprotective agent that has been successfully developed to date, however, there are many candidates in the pipeline which are showing promising pre-clinical results such as exendin (Aviles-Olmos *et al.*, 2013), osteopontin (Ailane, 2011, personal communication; Broom, 2012, personal communication) and most recently, histone deacetylase inhibitors involved in epigenetic modifications.

Therefore, due to the multi-factorial origins of PD development and progression, an effective treatment approach that would not only protect neurones but also limit inflammation by inhibiting microglial over-activation, while maintaining a 'stress-free' environment favourable to health and repair is needed. These multi-targeted demands have resulted in manipulation of gene expression underlying several cellular processes through genetic approaches (Dietz & Casaccia, 2010).

Table 1-3 Overview of neuroprotection clinical trials in PD.
(Adapted and modified from Lohle and Reichmann, 2010; Lang *et al.*, 2012)

Class	Drug	Aim	Primary outcome(s)	Duration	Result(s)	Reference
Antiapoptotic Agents	TCH346	Assess as neuroprotective drug	Need for symptomatic treatment	12–18 months	Negative	(Olanow *et al.*, 2006)
	CEP-1347	Assess disease-modifying potential in early PD	Need for symptomatic treatment	Terminated after ~21 months	Negative	(Parkinson Study Group PRECEPT Investigators., 2007)
	Minocycline	Alter course of early PD	Change in total UPDRS	12 months	Non-futile	(NINDS NET-PD Investigators., 2006)
Antioxidants	Coenzyme Q10	Determine safe dose which slows functional decline	Change in total UPDRS	16 months	Positive	(Shults *et al.*, 2002)
		Determine if future studies may be warranted	Change in total UPDRS	12 months	Non-futile	(NINDS NET-PD Investigators., 2007)
	Creatine	Determine effect in patients	Surrogate imaging marker	24 months	Negative	(Bender *et al.*, 2006)
		Alter course of early PD	Change in total UPDRS	12 months	Non-futile	(NINDS NET-PD Investigators., 2006)
	Mitoquinone	Slow disease progression	Change in total UPDRS	12 months	Negative	(Snow *et al.*, 2010)

Continues on next page

Dopamine Agonists	Pramipexole	Modify disease progression with delayed-start design	Change in UPDRS	15 months	Negative	(Schapira *et al.*, 2010)
		Assess motor complications after initial treatment in early PD	Surrogate imaging marker	23.5 months	Slow loss in striatal ^{123}I-β-CIT changes	(Parkinson Study Group., 2000)
	Ropinirole	Determine rate of loss of dopamine-terminal function	Surrogate imaging marker	24 months	Slower loss in striatal ^{18}F-DOPA uptake	(Whone *et al.*, 2003)
	α-dihydroergocryptine	Determine effect of monotherapy	Surrogate imaging marker	52 weeks	Slow loss in striatal ^{123}I-IPT changes	(Popperl *et al.*, 2004)
Glutamate Antagonist	Riluzole	Assess disease-modifying potential	Need for symptomatic treatment	Prematurely terminated	Negative	(Rascol *et al.*, 2002)
Levodopa	Levodopa	Assess on the rate of progression	Change in total UPDRS; Surrogate imaging marker	40 weeks	Positive for UPDRS; Fast loss in striatal 123I-β-CIT changes	(Fahn *et al.*, 2004)
MAO Inhibitors	Selegiline	Effect on symptoms progression in mild PD	Change in total UPDRS; Need for symptomatic treatment	14 months	Positive	(Olanow *et al.*, 1995)
		long-term effect in early PD	Need for symptomatic treatment	1–3 years	Positive	(Palhagen *et al.*, 1998)
		long-term effect on progression	Change in total UPDRS	60 months	Positive	(Larsen *et al.*, 1999)
		Study long-term effect in early PD	Change in total UPDRS	7 years	Positive	(Palhagen *et al.*, 2006)
	Rasagiline	Disease modifying effect	Change in total UPDRS	12 months	Positive with low dose	(Olanow *et al.*, 2009)
Neuro-immunophilin Ligands	GPI-1485	Determine if future studies may be warranted	Change in total UPDRS	12 months	Non-futile	(NINDS NET-PD Investigators., 2007)
Neurotrophic Factors	GDNF	Assess effect in advanced PD by ICV catheter	Change in UPDRS motor score	8 months	Negative	(Nutt *et al.*, 2003)
		Assess effect using Ipu infusion of recombinant human GDNF (liatermin)	Change in UPDRS motor score	6 months	Negative	(Lang *et al.*, 2006)
	Cogane	Assess effect in early PD	Change in UPDRS score	28 weeks	Negative	www.clinicaltrials.gov www.ft.com
Ganglioside	GM1 ganglioside	evaluate the long-term safety and efficacy	Change in total UPDRS	5 years	lower scores at 5 yrs than baseline at 'OFF' periods	(Schneider *et al.*, 2010)

Abbreviations: UPDRS - Unified Parkinson's Disease Rating Scale; ^{123}I-β-CIT - 2β-carbomethoxy-3β-[4-iodophenyl]tropane; ^{18}F-DOPA - L-3,4-dihydroxyphenylalanin; ICV - Intracerebroventricular; Ipu - Intraputamenal

1.2 Epigenetic modification

The genetic code and material inherited amongst all cells is the same, but the changes and regulations of these genes enables each cell to retain its specific physical characteristic and biological function in line with the tissue or organ it resides (Bernstein *et al.*, 2007). These changes in gene expression that does not involve any alterations in the DNA is termed as epigenetic modification. It is a crucial physiological mechanism essential for cellular differentiation, development and behaviour (Abel & Zukin, 2008; Portela & Esteller, 2010). Dysregulation of this mechanism has been a premise in disorders of synaptic plasticity and cognition including neurodegenerative disorders, mood disorders and neurodevelopmental disorders (such as Rett syndrome and Fragile X syndrome) (Abel & Zukin, 2008) in addition to cancer and metabolic diseases (Portela & Esteller, 2010).

Eukaryotic DNA is compacted through its association with an octamer of 4 histone core particles- H3/H4 tetramer and H2A/H2B dimer, to form nucleosomes. Together with a linker DNA of 10 – 60 base pairs, they assemble into a dynamic structure known as a chromatin (Stein, 1980) (Figure 1-3). This tight wrapping is due to electrostatic interactions between the negatively charged DNA and positively charged octamer (Stein, 1980). The amino terminal 'tails' of the histone proteins are sites for post-translational modifications, which include acetylation, methylation, phosphorylation, ubiquitination and SUMOlyation. These modifications alter the chromatin structure and make specific regions of the genome more or less accessible for transcription (Peterson & Laniel, 2004). Post translational histone modifications and DNA methylation are the two main categories of epigenetic modifications (Bernstein *et al.*, 2007).

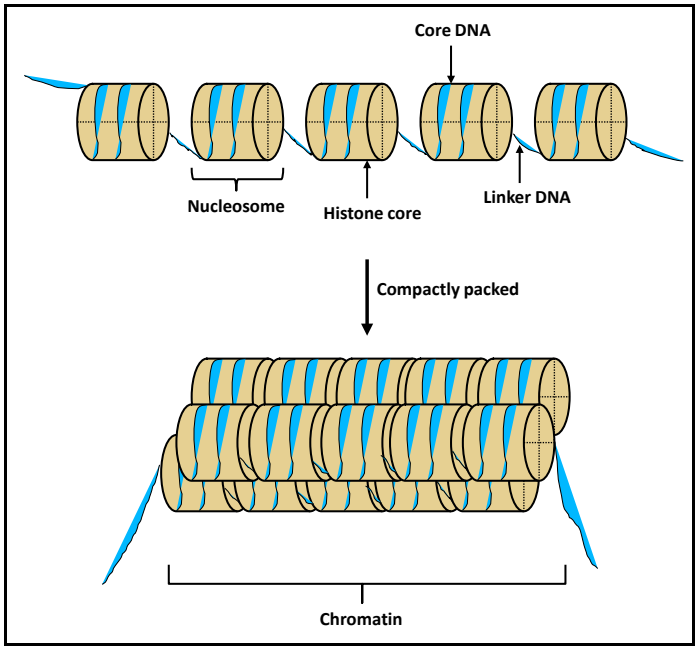

Figure 1-3 Nucleosome and chromatin structure.
DNA wrapped around core histones form a nucleosome. They are connected by linker DNA strands. These structures compacted together forms a chromatin. (Adapted and modified from Schlissel, 2003; Kouzarides, 2007).

DNA methylation occurs at the highest level in the brain and exclusively at CpG dinucleotide sites in mammals (Ehrlich *et al.*, 1982). It plays a role in long-term transcription silencing and heterochromatin organisation (Miranda & Jones, 2007). This process is regulated by the DNA methyltransferases (DNMT1, DMNT3a and DMNT3b) and that transfer a methyl group from S-adenosyl methionine (SAM) to the fifth carbon of a cytosine residue to form 5-methylcytosine (5-mC) (Miranda & Jones, 2007). S-adenosyl methionine is a compound which results from one-carbon metabolism of B vitamins including folic acid, B6 and B12 (Rottach *et al.*, 2009). Alterations of this metabolic cycle leads to aberrant DNA methylation processes where hypermethylation of CCG repeats causes *Fragile X mental retardation-1* (*FMR1*) gene repression is associated with Fragile X syndrome (Rottach *et al.*, 2009). In addition, mutation in genes for proteins involved in DNA methylation homeostasis such as methyl-CpG binding domain (MBD) protein (MECP2) results in Rett syndrome (Kumar, 2000; Rottach *et al.*, 2009).

Post-translational histone methylation of either arginine or lysine residues occurs on the N-terminal tails of histone H3 or H4 proteins (Kouzarides, 2007). This process is facilitated by histone methyl-transferases (HMTs) specific to arginine or lysine. Similar to DNA methylation, HMTs use SAM as a methyl donor (Arrowsmith *et al.*, 2012). The addition of a methyl group does not affect the chromatin structure directly as it does not change the charged state of the arginine or lysine resides. Methylation therefore acts as a binding site for other proteins that promote chromatin condensation or transcriptionally regulating proteins (Nielsen *et al.*, 2001; Trojer *et al.*, 2007). The effect of methylation on transcription activation or repression is determined by the site of the residue on the histone tail and the degree of methylation (Kouzarides, 2007; Arrowsmith *et al.*, 2012). It has important roles in many biological processes, including cell-cycle regulation, DNA damage and stress response, development and differentiation (Kouzarides, 2007). Mutations in or altered expression of histone methyl modifiers and methyl-binding proteins correlate with increased incidence of various different cancers such as leukaemia, breast cancer and lymphoma among others (Albert & Helin, 2010; Greer & Shi, 2012).

Histone acetylation is the most investigated post-translational process. It is regulated by the activities of two antagonistic enzymes: Histone Acetylases (HATs) and Histone Deacetylases (HDACs). HATs covalently bind acetyl moieties to ε-amino groups of lysine residues within the N-terminal tail of histones on nucleosomes (Yang & Seto, 2007). This neutralises the basic charge of the lysine and promotes a more relaxed chromatin structure, allowing transcription activation. In addition to transcription, acetylation regulates microtubule dynamics and intracellular transport, repair, replication and chromatin remodelling (Kouzarides, 2007;

Kazantsev, 2007). HDACs on the other hand act as transcription repressors, by removing the acetyl groups and promoting chromatin condensation and transcription silencing (Hanen *et al.*, 2008).

Under physiological conditions, the equilibrium between HATs and HDACs is maintained to achieve normal cellular function and survival. It is now believed that this balance is disturbed in pathological circumstances, where HAT activity is greatly reduced in neurodegenerative diseases (Saha & Pahan, 2006). In other words, there is a relative HDAC over-activity in degenerating neurones, which results in not only hypoacetylation, but reduced expression of cell survival genes and increased expression of apoptotic genes (Saha & Pahan, 2006). In fact, Rouaux *et al.* (2003) reported that the HAT and transcription factor, cAMP response element-binding (CREB)-binding protein (CBP) which is neuroprotective, specifically looses activity during apoptotic conditions following potassium deprivation, and results in hypoacetylation and subsequent activation of caspases (Rouaux *et al.*, 2003). Therefore, as the imbalance towards HDAC dominance is assumed to be a contributor to the development and progression of neurodegenerative diseases, inhibiting the activity of these enzymes would be an obvious therapeutic approach to rescue degenerating neurones.

Transcriptome-wide studies on neoplastic cells have shown that the substrates of HATs and HDACs are not only histones, as HDAC inhibitors affected the transcription levels of only 7 – 10 % of all genes (Xu & Marks, 2007). Some of the non-histone protein targets include transcription factors and regulators, signal transduction mediators, DNA repair enzymes, nuclear import regulators, chaperone proteins, structural proteins and inflammation mediators. This therefore implies that HDAC inhibitors possess the ability to induce transcriptional activation of disease-modifying genes (Lu *et al.*, 2006; Feinberg, 2007; Hanen *et al.*, 2008), which may revive neurones undergoing stress or damage during neurodegeneration in diseases such as Parkinson's disease.

1.3 Histone deacetylase (HDAC)

Eighteen mammalian HDACs have been identified and are grouped into four categories based on yeast homology, including structure and localisation (Table 1-4). Class I, II and IV HDACs, are also known as classical HDACs, and consist of 11 enzymes which share a zinc catalytic domain (de Ruijter *et al.*, 2003). Class III HDACs are known as sirtuins and have 7 members. Their catalytic mechanism on the other hand requires nicotinamide adenine dinucleotide (NAD^+) as a cofactor (Michishita *et al.*, 2005).

Classical HDACs

Class I (HDAC1, 2, 3 and 8) are enzymes closely related to the yeast transcriptional regulator Rpd3, with molecular weights between 22 – 55 kDa (de Ruijter *et al.*, 2003). They are ubiquitiously expressed and predominantly nuclear proteins, with the exception of HDAC3 which migrates between the nucleus and cytoplasm (de Ruijter *et al.*, 2003; Longworth & Laimins, 2006). Class IIa (HDAC4, 5, 7 and 9) and Class IIb (HDAC6 and 10) are homologous to the yeast Hda1, with molecular weights between 120 – 135 kDa (Witt *et al.*, 2008). They are found in both nucleus and cytoplasm (Witt *et al.*, 2008). Grozinger *et al.,* (2000) showed that HDACs 4 and 5 interact with 14-3-3 proteins to shuttle to the cytoplasm; whereas loss of the interaction resulted in their translocation to the nucleus (Grozinger & Schreiber, 2000). Unlike Class I, Class IIa HDACs display tissue-specific expression and are highly expressed in the heart, skeletal muscle and brain (Lucio-Eterovic *et al.*, 2008). HDAC6 and 10 differ from Class IIa HDACs through the possession of a second catalytic domain which function together and site-directed mutagenesis results in loss of enzymatic function (Guardiola & Yao, 2002; Verdin *et al.*, 2003). Class IV, consists solely of nuclear HDAC 11, which displays characteristics of both Classes I and II, and is highly expressed in kidney, heart, brain, skeletal muscle and testis (Gao *et al.*, 2002b), but has distinct physiological roles (Broide *et al.*, 2007).

Sirtuins

Class III HDACs, referred to as sirtuins are highly homologous to the yeast Sir2 (Michan & Sinclair, 2007). All 7 enzymes show different cellular localisation, where SIRT 1, 6 and 7 localise to the nucleus, SIRT 3, 4 and 5 to the mitochondria and SIRT 2 to the cytoplasm (Frye, 1999; Michishita *et al.*, 2005).

The widespread expression of these HDACs shows their importance in cell survival processes. But the existence of this many isoforms raises the question about whether they have specific functions in gene expression and development, and this has resulted in recent analyses of the role of each HDAC in development and disease.

Table 1-4 Summary of HDAC classes.
Including, expression pattern and cellular localisation. (Adapated from McKinsey *et al.*, 2002; Broide *et al.*, 2007; Lucio-Eterovic *et al.*, 2008; Di Marcotullio *et al.*, 2011; Karagiannis & Ververis, 2012).

Class	HDAC Isoform	Length (amino acids)	Chromosite	Cellular Localisatin	Expression Pattern
Class I	HDAC1	482	1p34.1	Nucleus	Ubiquitous
	HDAC2	488	6q21	Nucleus	Ubiquitous
	HDAC3	428	5q31.3	Nucleus/Cytoplasm	Ubiquitous
	HDAC8	377	Xq13	Nucleus	Ubiquitous
Class IIa	HDAC4	1084	2q37.2	Nucleus/Cytoplasm	Heart, Brain, Skeletal muscle, Thymus
	HDAC5	1122	17q21	Nucleus/Cytoplasm	Heart, Brain, Skeletal muscle, Placenta
	HDAC7	855	12q13.1	Nucleus/Cytoplasm	Heart, Skeletal muscle, Lung
	HDAC9	1011	7p12.1	Nucleus/Cytoplasm	Heart, Brain, Skeletal muscle, Spleen
Class IIb	HDAC6	1215	1p34.1	Nucleus/Cytoplasm	Heart, Kidney, Pancreas
	HDAC10	669	22q13.3	Nucleus/Cytoplasm	Ubiquitous
Class III	Sirtuins 1-7	747	-	Nucleus/ Mitochondria	Ubiquitous
Class IV	HDAC11	347	3p25.2	Nucleus/Cytoplasm	Heart, Brain, Kidney

1.3.1 Role of HDACs

The physiological role of each HDAC is not clearly defined, however, evidence shows that HDACs are involved in the development of the nervous system, and play a key role in cognition and neuronal death (Shen *et al.*, 2005; Cunliffe & Casaccia-Bonnefil, 2006). This is due to their effects not only on histone proteins, but also on transcriptional factors such as E2F and Sp1, and tumour suppressor proteins such as p53 (Morrison *et al.*, 2007). Through isoform-specific knockdown analyses and treatment with HDAC inhibitors, it has been suggested that the consequences of HDAC inhibition depends on the cell-type. Therefore, Class I HDACs, which are ubiquitous, are involved in cell proliferation and survival, whereas Class II HDACs seem to have tissue-specific roles (de Ruijter *et al.*, 2003; Dietz & Casaccia, 2010).

Table 1-5 Functions of HDACs in CNS and Periphery.

Class I

HDAC	CNS Role	Peripheral role
1	• Deletion results in early embryonic lethality in mice (Lagger *et al.*, 2002). • Promote generation and differentiation of neurones in the retina and spinal cord of zebrafish (Yamaguchi *et al.*, 2005; Cunliffe, 2004). • Over-expression in *in vitro* and *in vivo* ischemia models rescued neurones from p25 toxicity whereas HDAC1 inhibition resulted in p25-induced DNA damage and aberrant cell cycle activity, and subsequently neuronal loss (Kim *et al.*, 2008).	
2	• Reduction in HDAC2 levels in mature neurones attenuated basal excitatory neurotransmission without a significant change in the nerve terminal numbers, however, over-expression of HDAC2 increased excitatory synapses in mature neurones (Akhtar *et al.*, 2009). • Negatively regulates memory facilitation in transgenic mice which was overcome by chronic HDAC inhibition with Suberoylanilide hydroxamic acid (SAHA) (Guan *et al.*, 2009).	
3	• Homozygous HDAC3 deletions, as well as treatments with HDAC3 specific inhibitor, RGFP136 significantly improved long-term memory (McQuown *et al.*, 2011). • HDAC3 over-expression proved to be cytotoxic to cortical neurones, and in hippocampally derived HT22 cell line it exacerbated toxic effects of the toxin homo-cysteic acid (HCA), an oxidative stress inducer (Bardai & D'Mello, 2011).	
8	• Implicated in the negative regulation of CREB-dependent gene expression (Fischer *et al.*, 2010), which is critical for various cellular processes including glucose metabolism, cell survival and neuronal plasticity, which are essential for learning and memory (Gao *et al.*, 2009).	

Continues on next page

Class IIa

HDAC	CNS role	Peripheral role
4	• HDAC4 mediates neuronal death in normal cells through intracellular shuttling from the cytoplasm to the nucleus in response to stress, however, neuronal death is suppressed when HDAC4 is inhibited by Trichostatin A (TSA) or Trapoxin A (TPX), or inactivated by SiRNA in cultured cerebellar granules (Bolger & Yao, 2005). • Decline in HDAC4 expression during normal retina development has resulted in apoptosis of rod photoreceptors and bipolar (BP) interneurones, however, over-expression of HDAC4 in a mouse model of retinal degeneration prolonged photoreceptor survival and reduced the naturally occurring cell death of the BP cells (Chen & Cepko, 2009), • Deletion of HDAC4 has an inhibitory effect in regulating memory, and enhances learning and LTM formation (Wang *et al.*, 2011).	• HDAC4 is a critical modulator of the muscle transcription factor myocyte enhancer factor-2 (MEF2)-dependent structural and contractile gene expression in response to neural activity. In chronically reduced neural activity, HDAC4 binds and suppresses MEF2-dependent gene expression and contributes to the progressive muscle dysfunction observed in neuromuscular diseases such as ALS (Cohen *et al.*, 2007; Cohen *et al.*, 2009).
5	• HDAC5 appears to act as a regulator of adaptive responses to chronic stress and cocaine consumption, where there is decreases of HDAC5 function in the nucleus accumbens (NAc), a major brain reward region (Renthal *et al.*, 2007) • Mouse models of depression lacking HDAC5 exhibited hypersensitive responses to chronic stress and the anti-depressant effect of imipramine was linked to down-regulation of HDAC5 in the hippocampus, which is implicated in the pathophysiology of depression (Tsankova *et al.*, 2006).	
7	• Remains to be investigated	• Specifically expressed in the vascular endothelium where it maintains vascular integrity by repressing the expression of matrix metalloproteinase 10. • Lack of HDAC7 results in embryonic lethality due to impaired endothelial cell–cell adhesion and disrupted integrity of blood vessels (Chang *et al.*, 2006). • Controls endothelial cell growth via modulation of β-catenin, which is important as defects in signaling of Wnt/β-catenin has been implicated in AD, autism and schizophrenia (Margariti *et al.*, 2010; Freese *et al.*, 2010).
9	• Nucleocytoplasmic tanslocation of HDAC9, induced by spontaneous neural activity, regulates the expression of immediate-early genes (such as c-fos) and dendritic growth in developing cortical neurons. (Sugo *et al.*, 2010).	• Roles overlap with HDAC5 in cardiac development, as loss of either gene sensitizes the heart to stress signals, but knockout of both result in lethal ventricular septal defects (Chang *et al.*, 2004).

Continues on next page

Class IIb

HDAC	CNS role	Peripheral role
6	• Implicated in cellular processes such as neuronal transport, where it is a regulator of the cytoskeletal network (Gao *et al.*, 2007); co-ordinates the cell response to stress via the regulation of heat-shock protein (HSP)-90 (Kovacs *et al.*, 2005); a component of aggresome which recruits misfolded protein to dynein motors for transport to aggresome (Kawaguchi *et al.*, 2003). • HDAC6 interacted with polyubiquitinated proteins when the UPS was impaired for degradation via autophagy in *Drosophila melangaster* (Pandey *et al.*, 2007). • Recruited by Parkin to aid the clearance of impaired mitochondria via autophagy (Lee *et al.*, 2010b). • Contrary, inhibition of HDAC6 has been suggested to be neuroprotective, as HDAC6 is involved in the deacetylation of antioxidant enzymes, peroxiredoxin-1 and peroxiredoxin-2, to enable reduction of peroxides which contribute to ROS production and oxidative stress (Parmigiani *et al.*, 2008). • Loss of HDAC6 has been shown to be neuroprotective in primary neurons over-expressing mutant Huntington protein, where this loss significantly facilitated the axonal transport of neurotrophic factors such as BDNF (Dompierre *et al.*, 2007)	
10	• Remains to be investigated.	• In SNU-human gastric cells, HDAC10 knockdown increased the expression levels of thioredoxin-interacting protein, an endogenous inhibitor of thioredoxin which acts as a cellular antioxidant, and caused an accumulation of ROS (Lee *et al.*, 2010a).

Class IV

HDAC	CNS role	Peripheral role
11	• Acts as a regulator of the gene encoding interleukin 10 (IL-10), where overexpression of HDAC11 inhibited IL-10 expression and induced inflammatory bone marrow-derived antigen-presenting cells (APC) to prime naive T cells and restore the responsiveness of tolerant $CD4^+$ T cells (Villagra *et al.*, 2009). • HDAC11 has also been demonstrated to regulate oligodendrocyte-specific protein gene expression and cell development in OL-1 Oligodendroglia cells, non-transformed oligodendrocyte precursor cell line (Liu *et al.*, 2009).	

These functions show that these classical HDACs have specific and extensive roles in memory formation, synaptic plasticity, neuronal growth and differentiation, which are essential for neuronal survival. In PD, preventing dopaminergic neuronal loss is the ultimate goal as highlighted earlier, and the tabulated evidence show that inhibition of Class I HDAC3, and Class II HADC4 and 6 would be particularly beneficial in PD therapeutics, as they are proteins identified with neurotoxic activity (Bolger & Yao, 2005; Dompierre *et al.*, 2007; Bardai & D'Mello, 2011) (Table 1-5). However, it seems that inhibition of some HDAC isoforms may have more damaging effects than beneficial ones on neurones. For example, overexpression rather than inhibition of HDAC1, protects neurones from p25 toxicity (Kim *et al.*, 2008); and inhibition of HDAC5, which controls behavioural adaptations to chronic emotional stimuli such as stress and addiction (Renthal *et al.*, 2007), would augment and contribute to this non-motor symptom of PD (Dagher & Robbins, 2009). Irrespective of this issue, the bigger picture of PD pathology needs to be taken into consideration, where neuroprotective agents for dopaminergic neurones are urgently sought after, as this would alleviate the onset of motor symptoms and improve the quality of life for patients.

1.4 Histone deacetylase Inhibitors (HDAC-I)

As the search for potential disease-modifying agents for PD increases, small molecules which are able to cross the blood-brain barrier are required. In this case, the efficacy of HDAC-Is have been observed in an array of disorders from immune disorders, diabetes, sickle-cell anaemia, and importantly stroke to neurodegenerative disorders (Kazantsev & Thompson, 2008). Interestingly, they are most commonly used as anti-cancer agents. Their ability to induce cell growth arrest, differentiation and/ or apoptotic cell death by selectively altering the transcription of approximately 2 % of genes expressed in tumour cells make them ideal candidates (Marks *et al.*, 2001). Not surprisingly, various HDAC-Is are in clinical trials for numerous of cancers including leukaemia, T-cell lymphoma, non-small cell cancer, solid tumour and haematological malignancies (Wagner *et al.*, 2010). The idea that drugs used in cancer therapeutics to reduce proliferation and induce apoptosis, could be beneficial in neurodegenerative disorders, where cells die prematurely is conflicting. Yet, recent genetic studies have shown that there are overlapping pathways involved in the progression of both diseases, such as, mitochondrial dysfunction, oxidative stress and inflammation (Devine *et al.*, 2011a). This therefore makes agents that have an array of targets and functions, such as HDAC-Is, seem like ideal candidates for PD treatment.

HDAC-Is, which differ in classical HDAC isoenzyme selectivity are classed into four main chemical families. These are the short-chain fatty acids, hydroxamates, cyclic pepetides and benzamides

(Table 1-6). Majority of the inhibitors currently available non-selectively influence all eleven HDAC isoforms (Bieliauskas & Pflum, 2008).

Short chain fatty acids are relatively small and simple structured. The most common examples are sodium butyrate (Nab), valproic acid (VPA; valproate) and phenylbutyrate, which mainly inhibit Class I HDACs in the range of millimoles (Khan *et al.*, 2008). Sodium butyrate has been shown to exert anti-depressant properties in the mouse brain and stimulate neurogenesis in the rat brain following cerebral ischemia (Schroeder *et al.*, 2007; Kim *et al.*, 2009). VPA is an established central nervous system (CNS) drug used as an anti-convulsant, mood stabiliser and adjuvant treatment for schizophrenia (Grayson *et al.*, 2010). Both sodium butyrate and VPA have exhibited anti-inflammatory properties and have shown to be neuroprotective in rat ischemia models (Kim *et al.*, 2007), suggesting an anti-inflammatory role of this class of HDAC-Is in PD pathogenesis.

Hydroxamates bind to the zinc ion in the catalytic domain of HDAC to inactivate the enzyme (Marks *et al.*, 2004). For this reason, they act as pan-HDAC-Is and are selective for Class I and II HDACs without showing isoform selectivity with high nanomolar potency (Grayson *et al.*, 2010). Examples include, Trichostatin A (TSA), Suberoylanilide hydroxamic acid (SAHA; vorinostat), Oxamflatin, Panobinostat, Givinostat, Belinostat. Most of these compounds are undergoing clinical trials for cancer (Wagner *et al.*, 2010), but SAHA is the most clinically advanced as it has obtained US Food and Drug Administration (FDA) approval for T-cell lymphoma (Grant *et al.*, 2007). Its ability to cross the brain blood barrier (BBB) makes it an ideal agent for neurological disorders (Chuang *et al.*, 2009).

Cyclic peptides induce inhibition of HDACs by binding to the zinc ion site, and show selectivity for Class I HDAC isoforms (Grayson *et al.*, 2010; Furumai *et al.*, 2002; Grayson *et al.*, 2010). Two common examples of this class are romidepsin (FK-228; desipeptide) and apicidin. Romidepsin shows potent efficacy for HDAC1 and 2, whereas apicidin is selective for HDAC2, 3 and 8 (Furumai *et al.*, 2002; Khan *et al.*, 2008). Romidepsin has also recently obtained FDA approval for T-cell lymphoma (VanderMolen *et al.*, 2011). The HDAC isoform selectivity of these inhibitors make them ideal agents for multi-factorial disorders such as PD, as their treatment would limit possible side effects.

Benzamides are relatively new HDAC-Is which also exhibit isoform selectivity. Examples currently in clinical trials include MS-275 and CI-994 (Grayson *et al.*, 2010). They are both selective for

HDAC1. Similar to the cyclic peptides, the isoform selectivity of these inhibitors could limit toxic side effects which are exerted by pan-HDAC-Is and class selective HDAC-Is.

The extensive use of HDAC-Is in cancer therapeutics, has expanded the portfolio of the inhibitors. For this reason, it would be relatively quick to get HDAC-Is prescribed once they have successfully passed trials for PD. The overlap between cancer and PD progression instills some optimism that these agents may exert beneficial effects in PD. However, the contradicting effects that HDAC-Is have on the HDAC isoforms, enhances the crucial need for isoform-selective HDAC-Is.

Table 1-6 Structure and inhibitory profile of some inhibitors.
(Modified from Blanchard & Chipoy, 2005; Bolden *et al.*, 2006; Witt *et al.*, 2008; Khan *et al.*, 2008).

Class	Structure	Class Inhibited
Short-chain fatty acid	*Butyrate* 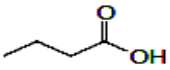 *Valproic Acid* 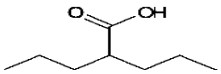	**Class I**
Hydroxamate	*Suberoylanilide Hydroxamic Acid (SAHA)* 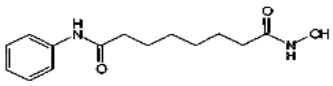 *Trichostatin A* 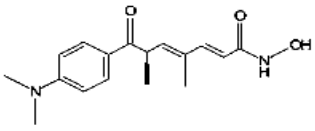	**Class I and II**
Benzamide	*MS-275* 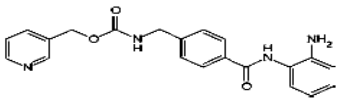 *MGCD010* 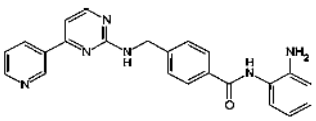	**HDAC1**
Cyclic-Tetrapeptide	*Apicidin* 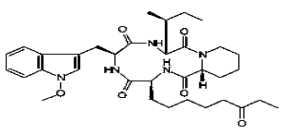 *Romidepsin* 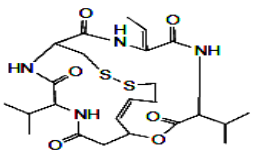	**Class I**

1.4.1 Evidence of HDAC-I therapeutic role in neurodegenerative diseases

Despite the vast use of HDAC-I's in cancer therapy, there has recently been an explosion of interest in the potential therapeutic role of HDAC-Is in neurodegenerative disorders. In fact a beneficial role for HDAC-Is was first discovered in Huntington's disease (HD) when HDAC-Is attenuated cell death and improved motor function and survival in *Drosophila* (Steffan *et al.*, 2001). Additional studies showed SAHA ameliorated the cognitive and motor deficit characteristics of the disorder in transgenic mouse models through increased histone acetylation (Hockly *et al.*, 2003). Sodium butyrate also protected R6/2 transgenic mice models from the lethality of the CAG expansion disorder in the coding region for the protein huntingtin, and caused less brain atrophy in transgenic mice compared to vehicle treated mice (Ferrante *et al.*, 2003). Further studies found phenylbutyrate exerted neuroprotective effects in the N171-82Q transgenic mouse models of HD (Gardian *et al.*, 2005).

Moreover, investigations in mouse models of spinal muscular atrophy (SMA), with low levels of survival motor neurone (SMN) protein involved in motor neurone degeneration, had increased levels of SMN protein and less regions exhibiting muscle atrophy, following sodium butyrate treatment (Chang *et al.*, 2001; Brichta *et al.*, 2003). Further studies, also reported that VPA-treated SMA mice displayed elevated levels of SMN protein, which resulted in improved motor function, reduced motor neurone degeneration and decreased muscle atrophy compared to the control group, through activation of the survival motor neurone gene (SMN2) (Tsai *et al.*, 2008).

Furthermore, VPA and phenylbutyrate administration ameliorated histone hypoacetylation in G86R and G93A transgenic amyotrophic lateral sclerosis (ALS) mice, and prevented motor neurone death in the rodents (Ryu *et al.*, 2005; Rouaux *et al.*, 2007). Finally, treatment of ischemic brain tissue with SAHA prevented histone deacetylation, thus increasing histone H3 acteylated levels. This was accompanied by increased expression of the neuroprotective proteins heat-shock protein 70 (Hsp70) and Bcl-2 (Faraco *et al.*, 2006).

So far, these promising evidences confirm the theory that epigenetic modifications could potentially be disease-modifying. This has led to the assumption that such beneficial effects could also be achieved in PD models, and has therefore increased the recent interest of HDAC inhibition in PD.

1.4.2 Therapeutic role for HDAC-I in PD

There is very limited evidence of the role of HDAC-Is in PD. However, the findings that have been reported so far implies that HDAC-Is may have the potential to be promising neuroprotective

agents in the disorder. Pionneering work from Beal and colleagues (2004) reported that phenylbutyrate administration significantly reduced striatal depletion of dopamine and dopaminergic cell death in mice following MPTP treatment (Gardian *et al.*, 2004).

Other studies also reported that mutant α-synuclein (A30P and A53T) present in Lewy bodies and associated with familial forms of PD, acted in the nucleus to bind to histones and reduce levels of acetylated histone H3, by inactivating HATs CBP, p300 and P/CAF (Kontopoulos *et al.*, 2006). This resulted in hypoacetylation, inhibited transcription, and promotion of apoptosis and neurotoxicity in human neuroblastoma cell lines. These cells were rescued from α-synuclein neurotoxicity and apoptosis by HDAC-Is, suberoylanilide hydroxamic acid (SAHA) and sodium butyrate (Kontopoulos *et al.*, 2006).

In summary, even though these findings are limited, they are positive and provide optimistic evidence that HDAC inhibition in PD could potentially protect dopaminergic cells from toxin- or stress-induced cell death and subsequently be useful as a treatment of PD. However, the effects of these drugs on the survival of dopaminergic neurones remain uncertain and will be addressed in these studies.

1.5 Thesis hypothesis

The identification of neuroprotective approaches that can delay or halt disease progression is the primary goal in PD research. Despite promising results from a number of compounds including cogane in animal studies (Table 1-3), all of the putative agents have failed to demonstrate unequivocal neuroprotection in clinical trials. As there is increasing evidence suggesting the potential neuroprotective effect of HDAC inhibitors in neurodegenerative diseases, it was hypothesised that HDAC inhibitors will protect dopaminergic neurones from oxidative stress- and inflammation-induced cell death in PD.

1.6 Thesis aims

In order to test this hypothesis, the studies described in this thesis aimed to investigate the role of HDAC-Is, VPA and SAHA, as potential neuroprotective agents against dopaminergic cell death in models of PD. Specifically, the thesis aimed to:

1. Model dopaminergic cell death in PD using *in vitro* and *in vivo* models with toxins H_2O_2 MPP^+, LPS and 6-OHDA.
2. Determine the effect of HDAC-Is on toxin-induced neuronal cell death in *in vitro* and *in vivo* models.

3. Determine the effect of HDAC-Is on inflammation associated with cell death *in vitro* and *in vivo* models of PD.

Chapter 2 Materials and Methods

2.1 Introduction

The aim of the studies described in this thesis was to investigate the neuroprotective effect of HDAC inhibitors on dopaminergic neurone cell death in *in vitro* and *in vivo* models of PD. The following studies were performed:

1. Neuroprotection studies in cell lines.

Neuroblastoma cell lines N1E-115 and SH-SY5Y were treated with HDAC inhibitors in the presence and absence of hydrogen peroxide (H_2O_2) and 1-methyl-4-phenylpyridinium (MPP^+). These act through reactive oxygen species (ROS) generation and inhibition of mitochondrial complex I respectively. The effect of the HDAC inhibitors on cell survival was determined by measuring the release of lactate dehydrogenase (LDH) and differentiating between the viable and non-viable cells by trypan blue exclusion.

2. Neuroprotection studies in rat primary ventral mesencephalic cultures.

Primary ventral mesencephalic cell cultures were prepared from 14 day old rat embryos. The cells were treated with HDAC inhibitors in the presence and absence of MPP^+ and lipopolysaccharide (LPS). The effects of the inhibitors were assessed by immunocytochemical staining for tyrosine hydroxylase (TH), astrocytes (GFAP) and microglia (OX-42).

3. Neuroprotection studies in 6-hydroxydopamine and LPS- lesioned mice.

Mice were lesioned with 6-hydroxydopamine (6-OHDA) and LPS to induce a partial lesion of the nigro-striatal pathway. HDAC inhibitors were administered to the animals before, during and after lesioning, and their effects were observed by immunohistochemistry with antibodies against TH, GFAP and OX-42.

This chapter describes the general materials and methods, common between the *in vitro* and *in vivo* models, used in these studies. Methods specific to each model is detailed in the individual results chapters.

2.1.1 Toxin-induced models of PD

Toxin-induced models are widely used *in vitro* and *in vivo* as tools to increase the understanding of the pathological process of PD, however, it is important that they are biologically relevant to the human disease reflecting the pathological processes involved. For this reason, in this study, MPP^+- and H_2O_2-induced toxicity was used to cause dopaminergic cell death *in vitro*, and 6-OHDA- and LPS-lesioned mice *in vivo*. Partial destruction of the nigro-striatal pathway was induced following unilateral stereotaxic injection of 6-OHDA or LPS into the striatum. These models produce irreversible dopaminergic cell death and the mechanism by which this occurs is described below.

2.1.1.1 MPP^+

MPP^+ is the toxic active metabolite of the neurotoxin 1-methyl-4-phenyl-1,2,3,6-tetrahydropyridine (MPTP). In 1982, MPTP was found to induce parkinsonism in man when young drug addicts accidentally injected this drug (Langston *et al.*, 1983b). Subsequent investigations of MPTP in rodent and primate models have shown it induces selective destruction of the dopaminergic neurones of the nigro-striatal tract as well as the observation of motor deficits (Langston *et al.*, 1984; Jenner *et al.*, 1984).

When MPP^+ is administered to culture media, it is taken up into dopaminergic neurones via the dopamine transporter (DAT) (Javitch *et al.*, 1985; Gainetdinov *et al.*, 1997). Once in the neurones, MPP^+ accumulates in the mitochondria where it inhibits complex I of the electron transport chain. This impairs mitochondrial respiration by inhibiting aerobic glycolysis and increasing lactate production, resulting in reduced ATP production and increased ROS release such as superoxides (Nicklas *et al.*, 1987). This dual effect of decreased ATP and increased ROS increases NO-dependent increase in pro-apoptotic protein bax (Dennis & Bennett, 2003), as well as initiating other cell death-related pathways such as p38 mitogen-activated kinase (Karunakaran *et al.*, 2008) and c-jun N-terminal kinase (JNK) (Saporito *et al.*, 2000) which all contribute to apoptotic cell death (Tatton & Kish, 1997). MPP^+ is also stored in the vesicles through uptake by the vesicular monoamine transporter (VMAT2) (Gainetdinov *et al.*, 1998). In the vesicles, MPP^+ displaces stored dopamine into the extracellular space where it is oxidised by MAO into metabolites such as 3,4-dihydroxyphenylacetaldehyde (DOPAL) which is toxic to dopaminergic neurones (Burke *et al.*, 2008b; Panneton *et al.*, 2010), dopamine quinones and free radicals (LaVoie & Hastings, 1999).

2.1.1.2 H_2O_2

Unlike MPP^+, H_2O_2 is not selective for the mitochondria, but it is commonly used to induce oxidative stress in culture. H_2O_2 is a ubiquitous molecule to living organisms (Halliwell *et al.*, 2000). At cellular levels, oxygenated species such as H_2O_2 is generated normally and detoxified by antioxidant enzymes such as catalase and glutathione to produce oxygen and water (Makino *et al.*, 1994; Hashida *et al.*, 2002). For this reason, H_2O_2 is added as a bolus to culture medium (Gille & Joenje, 1992). The oxygenated species become hazardous when the balance between radical formation and removal is disturbed. H_2O_2 is an unreactive species, but its deleterious effects are due to its ability to stimulate the super hydroxyl radical formation by the Fenton and Haber-Weiss reactions, both mediated by iron, to subsequently induce lipid peroxidation and DNA damage (Mello Filho & Meneghini, 1984; Starke & Farber, 1985).

When H_2O_2 is administered to culture medium, it readily penetrates the cellular envelope where it causes a reduction in the activity of antioxidant enzymes. This results in the formation of hydroxyls close to the chromatin which initiate DNA single-strand breaks (Mello Filho & Meneghini, 1984). This in turn activates poly(ADP-ribose) polymerase to deplete the levels of the coenzyme nicotinamide adenine dinucleotide (NAD) (Schraufstatter *et al.*, 1986), which is needed for electron transfer during redox reactions. H_2O_2 induces ATP depletion by inactivating glyceraldehyde 3-phosphate dehydrogenase (GAPDH), which catalyses glycolysis (Hinshaw *et al.*, 1990), and this in turn results in mitochondrial impairment. Furthermore, H_2O_2 increases intracellular free calcium, which has been implicated to be associated with cell death (Whittemore *et al.*, 1995). These effects of H_2O_2 combined, results in the induction of apoptotic neuronal death (Whittemore *et al.*, 1995).

MPP^+ and H_2O_2 are ideal candidates to investigate HDAC-Is potential antioxidant characteristic. This is due to the fact that both of the toxins induce oxidative stress, mitochondria impairment and apoptosis, which are implicated in the pathogenesis of PD.

2.1.1.3 6-OHDA

Since it was first reported to lesion the nigro-striatal dopaminergic pathway over 50 years ago (Ungerstedt, 1968), 6-OHDA has become the most routinely utilised and characterised toxin-based model of PD. It is commonly used in rats but other species, for example mice, monkeys, cats and dogs, are also sensitive to this toxin (Thomas *et al.*, 1991). The structure of 6-OHDA resembles that of dopamine but has an additional hydroxyl group thereby making it toxic to neurones (Kostrzewa & Jacobowitz, 1974). 6-OHDA does not cross the BBB so it is directly injected into the SNpc, medial forebrain bundle (MFB) or striatum (Carvey *et al.*, 2005) where it initiates dopaminergic cell death.

Although the exact mechanism of 6-OHDA toxicity is unclear, the current understanding is that, following injection, it enters neurones via the plasma membrane DAT into the cytoplasm (Choi *et al.*, 1999), where 6-OHDA destroys catecholaminergic neurones by a combination of cellular oxidative stress and mitochondrial dysfunction (Hanrott *et al.*, 2006). 6-OHDA oxidises to form ROS including H_2O_2 (Mazzio *et al.*, 2004) which is induced by MAO (Karoum *et al.*, 1993), and quinones (Saner & Thoenen, 1971) to directly damage neurones. It elevates the levels of iron in the SN (Oestreicher *et al.*, 1994) which drives the generation of ROS as well as damaging the electron transport system through membrane lipid peroxidation (Glinka & Youdim, 1995). It decreases the levels of striatal anti-oxidant enzymes including superoxide dismutase (SOD) and glutathione (GSH) (Perumal *et al.*, 1992) promoting ROS accumulation. Furthermore, 6-OHDA

potently inhibits complexes I and IV of the mitochondrial respiratory chain, particularly NADH dehydrogenase (complex I) and cytochrome c oxidase (complex IV) (Glinka & Youdim, 1995; Glinka *et al.*, 1997). This consequently causes ATP depletion, further oxidative stress and decrease in cell protective mechanism which results in cellular degeneration (Glinka & Youdim, 1995). Moreover, dopamine depletion, nigral dopamine cell loss, and neurobehavioral deficits have been successfully achieved using this model (Ungerstedt, 1968). Furthermore, this toxin induces neuro-inflammation in the brain (Cicchetti *et al.*, 2002), which is ongoing and implicated in the pathogenesis and progression of PD. Many of the effects of 6-OHDA mirrors the events occurring in PD, thus making it a good model to investigate the effects of HDAC-Is.

2.1.1.4 LPS

The use of the gram-negative bacteria endotoxin LPS has been a useful tool to demonstrate and study neuro-inflammation in the pathogenesis of PD and anti-inflammatory agents for PD therapy. LPS-induced inflammation replicates some characteristics of PD, such as glia activation and loss of dopaminergic neurones (Iravani *et al.*, 2005). LPS is not directly toxic to neurones, but can become more toxic to neurones in the presence of glial cells than 6-OHDA (Bronstein *et al.*, 1995). LPS is commonly used in rodents and can be administered systemically or injected into the striatum or SN (Hunter *et al.*, 2009).

Following injection into the brain, LPS initially binds to the LPS-binding protein (LBP) to transfer LPS to the CD14/Toll-like receptor (TLR) 4 complex expressed on glia cells to induce their activation and a cellular response (Ulevitch & Tobias, 1995; Castano *et al.*, 1998; Herrera *et al.*, 2000; Palsson-McDermott & O'Neill, 2004). This activation of glial cells induces the expression of iNOS which in turn up-regulates NO and 3-nitrotyrosine (3-NT) generation release to mediate toxicity (Iravani *et al.*, 2002; Arimoto & Bing, 2003). The activation of glial cells also induces the release of inflammatory cytokines, IL-1α, IL-1β, IL-6 and TNF-α, which are thought to be responsible for increased iNOS expression (Arimoto & Bing, 2003; Lehnardt *et al.*, 2003). NO interacts with metals, thiols and oxides leading to the increased generation of oxidative and nitrative stress which are deleterious to neurones (Dawson & Dawson, 1996). This stress is promoted by the increased levels of iron in the SN following intrastriatal injection of LPS (Hunter *et al.*, 2008). Similar to the 6-OHDA model, the LPS model also exhibits features of PD such as progressive degeneration of dopaminergic cell bodies in the SN and their striatal terminals, depletion dopamine content in the striatum, in addition to mitochondrial impairment (Hunter *et al.*, 2007; Hunter *et al.*, 2009).

Even though no model exists to completely and accurately portray the pathology of PD, the toxic models of 6-OHDA and LPS have been useful for understanding PD pathogenesis as well as testing new potential agents such as HDAC-Is in this study.

2.1.2 HDACs and HDAC-Is

This study focussed exclusively on the activities of the classical HDACs. This is because this class of enzymes have been widely investigated in cancer, and more recently in neurodegenerative disorders, such as HD and AD. In particular Class I HDAC3, Class II HDAC4 and 5, and Class IV HDAC11 were shown by gene expression mapping of the rat brain to have the highest expression in nigro-striatal pathway, particularly, the substantia nigra pars compacta (Broide *et al.*, 2007) which is affected in PD (Ehringer & Hornykiewicz, 1998).

The two chosen inhibitors utilised in this present study are VPA and SAHA, as they have been thoroughly examined in terms of toxicology, side effects and dose; and are already in clinical use for mood disorders and T cell lymphoma, respectively. In addition, they have already been shown to have positive effects in the neurodegenerative disorders HD and AD (Chapter 1). VPA shows selectivity for class I isoforms in millimolar range but has been confirmed by biochemical assays to have very little effect on Class II HDAC isoforms (Khan *et al.*, 2008). It is widely prescribed as an anti-convulsant and mood-stabilising drug commonly used to treat epilepsy and bipolar disorder and has been on the market for over 3 decades (Phiel *et al.*, 2001; Brichta *et al.*, 2003). SAHA, on the other hand, is a pan inhibitor which is selective for both class I and II HDAC isoforms (Bieliauskas & Pflum, 2008). It has been FDA approved for cutaneous T cell lymphoma, and has shown promising results in HD mice models (Hockly *et al.*, 2003).

2.2 Animals for biochemical analysis

Male C57BL/6J mice (Harlan, Bicester, UK), weighing 25-30 g, were singly housed in a temperature controlled room of 23^{o}C (King's College London Biological Services Unit) with a 12 hour light-dark cycle and free access to pelleted food and water. All experimental procedures were carried out in accordance with the Animals (Scientific Procedures) Act 1986 under the UK Home Office licence number 70/6898.

2.3 Preparation of mouse brains

2.3.1 Transcardial Perfusion and dissection for western blot and immunohistochemistry

Mice were terminally-anaesthetised with sodium pentobarbital solution (20 %; 100 mg/kg ip). The thoracic cavity was cut open and transcardially perfused with 0.1 M PBS pH 7.4, containing sodium chloride (NaCl; 137 mM), diSodium hydrogen orthophosphate anhydrous (Na_2HPO_4; 8 mM), Potassium dihydrogen orthophosphate (KH_2PO_4; 1.5 mM). The brains were removed and cut at the level of the optic chiasm forming a rostral and a caudal compartment of the brain. The rostral part of the brain was flash-frozen in liquid nitrogen, followed by storage -70^{o}C, until used for western blot (Section 2.4). The caudal part was post-fixed in PFA (4 %) in 0.1 M PBS for 7 days at 4^{o}C, followed by storage in cryoprotective solution composed 0.1 M PBS containing sucrose (30 %) and sodium azide (0.05 %) also at 4^{o}C, until used for immunohistochemistry (Section 2.6.6.2).

2.4 Western blotting

This is an analytical technique to detect proteins according to their molecular weights in brain homogenates or cell lysates.

2.4.1 Preparation of cell lysates

Cell lines were grown in a 175 cm^2 flask to confluence, and washed with 0.1 M PBS as described in Chapter 3. Using a sterile cell scraper the cells were released from the flask, collected and centrifuged at 1000 g. The pellet was resuspended in lysis buffer (250 μl) containing sodium dodecyl sulphate (SDS; 1%) and Tris (hydroxymethyl) aminomethane hydrochloride (Tris-HCL; 50 mM) (pH 7.4); heated at 98^{o}C for 10 minutes followed by centrifugation at 1000 g. The supernatant (150 μl) was transferred to a new eppendorf and stored at -80^{o}C until analysis.

2.4.2 Preparation of brain tissue homogenates

Brain tissue stored at -80^{o}C was weighed and homogenised (1:5 w/v) in Tris-base lysis buffer (50 mM; pH 8.0) containing Triton-X-100 (1 %), sodium chloride (150 mM), ethylenediamine-tetraacetic acid (EDTA; 5 mM), phenylmethylsulphonyl fluoride (PMSF; 2 mM) and protease

inhibitor cocktail set III (5 %). Homogenates were centrifuged (Biofuge Fresco, Heraeus) at 13000 g for 30 minutes at 4^{o}C.The supernatant was collected and stored at -80^{o}C.

2.4.3 Gel electrophoresis

Sodium dodecyl sulphate polyacrylamide gel electrophoresis (SDS-PAGE) was used to detect proteins in tissue homogenates and cell lysates. The components of the gel comprised of a resolving and stacking gel (Table 2-1). Sample protein concentrations were determined using the NanoDrop® detailed in Section 2.5. They were mixed with an equal amount of loading buffer, boiled for 3 minutes at 95^{o}C, and then each sample (15 μl) was loaded onto the gel. The ladder marker (precision plus protein standard) (10 μl) was also loaded onto the gel. Protein separation by electrophoresis was performed in running buffer (Table 2-1) at a constant current of 30 mA for 90 minutes.

2.4.4 Immunoblotting

On completion of electrophoresis, polyvinylidene difluoride (PVDF) membranes were rinsed in methanol (100 %) and deionised water and then soaked in blot buffer (Table 2-1). The gel and PVDF membrane were sandwiched between 2 layers each consisting of 4 filter papers, soaked in blot buffer. Protein transfer onto the membrane was performed at 20 V for 20 minutes using a Bio-Rad transblotter.

Following transfer, the membranes were blocked in milk (5 %) in 1 X Tris-buffered saline (TBS) and Tween-20 (0.1 %) (TBS-T) at room temperature, with gentle agitation on a shaker (DS-500E Orbital shaker, VWR International, UK). After 1 hour, the membranes were incubated with the primary antibody (at the appropriate dilution listed in Table 2-2) in albumin bovine serum (5 %)/ TBS-T at 4^{o}C overnight on a shaker. Membranes were washed 3 times for 5 minutes with TBST-T, and followed by 1 hour incubation at room temperature with the polyclonal goat anti-rabbit horseradish peroxidise (HRP) - conjugated secondary antibody (Table 2-3) diluted in milk (5 %)/ TBS-T.

Membranes were washed with TBS-T (3 X 5 minutes) and protein bands were detected by enhanced chemiluminescence (ECL) western blot detection kit (Table 2-4). Following manufacturer's instructions, the reagents were mixed and pipette over the membranes and incubated in the dark for 5 minutes. The membranes were sandwiched in clear acetate sheets, placed in an X-ray film cassette and exposed to Kodak® Hyperfilm at different time points (5 seconds to 3 minutes). The films were developed by a fully automated X-ray film processor (Compact X4, Xograph healthcare, UK).

To recognise differences in protein loading, the membrane was stripped with antibodies by incubating with stripping buffer (Table 2-1) for 30 minutes at 5°C. Following washes with TBS-T (3 X 10 minutes), the membrane was blocked with milk (5 %)/ TBS-T, reprobed with β-actin primary antibody (Table 2-2) followed by mouse HRP secondary antibody (Table 2-3), 1 hour each. Band detection with ECL was done as detailed above.

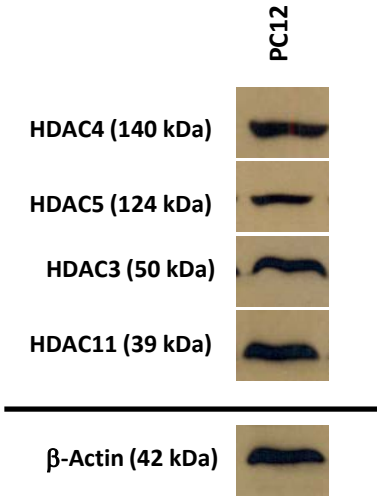

Figure 2-1 Protein expression of HDAC isoforms by western blot.
PC12 cell line was screened for the expression of HDAC3, 4, 5 and 11. β-Actin was used as a loading control. Images are typical of duplicate analyses.

Table 2-1 List of buffers used for western blot.

Buffer	Components	Source
4X Resolving Gel Buffer (RGB), pH 8.8	1.5 M Tris-base Adjust pH with HCl	Sigma-Aldrich, Dorset, UK
4X Stacking Gel Buffer (SGB), pH 6.8	0.5 M Tris-base Adjust pH with HCl	Sigma-Aldrich, Dorset, UK
10X Running buffer (RB)	25 mM Tris 200 mM Glycine 10 % Sodium dodecyl sulphate (SDS)	Sigma-Aldrich, Dorset, UK BDH, VWR International, Lutterworth, UK Sigma-Aldrich, Dorset, UK
10X TBS	50 mM Tris-base 150 mM NaCl	Sigma-Aldrich, Dorset, UK Sigma-Aldrich, Dorset, UK
Blot Buffer	48 mM Tris 39 mM Glycine 20 % Methanol	Sigma-Aldrich, Dorset, UK BDH, VWR International, Lutterworth, UK
Loading Buffer	5 mM Tris, pH 6.8 2 % SDS 10 % Glycerol 0.1 % Bromophenol blue 5 % β-mercaptoethanol	Sigma-Aldrich, Dorset, UK Sigma-Aldrich, Dorset, UK Alfa Aesar, Lancashire, UK
Stripping Buffer	62.5 mM Tris, pH 6.8 100 mM β-mercaptoethanol 2 % SDS	Sigma-Aldrich, Dorset, UK Sigma-Aldrich, Dorset, UK

2.5 Measurement of Protein Content

2.5.1 Protein concentration

Protein concentration of cell lysates and tissue homogenates prepared as described in Sections 2.4.1 and 2.4.2, was determined using the NanoDrop® ND-10000 spectrophotometer (Labtech international Ltd., East Sussex, UK). Using the module 'Protein A280' on the ND-1000 3.5.1 software, an aliquot of the sample (2 μl) was loaded onto the measurement pedestal and the protein absorbance at 280 nm wavelength was measured (Figure 2-2). Protein measurements for each sample were determined in triplicate, and the mean was used as final concentration.

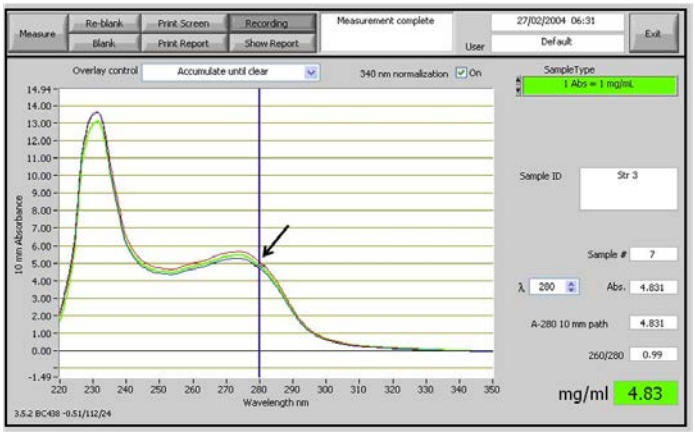

Figure 2-2 An example of an absorbent spectrum using the NanoDrop spectrophotometer.
The protein content of a mouse brain striatum homogenate (1:10 w/v) was measured in triplicate using the NanoDrop ND-1000 Spectrophotometer. The protein absorbance of all three runs (red, green and blue) at 280 nm wavelength (arrow) was compared to an internal Bovine serum albumin (BSA) protein standard. The protein concentration is recorded as mg/ml.

To assess the accuracy and linearity of the Nanodrop, a series of Bovine serum albumin (BSA) dilutions ranging from 0.4 - 25 mg/ml were measured and compared to actual concentrations. The concentrations obtained for cell lysates and tissue homogenates examined in this thesis were 1 – 12 mg/ml, which lies within the most accurate range of the Nanodrop (Figure 2-3) therefore no correction was made. The BSA standard was linear (r^2= 0.9971), but deviated from the expected measurements at concentrations above 10 mg/ml.

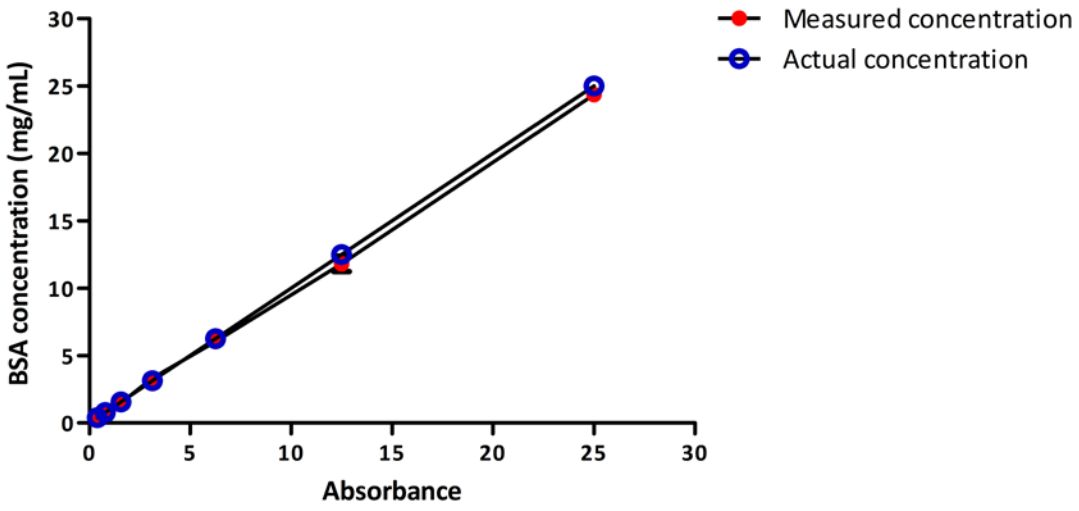

Figure 2-3 Comparison of protein concentration of BSA standard curve using Nanodrop.
BSA (0.4 - 25 mg/ml) was measured using the internal standard (blue) and to compared the actual concentrations (red). Measurements were repeated in triplicate. Data are expressed as mean ± SEM.

2.6 Immunochemical Staining

2.6.1 Plate preparation

Glass coverslips (13 mm diameter; Scientific Laboratories supplies, UK) were washed three times with ethanol (70 %) followed by three washes with sterile distilled water. They were then sterilised in an autoclave (Dixons Surgical Ltd, Wickford, Essex, UK) at 121^{o}C for 30 minutes and air-dried under a safety cabinet. They were soaked in poly-D-lysine solution (0.01 % in sterile distilled water) for 30 minutes at room temperature. The coverslips were then rinsed twice with sterile distilled water to wash off any unbound material, and left to dry overnight under a safety cabinet.

2.6.2 Preparation of cell culture

Cell lines were seeded onto poly-D-Lysine (0.05 %; Sigma-Aldrich, Dorset, UK) coated coverslips in 24 well plates at a density of 1x10^{5}. They were grown and maintained at 37^{o}C (described in detail in Chapter 3) for 2 days. The media was aspirated and the cells were washed with 0.1 M PBS, followed by paraformaldehyde (PFA) (4 %; 500 μl) at room temperature for 30 minutes. The PFA was then discarded, and the wells were rinsed three times with sterile PBS (0.1 M; pH 7.4; 500 μl) and stored in sterile PBS (1 ml) at 4^{o}C, until immunolabelling (Section 2.6.3).

A similar process was followed for primary culture; however, the cells were grown for 7 days in an incubator (detailed in Chapter 4). The cells were processed in a similar manner to cell lines and stored in PBS (0.1 M; 1ml) at 4^{o}C, until processed for staining (Sections 2.6.3, 2.6.5 and 2.6.6.1).

2.6.3 Single immunoflourescence staining

Cell lines and primary culture cells fixed on coverslips detailed in Section 2.6.2, were labelled by single immunoflourescence in 24 well plates (500 μl per well), and were agitated using a plate shaker (VXR basic Vibrax ®, IKA, Germany). The cells were first washed 3 X 5 minutes with 0.1 M PBS and blocked with goat serum (10 %) in 0.1 M PBS at room temperature for 1 hour. Primary antibodies were prepared in goat serum (GS; 1 %) in 0.1 M PBS at dilutions detailed in Table 2-2, and the cells were incubated at 4^{o}C overnight. On the next day, the cells were washed 3 X 5 minutes with Triton-X 100 (0.05 %)/ 0.1 M PBS (PBS-T), followed by 2 hours incubation with the secondary antibody (Table 2-3) at room temperature in the dark. Following 3 X 5 minutes washes, the cells were mounted with Vectashield® Hard set mounting medium containing 4, 6-diamidino-2-phenylindole (DAPI; Vector Laboratories, Peterborough, UK) and left to dry at 4^{o}C for 24 hours. Cells were examined using an immunofluorescence microscope (Zeiss Axioskop, Carl Zeiss, Hertfordshire, UK) (Figure 2-4).

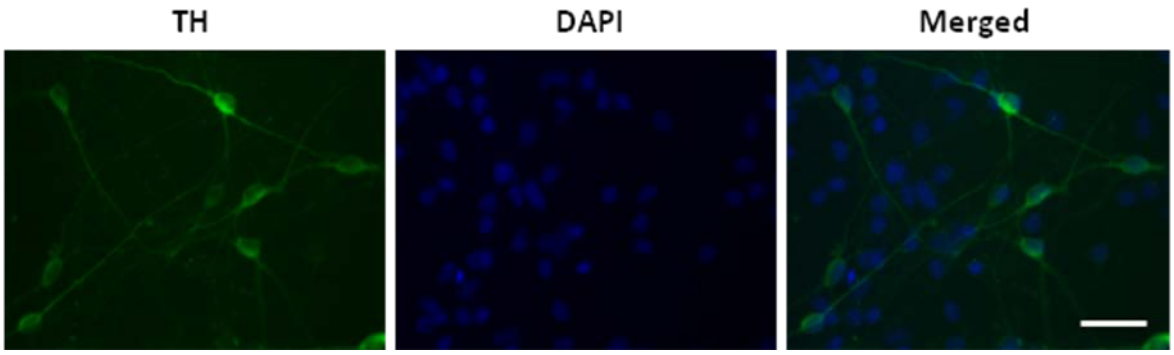

Figure 2-4 Single immunoflourescence labelling of primary culture cells.
Ventral mesencephalic (VM) cultures were stained with antibodies against tyrosine hydroxylase (TH) (green). DAPI was used as counter stain for nucleus staining (blue). Scale bar = 100 μm

2.6.4 Preparation of mouse brain tissue

Coronal sections (30 μm) of mouse brains were cut using a freezing microtome (Leica SM 2000R). Substantia nigra pars compacta (SNpc) was sectioned at the level of the third nerve (Paxinos G. & Franklin F., 2004). Free floating sections were collected into 96 well plates (1 section/ well) filled with 0.1 M PBS and NaN_3 (0.05 %), and processed for double immunofluorescence (Section 2.6.5) or immunohistochemical staining (Section 2.6.6.2).

2.6.5 Double immunoflourescence staining

Primary VM cultures fixed on coverlips (Section 2.6.2) and free floating mouse brain sections (Section 2.6.4) were labelled in 24 well plates of 0.1 M PBS (pH 7.4) (500 μl per well) on a plate shaker providing constant gentle agitation. First, both cell cultures and brain sections were washed with 0.1 M PBS 3 X 5 minutes. Subsequently, they were incubated with blocking solution (10 %) containing GS and donkey serum (DS), in PBS-T for 1 hour at room temperature. They were then incubated with two different primary antibodies (Table 2-2) diluted in blocking solution (1 %) at 4^{o}C overnight. Following 3 X 5 minutes washes in PBS-T, the samples were subjected to incubation with the two respective secondary antibodies in PBS-T (Table 2-3), for 2 hours at room temperature. After 3 X 5 minutes washes in 0.1 M PBS, the labelled cells and sections were mounted with Vectashield® Hard set mounting medium containing DAPI, or Vectashield® Hard set mounting medium for fluorescence, respectively. They were then examined as previously mentioned in Section 2.6.3 (Figure 2-5).

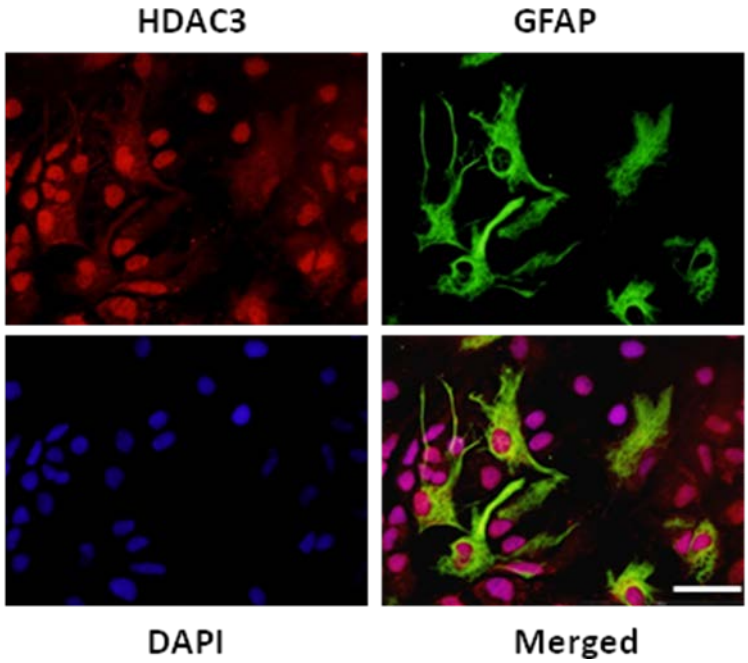

Figure 2-5 Double immunoflourescence labelling of primary culture cells.
Fixed VM cultures were double stained for histone deacetylase 3 (HDAC3) (red) and glial fibrilliary acidic protein (GFAP) (green). The nucleus was counter stained with DAPI (blue). Scale bar = 100 μm

2.6.6 Immunoperoxidase staining

2.6.6.1 Immunocytochemical staining of fixed cells

Fixed VM cells on coverslips underwent immunocytochemistry in 24 well plates of 0.1 M PBS (pH 7.4) (500 μl per well). The cells were first washed for 10 minutes with 0.1 M PBS and then incubated with methanol (70 %)/ hydrogen peroxide (H_2O_2; 0.3 %) in deionised water (DI H_2O) for 30 minutes to quench the endogenous peroxidase activity. The cells were washed 3 x 10 minutes with 0.1 M PBS followed by incubation with blocking solution (20 %) containing GS in 0.1 M PBS for 1 hour at room temperature. Next the cells were washed rinsed with GS (1 %) in PBS-T to permeabilise the membrane, and incubated overnight in the desired primary antibody dilution (Table 2-2) in GS (1 %)/ PBS-T overnight at room temperature. On the next day, the antibody was removed and the coverslips washed with GS (1 %)/ 0.1 M PBS, and subsequently incubated with biotinylated secondary antibody (Table 2-3) in 0.1 M PBS for 1 hour at room temperature. On completion, the cells were washed with 0.1 M PBS and incubated for 1 hour at room temperature with avidin-biotin peroxidise complex (ABC-kit; Vector laboratories, Peterborough, UK). They were then washed with 0.1 M Tris-HCl 3 X 10 minutes. To visualise the staining, the cells were incubated with 3, 3'-diaminobenzidine tetrahydrochloride (DAB; 0.05 %)/ 0.1 M Trisl-HCl (500 μl) for 1 minute. The reaction was initiated on addition of H_2O_2 (30 %, 1 μl). The reaction was then terminated by rinsing the coverslips with 0.1 M Tris-HCl followed by a

final DI H_2O wash. The cell containing coverslips were hydrated in ethanol baths (100 %, 98 %, and 70 %) for 1 second each, followed by a DI H_2O rinse and counterstained with cresyl violet for 1 minute. The cells were then rinsed once with DI H_2O and dehydrated in ethanol (70 %, 98 %, and 100 %) for 5 seconds each and delipidated in Histoclear for 2 minutes. The coverslips were mounted onto superfrost slides with DePeX mounting medium and left overnight to dry. Cells were examined using a light microscope (Zeiss Axioskop, Carl Zeiss, Hertfordshire, UK) (Figure 2-6).

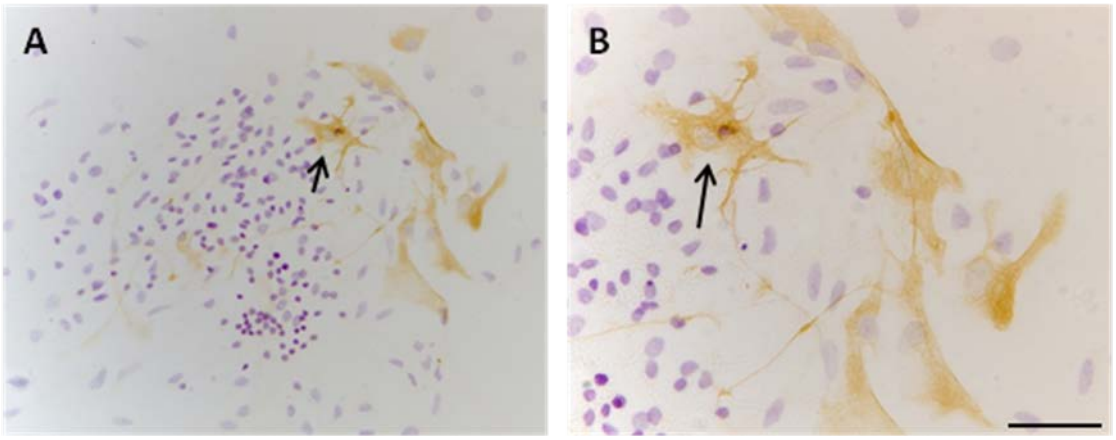

Figure 2-6 A typical GFAP staining in rat primary cultures.
Rat VM cell cultures were stained with antibodies against GFAP (brown) and counterstained with cresyl violet (violet). Scale bar = 100 μm (A) and 50 μm (B).

2.6.6.2 Immunohistochemical staining of free floating sections

Free floating mouse brain sections were first washed in 0.1 M PBS (500 μl) for 10 minutes and transferred into methanol (70 %)/H_2O_2 (0.3 %) in DI H_2O for 20 minutes. The sections were washed 3 x 10 minutes in PBS-T and then blocked with GS (20 %) in PBS-T for 1 hour at room temperature. Following this, the sections were incubated with the primary antibody (Table 2-2) at the desired dilution in GS (1 %)/ PBS-T overnight at room temperature. On day 2, the sections were rinsed with PBS-T and incubated with the appropriate biotinylated secondary antibody (Table 2-3) diluted in GS (1 %)/ PBS-T for 1 hour at room temperature. Following 3 x 10 minutes washes with PBS-T, sections were incubated in ABC solution for 1 hour at room temperature. The sections were once again washed in 0.1 M Tris-HCl, and then incubated in DAB (0.05 %)/ Tris-HCl for 1 minute for visualisation of the cells. H_2O_2 (30 %, 1 μl) was added to initiate the reaction. Termination of the reaction occurred when the cells were washed in Tris-HCl 3 X 10 minutes, and then mounted on polysine coated microscope slides and left to dry overnight. On day 3, the sections were hydrated through a series of ethanol dilutions (100 %, 98 %, and 70 %) and DI H_2O for 5 minutes each. They were counterstained in cresyl violet for 2 minutes

dehydrated in the order of DI H_2O, 70 %, 98 % and 100 % for 5 minutes each and delipidated in Histoclear for 15 minutes. The slides were then cover slipped using DePeX mounting medium (VWR International, Lutterworth, UK) and allowed to dry overnight. Sections were examined as described in Section 2.6.6.1 (Figure 2-7).

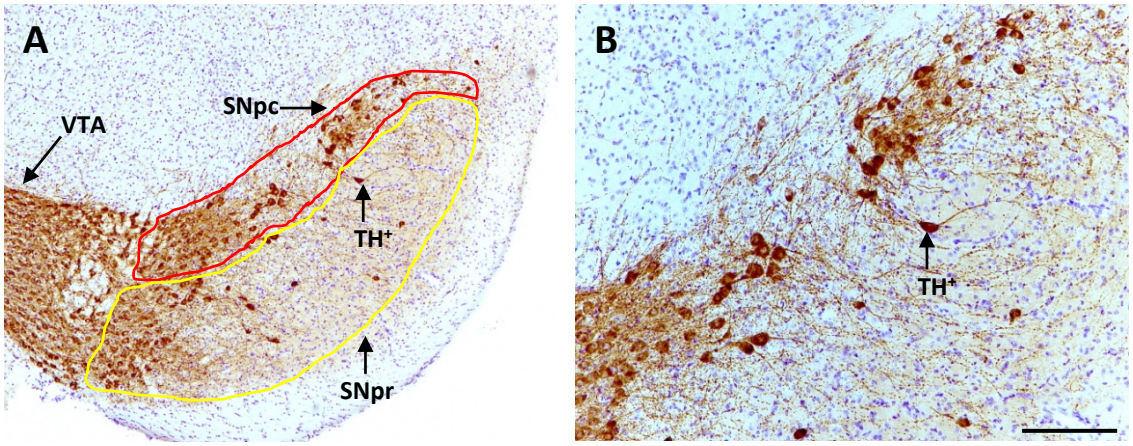

Figure 2-7 Typical TH immunoperoxidase staining in the mouse SN.
Mouse brain sections (30 μm) were stained with an antibody against TH (brown) and counterstained with cresyl violet (violet) at the level of the substantia nigra. Abbreviations: VTA, ventral tegmental area; SNpc, Substantia nigra pars compacta; SNpr, Substantia nigra pars reticulate; TH^+, Tyrosine hydroxylase positive. Scale bars = 200 μm (A) and 100 μm (B).

2.6.7 Quantification of positive staining in cell culture

Positively labelled mounted VM cells were counted on 3 coverslips per culture at X20 magnification under a light/ fluorescence microscope (Zeiss Axioskop, Carl Zeiss, Hertfordshire, UK), using the Axio vision software, powered by the Zeiss Axiocam camera. Immunoreactive cells were counted in 8 random areas on each coverslip using an eye piece reticule, where total area was equivalent to 8 mm^2. The total number of cells counted was calculated and expressed as 'the number of positively stained cells per 8 mm^{2}' or a 'percentage of immunoreactive cells' (n=3).

2.6.8 Quantification of positive staining in mouse tissue

Positively stained cells on mounted brains sections was counted bilaterally on 3 sections per animal at X10 magnification using an eye piece grid, where total area was equal to 1 mm^2. Slides were examined in a blind manner using the equipment and software detailed in Section 2.6.7. The number of positively labelled cells was expressed as the mean of the counts obtained from representative sections (n=3).

Table 2-2 List of primary antibodies.

Primary antibody	Dilution			Supplier
	IHC	IF	WB	
Polyclonal rabbit anti-rat tyrosine hydroxylase (TH)	1:500	1:200	-	Pel-Freeze Biologicals, USA
Monoclonal mouse anti-tyrosine hydroxylase (TH)	1:500	1:200	-	Sigma-Aldrich, Dorset, UK
Polyclonal rabbit anti-glial fibrillary acidic protein (GFAP)	1:500	1:200	-	Dako UK Ltd., Cambridgeshire, UK
Polyclonal rabbit anti-glutamic acid decarboxylase (GAD)	1:500	-	-	Sigma-Aldrich, Dorset, UK
Monoclonal rat anti-mouse CDIIb (OX-42)	1:100	1:200	-	AbD Serotec, Oxon, UK
Monoclonal mouse anti-rat CDIIb (OX-42)	1:100	1:200	-	AbD Serotec, Oxon, UK
Polyclonal rabbit anti-HDAC3	-	1:500	1:1000	Abcam Ltd., Cambridge, UK
Polyclonal rabbit anti-HDAC4	-	1:500	1:1000	Abcam Ltd., Cambridge, UK
Polyclonal rabbit anti-Histone deacetylase (HDAC5)	-	1:200	1:1000	New England Biolabs Ltd., Hertfordshire, UK
Polyclonal rabbit anti-HDAC11	-	1:500	1:1000	Abcam Ltd., Cambridge, UK
Polyclonal rabbit anti-acetyl-Histone H4	-	-	1:2000	Millipore UK Ltd., Watford, UK
Monoclonal mouse anti β-actin	-	-	1:5000	Insight Biotechnology Ltd., Middlesex, UK

IF – Immunoflourescence; IHC – Immunohistochemistry; WB – Western blot

Table 2-3 List of secondary antibodies.

Secondary antibody	Dilution			Supplier
	IF	IHC	WB	
Alexa Fluor® 488 donkey anti-mouse IgG (H+L)	1:500	-	-	Invitrogen life technologies, Paisley, UK
Alexa Fluor® 594 goat anti-rabbit IgG (H+L)	1:500	-	-	Invitrogen life technologies, Paisley, UK
Biotinylated goat anti-mouse IgG	-	1:250	-	Vector laboratories, Peterborough, UK
Biotinylated goat anti-rabbit IgG	-	1:250	-	Vector laboratories, Peterborough, UK
Polyclonal goat anti-rabbit HRP conjugate	-	-	1:1000	Dako UK Ltd., Cambridgeshire, UK
Polyclonal goat anti-mouse HRP conjugate.	-	-	1:1000	Dako UK Ltd., Cambridgeshire, UK

IF – Immunoflourescence; IHC – Immunohistochemistry; WB – Western blot

Table 2-4 List of reagents and compounds.

Name	Supplier
30% Acrylamide/bis solution, 37.5:1	Bio-Rad, Hertfordshire, UK
Boc-Lys(Ac)-7-Amino-4-Methylcoumarin	MP Biomedicals Europe, Cambridge, UK
CytoTox-ONE™ Homogenous membrane integrity assay	Promega, Southampton, UK
DePeX mounting medium	VWR international, Lutterworth, UK
Dulbecco's modified eagle medium (DMEM)	Invitrogen, Paisley, UK
Emla cream	BSU, KCL, UK
Enhanced Chemiluminescence (ECL) plus blotting detection system	Amersham Biosciences, Buckinghamshire, UK
Foetal bovine serum (FBS)	Invitrogen, Paisley, UK
HDAC developer	Cambridge Bioscience, Cambridge, UK
HDAC deacetylated standard	Cambridge Bioscience, Cambridge, UK
Histoclear	Fisher scientific, Leicestershire, UK
Isofluorane	BSU, KCL, UK
Lipopolysaccaride E. Coli O55:B5	Merck chemicals Ltd., Nottingham,UK
Marcain	BSU, KCL, UK
Methanol	BDH, VWR international, Lutterworth, UK
Penicillin-Streptomycin-Neomycin (PSN)	Invitrogen, Paisley, UK
Precision Plus protein standard	Bio-Rad, Hertfordshire, UK
Protease inhibitor cocktail set III	Merck chemicals Ltd., Nottingham, UK
PVDF membrane	Bio-Rad, Hertfordshire, UK
Sodium pentobarbitone (Euthatal®)	Merial, Dundee, UK
Standard Avidin biotin complex (ABC)	Vector laboratories, Peterborough, UK
Sterile distilled water	PAA laboratories Ltd., Yeovil, UK
Suberoylanilide Hydroxamic Acid (SAHA)	Cambridge Bioscience, Cambridge, UK
Tris-(hydroxymethyl) methylamonium chloride (Tis-HCl)	BDH, VWR international, Lutterworth, UK
Trypsin (1x)	Invitrogen, Paisley, UK
Vectashield® Hard set mounting medium (with DAPI)	Vector laboratories, Peterborough, UK
Vectashield® Hard set mounting medium for fluorescence	Vector laboratories, Peterborough, UK

Chemicals and reagents which are not listed were obtained from Sigma-Aldrich, Dorset, UK

Table 2-5 List of equipments and consumables.

Name	Supplier
16 mm coated Vicryl	Ethicon, Berkshire, UK
26s Hamilton needle	Essex scientific laboratory supplies Ltd., Essex, UK
70IRN Hamilton syringe	Essex scientific laboratory supplies Ltd., Essex. UK
Acetate sheets	KCL stores, UK
Autoclave	Meadowrose scientific Ltd., Oxfordshire, UK
Bisafety cabinet II	Walker safety cabinets Ltd., Derbyshire, UK
Centrifuge	Meadowrose scientific Ltd., Oxfordshire, UK
Cryospray	Bright instrument company Ltd., Cambridgeshire, UK
CO_2 incubator	SANYO E&E Europe BV, Leicestershire, UK
Compact X4, Xograph	Imaging system, Gloucestershire, UK
Cover slips (22 x 50 mm)	VWR international Ltd., Lutterworth, UK
Cover slips round (13 mm)	VWR international Ltd., Lutterworth, UK
Dissecting Microscope	Vickers Instruments, Croydon, UK
Kodak hyperfilm	GE Healthcare Ltd., Buckinghamshire, UK
Light/ Fluorescence Microscope	Carl Zeiss Ltd, Hertfordshire, UK
Multidish 24 well plates	VWR international Ltd., Lutterworth, UK
Microplate Corning 96 well plate	Fisher scientific, Leicestershire, UK
The Nanodrop® ND-10000 Spectrophotometer	Labtech international Ltd., East Sussex, UK
Microplate reader, GeminiXS	Molecular devices, Cambridgeshire, UK
Microplate reader, Vmax	Molecular devices, Cambridgeshire, UK
Microscope slide, polysine coated	VWR international Ltd., Lutterworth, UK
Microtome SM 2000R	Leica Microsystems, Milton Keynes, UK

Chapter 3 The effect of HDAC inhibitors on toxin-induced cell death on neuroblastoma cell lines.

3.1 Introduction

Aberrant recruitment of HDACs to repress transcription and silence gene expression of possible disease-modifying genes has been associated with a wide number of neurodegenerative disorders such as Huntington's (HD), Parkinson's (PD) and Alzheimer's (AD) disease, spinal muscular atrophy (SMA) and amyotrophic lateral sclerosis (ALS).

The most prominent evidence for the protective effects of HDAC inhibitors comes from *in vivo* models of HD, where photoreceptor neurodegeneration was retarded in a *Drosophila* model of polyglutamine-repeat disease (Steffan *et al.*, 2001). The pan HDAC-I, suberoylanilide Hydroxamic acid (SAHA), also slowed neurodegeneration and improved motor impairments in R6/2 genetic mouse models (Hockly *et al.*, 2003). These are mice generated to express exon 1 of human HD carrying $(CAG)_{115}$–$(CAG)_{150}$ repeat expansions. They develop the progressive neurological symptoms exhibited in HD such as deficits of motor skills, altered locomotor activity, seizures and impaired cognitive performance (Mangiarini *et al.*, 1996; Davies *et al.*, 1997). SAHA did not inhibit the polyglutamine aggregation associated with HD pathogenesis, but increased histone acetylation, indicating that it probably acts by redressing transcriptional repression.

In PD, accumulation of mutated neuronal protein α-synuclein has been implicated in disease progression. Kontopoulos *et al.,* (2006) showed that α-synuclein bound to histones in the nucleus to inhibit acetylation of histone H3 and contribute to neurotoxicity (Kontopoulos *et al.*, 2006). This cellular toxicity was ameliorated by HDAC inhibitors in SH-SY5Y cultured cells transfected with A30P and A53T α-synuclein and α-synuclein transgenic *Drosophila*, similarly to that observed in HD. Evidence from a small molecule inhibitor of sirtuin 2, a Class III histone deacetylase, was also found to protect dopaminergic cells transfected with A53T α-synuclein and transgenic *Drosophila* (*elav-GAL4/+*) from toxicity *(Outeiro et al., 2007)*. However, very little is known about the ability of HDAC-Is to protect dopaminergic cells from oxidative stress implicated in the pathogenesis of idiopathic PD (detailed in Chapter 1). One of the possible major causes of degeneration in PD progression as previously described is oxidative stress, which is linked to other components of the degenerative process including mitochondrial dysfunction, excitotoxicty, nitric oxide toxicity and inflammation (Jenner, 2003b).

Despite the limitations, there are indications that HDAC-Is may have the potential to arrest oxidative stress exerted during disease progression. Such as, evidence from Ryu and colleagues (2003), which showed that transcription factor Specific protein-1 (Sp1) is acetylated in response to oxidative stress in neurones, but is suppressed by HDACs. HDAC-Is augment Sp1 acetylation, Sp1 DNA binding and Sp1 gene expression, which confers resistance to oxidative stress-induced

death *in vitro* and *in vivo* (Ryu et al., 2003). Langley *et al.,* (2008) also showed that pulse exposure of cortical neurones to HDAC-Is resulted in resistance to oxidative stress toxicity associated with transcriptional up-regulation of the cell cycle inhibitor $p21^{waf1/cip1}$ (Langley *et al.*, 2008).

3.1.1 Hypothesis

It was hypothesised that the HDAC inhibitors would protect dopaminergic cells against H_2O_2- and MPP^+-induced cell death.

3.1.2 Aims

To test the hypotheses, the susceptibility of dopaminergic cell lines which expressed HDAC to the toxins H_2O_2 and MPP^+ was assessed. The effect of HDAC inhibitors on toxin-induced cell death was measured. Specifically, the main aims were to:

1. Determine the dopaminergic phenotype of mouse adrenergic N1E-115 and human catecholaminergic SH-SY5Y cell lines and their expression of HDAC3, 4, 5 and 11.
2. Investigate the effect of neurotoxins, H_2O_2 and MPP^+, which induce oxidative stress in N1E-115 and SH-SY5Y cell lines.
3. Determine the neuroprotective effect of HDAC inhibitors, SAHA and valproic acid (VPA), on H_2O_2- and MPP^+-induced cell death in N1E-115 and SH-SY5Y cell lines.

3.2 Material and Methods

3.2.1 Cell culture

Human neuroblastoma SH-SY5Y and mouse neuroblastoma N1E-115 cells were purchased from American Type Culture Collection (Manassas, USA) and maintained in high glucose Dulbecco's Modified Eagle's medium (DMEM) supplemented with heat-inactivated Foetal Bovine Serum (FBS) (10 %) and penicillin (5 mg/ml), streptomycin (5 mg/ml) and neomycin (10 mg/ml) in 0.85 % saline (PSN 1 %). The medium was changed every 2-3 days. The cells were grown in T75 cm^2 flasks at 37^oC incubator (MCO-18AIC, Sanyo), with atmosphere of CO_2 (5 %) and relative humidity (95 %).

3.2.2 Trypsinisation of cells

Confluent cultured cells were passaged by discarding the culture media and washing twice with sterile phosphate buffered saline (PBS; 0.1 M). Trypsin-EDTA (0.25 %) was added to the flasks and incubated at 37^oC for 2 minutes. Flasks were tapped gently to detach the cells, followed by the addition of culture medium (prepared in Section 3.2.1) to inhibit the trypsin activity. The detached cells were collected and centrifuged (Jouan centrifuge cr3i, Meadowrose Scientific Ltd) at 1000 g for 5 minutes. The pellet was re-suspended in culture medium (5 ml) and the suspension was re-plated at half the original density into 75 cm^2 culture flasks or utilised for subsequent experiments.

3.2.3 Cell counting

The cell density was determined using a haemocytometer (improved Neubauer). Cell suspension (50 μl) was first diluted (1:1 v/v) with trypan blue solution (0.4 %). The haemocytometer was covered with a cover slip, and cell/ trypan blue solution (50 μl) gently filled by resting the pipette tip on the edge of the chambers allowing it to be filled by capillary action. Non-viable cells were stained blue, while viable cells remained unstained. Viable cells were counted in four sets of 16 corner squares (highlighted in red in Figure 3-1) using an inverted microscope (Nikon TMS) with a magnification of x 0.25. Each set of 16 corner squares represents the number of cells x 10^4 per ml. The following equation was therefore employed to calculate the cell density per ml:

Average count of cells per 16 corner square x dilution factor x 10^4

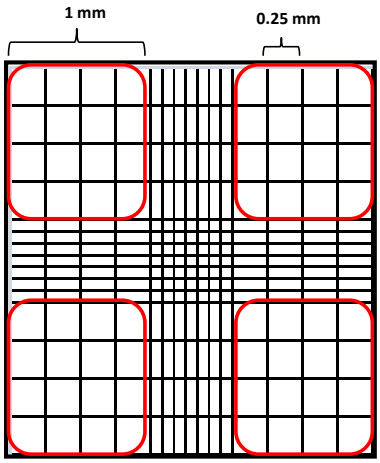

Figure 3-1 Diagram of haemocytometer gridlines.
Image shows the 16 corner square that are counted, highlighted in red. Adapted and modified from www.deltaenvironmental.com.au.

3.2.4 Characterisation of dopaminergic and HDAC phenotype

3.2.4.1 Immunofluorescence

Immunofluorescence was used to detect the presence of tyrosine hydroxylase (TH), and HDAC3, 4, 5 and 11 in SH-SY5Y and N1E-15 cell lines, as described in Section 2.6. In summary, the cell lines were seeded at a density of 1 x 10^5 in 24 well plates on 0.05 % poly-D-lysine coated cover slips. Once grown, they were fixed with paraformaldehyde (PFA) (4 %), blocked with goat serum (20 %) and incubated at 4^{o}C overnight with primary antibodies raised in rabbit against TH (1:200), HDAC3 (1:500), HDAC4 (1:500), HDAC5 (1:200) and HDAC11 (1:500) (Table 2-2). On the subsequent day, the cells were incubated with Alexa Fluor 594 IgG secondary antibody (1:500) (Table 2-3) for 2 hours at room temperature. The cells were processed as in Section 2.6.3 and visualised using an immunofluorescence microscope (Zeiss Axioskop, Carl Zeiss).

3.2.4.2 Western blot analysis

Western blot technique was used to detect the expression of HDAC3, 4, 5 and 11 proteins in SH-SY5Y and N1E-115 cells. The technique is described in detail in Section 2.4. Cell lysates, prepared as described in Section 2.4.1, were resolved onto a SDS-PAGE gel (8-10 %) and transferred onto a PVDF membrane. The membrane was blocked with milk (5 %) in TBS-T for 1 hour, and incubated with primary antibodies against HDAC3, 4, 5, 11 (1:1000) and β-actin (1:5000) (Table 2-2), as loading control overnight at 4^{o}C. After incubation with anti-rabbit or anti-mouse IgG-horseradish peroxidise (HRP)-conjugated secondary antibody (1:2000) (Table 2-3) for 1 hour, bands were visualised by the enhanced chemiluminescence system detailed in Section 2.4.4.

3.2.5 Neuroprotection study

3.2.5.1 Induction of toxin-induced cell death

SH-SY5Y and N1E-115 cell lines were plated at 2 x 10^4 and 1 x 10^4, respectively into 96 well plates, and grown in growth medium for 24 hours at 37°C in an incubator as described in Section 3.2.1. On day 2, the cells were incubated with heat-inactivated foetal bovine serum free media (Serum-free media) for 2 hours, prior to 24 hours incubation with serum-free media containing hydrogen peroxide (H_2O_2) (10^{-6} to 10^{-3} M) or 1-methyl-4-phenylpyridinium (MPP^+) ($10^{-1.5}$ to $10^{-3.5}$ M). Cells treated with serum-free media served as controls. Lactate dehydrogenase (LDH) release, a marker for damaged cells, was determined by a commercially available LDH assay (Section 3.2.6.1), and viability of cells was determined trypan blue assay as described in Section 3.2.6.2. EC_{50} values for the effect of H_2O_2 and MPP^+ on LDH release and trypan blue were determined by using non-linear regression as described in Section 3.2.7. The rationale for using these EC_{50} concentrations was to generate 50 % cell death in the cultures, a difference which is substantial enough to allow any changes measured in the cultures to be attributed to the effects of the HDAC-Is following their treatment in the Neuroprotection experiments.

3.2.5.2 Effect of HDAC inhibitors on toxin-induced cell death

To assess the effect of HDAC inhibitors on toxic insult, cells were grown in 96 well plates for 24 hours. VPA (10^{-9} to 10^{-3} M) and SAHA (10^{-9} to 10^{-3} M) were diluted in serum-free media and applied to the cells for a 2 hour incubation period. On completion, the media was removed and the cells were incubated for further 24 hours with a mixture of HDAC inhibitors and EC_{50} concentrations of H_2O_2 and MPP^+ in serum-free media, similar to Section 3.2.5.1. Control cells were incubated with HDAC inhibitors or toxin alone in serum-free media for 24 hours. Untreated control cells were treated with serum-free medium only. LDH release and cell viability was assessed as described in Section 3.2.6. Figure 3-2 summarises the experimental timeline.

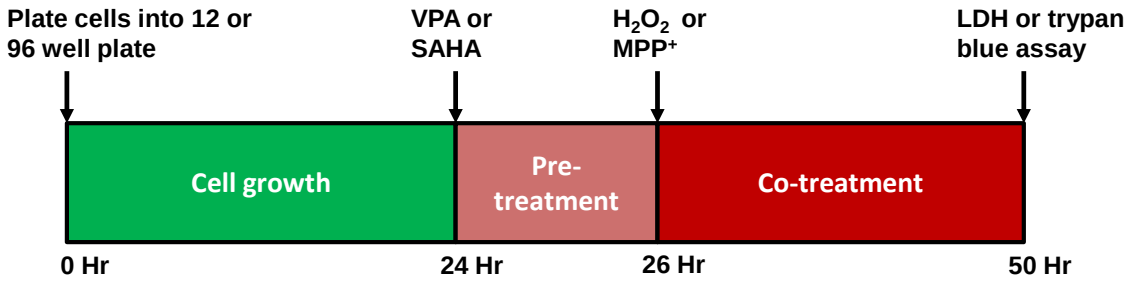

Figure 3-2 Experimental outline.
SH-SY5Y and N1E-115 cell lines were plated at 0 hour and grown 24 hours in serum-containing medium. At 24 hours, the medium was aspirated and changed to serum-free medium (SFM), VPA (0.3, 0.6, 1.2 mM) or SAHA (0.01, 0.1, 1 μM) for 2 hours followed by the same concentrations with or without EC_{50} concentrations of H_2O_2 or MPP^+. Twenty-four hours later cell viability assays were performed.

3.2.6 Determination of cell death

The effect of the toxins and HDAC inhibitors were assessed either through the release of lactate dehydrogenase (LDH) of damaged cells or by counting viable cells which were not stained by the trypan blue dye.

3.2.6.1 Lactate dehydrogenase (LDH) assay

Lactate dehydrogenase (LDH) is released from cells with damaged membranes. It is measured by supplying lactate, NAD^+ and resazurin as substrates in the presence of diaphorase. Diaphorase catalyses the conversion of resazurin to resorufin and produces a red fluorescent compound. The CytoTox-ONE^{TM} homogeneous membrane integrity assay was performed according to the manufacturer's instructions (Promega, Southampton, UK). Briefly, the Cyto-Tox-ONE reagent (100 μl) was added to the cell culture media of each treated well, and incubated for 10 minutes at 22^{o}C. Stop solution (50 μl) was added to each well to end the reaction. A fluorescent signal was measured using a spectrophotometer (SpectraMax Gemini XS, Molecular Devices) with an excitation wavelength of 560 nm and an emission wavelength of 590 nm. Experiments were performed in triplicate on three separate occasions. A lysis solution (9 % w/v, Triton®-X-100 in water) supplied in the kit generated maximum LDH release, served as a positive control, and culture media only wells were used as background readings. The data was displayed as average percent cytotoxicity employing the following equation:

$$\text{Percent cytotoxicity} = 100 \times \frac{\text{(Experimental – Culture Medium Background)}}{\text{(Maximum LDH Release – Culture Medium Background)}}$$

3.2.6.2 Trypan blue exclusion assay

The trypan blue exclusion test estimates the proportion of viable cells in a cell suspension. It works on the notion that viable cells have intact membranes, so prevents penetration of the dye, however dead cells have damaged membranes, so allows the nuclei to be stained. In this assay, cells were collected from 12 well plates using a cell scraper and resuspended in 500 μl PBS. Cell suspension in PBS (100 μl) was combined with 0.4 % trypan blue (100 μl). Cells were counted using a haemocytometer. The number of blue stained cells (Figure 3-3) was subtracted from the total cell number which was then divided by the total number of cells counted to estimate percent viability as follows:

$$\text{Percent viability} = 100 \times \frac{\text{Viable cell}}{\text{Total cells (viable and non-viable cells)}}$$

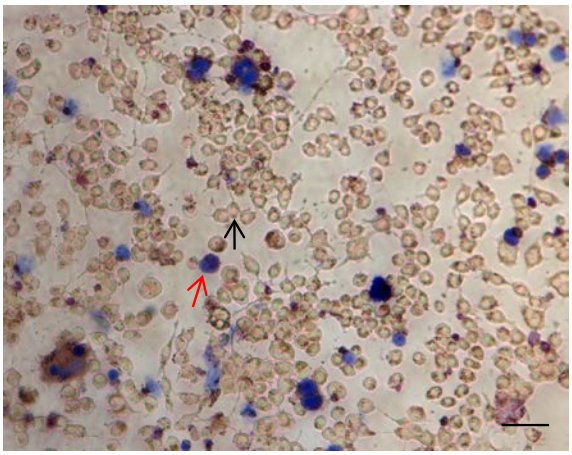

Figure 3-3 An example of trypan blue exclusion in N1E-115 cells.
Cells grown in a 12 well plate were incubated with 0.4 % trypan blue solution. Viable cells remained unstained (black arrow) and nonviable cells were stained blue (red arrow) with trypan blue. Scale bar = 200μm.

3.2.7 Statistical Analysis

All experiments were performed in duplicate (trypan blue exclusion assay) or in triplicate (LDH assay) on three separate occasions (n=3). To analyse toxin-induced effects, data from each experiment were plotted as logarithmic values and a sigmoidal concentration-response curve was established using non-linear regression (Graph Pad Prism 5 software, USA). The software also determined the half maximal effective concentration (EC_{50}). For HDAC inhibitor effect, data were analysed using one-way or two-way ANOVA followed by Newman Keuls post-hoc multiple test where appropriate (GraphPad Prism®). Data are expressed as mean ± SEM.

3.3 Results

3.3.1 Characterisation of dopaminergic phenotype in cell lines

N1E-115 and SH-SY5Y cell lines were characterised for tyrosine hydroxylase (TH) by immunoflourescence. Both cell lines showed positive TH immunostaining which is mainly present in the cytoplasm (Figure 3-4).

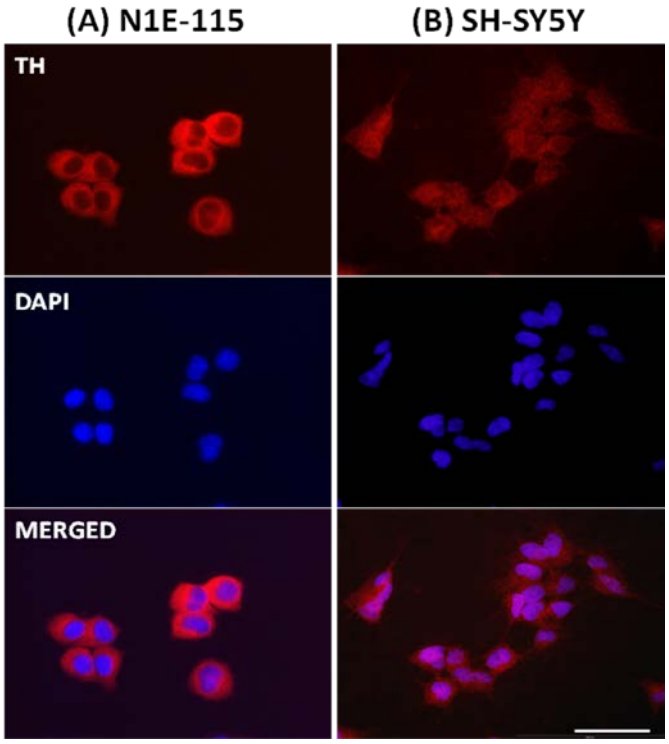

Figure 3-4 Expression of dopaminergic marker in N1E-115 and SH-SY5Y cell lines.
Cell lines (A) N1E-115 and (B) SH-SY5Y were stained with antibodies against tyrosine hydroxylase (TH) (red). The nuclei were counterstained with DAPI (blue). Photomicrographs are typical of duplicate analyses. Scale bar = 100 μm.

3.3.2 Determination of HDAC expression in cell lines

N1E-115 and SH-SY5Y cells were characterised for the presence and localisation of the HDAC isoforms, 3, 4, 5 and 11. For all isoforms stronger immunoreactive fluorescence signals was visualised for the enzymes in N1E-115 than in SH-SY5Y (Figure 3-5).

HDAC3 was mainly localised in the nucleus and HDAC4 and 5 was localised mainly in the cytoplasm of N1E-115 cells. Diffused HDAC11 staining was visualised in both the cytoplasm and nucleus of N1E-115 cells (Figure 3-5A).

Similarly, HDAC3 was localised in the nucleus of SH-SY5Y cells. HDAC4, HDAC5 and HDAC11 were found in nucleus and cytoplasm of SH-SY5Y cells (Figure 3-5B).

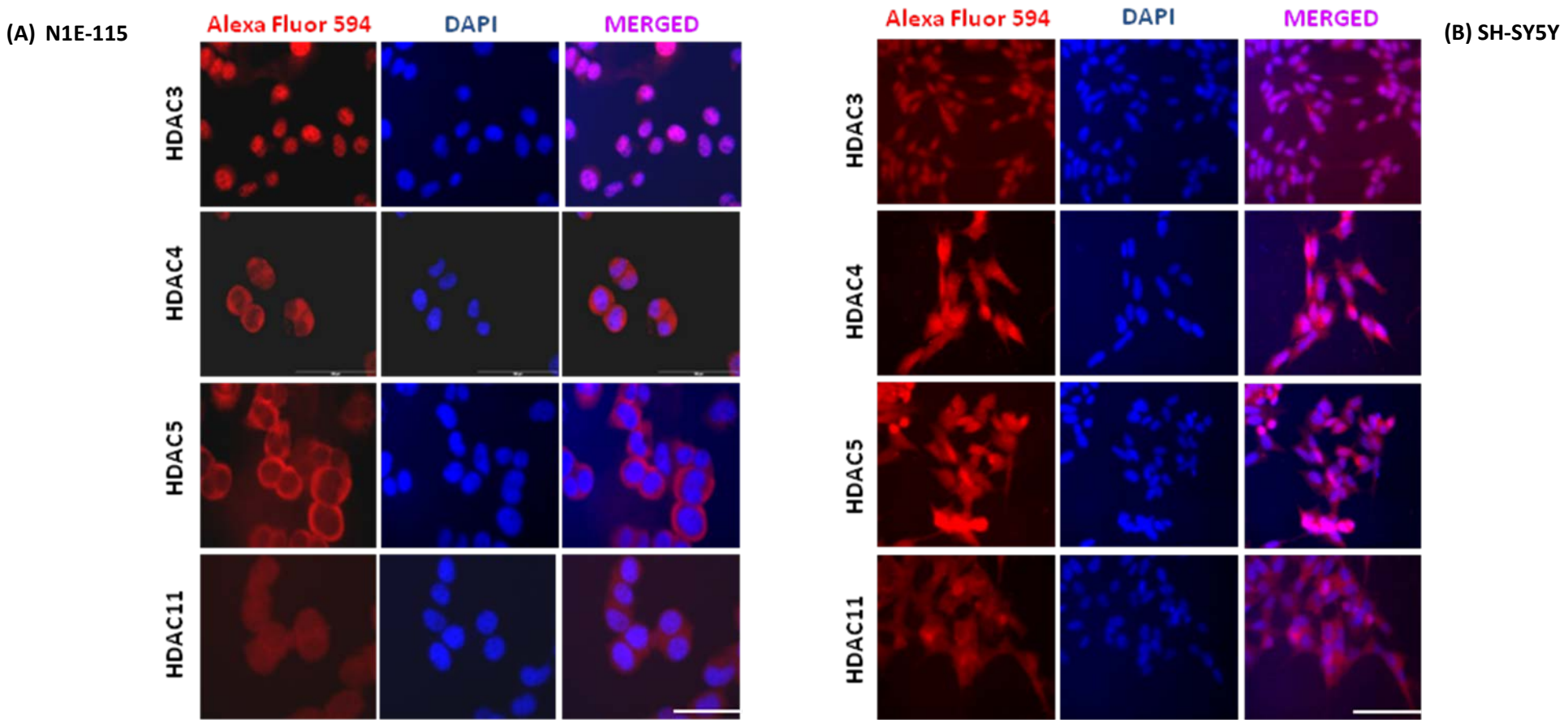

Figure 3-5 Expression of HDAC phenotype in cell lines.
(A) N1E-115 and (B) SH-SY5Y cell lines were stained with antibodies against HDAC3, 4, 5 and 11 (red). Dapi (blue) was used to counterstain the nucleus. Photomicrographs are typical of duplicate analyses. Scale bar = 100 μm.

Western blotting was also used to confirm the protein expression of the HDAC isoforms 3, 4, 5 and 11 in N1E-115 and SH-SY5Y cell lines. In both cell lines, HDAC3 was detected as a band at 50 kDa, HDAC4 at 140 kDa, HDAC5 at 124 kDa and HDAC11 at 39 kDa (Figure 3-6).

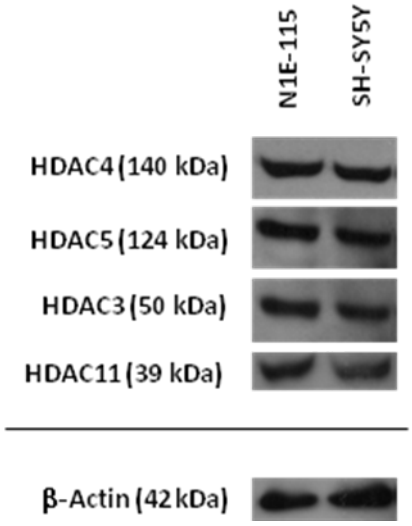

Figure 3-6 Protein expression of HDAC isoforms by western blotting.
N1E-115 and SH-SY5Y cell lines were screened for the expression of HDAC3, 4, 5 and 11. β-Actin was used as a loading control. Images are typical of duplicate analyses.

3.3.3 Effect of H_2O_2 and MPP^+ on cell survival

To assess the effect of HDAC inhibitors on toxin-induced cell death, N1E-115 and SH-SY5Y cell lines were treated with H_2O_2 (10^{-6} – 10^{-3} M) and MPP^+ ($10^{-3.5}$ – $10^{-1.5}$ M) for 24 hours and cell death was measured by the LDH assay. Both toxins produced a concentration-related cell death in N1E-115 and SH-SY5Y cell lines. The EC_{50} values for H_2O_2-induced cytotoxicity was calculated for N1E-115 (60.0 ± 0.4 μM) and SH-SY5Y (350.0 ± 0.5 μM) (Figure 3-7A-B). Following MPP^+-induced cytotoxicity, EC_{50} values were calculated for N1E-115 (3.0 ± 0.2 mM) and SH-SY5Y (3.0 ± 0.4 mM) cell lines (Figure 3-7C-D).

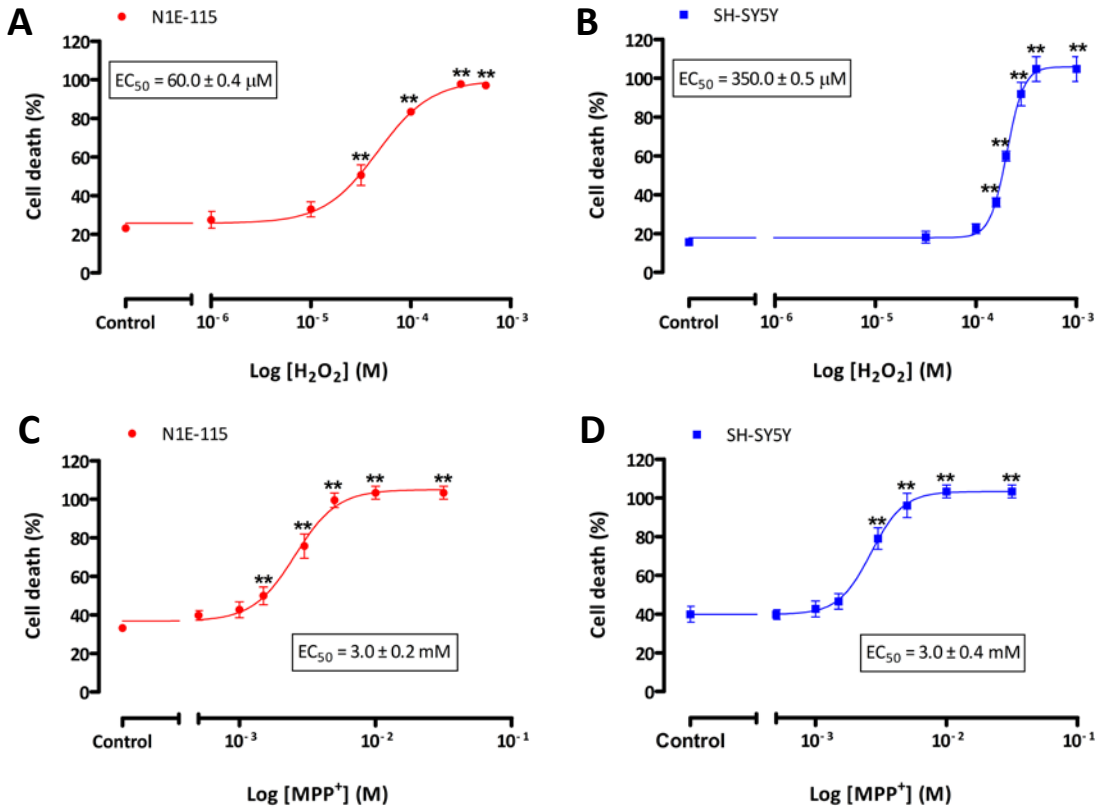

Figure 3-7 Cell death in N1E-115 and SH-SY5Y cells following H_2O_2 and MPP^+ treatment. N1E-115 and SH-SY5Y cells were subjected to (A-B) H_2O_2 (10^{-6}-10^{-3}M) and (C-D) MPP^+ ($10^{-3.5}$-$10^{-1.5}$ M) for 24 hours. Cell loss was assessed by the LDH assay, where maximum LDH released was recorded at 100%. Non-linear regression curve was fitted to calculate EC_{50}. Data are expressed as mean ± SEM (n=3); **p<0.01 compared to control cells (one-way ANOVA followed by Newman-Keuls test).

Similarly to LDH assay, N1E-115 and SH-SY5Y cell lines were incubated with H_2O_2 and MPP^+ (10^{-9} – 10^{-1} M) for 24 hours and cell viability was assessed by trypan blue dye exclusion assay. Viable cells were counted and the EC_{50} values for H_2O_2-induced cell death were calculated for N1E-115 (96.0 ± 4.0 µM) and SH-SY5Y (935.0 ± 6.0 µM) (Figure 3-8A-B). Subsequently, the EC_{50} values for MPP^+-induced cell death was also determined for N1E-115 (62.0 ± 5.0 µM) and SH-SY5Y (82.0 ± 5.0 µM) cell lines (Figure 3-8C-D).

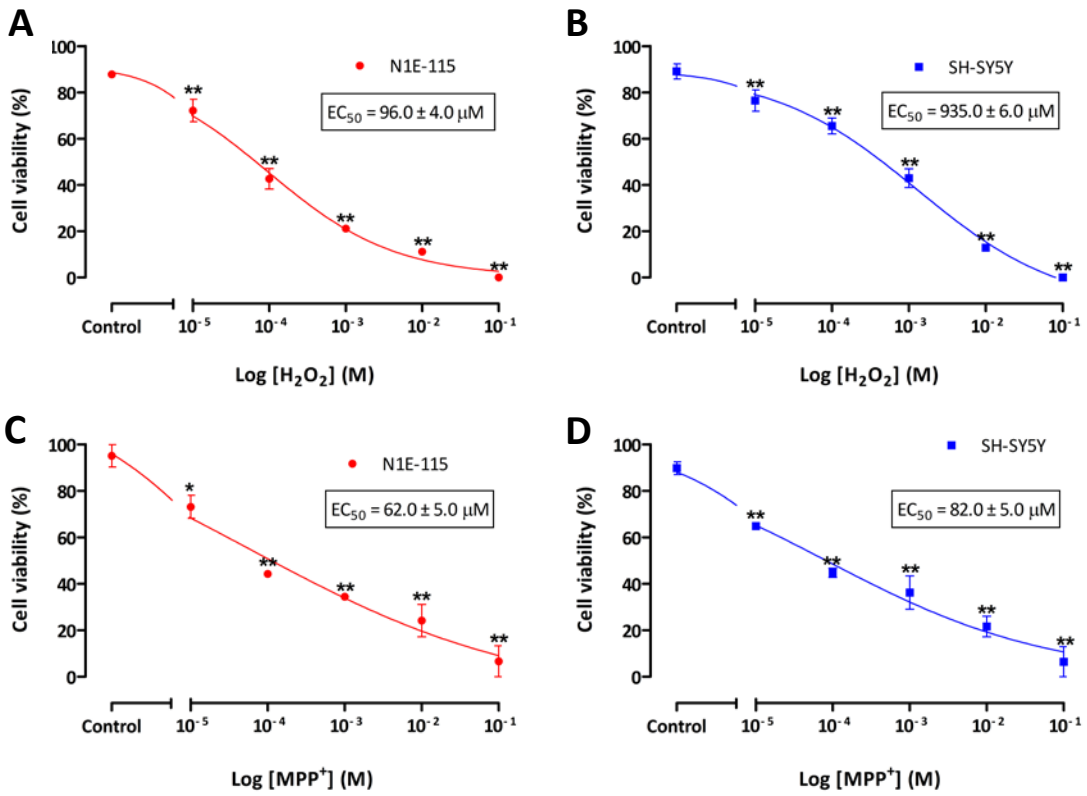

Figure 3-8 Viable N1E-115 and SH-SY5Y cells following H_2O_2 treatment and MPP^+ treatment. N1E-115 and SH-SY5Y cells were exposed to (A-B) H_2O_2 (10^{-9}-10^{-1} M) and (C-D) MPP^+ (10^{-9}-10^{-1} M) for 24 hours. Cell viability was assessed by the trypan blue exclusion assay. Non-linear regression curve was fitted to calculate EC_{50}. Data are expressed as mean ± SEM (n=3); **p<0.01, *p<0.05 compared to control cells (one-way ANOVA followed by Newman-Keuls test).

3.3.4 Involvement of HDAC inhibitors in toxin-induced LDH release

3.3.4.1 Effect of HDAC inhibitors on cell survival following H_2O_2 treatment.

N1E-115 and SH-SY5Y cell lines were treated with EC_{50} concentrations of H_2O_2 (60 µM and 350 µM for LDH assay; 96 µM and 935 µM for trypan blue assay, respectively) in the presence and absence of a range of SAHA and VPA (10^{-9} – 10^{-3} M) concentrations. Control cells were treated with serum-free medium only or toxin in serum-free medium.

<u>SAHA Treatments</u>

In N1E-115, there was 73 % cell survival in the control culture (Figure 3-9A) treated with serum-free medium only. SAHA alone only affected the degree of cell loss at 10^{-4} M and 10^{-3} M, where cell survival decreased to 45 % and 30 %, respectively. Although this was only significantly different to control at 10^{-3} M. H_2O_2 (60 µM) alone induced 36 % cell survival which was significant to the serum-free only culture. SAHA (10^{-9} - 10^{-3} M) added 2 hours before and during H_2O_2 incubation had no effect on H_2O_2–induced cell death, except at the highest concentration, 10^{-3} M, where the cell survival tended to be increased to 53 % although this was not significantly different to H_2O_2 alone.

In SH-SY5Y cells, 83 % cell survival was observed in untreated cultures. Treatment with SAHA did not alter the degree of cell viability, except at the high concentrations, 10^{-4} and 10^{-3} M, where cell survival significantly decreased to 73 % and 58 % respectively (Figure 3-9B). H_2O_2 (350 μM) alone induced 40 % cell survival. SAHA (10^{-9} - 10^{-3} M) incubation had effects on H_2O_2-induced cell death, at 10^{-8}, 10^{-7} and 10^{-3} M where cell continued existence decreased to 26 %, 30 % and 71 %, respectively.

In untreated N1E-115 cultures, 78 % viable cells were counted. SAHA alone treatments decreased the number of surviving cells to a range of 59 % and 39 %, which were statistically significant to the control (Figure 3-9C). H_2O_2 (96 μM) generated 45 % surviving cells. SAHA administration for 2 hours prior to H_2O_2 had no effect on cell survival, except at the highest concentration (10^{-3} M) where 29 % of viable cells was recorded.

In SH-SY5Y untreated cultures, 85 % cells survived serum-free treatments (Figure 3-9D). SAHA alone caused a statistically significant decline in the number of viable cells to approximately 60 % across all the concentrations. H_2O_2 (935 μM) alone produced 46 % viable cells, and SAHA administration had no effect on the viable cells counted.

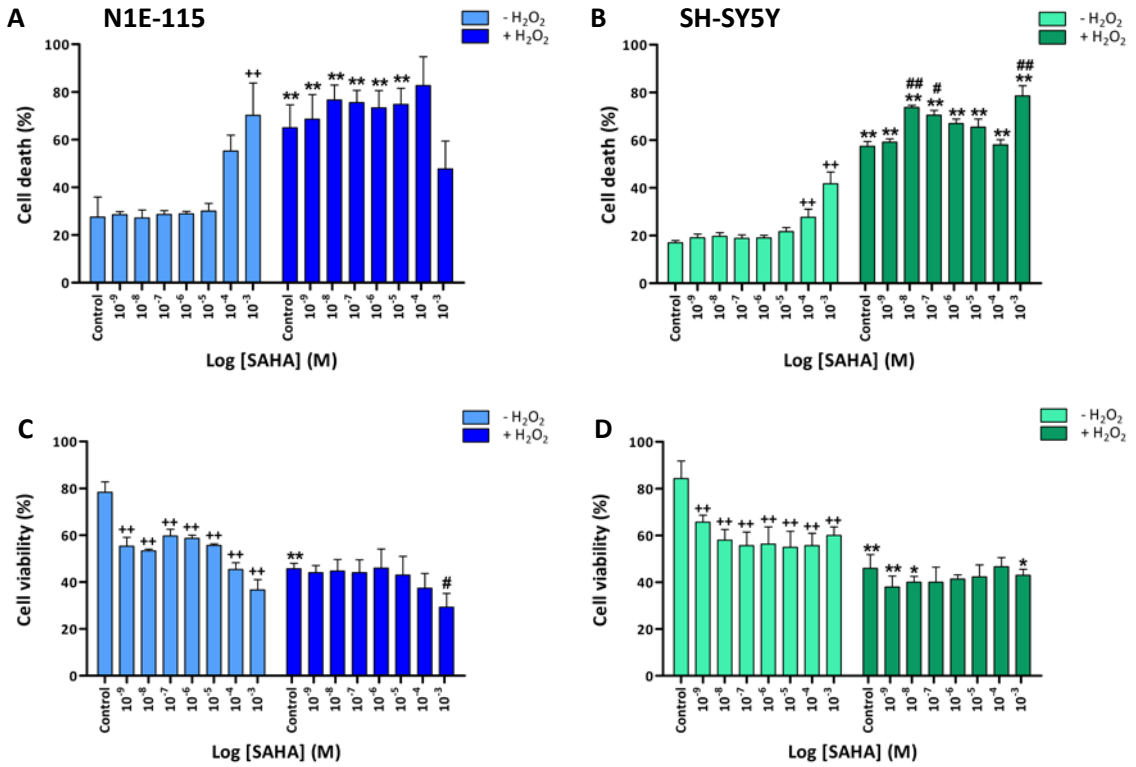

Figure 3-9 Effect of H_2O_2 on cell survival following SAHA pre-treatment.
N1E-115 (A & C) and SH-SY5Y (B & D) cell survival was assessed by LDH assay (A & B) and trypan blue exclusion assay (C & D). The cells were exposed to SAHA (10^{-9} - 10^{-3} M) pre-treatment for 2 hours, followed by 24 hours co-treatment with H_2O_2 (60 μM and 350 μM for the LDH assay; 96 μM and 935 μM for the trypan blue assay, respectively). Cell death was measured by the LDH assay, where maximum LDH release was recorded at 100 %. Viable cells for the trypan blue assay were counted and percentages were calculated from total cell counts of dead and surviving cells. Data are expressed as mean ± SEM (n=3); **p<0.01, *p<0.05 comparison between H_2O_2-free treatments; ++p<0.01 compared to serum-free control; ##p<0.01, #p<0.05 compared to H_2O_2 only treated control cells (two-way ANOVA followed by Newman-Keuls test).

VPA Treatments

Approximately 74 % viable cells were observed in untreated N1E-115 cultures. VPA alone treatments had no effect on the cell viability (Figure 3-10A). As expected, H_2O_2 (60 μM) alone treatment induced 57 % cell survival. VPA administration for 2 hours prior to H_2O_2 significantly increased H_2O_2-induced cell loss to approximately 68 % at all concentrations, although this was not dose dependent.

In SH-SY5Y cells, 81 % viable cells were observed in untreated cultures (Figure 3-10B). As for N1E-115 cultures, VPA treatments did not alter the cell viability at any of the concentrations tested, and H_2O_2 (350 μM) alone induced approximately 43 % cell viability. VPA (10^{-9} – 10^{-3} M) administration prior to H_2O_2 had no significant effect on H_2O_2-induced cell death, although there tended to be an increase in the cytotoxicity at all doses.

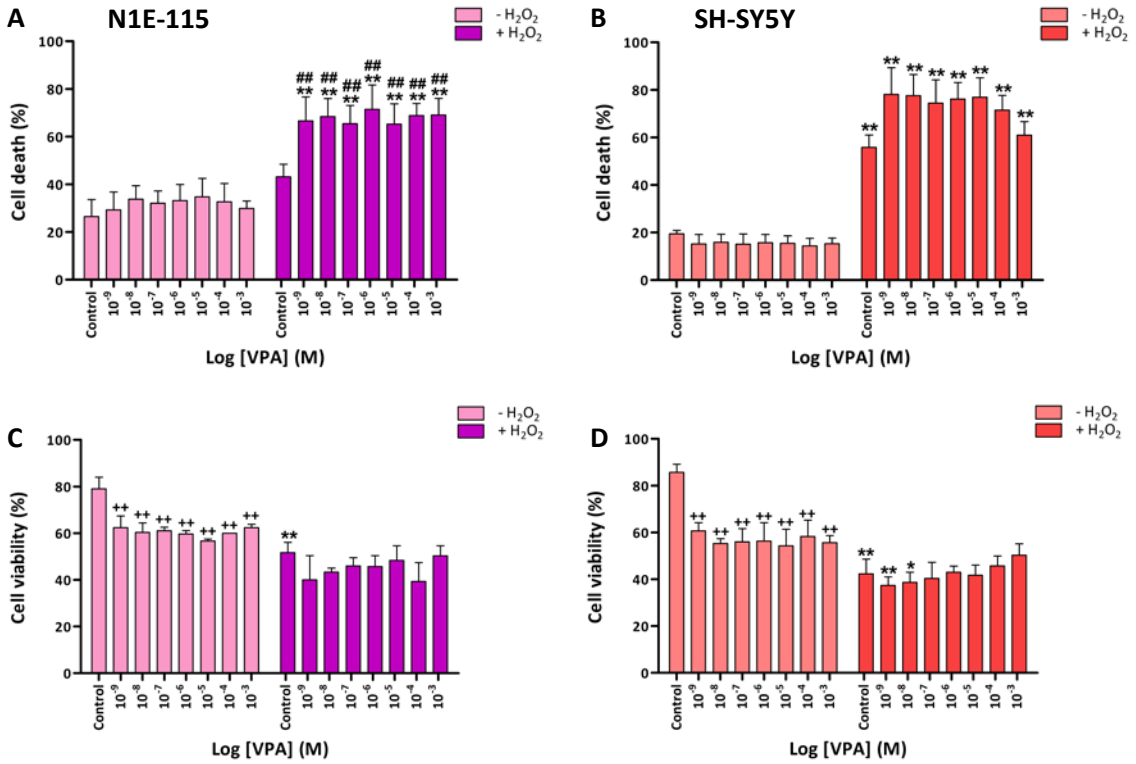

Figure 3-10 Effect of H_2O_2 on cell survival following VPA pre-treatment.
N1E-115 (A & C) and SH-SY5Y (B & D) cell survival was assessed by LDH assay (A & B) and trypan blue exclusion assay (C & D). The cells were exposed to VPA (10^{-9} - 10^{-3} M) pre-treatment for 2 hours, followed by 24 hours co-treatment with H_2O_2 (60 μM and 350 μM for the LDH assay; 96 μM and 935 μM for the trypan blue assay, respectively). Cell death was measured by the LDH assay, where maximum LDH release was recorded at 100 %. Viable cells for the trypan blue assay were counted and percentages were calculated from total cell counts of dead and surviving cells. Data are expressed as mean ± SEM (n=3); **p<0.01, *p<0.05 comparison between H_2O_2-free treatments; ++p<0.01 compared to serum-free control; ##p<0.01 compared to H_2O_2 only treated control cells (two-way ANOVA followed by Newman-Keuls test).

In N1E-115 untreated cultures 79 % of viable cells was counted (Figure 3-10C). VPA alone significantly declined the number of viable cells by approximately 18 % across all the concentrations. H_2O_2 alone treatment had 51 % surviving cells. VPA administration had no significant effect on cell survival.

In untreated SH-SY5Y cultures, 86 % of viable cells were represented. VPA administration statistically decreased the percentage of viable cells to approximately 59 % across the treatments (Figure 3-10D). H_2O_2 alone induced 42 % of viable cells. VPA administration for 2 hours prior to H_2O_2 administration had no significant effect on cell viability.

3.3.4.2 Effect of HDAC inhibitors on cell viability following MPP^+ administration

N1E-115 and SH-SY5Y cell lines were treated with EC_{50} concentrations of MPP^+ (3 mM and 3 mM for LDH assay; 62 μM and 82 μM for trypan blue assay, respectively) in the presence and absence of a range of SAHA and VPA (10^{-9} – 10^{-3} M) concentrations. Control cultures were treated with serum-free medium only or toxin in serum-free medium.

SAHA Treatments

In untreated N1E-115 cultures, approximately 76 % cell viability was observed (Figure 3-11A). SAHA decreased cell survival in a bell shaped concentration-dependent manner, with significant decrease to 40 % and 31 % at 10^{-5} and 10^{-4} M, respectively. MPP^+ (3 mM) alone induced 53 % cell viability, however, although SAHA (10^{-9} – 10^{-3} M) administration had no significant effect on MPP^+-induced cell survival, cell loss tended to be greater than for MPP^+ alone control at all concentrations.

In untreated SH-SY5Y cultures, approximately 83 % cell survival was observed. Treatment with SAHA did not alter the degree of cell loss except at the highest concentration (10^{-3} M) where 36 % cell viability was observed (Figure 3-11B). MPP^+ (3 mM) alone induced 57 % cell survival in the control condition. SAHA had no effect on MPP^+-induced cell death, except at the highest concentration where cell viability of 8 % was measured, which was significantly greater than that of MPP^+ alone.

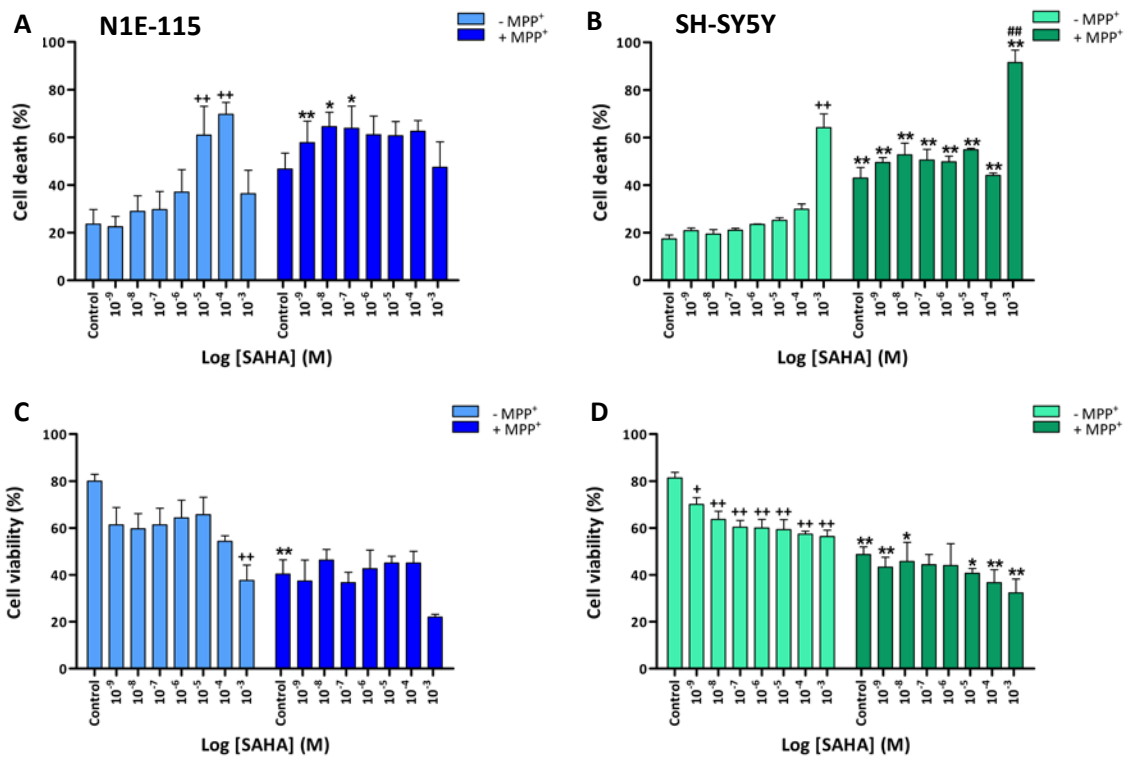

Figure 3-11 Effect of MPP^+ on cell survival following SAHA pre-treatment.
N1E-115 (A & C) and SH-SY5Y (B & D) cell survival was assessed by LDH assay (A & B) and trypan blue exclusion assay (C & D). The cells were exposed to SAHA (10^{-9} - 10^{-3} M) pre-treatment for 2 hours, followed by 24 hours co-treatment with MPP^+ (3 mM and 3 mM for the LDH assay; 62 μM and 82 μM for the trypan blue assay, respectively). Cell death was measured by the LDH assay, where maximum LDH release was recorded at 100 %. Viable cells for the trypan blue assay were counted and percentages were calculated from total cell counts of dead and surviving cells. Data are expressed as mean ± SEM (n=3); **p<0.01, *p<0.05 comparison between MPP^+-free treatments; ++p<0.01, +p<0.05 compared to serum-free control; ##p<0.01 compared to MPP^+ only treated control cells (two-way ANOVA followed by Newman-Keuls test).

In untreated N1E-115 cultures 80 % cell viability was observed. SAHA alone caused a decrease across the concentrations, but was only statistically significant at 10^{-3} M, where 37 % viable cells were counted (Figure 3-11C). MPP^+ (62 μM) alone had 40 % cell viability. SAHA administration for 2 hrs prior to MPP+ administration had no significant effect on the cells, even at 10^{-3} M, where the lowest cell count was recorded at 22 %.

In SH-SY5Y control cultures, 81 % cell survival was recorded (Figure 3-11D). SAHA alone statistically decreased the cell survival gradually from 70 % at 10^{-9} M to 56 % at 10^{-3} M. MPP^+ (82 μM) alone induced 48 % cell viability, and SAHA administration caused a gradual decline in cell viability from to 32 % at 10^{-3} M which was not significant.

VPA Treatments

In N1E-115 cultures, 70 % cell viability was measured in untreated cells. VPA alone did not alter the degree of cell death at any concentration tested (Figure 3-12A). MPP^+ (3 mM) alone significantly decreased cell survival to 38 %. VPA administration (10^{-9} – 10^{-3} M) had no significant effect on the degree of MPP^+-induced cell loss at any concentration tested.

In untreated SH-SY5Y cultures, 78 % cell viability was observed. Treatment with VPA alone did not significantly affect cell loss at any concentration tested (Figure 3-12B). MPP^+ (3 mM) alone induced 58 % cell survival. VPA administration prior to MPP^+ addition had no effect on MPP^+-induced cell loss, except at the highest concentrations 10^{-4} M and 10^{-3} M, where cell loss was significantly increased to 58 % and 63 %, respectively.

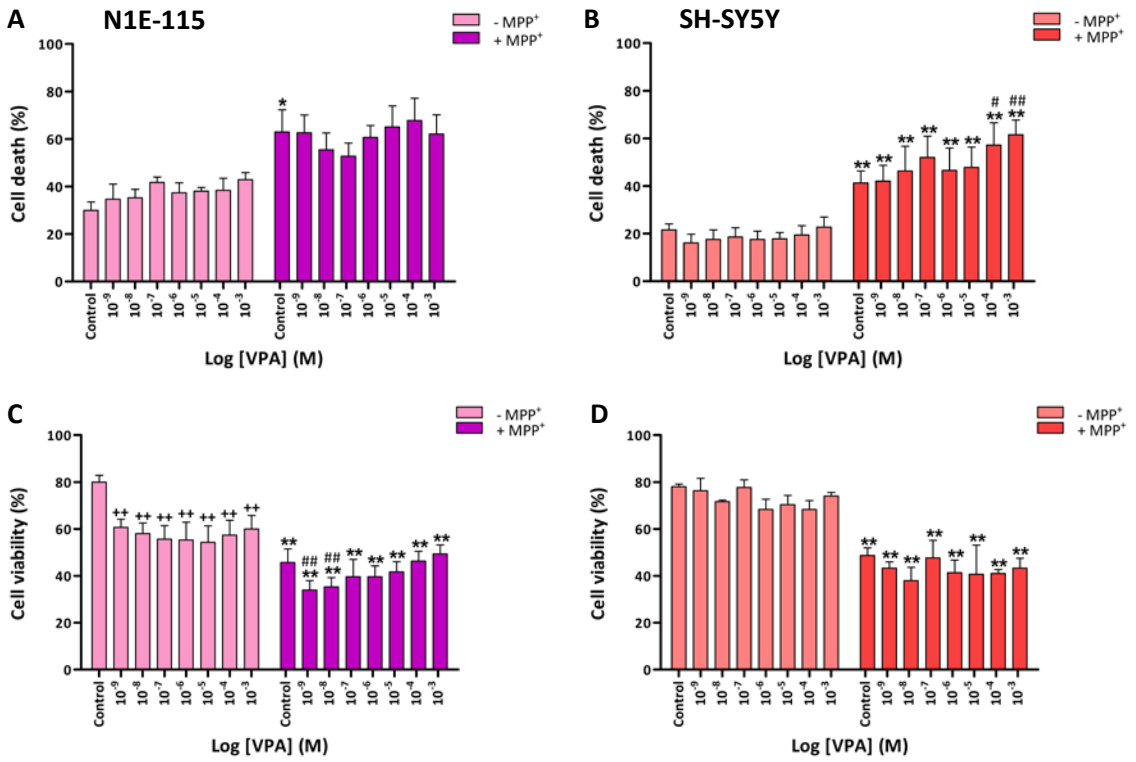

Figure 3-12 Effect of MPP^+ on cell survival following VPA pre-treatment.
N1E-115 (A & C) and SH-SY5Y (B & D) cell survival was assessed by LDH assay (A & B) and trypan blue exclusion assay (C & D). The cells were exposed to VPA (10^{-9} - 10^{-3} M) pre-treatment for 2 hours, followed by 24 hours co-treatment with MPP^+ (3 mM and 3 mM for the LDH assay; 62 μM and 82 μM for the trypan blue assay, respectively). Cell death was measured by the LDH assay, where maximum LDH release was recorded at 100 %. Viable cells for the trypan blue assay were counted and percentages were calculated from total cell counts of dead and surviving cells. Data are expressed as mean ± SEM (n=3); **p<0.01, *p<0.05 comparison between MPP^+-free treatments; ++p<0.01 compared to serum-free control; ##p<0.01, #p<0.05 compared to MPP^+ only treated control cells (two-way ANOVA followed by Newman-Keuls test).

In N1E-115 untreated cells, 80 % cell viability was observed (Figure 3-12C). VPA alone significantly decreased viability by approximately 18 % across all the concentrations tested. MPP^+ (62 μM) alone induced 45 % cell viability. Administration of VPA 2 hours prior to MPP^+ incubation induced further significant decline to 35 % at 10^{-9} and 10^{-8} M, and then a gradual increase to 49 % at 10^{-3} M, which was not significant.

SH-SY5Y untreated cells generated 78 % cell survival (Figure 3-12D). VPA alone did not have an effect on cell viability across all the concentrations tested. MPP^+ (82 μM) alone induced 48 % cell survival, and administration of VPA prior to MPP^+ incubation did not have any effect on cell survival across the concentrations tested.

3.4 Discussion

The hypothesis that the HDAC inhibitors would protect dopaminergic cells against toxin-induced cell death in cell lines, due to the presence of HDAC isoforms, was first tested by characterising the cell lines for dopaminergic and HDAC phenotype. The susceptibility of the cell lines to toxin-induced toxicity was then compared.

3.4.1 Characterisation of cell lines

Positive staining for TH in both mouse adrenergic N1E-115 and human catecholaminergic SH-SY5Y confirms they have dopaminergic phenotype. This is in agreement with previous evidence, where both cell lines were shown to possess dopaminergic characteristics by staining positive for TH (Amano *et al.*, 1972; Richelson, 1973; Biedler *et al.*, 1978).

Immunofluorescence staining of SH-SY5Y and N1E-115 cells for the HDAC isoforms showed that HDAC3 is localised mainly in the nucleus, whereas HDAC5 is primarily localised in the cytoplasm. HDAC4 and HDAC11 are present in both the nucleus and cytoplasm but stronger stains in the cytoplasm may indicate greater levels of protein outside the nucleus. These results are in agreement with previous reports where Class I (HDAC3) are predominantly nuclear and Class II (HDAC4 and 5) shuttle between the nucleus and cytoplasm (Verdin *et al.*, 2003; Lucio-Eterovic *et al.*, 2008). HDAC4 and 5 remain mainly in the cytoplasm due to their association with 14-3-3 protein which excludes them from the nucleus. In addition, a conserved nuclear import signal mapped to their N-terminal and binding to 14-3-3, has been suggested to mask their nuclear localisation (Wang & Yang, 2001; Sengupta & Seto, 2004).

HDAC11, which has previously been demonstrated to be localised mainly in the nucleus (Gao *et al.*, 2002b; Liu *et al.*, 2008) was found in both nucleus and cytoplasm in this study. This agrees with reports that this isoform has the characteristics of both Classes I and II HDACs (Broide *et al.*, 2007). If this is the case, it suggests that HDAC11 may also interact with 14-3-3 protein to localise predominantly in the cytoplasm, although this has not been confirmed.

Analysis by Western blot (Figure 3-6) confirmed the expression of the HDAC isoforms 3, 4, 5 and 11 in the two cell lines. In summary, positive staining of the two cell lines for dopaminergic phenotype and HDAC phenotype makes them a good *in vitro* model for this study.

3.4.2 The effect of H_2O_2 and MPP^+ on cell viability

The main aim of the study was to investigate the effect of HDAC-I in *in vitro* models of PD in these cell lines. Initial studies investigated the concentration-response relationship of neurotoxins H_2O_2 and MPP^+, which results in the inhibition of mitochondrial complex I and induces oxidative stress in N1E-115 and SH-SY5Y cell lines.

H_2O_2 was chosen as it induces the oxidative stress as observed in PD. It exerts its effects via ROS generation which inhibits mitochondrial complex I and causes lipid peroxidation and DNA and protein damage in cells (Halliwell & Aruoma, 1991). It has also been reported to activate caspase-3 (Jeon *et al.*, 1999), and stimulate cytochrome *c* release from mitochondria (Li *et al.*, 1997), both involved in cell death.

The second toxin, MPP^+, a metabolite of MPTP, on the other hand acts via inhibiting complex I (nicotinamide adenine dinucleotide coenzyme Q reductase) of the mitochondrial respiratory system (Chiba *et al.*, 1985). This leads to energy depletion and generation of ROS, similar to H_2O_2, resulting in oxidative stress and cell death (Mizuno *et al.*, 1987).

Both toxins induced concentration-dependent cell loss in N1E-115 and SH-SY5Y cell lines, indicating their vulnerability towards the toxins. Induction of LDH leakage and trypan blue stain of non-viable cells after toxin treatment confirms cell death by loss of membrane integrity which is probably the result of mitochondrial complex I activity impairment. Previous evidence have shown that MPP^+ induced the production of ROS in SH-SY5Y neuroblastoma cells, resulting in the initiation of apoptosis (Fall & Bennett, 1999). Even though this was not tested, caspase-3 assay could have been employed to test this notion and confirm that the cell loss observed in the cultures was probably due to apoptosis. In fact, H_2O_2 and MPP^+ used in previous studies have been shown to induce apoptosis in dopaminergic cells (Sheehan *et al.*, 1997; Gomez *et al.*, 2001; Uberti *et al.*, 2002; Dennis & Bennett, 2003; King & Jope, 2005; Wang *et al.*, 2009a). EC_{50} concentrations reported in these studies are comparable to the concentrations reported in here: H_2O_2 (100 – 935 μM) and MPP^+ (3 mM). The low concentrations reported in this study for MPP^+ (100 – 200 μM) assessed by trypan blue exclusion assays however does not correlate to previous findings. This variation is because the trypan blue dye is able to stain all dead cells as well as those with cell membrane damages, whereas the LDH assay only measures the leakage of LDH from cells with damaged membranes (Lappalainen *et al.*, 1994), therefore requiring higher toxin concentrations.

The cell death was determined and expressed as percentage cytotoxicity in both assays. The LDH assay, which measures LDH leakage from cells with disrupted membranes is indicative of necrotic cell death (Lobner, 2000). The trypan blue exclusion assay on the other hand stains all dead cells indicating that it measures both apoptotic and necrotic cell loss. Therefore, caspase-3 assay which measures apoptosis would have been an appropriate test to determine whether HDAC-Is were inducing apoptotic or necrotic neuronal loss in the cultures. Assays such as MTT and ATP were considered, however as both toxins inhibit mitochondrial function, they were concluded to be inappropriate.

3.4.3 HDAC-I's do not protect dopaminergic cell lines against toxin induced cell death

To investigate the effects of HDAC-Is in the presence of H_2O_2 and MPP^+, N1E-115 and SH-SY5Y cells were subjected to 2 hours pre-treatment prior to toxin exposure for 24 hours. LDH assay results, showed SAHA alone treatments had the tendency to increase cell death only at high concentrations (10^{-4} and 10^{-3} M) in both cell lines. This result was similar for trypan blue exclusion assay where absolute cell numbers were counted. Concomitant treatment of the HDAC-I and both toxins, showed SAHA to exacerbate to effects of the toxins at all concentrations tested in both assays, except for N1E-115 cells where SAHA proved to be potentially protective at the highest concentration (10^{-3} M) which was not significant (Figure 3-9A&C; Figure 3-11C).

VPA, on the other hand, had little or no effect on cells when they were treated with VPA alone or concomitantly with the toxins. Similarly to SAHA, VPA also exacerbated the effects of the toxins H_2O_2 and MPP^+ in both LDH and trypan blue exclusion assay.

The toxic effects of the HDAC-Is observed here contradicts previous reports where inhibition of HDAC with sodium butyrate (Nab) reduced cell death at millimolar concentrations (Candido *et al.*, 1978) and also recently confirmed by Kidd & Schneider (2010) where VPA and Nab (both 1 mM) protected against MPP^+-induced apoptotic cell loss in dopaminergic cell lines (Kidd & Schneider, 2010). The protective effect implicated by these studies was achieved at concentrations which are not physiologically plausible as they are too high, and would hinder the use of these inhibitors as a therapeutic approach. In addition, due to the nature of cell lines to withstand harsh conditions, this cannot be a true representation of a neuroprotective effect, and other models will have to be investigated. Moreover, it is unlikely that such high levels can be translated and sustained in *in vivo* models due to the pharmacotoxicity effects of these HDAC-Is even at low concentrations. A contributory factor to their toxicity could be due to the fact that their mechanisms of action are highly non-specific and non-targeted.

Treating the cells with serum-free media, also contributed to the decline in cell viability. Serum deprivation has been shown to be toxic to cells (Takeshima *et al.*, 1994a; Bar-Am *et al.*, 2005). Despite this finding, serum deprivation was still encouraged as it helps to synchronise the development stage of the cancer cell lines, by enabling cells to exit from cell cycle into the non-dividing state termed G0 characterised by low metabolic activity (Kues *et al.*, 2000). This also makes the cells less resistant to toxin insults, because serum enriches the media and promotes growth. Therefore, higher toxin concentrations were required to observe maximum cell loss, especially when generating the concentration-response curves.

More recently, it has also been reported that serum deprivation induces autophagy by starvation (Steiger-Barraissoul & Rami, 2009). To some extent, this may have contributed to the degree of cell death assessed, but as the DMEM used in the study contains a variety of amino acids and vitamins, it seems unlikely that a major proportion of the cell death measured can be attributed to the induction of autophagy. This concept therefore needs to be examined further for confirmation. However, if this hypothesised view is false, then it would result in an over-exaggeration of the toxic effects of the HDAC-Is and toxins, as the cell death measured would be attributed to their toxicity. In this case, to overcome the problem of autophagy induction, the concentration of FBS could be reduced from 10 %, in the serum-containing media, to 1 %, to prevent a complete starvation, and minimise the onset of autophagy.

Treatment with SAHA and VPA resulted in exacerbated neurotoxic damage to the cell lines induced by H_2O_2 and MPP^+. A similar effect in SH-SY5Y cells when treated with Trichostatin A (TSA) and rotenone was previously reported (Wang *et al.*, 2009b) . Confirmation of these results are by Subramanian and group who reported HDAC-Is induced apoptosis in neuronal neuroblastoma cells, via Ku70 hyperacetylation which led to Bax activation and translocation to the mitochondria to result in the release of cytochrome *c* and caspase dependent apoptosis in the cytoplasm (Subramanian *et al.*, 2005a; Subramanian *et al.*, 2005b). This indicates that the inhibitors may be exerting their anti-cancer effects in the assays as both N1E-115 and SH-SY5Y cells are mouse and human neuroblastoma-derived, respectively. This is confirmed by Marks *et al.* (2000) who suggested that small molecule Class I and II HDAC-Is, such as VPA and SAHA, produce responses in a wide variety of cultured transformed cells including neuroblastoma cells associated with anti-tumour agents, which triggers apoptosis, cell cycle arrest and differentiation (Marks *et al.*, 2000).

3.4.4 Conclusion

In conclusion, this study showed that N1E-115 and SH-SY5Y possess dopaminergic and HDAC phenotype. In addition to expressing their vulnerability to neurotoxins to enable the effects of HDAC-Is to be investigated. Inhibition of HDACs showed the inhibitors are toxic to the cell lines and exacerbate the effects of H_2O_2 and MPP^+, except at high concentrations where they tend to be protective. As the cell lines are immortalised, they are able to withstand such high concentrations which are not pharmacologically possible to translate into *in vivo* models. Secondly, the cell lines were not induced to differentiate into neuronal-like morphology with retinoic acid, where they resembled functionally mature neurones. Therefore the effects of the HDAC-Is observed in the cell lines is not a true representation of the effects they would have on mature neurones. Thirdly, they are of neuronal origin and lack the complexity of the 'real picture', where different cell types such as glial cells are present. This therefore only allowed the effects of HDAC-Is on oxidative stress to be investigated and not inflammation. For this reason, further investigation performed in primary mesencephalic cultures as an *in vitro* cell death model of PD is reported in the next chapter.

Chapter 4 The effect of HDAC inhibitors on MPP^+- and LPS-induced cell death in primary ventral mesencephalic cultures.

4.1 Introduction

In the preceding chapter, it was reported that HDAC-Is did not protect dopaminergic neuronal cell lines against toxin-induced cell death despite the presence of multiple HDAC isoforms. Indeed, at higher concentrations the inhibitors were toxic to the cell lines and exacerbated the toxic effects of both H_2O_2 and MPP^+, resulting in increased cell loss. Although this suggests that HDAC-Is may not be useful as neuroprotective agents mediated by a direct action on neuronal cells, it does not preclude other mechanisms of action which may have a beneficial protective effect.

HDAC-Is have been shown to have anti-inflammatory properties in models of autoimmune and inflammatory diseases (Leoni *et al.*, 2002; Leoni *et al.*, 2005; Camelo *et al.*, 2005; Lin *et al.*, 2007). This may be relevant to PD as glial cell toxicity plays a major role in the pathogenesis of the disease (see Chapter 1). Investigations in post mortem PD brains have shown increased numbers of activated microglia, phagocytes and astrocytes in the substantia nigra. These cells are activated in response to cellular damage, including oxidative stress and the increased expression of genes involved in nitric oxide (NO) and cytokine synthesis (McNaught & Jenner, 1999). Thus HDAC-Is may have an anti-inflammatory role that would result in protection against cell death in PD, however, this has not been investigated.

In order to study this anti-inflammatory role of HDAC-Is, it is important to use a cell system that is composed of a mixed population of neurones and glial cells. Primary rat cultures derived from foetal ventral mesencephalon are the best suited option, as they have been extensively used to investigate dopaminergic cell death in *in vitro* studies (Chung *et al.*, 2005; Ono *et al.*, 2007; Pruszak *et al.*, 2009). In addition, primary cultures closely mimic the *in vivo* state, and generate a more physiologically relevant effect as opposed to cell lines.

In the present study, primary cultures were used to investigate and compare the effects of HDAC-Is in MPP^+-induced oxidative stress and LPS-induced inflammation on dopaminergic neurones. The two toxins were chosen because they both exert their effects in different pathways in cultures and exert different levels of gliosis (Block *et al.*, 2007; MCNaught & Jenner, 2000; Gao *et al.*, 2003).

Even though HDAC-Is did not protect dopaminergic neurones from MPP^+-induced toxicity as shown in the previous chapter, their effects on cultures with mixed cell populations including glial cells is of particular interest. This is because besides the harmful effects of glial cells detailed in Chapter 1, they do have beneficial effects such as: 1) promoting neuronal survival through the

release of endogenous neuroprotective proteins termed neurotrophic factors, such as GDNF (Hou *et al.*, 1996; Burke *et al.*, 1998); 2) scavenging toxic compounds released by dying neurones (Rosenberg, 1991; Aloisi, 2001); and 3) protecting neurones against oxidative stress by up-regulating the synthesis of the antioxidant glutathione (Iwata-Ichikawa *et al.*, 1999). These properties may in turn protect neurones from toxin-induced damage.

4.1.1 Hypothesis

It was hypothesised that HDAC inhibition will protect dopaminergic neurones from the biochemical and pathological changes linked to cell death in the substantia nigra induced by MPP^+ and LPS by reducing the inflammatory response.

4.1.2 Aims

To test this hypothesis, the effect of HDAC inhibition on MPP^+ and LPS-induced cell death was investigated in the rat primary VM cell cultures. The main aims were to:

1. Characterise VM cultures for constituent cell types.
2. Determine the expression of HDACs in VM cultures.
3. Assess the effect of HDAC inhibitors on dopaminergic cell death following MPP^+ and LPS treatment.
4. Investigate the effect of HDAC inhibitors on the inflammatory changes induced by MPP^+ and LPS treatment in VM cultures.

4.2 Materials and methods

4.2.1 Primary cell culture

Pregnant female Wistar rats (Charles River, Margate, UK), were housed in a temperature-controlled room (23^{o}C) (King's College London Biological Services Unit) with a 12 hour light-dark cycle and *ad libitum* access to pelleted diet and water. Experiments were conducted according to guidelines set out in the UK Animals (Scientific Procedures) Act, 1986.

4.2.2 Dissection of ventral mesencephalon

Pregnant rats were killed by an overdose of carbon dioxide (CO_2) followed by cervical dislocation. The uterine horn was removed by caesarean section, cleared of blood and membranes, and placed into a petri dish containing ice-cold sterile PBS (0.1 M). The foetal ventral mesencephalon (VM) (Figure 4-1) was dissected under a microscope (Vickers Instruments, Croydon) and collected into a falcon tube containing ice-cold sterile PBS (0.1 M), using micro-dissection scissors and micro-forceps (World Precision Instuments, Hertfordshire).

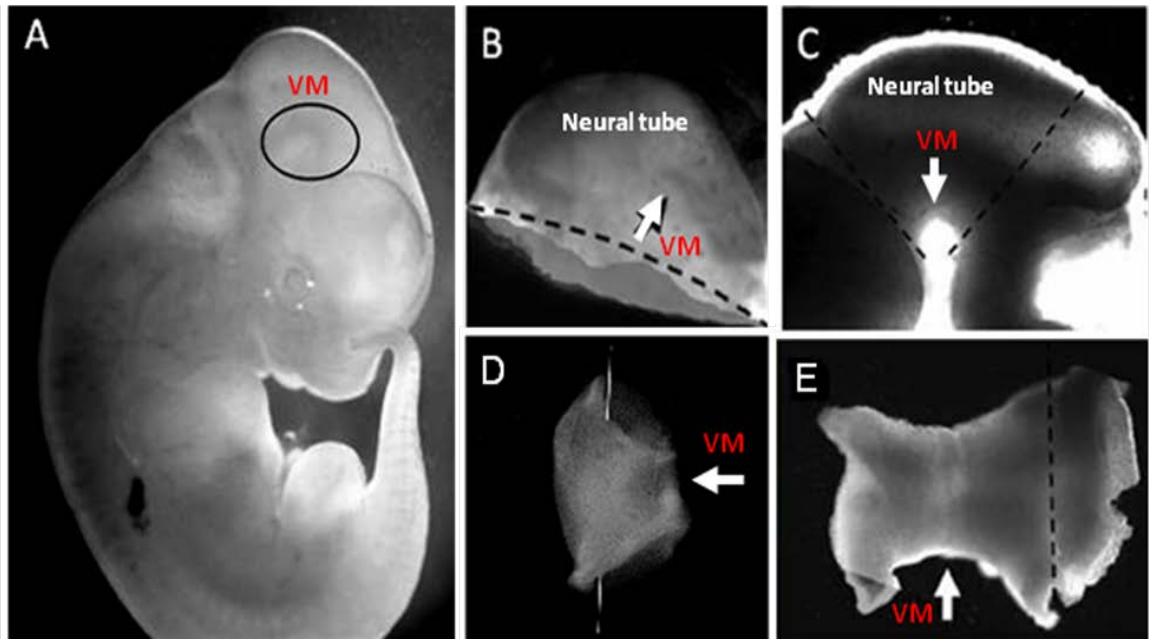

Figure 4-1 Outline of VM dissection.
(A) An E14 old rat embryo. Black circle shows the mesencephalon that develops into the ventral tegmental area and substantia nigra. (B & C) depicts the top of the head (neural tube) with the VM highlighted with white arrow. (D) The neural tube is isolated and cut open (at white line) to reveal a butterfly image with the VM in the middle (E). Adapted and Modified from Studer, 2001; Pruszak *et al.*, 2009)

4.2.3 Preparation of mesencephalic primary culture

Using aseptic technique, cell preparation was performed in a class II safety cabinet (Walker Safety Cabinets, Derbyshire) following tissue dissection. The collected mesencephalon was washed three times with ice-cold PBS and enzymatically digested with Trypsin-EDTA solution (2.5 %; 2 ml) at 37^{o}C for 2 minutes. Trypsin was inactivated by addition of high glucose Dulbecco's Modified Eagle Medium (DMEM) (10 ml) supplemented with heat-inactivated foetal bovine serum (10 %) and PSN (1 %; 100 IU/ml) and centrifuged at 1000 g for 90 seconds. The tissue pellet was resuspended in DMEM (1 ml) and dissociated with p1000 Gilson pipette followed by a fire-polished glass Pasteur pipette. The cell density was determined as described in Section 3.2.3 and the cells were plated at 2 x 10^5 cells per well into a 24 well plate containing poly-D-lysine coated 13 mm coverslips (Section 2.6.1). Cells were grown at 37^{o}C in an incubator (MCO-18AIC, Sanyo), with CO_2 (5 %) and humidity (95 %) in atmospheric air. Following 7 days *in vitro* (DIV7), the cells were processed for immunochemical staining (Section 4.2.6).

4.2.4 Characterisation of VM cultures

Primary culture cells were characterised for TH; glutamic acid decarboxylase (GAD), a GABA-ergic neurone marker; GFAP, a marker for astrocytes; and OX-42, for microglia. At DIV7 after dissection, the medium was aspirated and the cells were washed with cold sterile PBS followed by 15 minutes fixation with PFA (4 % in PBS). Immunoperoxidase staining was performed as described in Section 4.2.6.1.

4.2.5 Neuroprotection study

4.2.5.1 Effect of MPP^+ and LPS on VM cultures

Neuronal cell death was induced in VM cultures (DIV7) using MPP^+ (1 to 100 μM) or LPS (1 to 200 μg/ml) in serum-free medium for 24 hours. Control cells were grown in serum-free medium only for 24 hours. The media was aspirated and the cells were fixed with PFA (4 %) as described in Section 2.6.2. The cells were then stained for TH cell number by immunocytochemistry and counted as described in Section 4.2.7. EC_{50} calculation of MPP^+ and LPS were determined in Section 4.2.8.

4.2.5.2 Neuroprotection assays on MPP^+ and LPS induced toxicity

To assess and compare the effects of HDAC inhibition on MPP^+ and LPS-induced cell death, VM cultures (DIV7) were pre-treated with SAHA (0.01, 0.1 and 1 μM) or VPA (0.3, 0.6 and 1.2 mM) diluted in serum-free media for 2 hours (Figure 4-2). The media was then replaced with the same concentrations of VPA or SAHA with or without EC_{50} concentrations of MPP^+ or LPS determined in Section 4.2.5.1, for a further 24 hours. Control cells were incubated with serum-free medium

only, HDAC inhibitor only or toxin only for 24 hours. The cells were fixed as described in Section 2.6.2, and stained for TH, GFAP and OX-42 by immunocytochemistry as described in Section 4.2.6.

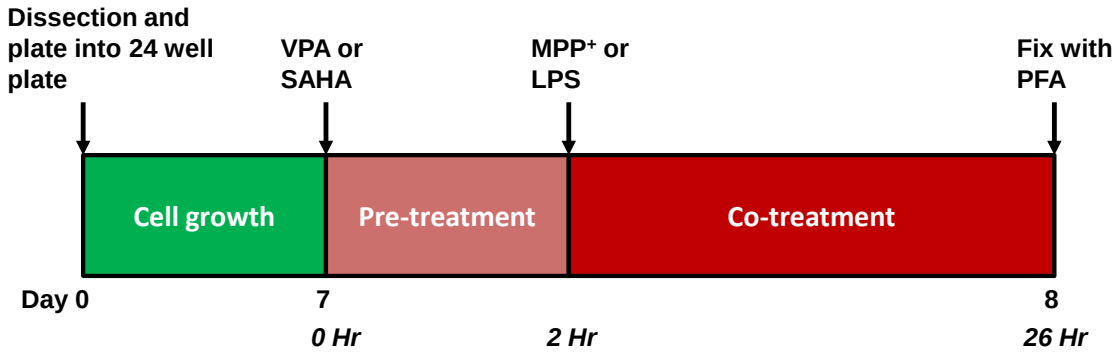

Figure 4-2 Schematic experimental outline.
VM cultures were plated at day 0, and grown for 7 days. On day 7, the medium was aspirated and changed to serum-free medium (SFM), VPA (0.3, 0.6, 1.2 mM) or SAHA (0.01, 0.1, 1 μM) for 2 hours followed by the same concentrations with or without EC_{50} concentrations of MPP^+ or LPS. Twenty-four hours later, the cells were fixed with PFA (4 %) and processed for immunocytochemistry.

4.2.6 Immunocytochemistry

4.2.6.1 Immunoperoxidase staining of fixed VM cells

Immunoperoxidase staining was used to identify the expression of TH, GAD, GFAP and OX-42 in VM cultures. This is described in detail in Section 2.6.6. To summarise, VM cell cultures attached to poly-D-lysine (0.05 %; Sigma-Aldrich, Dorset, UK) coated coverslips, were fixed with PFA (4 % in 0.1 M PBS) and incubated in 24 well plates with primary antibodies against TH (1:500), GAD (1:500), GFAP (1:500) and OX-42 (1:100) overnight at room temperature (Table 2-2). The following day, the cells were incubated with biotinylated secondary antibody (1:250) (Table 2-3) and ABC solution for 1 hour each at room temperature. Cells were visualised by exposing to DAB for 1 minute. The cells were hydrated in ethanol (100 %, 98 % and 70 %), counterstained with cresyl violet, dehydrated in ethanol (70 %, 98 % and 100 %) and mounted onto superfrost microscope slides.

4.2.6.2 Double immunofluorescence of fixed primary cultures

Double immunofluorescence histochemistry was used to assess the co-expression of TH, GFAP and OX-42 with HDAC isoforms 3, 4, 5 and 11 described in detail in Section 2.6.5. In brief, VM cultures fixed to poly-D-lysine coated coverslips were first blocked with blocking solution (10 %) followed by incubation of primary antibodies against HDAC3, 4, 5, 11 and TH, GFAP and OX-42 (dilutions in Table 2-2) overnight at 4°C. On the next day, the cells were incubated with the two

respective secondary antibodies (Table 2-3) for 2 hours at room temperature. The cells were mounted with Vectashield® Hard set mounting medium containing DAPI and examined using a fluorescence microscope (Zeiss Axioskop, Carl Zeiss, Hertfordshire, UK).

4.2.7 Cell Counting

Positively stained cells were counted in 8 randomly chosen areas at X20 magnification in one cover slip with total area equivalent to 8 mm^2, with three coverslips per experiment. For characterisation study, the number of TH, GAD and GFAP immunoreactive cells were calculated as a percentage of the total number of cells, including the cresyl violet stained cells. For the neuroprotection study, immunoreactive cells were counterstained with cresyl violet and expressed as the number of immunoreactive cells per 8 mm^2.

4.2.8 Data & Statistical Analysis

GraphPad Prism 5 software was employed for statistical analysis. Non-linear regression analysis was used to determine the EC_{50} for MPP^+ and LPS. One-way ANOVA followed by Newman Keul's post hoc test was performed on MPP^+ and LPS concentration-response data. Neuroprotection studies were analysed by two-way ANOVA followed by Newman Keul's test using toxin and HDAC treatment as variables. $P<0.05$ was considered significant. Data are expressed as mean ± SEM of three separate experiments (n = 3) performed in triplicate.

4.3 Results

4.3.1 Characterisation of VM primary cultures

VM cultures from E14 embryos were stained at DIV7 for the proportions of dopaminergic, GABAergic neurones, astrocytes and microglia by staining for TH, GAD, GFAP and OX-42, respectively, using immunoperoxidase and immunofluorescence for the latter (Figure 4-3). The majority of cell population were GAD positive cells (55 %), whereas TH positive cells made up only 5 % of the culture. Staining for both GAD and TH markers were observed in the cell bodies and dendritic processes (Figure 4-3A & B). GFAP-positive cells made up a small proportion of the population (8 %), where distinct staining of the cell body and fibrous processes was noted (Figure 4-3C), and OX-42-immunoreactive cells made up 0.2 % of the cell population (Figure 4-3D).

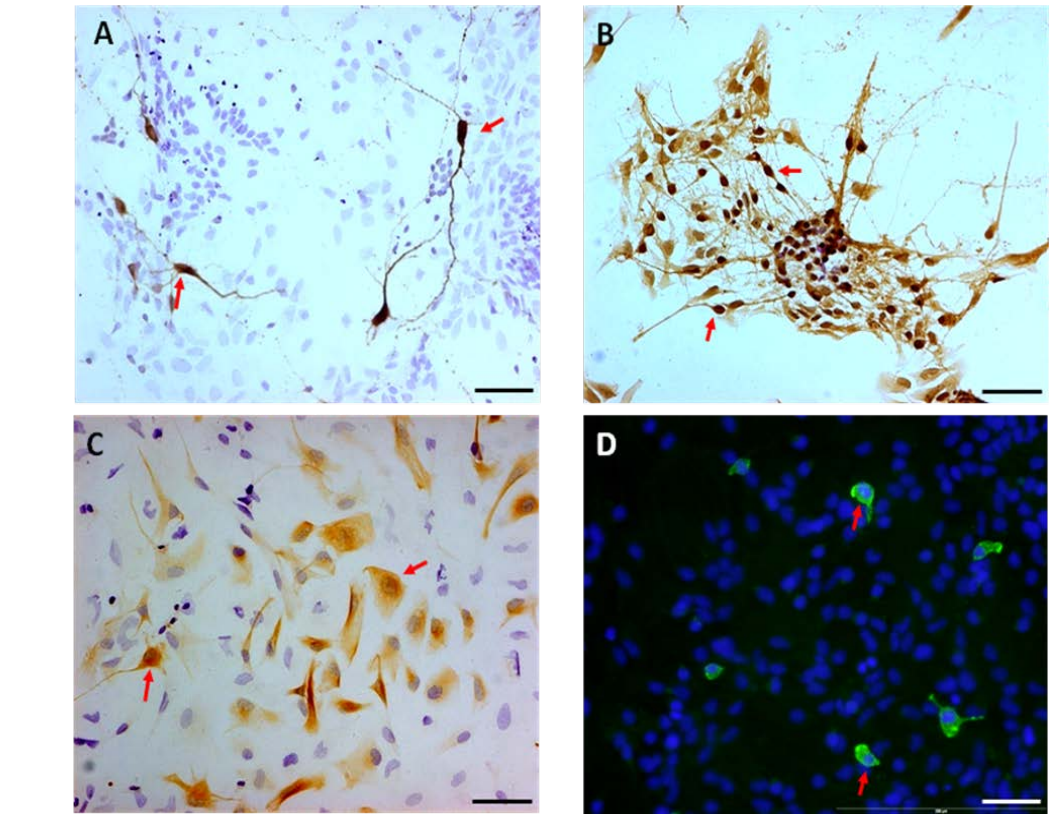

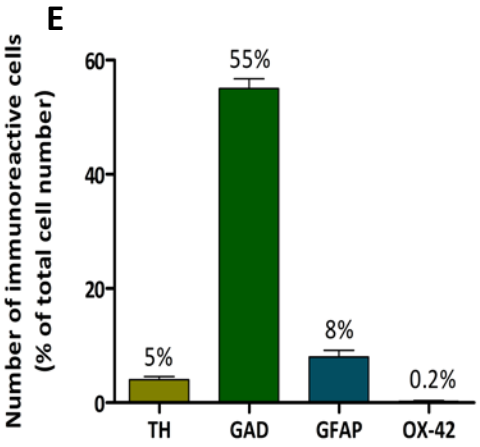

Figure 4-3 Positive immunoperoxidase and immunofluorescence staining of VM primary cultures for TH, GAD, GFAP and OX-42.
Representative photomicrographs of VM cell cultures (DIV7) stained with antibodies against (A) TH, (B) GAD, (C) GFAP, and (D) OX-42. Positively stained cells were stained brown (A-C) by immunoperoxidase, and green (D) by immunofluorescence. Typical stained cell bodies are indicated with red arrows. Cultures (A-C) were counterstained with cresyl violet and DAPI (D). Scale bar = 100 μm (A & B) 200 μm (C & D). (E) Data are expressed as percentage of total cell number indicated by cresyl violet and DAPI.

4.3.2 Co-expression of HDAC isoforms and dopaminergic cells in VM cultures.

In order to determine whether HDAC isoforms were co-expressed with dopaminergic cells, VM cultures fixed at DIV7 were double-labelled by immunoflourescence for TH and HDAC3, 4, 5 and 11 (Figure 4-4,). Similar to results observed in Section 3.3.2, HDAC3 was mainly localised in the nucleus of the cell body; whereas HDAC4, 5 and 11 were localised mainly in the both cell body and dendritic processes.

Double immunoflourescence labelling with anti-TH antibody showed that TH-positive cells expressed all four HDAC isoforms (Figure 4-4). These isoforms were also seen to be expressed in non-TH expressing cells in the culture.

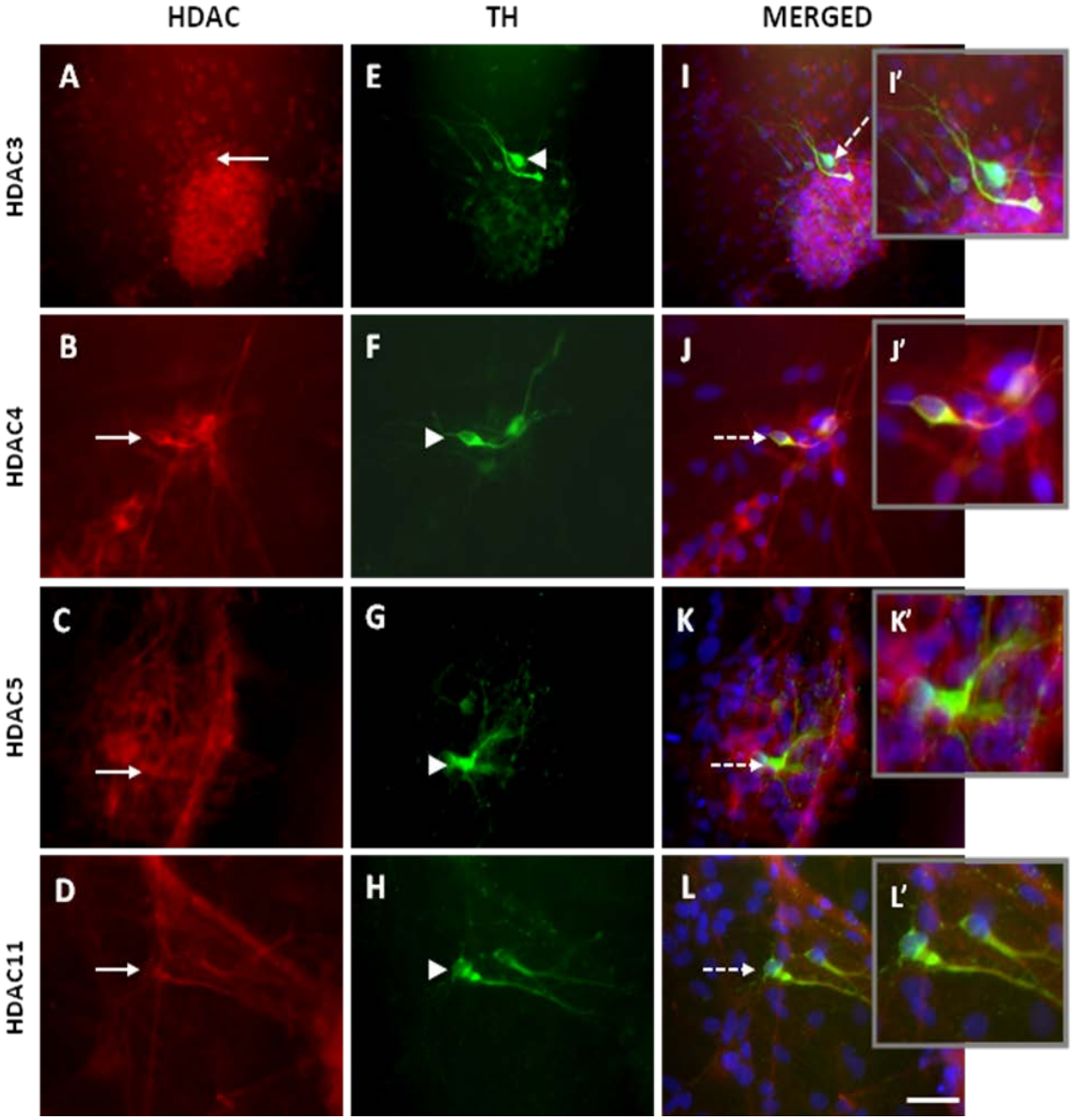

Figure 4-4 Expression of HDAC isoforms in TH immunopositive cells in VM cultures.
Representative photomicrographs showing (A-D) HDAC3, 4, 5 and 11 positive cells respectively (red; solid arrow); (E-H) TH positve cells (green; arrow head) and (I-L) merged images (typical cells depicted with broken arrow). DAPI (blue) was used to counterstain nuclei. Scale bar = 100 μm is representative of all images.

4.3.3 Co-expression of HDAC isoforms and inflammatory cells in VM cultures.

As expected, VM cultures were composed of multiple cell types including inflammatory cells. Thus, the expression of HDAC isoforms 3, 4, 5 and 11 was investigated in inflammatory cells, including astrocytes and microglial cells. Double-labelling by immunoflourescence with anti-GFAP (Figure 4-5) and anti-OX-42 (Figure 4-6), also showed that GFAP and OX-42 positive cells expressed all four HDAC isoforms.

HDAC3 was located primarily in the nucleus of the astrocytes (Figure 4-5-A, E, I), but in some cells HDAC3 was found to have some diffused cytoplasmic staining. HDACs 4, 5 and 11 were mainly found in the cytoplasm with diffused nucleic staining (Figure 4-5-B-L).

A similar staining pattern was observed in microglia (Figure 4-6). HDACs was primarily localised in the nucleus of the cells, whereas HDAC4, 5 and 11 were seen to have both nuclear and cytoplasmic staining of the microglial cells.

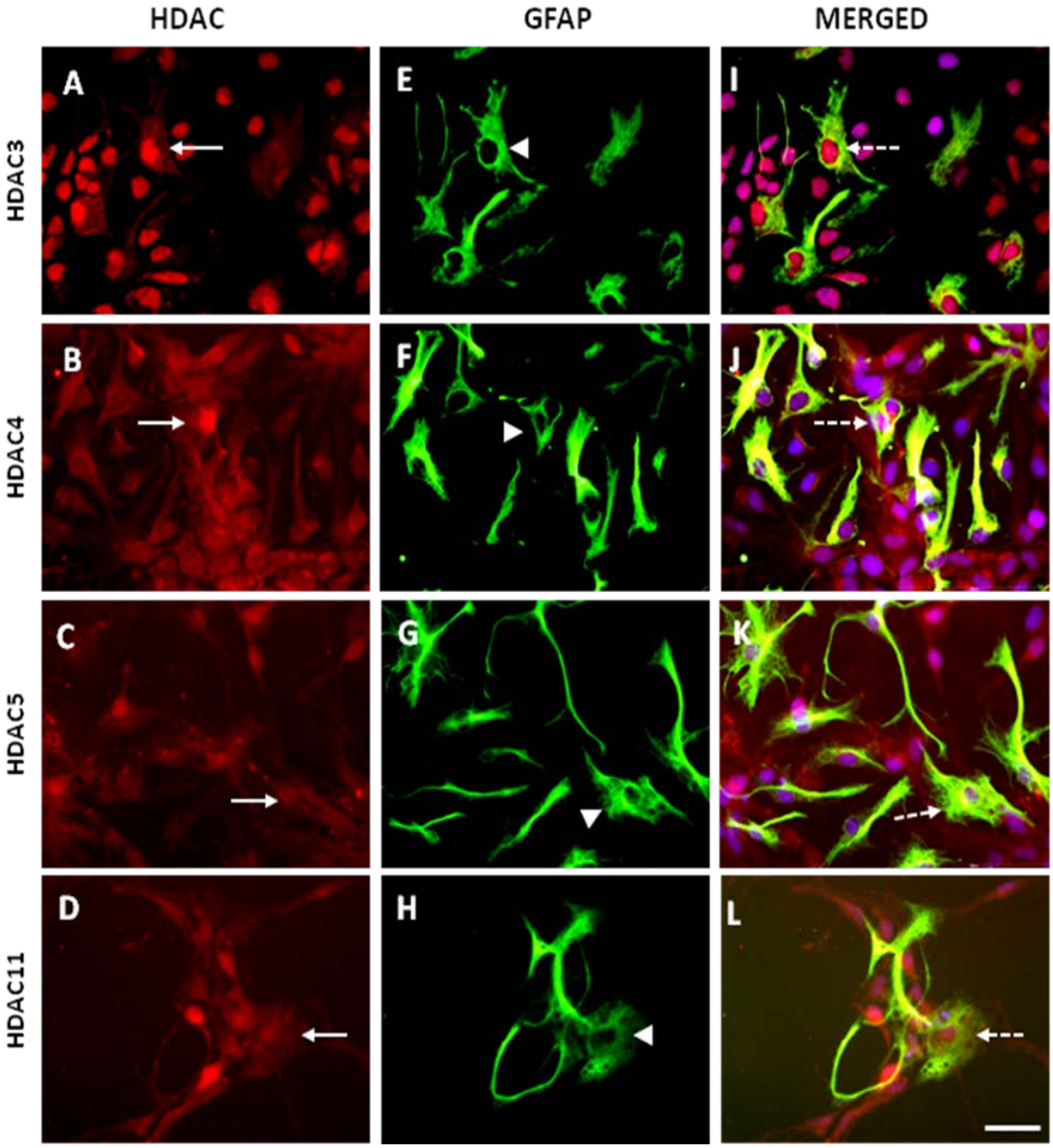

Figure 4-5 Expression of HDAC isoforms in GFAP immunopositive cells in VM cultures.
Representative photomicrographs showing (A-D) HDAC3, 4, 5 and 11 positive cells respectively (red; solid arrow); (E-H) GFAP positve cells (green; arrow head) and (I-L) merged images (broken arrow). DAPI (blue) was used to counterstain nuclei. Scale bar = 100 μm is representative of all images.

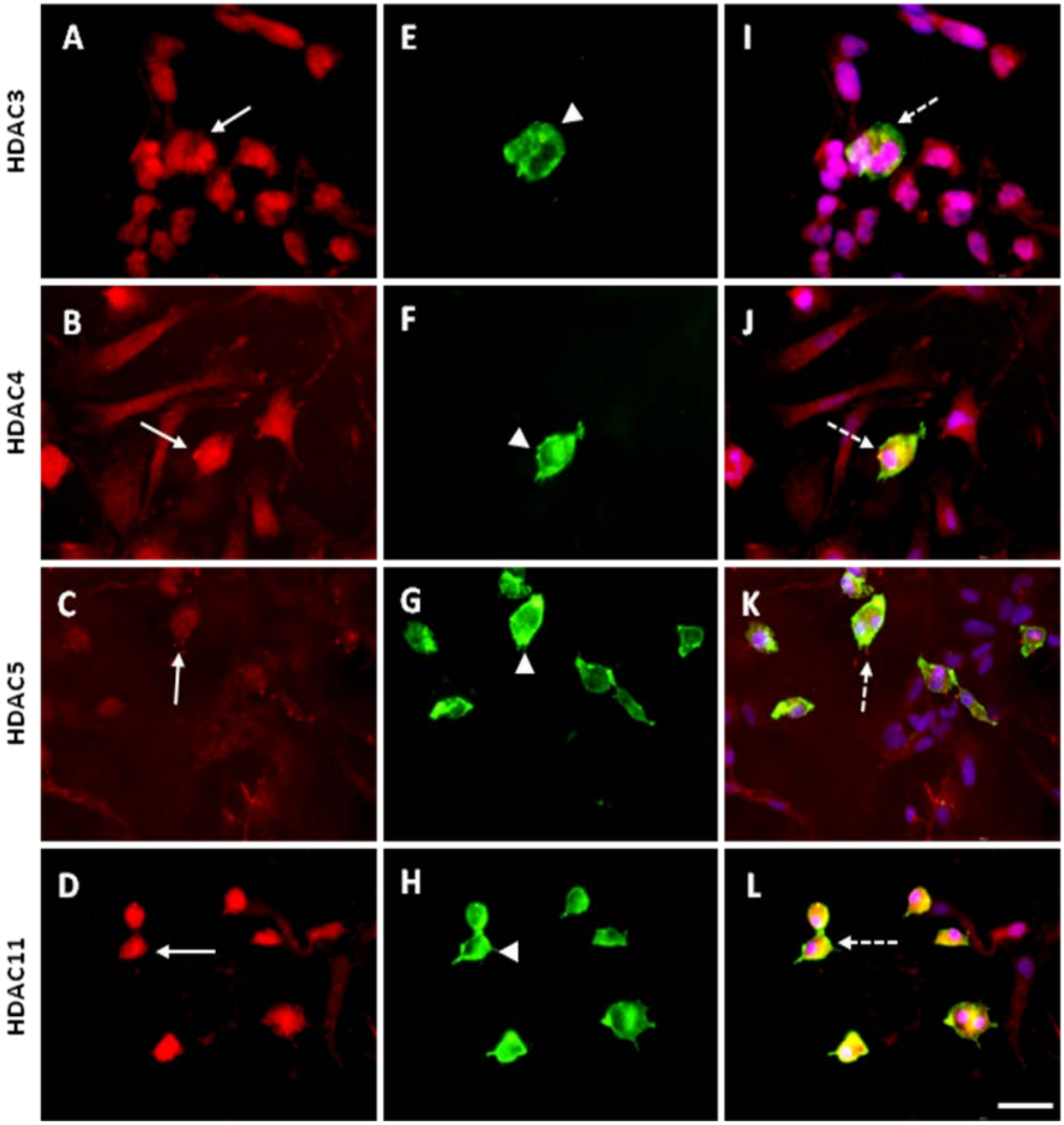

Figure 4-6 Expression of HDAC isoforms in OX42 immunopositive cells in VM cultures.
Representative photomicrographs showing (A-D) HDAC3, 4, 5 and 11 positive cells respectively (red; solid arrow); (E-H) GFAP positve cells (green; arrow head) and (I-L) merged images (broken arrow). DAPI (blue) was used to counterstain nuclei. Scale bar = 200 μm is representative of all images.

4.3.4 The effect of MPP^+ and LPS on TH-positive cells in VM cultures.

To assess the effect of the toxins MPP^+ and LPS on dopaminergic cells in VM cultures, the cultures (DIV7) were exposed to MPP^+ (1 - 100 μM) and LPS (1 - 200 μg/ml) and cell loss was determined by staining for TH-positive cell number by immunocytochemistry.

MPP^+ (1 – 100 μM) induced a concentration-related decline in TH positive stained neurones in the cultures (Figure 4-7A). The EC_{50} was calculated to be 3 ± 1.5 μM. Similarly, LPS (1 – 200

μg/ml) also induced a concentration-dependent loss of immunoreactive TH cells in VM cultures (Figure 4-7B). The EC_{50} concentration was calculated as 40 ± 0.6 μg/ml.

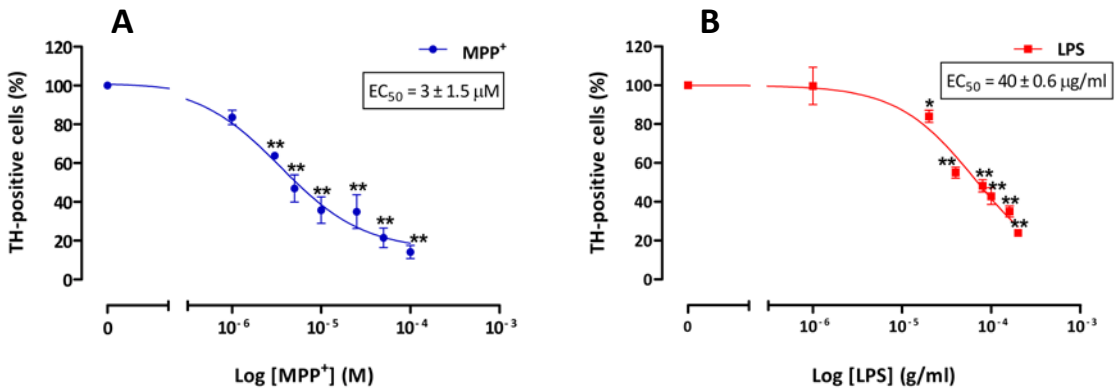

Figure 4-7 The effect of MPP+ and LPS on TH-positive cells in VM culture.
DIV7 embryonic cultures were incubated with serum-free medium for 2 hours prior (A) MPP^+ (1 – 100 μM) and (B) LPS (1 – 200 μg/ml). Positively stained TH cells were counted and displayed as percentage TH-positive cells compared to untreated control cells (100 %). Non-linear regression curve was fitted to determine EC_{50}. Data are expressed as mean ± SEM (n=3) and analysed by one-way ANOVA with Newman Keul's test. *p<0.05, **p<0.01 compared to untreated control cells.

4.3.5 The effects of SAHA and VPA on toxin-induced cell loss in rat mesencephalic culture.

The effects of HDAC-Is, SAHA and VPA, on toxin-induced cell loss in VM primary cultures were investigated. Culture cells were subjected to 2 hours pre-treatment with SAHA (0.01, 0.1, and 1 μM) and VPA (0.3, 0.6, and 1.2 mM) prior to concomitant treatment for a further 24 hours with EC_{50} concentrations of MPP^+ (3 μM) or LPS (40 μg/ml). The number of TH, GFAP or OX-42 cells was determined by immunocytochemistry as described in Section 2.6.6.

4.3.5.1 The effect of HDAC inhibitors on TH-positive cells following MPP^+ and LPS exposure.

<u>SAHA and MPP^+ Treatments</u>

Control VM cell cultures contained 42 ± 9 TH-positive cells per 8 mm^2 with intact cell bodies and dendritic processes (Figure 4-8A; Figure 4-9A). Treatment with SAHA alone caused significant decreases of TH-positive cells, with the highest percentage loss observed at 1 μM (71 %) which caused the loss of the dendritic nodes (Figure 4-9D). MPP^+ (3 μM) alone reduced the number of TH immunoreactive cells by 45 %. In some instances, some cells were left with intact cell bodies with completely disintegrated processes, whereas other cells had both damaged cell bodies and processes (Figure 4-9B). Pre-treatment with SAHA for 2 hours prior to MPP^+ incubation for 24 hours had no significant effect on TH cell survival compared to MPP^+ alone. However, both

treatments resulted in shortened processes in some surviving cells and complete loss of processes in others (Figure 4-9E).

VPA and MPP^+ treatments

Control VM cell cultures contained 36 ± 3 TH-positive cells per 8 mm^2 (Figure 4-8B). Similarly to SAHA, treatment with VPA alone caused a decline in the number of TH-positive cells where 50 % viable cells was observed with 1.2 mM VPA concentration. VPA caused cell processes to completely disintegrate leaving the cell bodies intact (Figure 4-9G). MPP^+ (3 μM) alone reduced the number of TH immunoreactive cells by 47 %. Pre-incubation of cultures with VPA for 2 hours prior to MPP^+ had no effect on the number of viable TH immunoreactive cells (Figure 4-9H).

SAHA and LPS treatments

Control VM cell cultures contained 40 ± 3 TH-positive cells per 8 mm^2 (Figure 4-8C). SAHA alone significantly decreased the number of TH-positive cells across the concentrations tested, where the lowest number of positive cells (16 ± 2 cells per 8 mm^2) was observed at 1 μm. Treatment with LPS (40 μg/ml) alone caused 45 % TH immunoreactive cell loss, with remaining cells showing loss of cell processes and damage to some cell bodies (Figure 4-9C). Pre-treatment with SAHA for 2 hours prior to LPS incubation for 24 hours decreased the number of surviving TH-positive cells at 0.10 μM to 43 %, causing a loss to both cell bodies and processes (Figure 4-9F).

VPA and LPS treatments

Control VM cell cultures had 35 ± 3 TH-positive cells per 8 mm^2 (Figure 4-8D). VPA alone significantly decreased the number of TH-positive cells by 38 % at 0.3 and 0.6 mM and by 55 % at 1.2 mM. LPS (40 μg/ml) alone declined the positive cells by 52 % to 17 ± 1 TH-positive cells per 8 mm^2. VPA pre-treatment for 2 hours prior to LPS treatment for 24 hours had no effect on the number of TH-positive cells across the concentrations tested, but caused a loss to the cell bodies and processes (Figure 4-9I).

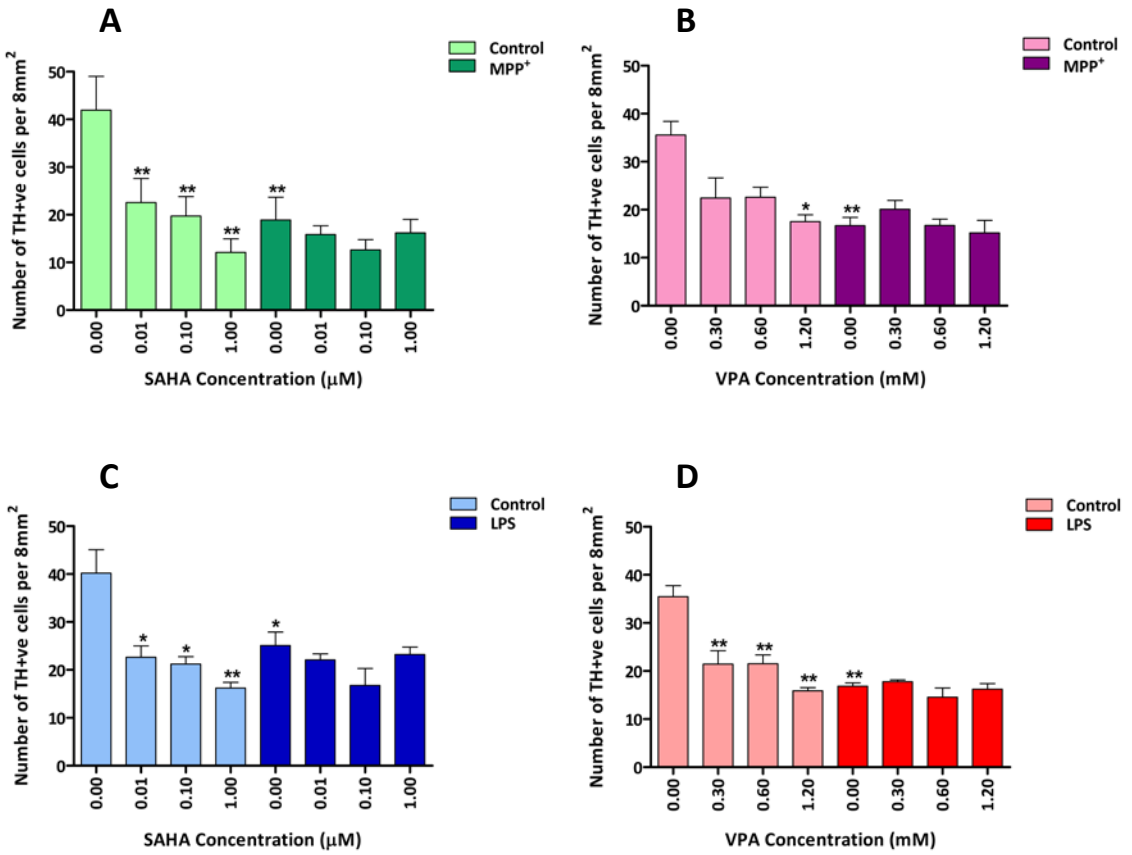

Figure 4-8 The effect of SAHA and VPA on the number of TH-positive cells following MPP^+ and LPS induced toxicity.

VM cultures (DIV7) were treated with (A-B) MPP^+ (3 µM) and (C-D) LPS (40 µg/ml) in the presence and absence of (A & C) SAHA (0.01, 0.1 and 1 µM) or (B & D) VPA (0.3, 0.6 and 1.2 mM). Dopaminergic cell loss was assessed by immunoperoxidase staining for TH. Data are the number of TH positive cells per 8 mm^2 and are expressed as mean ± SEM (n=3). *p<0.05, **p<0.01 compared to untreated control cells. Analysis by two-way ANOVA with Bonferroni test, followed by one-way ANOVA with Newman Keul's post hoc test.

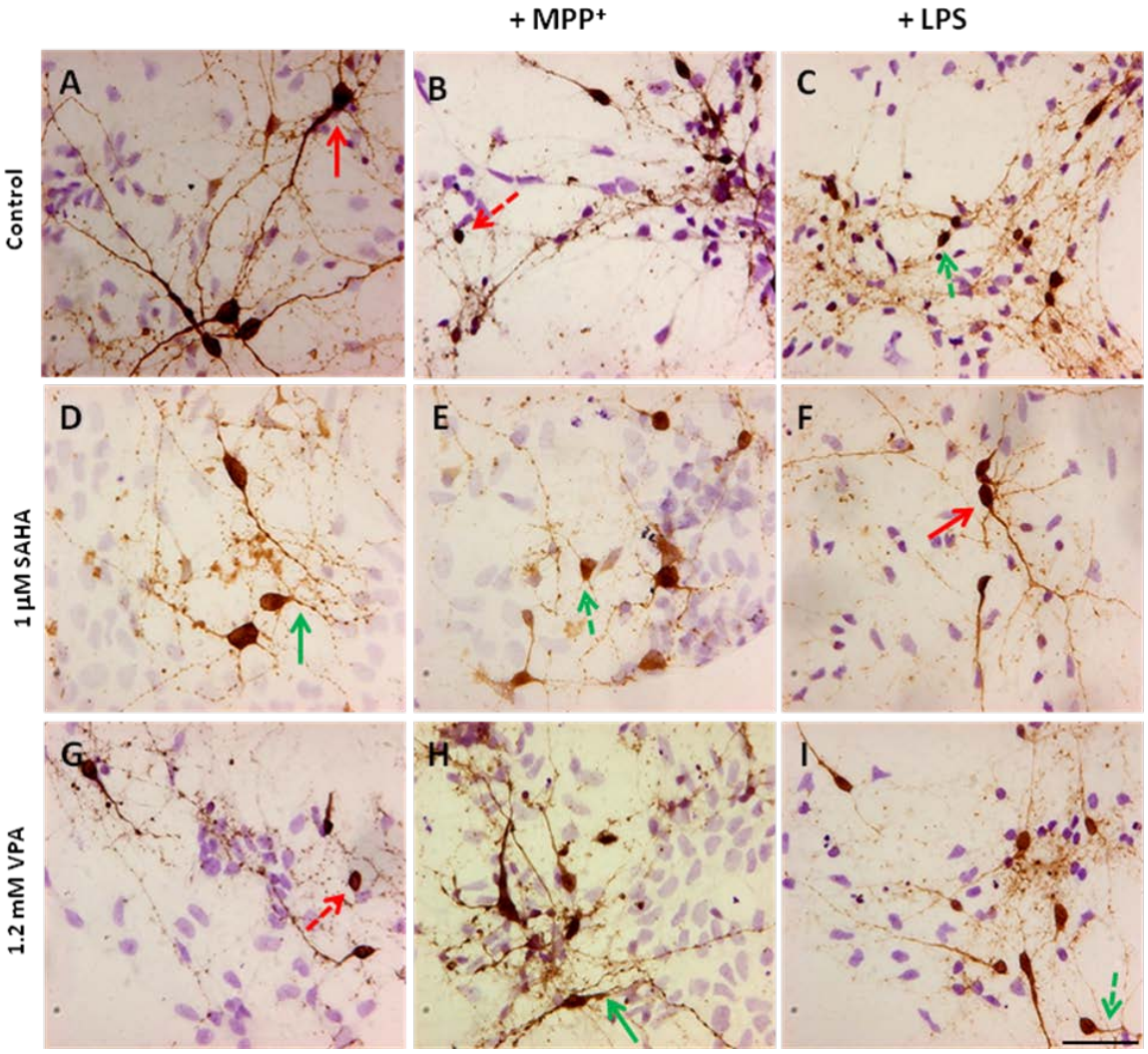

Figure 4-9 Immunoperoxidase staining of TH-positive cells in VM cultures following HDAC and toxin treatment.

VM cell cultures showing TH immunoreactivity in (A) untreated cells, and cells treated with: (B) MPP^+ (3 µM), (C) LPS (40 µg/ml), (D) SAHA (1.0 µM), (E) SAHA (1.0 µM) and MPP^+ (3 µM), (F) SAHA (1.0 µM) and LPS (40 µg/ml), (G) VPA (1.2 mM), (H) VPA (1.2 mM) and MPP^+ (3µM), (I) VPA (1.2 mM) and LPS (40 µg/ml). Cells were counterstained with cresyl violet (violet). Morphological changes are highlighted with arrows: normal TH-positive cell (solid red arrow), cell losing their dendritic nodes (solid green arrow), cell with shortened processes (broken green arrow) and complete loss of processes (broken red arrow). Scale bar = 100 µm is representative of all images. Photographs are typical of experiments performed in triplicate on 3 separate occasions.

4.3.5.2 The effect of HDAC inhibitors on GFAP-positive cells following MPP^+ and LPS exposure.

SAHA and MPP^+ treatments

Control VM cell cultures had 40 ± 10 GFAP-positive cells per 8 mm^2. Treatment with SAHA (0.01 - 1.00 µM) alone tended to increase the number of GFAP-positive cells by approximately 75 % (Figure 4-10A). MPP^+ (3 µM) alone increased the number of GFAP-positive cells by 185 % compared to the untreated cells. Pre-incubation of primary cultures with SAHA for 2 hours prior

to MPP^+ for 24 hours significantly prevented the MPP^+-induced increase in the number of GFAP-positive cells by 36 – 41 % across the concentrations tested.

VPA and MPP^+ treatments

Control VM cell cultures contained 40 ± 4 GFAP-positive cells per 8 mm^2. VPA (0.3 - 1.2 mM) alone tended to increase the number of GFAP-positive cells by approximately 73 % across the concentrations tested (Figure 4-10B). MPP^+ alone increased the number of GFAP-positive cells by 185 % compared to the untreated cells. Two hour pre-treatment with VPA prior to concomitant treatment with MPP^+ for 24 hours, prevented the MPP^+-induced increase in the number of GFAP-positive cells by 39 – 46 % across the concentrations tested, although it was only significant at the highest concentration of VPA (1.2 mM).

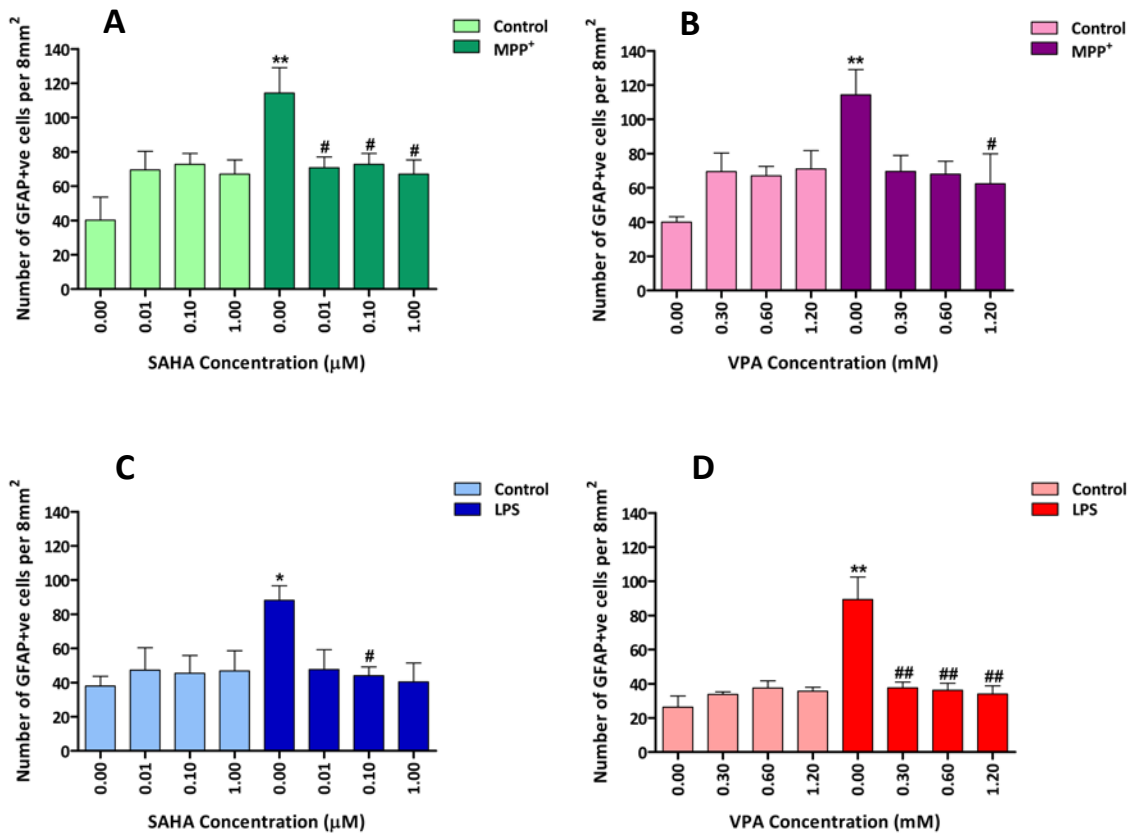

Figure 4-10 The effect of SAHA and VPA on the number of GFAP cells following MPP^+ and LPS exposure.

VM cultures (DIV7) were treated with (A-B) MPP^+ (3 μM) and (C-D) LPS (40 μg/ml) in the presence and absence of (A & C) SAHA (0.01, 0.1 and 1 μM) or (B & D) VPA (0.3, 0.6 and 1.2 mM). Astrocytic cell loss was assessed by immunoperoxidase staining for GFAP. Data are the number of GFAP positive cells per 8 mm^2 and are expressed as mean ± SEM (n=3). **p<0.01 compared to untreated control cells; #p<0.05, ##p<0.01 compared to MPP^+ or LPS alone. Analysis by one-way ANOVA with Newman Keul's post hoc test.

SAHA and LPS treatments

Control VM cell cultures had 38 ± 7 GFAP-positive cells per 8 mm^2. SAHA (0.01 – 1.00 μm) alone increased the number of GFAP-positive cells by approximately 20 % (Figure 4-10C). LPS (40 μg/ml) alone, increased the cells to 88 ± 8 GFAP-positive cells per 8 mm^2. Pre-treatment with SAHA for 2 hours prior to 24 hours treatment with LPS, prevented the LPS-induced increase in GFAP-positive cells in the range of 40 ± 3 - 47 ± 15 per 8 mm^2 at all the concentrations tested, with a significant effect at 0.10 μm.

VPA and LPS treatments

Control cultures had 25 ± 8 GFAP-positive cells per 8 mm^2 (Figure 4-10D). VPA (0.3 – 1.2 mm) alone caused a slight increase of approximately 20 % in the number of GFAP-positive cells. LPS (40 μg/ml) increased the number of cells to 89 ± 17 GFAP-positive cells per 8 mm^2 compared to the control. Two hours pre-treatment with VPA prior to 24 hours concomitant treatment with LPS prevented the increase in GFAP-positive cells by 34 ± 5 - 37 ± 5 per 8 mm^2 across all the concentrations tested compared to LPS alone.

The toxins and concentrations tested induced morphological changes of GFAP-positive cells (Figure 4-11). In the control sample, the cells looked fibrous with extended cytoskeleton with short processes (Figure 4-11A). However, treatment with MPP^+ and LPS caused some of the cells (approximately 60 - 70 %) to take on an activated morphology, with a re-organised cytoskeleton and long processes (Figure 4-11B & C), which is typical of a reactive astrocyte. SAHA and VPA alone treatments exhibited approximately 15 - 20 % of the activated morphology (Figure 4-11D & G). HDAC-I pre-treatment prior to MPP^+ and LPS incubations for 24 hours exhibited 30 – 40 % of the reactive astrocyte (Figure 4-11E & F, H & I).

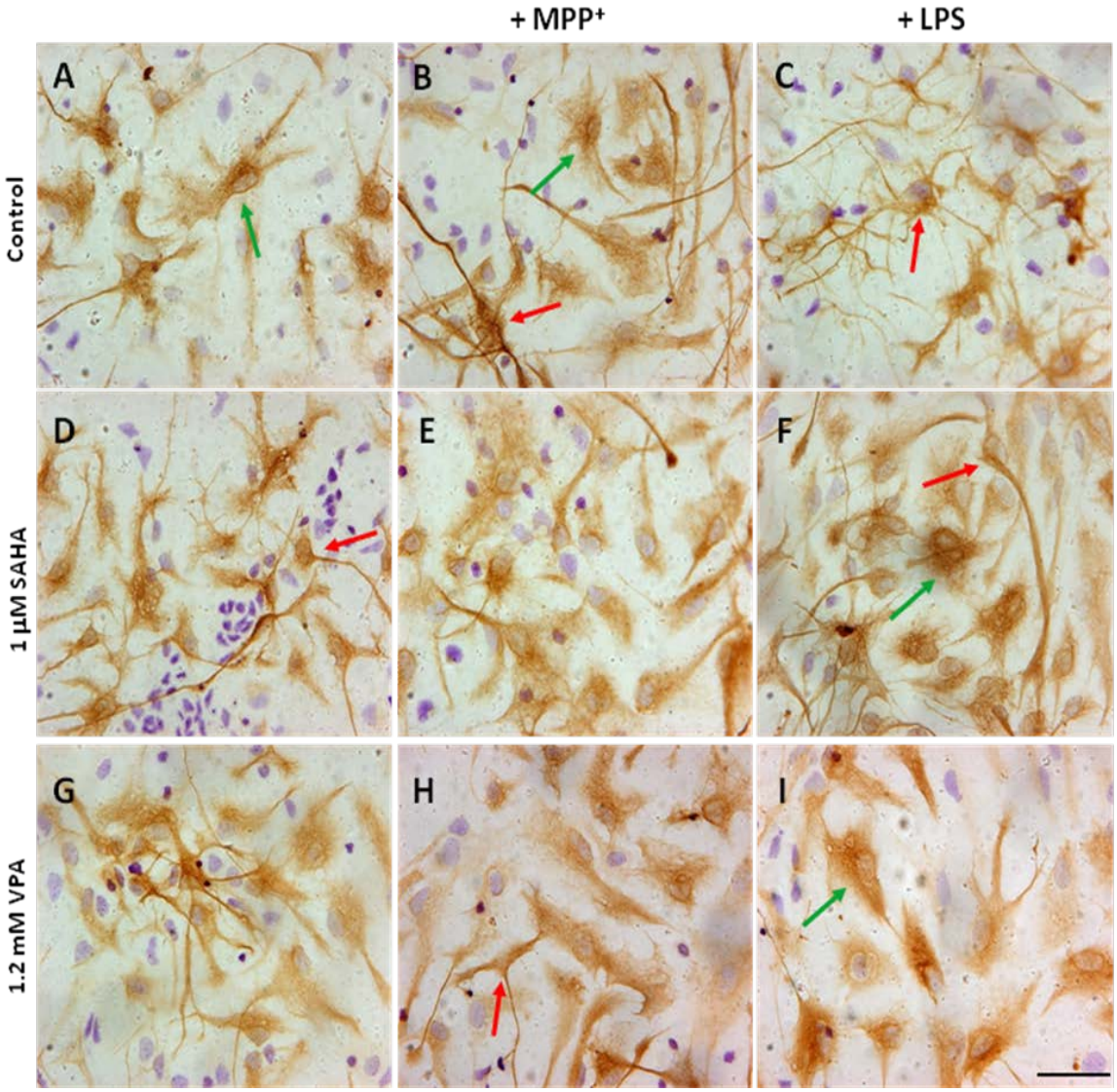

Figure 4-11 Immunoperoxidase staining of GFAP-positive cells in VM cultures following HDAC and toxin treatment.

VM cell cultures showing GFAP immunoreactivity in (A) untreated cells, and cells treated with: (B) MPP^+ (3 μM), (C) LPS (40 μg/ml), (D) SAHA (1.0 μM), (E) SAHA (1.0 μM) and MPP^+ (3 μM), (F) SAHA (1.0 μM) and LPS (40 μg/ml), (G) VPA (1.2 mM), (H) VPA (1.2 mM) and MPP^+ (3μM), (I) VPA (1.2 mM) and LPS (40 μg/ml). Cells were counterstained with cresyl violet (violet). Morphological changes are highlighted with arrows: normal GFAP-positive cell (green arrow), reactive GFAP-postive cell red arrow). Scale bar = 100 μm is representative of all images. Photographs are typical of experiments performed in triplicate on 3 separate occasions.

4.3.5.3 The effect of HDAC inhibitors on OX-42-positive cells following MPP^+ and LPS exposure.

SAHA and MPP^+ treatments

Control VM cell cultures contained 10 ± 2 OX-42-positive cells per $8mm^2$ (Figure 4-12). Treatment with SAHA (0.1 – 1 μM) alone induced approximately 36 – 63 % increase in the number of OX-42 immunoreactive cells. MPP^+ (3μM) alone increased the number of OX-42 cells to approximately 26 ± 2 cells/ 8 mm^2. Pre-treatment with SAHA for 2 hours prior to MPP^+

incubation for 24 hours significantly prevented the increase in the number of OX-42-positive cells by 27 – 38 % (Figure 4-12A).

VPA and MPP^+ treatments

Control VM cultures had 9 ± 1 OX-42 immunoreactive cells per 8 mm^2. Treatment with VPA (0.3 - 1.2 mM) alone significantly increased the number of OX-42 cells in a concentration dependent manner (Figure 4-12B). Treatment with MPP^+ (3 μM) alone significantly increased the number of OX-42-positive cells to 28 ± 2 cells per 8 mm^2 compared to the control. Pre-incubation with VPA for 2 hours prior to MPP^+ incubation for 24 hours significantly prevented the increase in the number of OX-42-positive cells by 30, 52 and 56 % at 0.3, 0.6 and 1.2 mM, respectively.

SAHA and LPS treatments

Control VM cultures contained 10 ± 2 OX-42-positive cells per 8mm^2 (Figure 4-12A). Treatment with SAHA (0.1 – 1 μM) alone increased the number of OX-42-positive cells by approximately 36 – 63 %. LPS (40 μg/ml) alone increased the number of OX-42 cells to around 26 ± 2 cells/ 8 mm^2. SAHA also tended to prevent the increase in the number of LPS-induced OX-42-positive cells, however, this difference was not statistically significant.

VPA and LPS treatments

Control VM cultures had 9 ± 1 OX-42-positive cells per 8 mm^2 (Figure 4-12B). VPA (0.3 - 1.2 mM) alone significantly increased the number of OX-42-positive cells in a concentration dependent manner. As expected, treatment with LPS (40 μg/ml) alone significantly increased the number of active OX-42-positive cells to 28 ± 2 cells per 8 mm^2 compared to the control. A similar effect was observed for the LPS treated cultures, where significant decreases by 29, 36 and 39 % were observed at 0.3, 0.6 and 1.2 mM respectively.

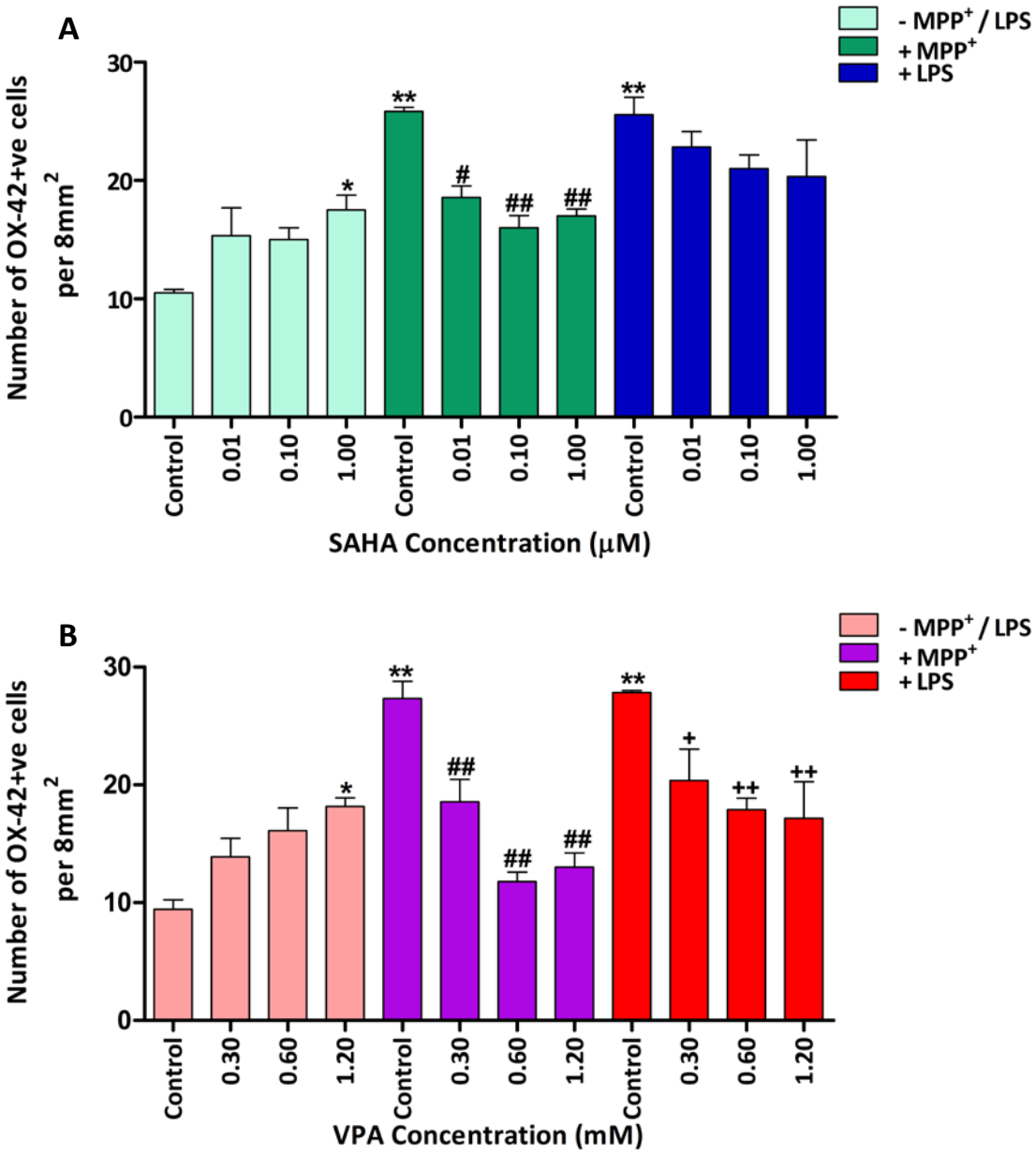

Figure 4-12 The effect of SAHA and VPA on the number of OX-42-positive cells following MPP^+ and LPS treatment.

VM cultures (DIV7) were treated with (A & B) MPP^+ (3 μM) and LPS (40 μg/ml) in the presence and absence of (A) SAHA (0.01, 0.1 and 1 μM) or (B) VPA (0.3, 0.6 and 1.2 mM). Cell loss was assessed by immunoperoxidase staining for OX-42. Data are the number of OX-42 positive cells per 8 mm^2 and are expressed as mean ± SEM (n=3). *p<0.05, **p<0.01 compared to untreated control cells; #p<0.05, ##p<0.01 compared to MPP^+ alone; +p<0.05, ++p<0.01 compared to LPS alone. Analysis by one-way ANOVA with Newman Keul's post hoc test.

The OX-42 immunoreactive cells were active taking an amoeboid morphology (Figure 4-13A-C). Approximately 2 % of partially active OX-42-positive cells were observed in the SAHA and VPA only treated conditions in the presence and absence of both MPP^+ and LPS (Figure 4-13D, G, F & I). In this state, the cells were more ramified and phagocytic, and processes were beginning to extend from the amoeboid cell body. Less than 1 % of OX-42 cells in the resting state were

124observed in the cultures, where the cells had very small cell bodies and extended processes (Figure 4-13F).

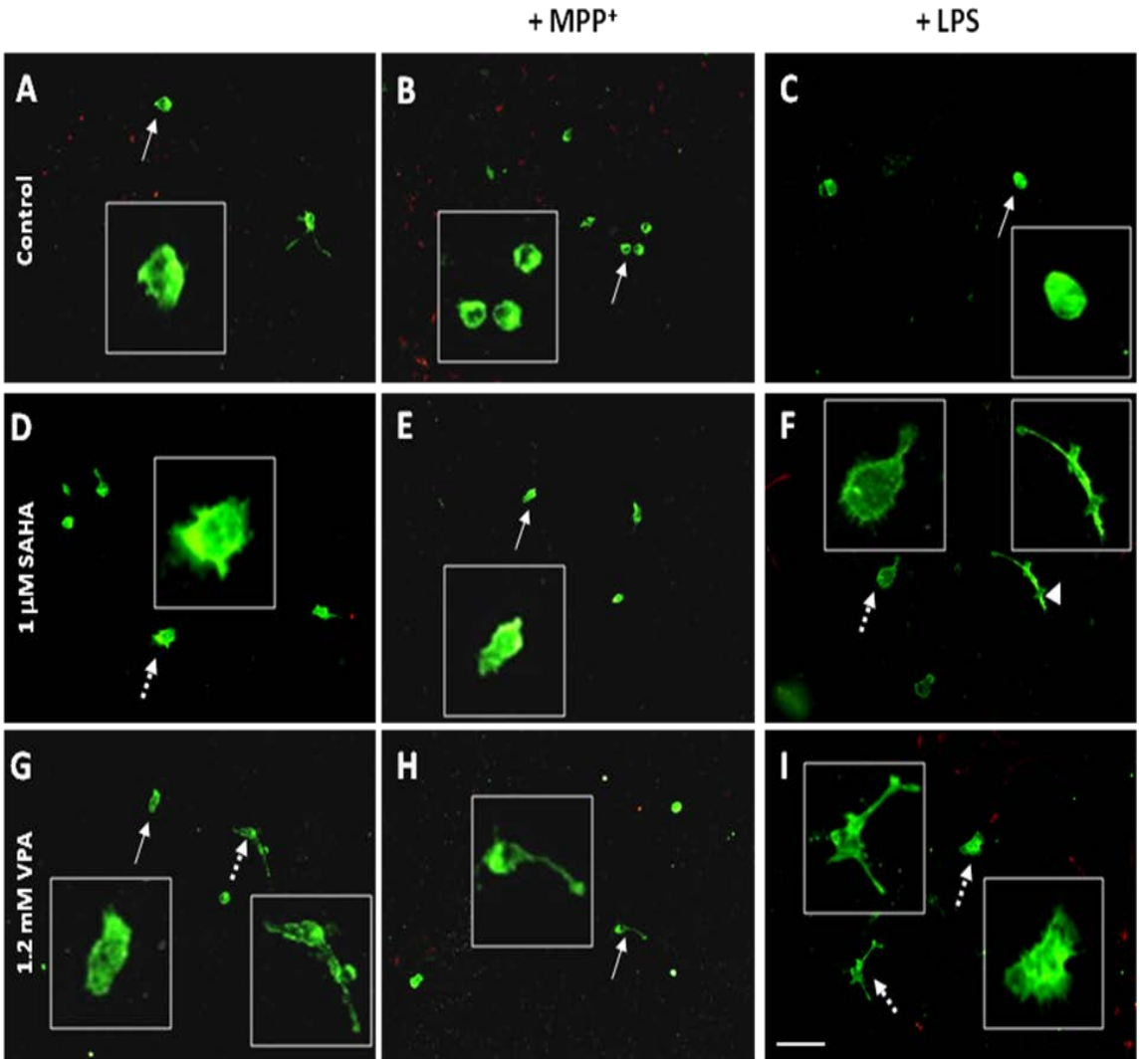

Figure 4-13 Immunofluorescence staining of OX-42 positive cells in VM cultures following HDAC and toxin treatment.

VM cell cultures showing OX-42 immunoreactivity in (A) untreated cells, and cells treated with: (B) MPP^+ (3 μM), (C) LPS (40 μg/ml), (D) SAHA (1.0 μM), (E) SAHA (1.0 μM) and MPP^+ (3 μM), (F) SAHA (1.0 μM) and LPS (40 μg/ml), (G) VPA (1.2 mM), (H) VPA (1.2 mM) and MPP^+ (3μM), (I) VPA (1.2 mM) and LPS (40 μg/ml). Cells were counterstained with cresyl violet (violet). Stages of microglial activation indicated with arrows: fully active state (solid arrow), partially active state (broken arrow), and resting state (arrow head). Scale bar = 200 μm. Photographs are typical of experiments performed in triplicate on 3 separate occasions.

4.4 Discussion

This study investigated the role of HDAC-Is in cell death induced by MPP^+ and LPS in VM cell cultures. It was hypothesised that HDAC inhibition would protect dopaminergic neurones from the biochemical and pathological changes linked to cell death in the SN induced by MPP^+ and LPS by reducing the number of inflammatory cells. In particular, this study aimed to: 1. characterise the dopaminergic and HDAC phenotype of the VM cell cultures. 2. determine the dopaminergic cell loss following MPP^+ and LPS-induced toxicity. 3. assess the role of HDAC inhibition on MPP^+ and LPS-induced loss of dopaminergic neurones, and 4. evaluate the effects of HDAC inhibition on the inflammatory changes induced by MPP^+ and LPS treatment.

4.4.1 Characterisation of VM cultures

The VM cultures (DIV7) showed positive immunolabelling for TH, GFAP and GAD confirming a mixed population of cells. The cultures were comprised of approximately 5 % dopaminergic cells, 55 % GABAergic cells, 8 % astrocytes and 0.2 % microglia. These results are in agreement with previous reports of 2-5 % TH, 48 % GAD, 2-17 % GFAP, and 0-0.1 % OX-42 immunopositive cells (Takeshima *et al.*, 1994a; Cheung *et al.*, 1997; Pardo *et al.*, 1997; Gilbert *et al.*, 2003; Qian *et al.*, 2006). ED-1 positive macrophages are also present in VM cultures (Ailane, 2011, personal communication), although this was not measured in this study. The characterisation of the remaining cell types were not determined in this study and is likely to be accounted for by other neuronal cells such as serotonergic, glutamatergic, cholinergic cells and cells that have not completely differentiated into dopaminergic neurones (Zurn & Werren, 1994; Spencer *et al.*, 1995; Rayport, 2001; Ducray *et al.*, 2006). The data however confirms the presence of other cell populations other than dopaminergic neurones in primary VM cultures, and importantly allows an interaction between cell types, particularly inflammatory cells and neurones to be closely investigated.

In order to establish whether HDAC-Is could have an effect on dopaminergic neurones, the expression and localisation of HDAC3, 4, 5, and 11 were determined in VM primary cultures. Double immunofluorescence staining showed that the four investigated HDACs are expressed in the mesencephalic cultures, and this study is the first to describe their localisation in dopaminergic neurones, although previous studies by Broide *et al.* (2007) showed their co-localisation of HDACs in neurones (anti-*NeuN* antibody) by double labelling, and Janssen *et al.* (2010) reported HDAC localisation in motor neurones (Broide *et al.*, 2007; Janssen *et al.*, 2010).

Importantly this study also showed that astrocytes and glial cells express HDACs. This is in agreement with Faraco *et al.* (2009) who showed that HDAC transcripts and activity are present

in mouse glial cultures, and that inhibition of HDAC with ITF2357 (SAHA structural analogue) increased acetylation levels in cultured astrocytes and microglia *in vitro* (Faraco *et al.*, 2009). The localisation of HDACs among these cell types, and the findings reported in this study are consistent with the widespread distribution of this enzyme family and specific HDAC expression in the brain (MacDonald & Roskams, 2008; Liu *et al.*, 2008; Shen *et al.*, 2008). The presence of HDACs suggests a role in cellular biological processes and provides a target for HDAC-Is.

4.4.2 Effect of HDAC-Is on MPP^+ and LPS-induced toxicity on dopaminergic neurones

As detailed in the previous chapter, MPP^+ causes dopaminergic toxicity by directly inhibiting mitochondrial complex I. LPS, on the other hand, does not exert its neurotoxicity directly on dopaminergic neurones, but through activation of microglia and astrocytes to release a variety of pro-inflammatory cytokines, such as TNF-α, IL-1α, IL-1β and IL-6 (Castano *et al.*, 1998; Le *et al.*, 2001).

As expected, increasing concentrations of MPP^+ caused a concentration-dependent decrease in the number of viable TH positive cells with an EC_{50} = 3 μM. This concentration is comparable to the range used in previous studies (1 – 10 μM) (Otto & Unsicker, 1993; Dodel *et al.*, 1998; Chung *et al.*, 2005; Jakobsen *et al.*, 2005). Similarly, LPS induced a concentration-dependent loss of dopaminergic cell with an EC_{50} of 40 μg/ml. This is in agreement with previously used LPS concentration in ranges of 30 – 80 μg/ml (Bronstein *et al.*, 1995; MCNaught & Jenner, 1999; Iczkiewicz *et al.*, 2010).

Pre-treatment with SAHA (0.01 – 1 μM) and VPA (0.3 – 1.2 mM) proved to be toxic to dopaminergic neurones by reducing the number of viable cells following treatment alone and in conjunction with MPP^+ and LPS at all concentrations tested. This supports the finding in the cell lines described in Chapter 3, but is contrary to previous work by Chen *et al.* (2006) and Wu *et al.* (2008), who both showed that HDAC-Is VPA, TSA and sodium butyrate protected dopaminergic neurones from MPP^+ and LPS-induced toxicity in neurone-glia cultures (Chen *et al.*, 2006; Wu *et al.*, 2008). This protective effect was also recently confirmed with SAHA by Chen and colleagues (Chen *et al.*, 2012). All three groups showed this protection to be dependent on the ability of the HDAC-Is to up-regulate the expression of neurotrophic factors GDNF and BDNF from astrocytes.

The toxicity of HDAC-Is, as exhibited in the cell lines (Chapter 3), has to be considered as a contributing factor to the neuronal cell loss. HDAC-Is have inherent toxicity and their prolonged treatment at high doses induces neuronal death, which compromises their neuroprotective effect in dopaminergic neurones (Jeong *et al.*, 2003). VPA, in particular, can exacerbate neuronal

death in primary cultures of cerebellar granule neurones (Jin *et al.*, 2005), similar to the effect observed in cell lines. This HDAC-I-induced toxicity may be partly due to the activation of transcription factor E2F1 by HDAC inhibition, which plays a part in pro-apoptotic signalling in these neurones and over-expression of this protein induces neuronal apoptosis (Boutillier *et al.*, 2002; Boutillier *et al.*, 2003). This finding makes it less surprising as HDAC-I alone treated cells were observed to look damaged, which was depicted by the disintegrated cell processes, as well as the loss of dopaminergic neurones.

Regardless of the above findings, other contributing factors to the neuronal cell loss are the presence of growth factors and medium composition. Growth factors produced by neurones and neurotrophic factors from astrocytes are known to play an important role in the development and survival of neurones in culture (Engele & Bohn, 1991; Walsh *et al.*, 1992; Takeshima *et al.*, 1994b; Young *et al.*, 2000). The cell density used in the present study (2×10^5) compared to densities in the previously mentioned studies (5×10^5) might result in the medium being enriched with growth factors in the latter. This would therefore have a positive effect on promoting neuronal survival (Peng *et al.*, 2005; Chen *et al.*, 2006; Wu *et al.*, 2008).

The HDAC-I administration in this study were performed in serum-free medium. This has been previously demonstrated to be toxic to cells (Takeshima *et al.*, 1994a; Bar-Am *et al.*, 2005) and confirmed by studies on cell lines as described in Chapter 3. This toxicity of serum-free medium was however not observed in characterisation studies and did not have an effect on the number of TH-positive cell numbers (Brzozowski, 2010, personal communication). However, it cannot be disputed that the absence of serum would make the cells more vulnerable to HDAC-I and/ or toxin treatment. HDAC-I and toxin challenges were chosen to be performed under serum-free conditions to ensure the protective effects of TH-positive cells was due to the HDAC-Is themselves and not the serum, as it contains cell survival promoters, such as fibronectin - the main cell attachment promoting protein in serum which encourages cell survival and growth (Hayman *et al.*, 1985; Takeshima *et al.*, 1994a).

Glial cell proliferation has been reported to be suppressed in serum-free mesencephalic cultures (Takeshima *et al.*, 1994a), but this study only looked at the effects of serum-deprivation from day 1 of seeding the cells. In the present study, cell suspensions were seeded and promoted to grow in serum-containing medium for 7 days prior to serum deprivation for 26 hours. Cell maturation, neurite elongation and complexity is complete at DIV5 and maintained till DIV10 (Shimoda *et al.*, 1992), thus indicating that at DIV7, the cells are in the mature phase. As 26 hours is a short period of time, it can be assumed that serum-deprivation would have no

significant effect on the levels of growth factors in medium and on the neuronal survival (Brzozowski, 2010, personal communication). This hypothesis will however have to be tested in the future for confirmation and clarification.

It is possible that the loss of TH-positive cells is due to the HDAC-Is affecting gene expression and in turn down-regulating TH expression. Indeed, experiments with HDAC-Is sodium butyrate and Trichostatin A reduced the mRNA levels of TH in PC12 cell lines (Aranyi *et al.*, 2007). This theory is probable as the number of TH-positive cells counted in the HDAC-I alone treatments is similar to the number of cells accounted for in the HDAC-I and toxin concomitant treatments. But as mRNA levels of TH were not measured in this study, further experiments will need to be undertaken to confirm this hypothesis.

Even though many factors mentioned above may have contributed to the loss of TH-positive cells, the evidence still shows that similar to cell lines, these HDAC-Is are also toxic to dopaminergic neurones and exacerbate the toxicity of MPP^+ and LPS.

4.4.3 Effect of HDAC-Is on MPP^+ and LPS-induced toxicity on inflammatory changes

This study hypothesised that HDAC-Is would modulate inflammatory processes. As expected, this study showed a significant increase in the number of astrocytes and microglia following MPP^+ and LPS treatment indicated by the increase in GFAP and OX-42 positive cells, signifying the induction of an inflammatory response in the cultures. This proliferation of astrocytes and microglia has been attributed to the secretion of a variety of pro-inflammatory and neurotoxic factors, including IL-1β, TNF-α, NO and ROS in mesencephalic cultures (Liu *et al.*, 2000; Gayle *et al.*, 2002; Qin *et al.*, 2002; Sofroniew, 2009). This suggests that the increase in glial cells is a result of cell death, but in turn become responsible for cell death. In other words, on the onset of neuronal damage, toxic compounds are released by the neurones and these are scavenged by glial cells to protect neighbouring neurones (Rosenberg, 1991; Aloisi, 2001). But the activation of the glial cells is associated with production and secretion of neurotoxic factors which in turn result in further neuronal damage.

Pre-treatment of VM cultures with SAHA (0.01 – 1 μM) and VPA (0.3 – 1.2 mM) alone initiated a glial reaction in astrocytes and microglia. This increase in astrocytes and microglia is understandable, as HDAC-Is alone have been shown to be toxic to TH-positive cells, so their incorporation to cultures would induce an activation of inflammatory cells to exert their defence mechanisms. Interestingly, this was not observed by Peng *et al.* (2005) and Chen *et al.* (2007) who both showed that HDAC-I's VPA, SB and TSA alone did not induce an inflammatory response

in their mesencephalic cultures, although this may reflect the differences in plating densities and medium composition to promote cell survival as discussed above. The two groups plated their cells at higher densities than that of this study, and also used serum-containing medium. Both factors have been explained to promote cell survival.

Importantly, this present study observed concomitant treatment of cultures with SAHA or VPA with MPP^+ or LPS significantly reduce the numbers of GFAP and OX-42 positive cells to levels similar to that of HDAC-I alone treatments. This is in agreement with Peng *et al.* (2005) and Chen *et al.* (2007), who also showed that VPA pre-treatment suppressed LPS-induced activation of microglia accompanied by a reduced release of pro-inflammatory factor TNF-α, decreased nitrite accumulation indicative of reduced NO production, and reduced ROS production.

Even though the levels of pro-inflammatory factors were not measured in this study, it is proposed that the suppression of microglia may be due to the HDAC-Is inhibiting the transcription of the pro-inflammatory factors and in turn resulting in a reduced number of inflammatory cells. This effect was shown by Faraco *et al.* (2009), who observed a reduction in transcript levels of pro-inflammatory factors iNOS, COX-2 and IL-1β; and a concentration-dependent reduction in TNF-α release following concomitant treatment with HDAC-Is SAHA and ITF2357 and LPS in primary mixed cultures of astrocytes and microglia (Faraco *et al.*, 2009).

Chen and colleagues (2007) suggested that the mechanism by which HDAC-Is reduced the inflammatory process may be due to apoptosis of microglia. This was demonstrated by typical hallmarks such as phosphatidylserine externalisation, internucleosomal DNA fragmentation and chromatin condensation. This theory is far from convincing because if the HDAC-Is were in actual fact inducing the apoptotic process, then one would expect little or no glial cells, in the HDAC-I alone treatments too, however the opposite was true. This confirms the most likely reason for the decrease in inflammatory cells to be due to inhibition of the transcription of pro-inflammatory factors.

4.4.4 Conclusion

In conclusion, this study confirms the toxicity of MPP^+ and LPS in VM cell culture, and shows the localisation of HDAC isoforms in dopaminergic neurones for the first time, as well as confirming their localisation in inflammatory cells. Similar to the previous chapter, the HDAC-Is did not protect dopaminergic neurones against MPP^+- and LPS-induced neurotoxicity, and proved to be toxic to the neurones when they were treated alone. Pre-treatment with SAHA and VPA, on the other hand had an impact on inflammation by reducing the number of astrocytes and microglial

cells following toxin treatment. In spite of the reduction in the number of inflammatory cells, the change in glia did not influence the loss of TH and resulted in decreases in the number TH-positive cells. The reason for this is unknown and was unfortunately not conclusive in the present study. These findings do however suggest an anti-inflammatory role for HDAC-Is.

In light of the contradictory results shown in the primary culture, which may relate to the expression of trophic factors, is dependent on the methodology used. These data do not preclude a protective effect of HDAC-Is *in vivo*. The HDAC-Is were toxic in both cell lines and primary culture and resulted in an increase in the loss of TH-positive cell loss. The only exception was the decrease in inflammatory cells. It is therefore necessary to confirm these present findings in an *in vivo* model of PD, as it possesses physiologically relevant systems to aid in assessing the effects of SAHA and VPA in a living organism. It has also been suggested that a decrease in inflammation, as observed in primary cultures, protect dopaminergic neurones *in vivo*. This may be dependent on the cell composition. Therefore an *in vivo study* will be undertaken to conclude what might happen in the PD brain.

Chapter 5 The effect of HDAC-Is in preventing pathological changes in 6-OHDA- and LPS-lesioned mice.

5.1 Introduction

It was originally hypothesised that inhibition of HDAC would protect dopaminergic cells from toxin-mediated cell death in PD. However, when testing this hypothesis, it was found that treatment of neuroblastoma cell lines with the HDAC-Is, VPA and SAHA, was in fact toxic to the cells. Indeed, the HDAC-Is enhanced cell death following exposure to H_2O_2 and MPP^+. It was proposed that this was due to the mono-cellular composition of the cell lines, and it was hypothesised that other cell types, in particular glia, would enable the HDAC-Is to exert a protective effect. However, this hypothesis was rejected in Chapter 4 as HDAC inhibition did not protect dopaminergic neurones from MPP^+- and LPS-induced cell death in rat E14 VM primary cultures where glial cells are present and have been shown to contribute to cell death. This finding contradicted the results of previous studies which reported that HDAC inhibition protected dopaminergic neurones against MPP^+- and LPS-induced cell death (Chen *et al.*, 2006; Wu *et al.*, 2008; Chen *et al.*, 2012), but this was assumed to be due to differences in protocols. However, the study in VM culture was not entirely negative as concomitant treatment of VM cultures with the HDAC-Is and MPP^+ or LPS prevented the expected increase in astrocytes and microglia compared to the toxin treatment alone. The interpretation of this finding is difficult to assess, however, HDAC-Is have previously been associated with anti-inflammatory activity in models of rheumatoid arthritis (Grabiec *et al.*, 2008), traumatic brain injury (Zhang *et al.*, 2008) and multiple sclerosis (Gray & Dangond, 2006); and this might explain the reduction in glial cell number observed.

Even though pro-inflammatory factors such as TNF-α and NO were not measured in the study, the possibility remains that HDAC-Is might protect dopaminergic neurones through an anti-inflammatory mechanism in a more complex physiological environment such as occurs *in vivo* in the mature rodent brain. So far there has been very little *in vivo* investigation of the protective effects of HDAC-Is, however, importantly, in the MPTP-treated mouse, HDAC-I phenylbutyrate attenuated the depletion of striatal dopamine content and protected nigral dopaminergic neurones (Gardian *et al.*, 2004). Although it was not determined whether this was mediated via an effect on gliosis. For this reason, the studies reported in this Chapter investigated the effects of the HDAC-Is, VPA and SAHA on dopaminergic neuronal survival and gliosis in the SN following unilateral lesioning using 6-OHDA and LPS in mice. In particular, this study addressed the potential mechanism through which the HDAC inhibitors might potentially exert a protective effect.

5.1.1 Hypothesis

It was hypothesised that inhibition of HDACs protect against 6-OHDA and LPS-induced degeneration of dopaminergic neurones in the mouse nigrostriatal pathway *in vivo* through a reduction in glial cell activation and recruitment.

5.1.2 Aims

To test this hypothesis, this study was devised to investigate the effect of SAHA and VPA on cell death and inflammatory cells induced by partial 6-OHDA- and LPS-lesions of the nigrostriatal pathway in mice. Specifically, the aims were to:

1. Determine the localisation of HDACs within dopaminergic and inflammatory cells in the SN of mouse brain.
2. Establish whether VPA and SAHA can cross the blood brain barrier and induce hyperacetylation.
3. Examine whether SAHA and VPA can protect against 6-OHDA- and LPS-induced dopaminergic cell loss in mouse SN.
4. Investigate whether HDAC-Is alter the inflammatory response induced by 6-OHDA and LPS.

5.2 Materials and Methods

Mouse brain sections were initially double-labelled to determine the presence of HDACs within dopaminergic and inflammatory cells (Section 5.2.2). Following that, HDAC activity in the mouse brain and penetration of the HDAC-Is, VPA and SAHA, across the blood brain barrier were investigated by HDAC assay (Section 5.2.3.4) and Western blotting (Section 5.2.3.6), on nuclear and histone extracts, respectively. Once these were established, mice were treated daily with HDAC-Is, VPA and SAHA, for 10 days following intrastriatal 6-OHDA and LPS lesions. On completion of drug administration, the mice were culled and their brain tissue was processed for immunoperoxidase staining, where the effects of VPA and SAHA on dopaminergic and inflammatory cells were investigated. Detailed methodologies are described below.

5.2.1 Animal husbandry

Male C57BL/6J mice (Harlan, Bicester, UK), weighing 25-30 g, were singly housed in a temperature controlled room of 23^{o}C (King's College London Biological Services Unit) with a 12 hour light-dark cycle and unlimited access to pelleted food and water. All experimental procedures were carried out in accordance with the Animals (Scientific Procedures) Act 1986 under the UK Home Office license number 70/6898.

5.2.2 Double immunoflourescence

Mouse brains were perfused with 0.1 M PBS, pH 7.4 and post-fixed in PFA (4 %) in 0.1 M PBS for 7 days at 4^{o}C. This was followed by storage in cryoprotective solution composed 0.1 M PB containing sucrose (30 %) and sodium azide (0.05 %) also at 4^{o}C as described in Section 2.3.1. The brains were cut into coronal sections (30 m) at the
Section 2.6.4. Double immunofluorescence staining was used to determine the co-expression of TH, GFAP and OX-42 with HDAC3, 4, 5 and 11 as described in Section 2.6.5. Briefly, brain sections were blocked with 1 % goat and donkey serum for 30 minutes at room temperature followed by overnight incubation in primary antibodies TH (1:200), GFAP (1:200), OX-42 (1:50) and HDAC 3 (1:500), HDAC 4 (1:500), HDAC 5 (1:200) and HDAC 11 (1:500) (Table 2-2), at 4^{o}C. On the next day, the sections were incubated with Alexa Fluor 488 (green) and Alexa Flour 594 (red) secondary antibodies (both 1:500) (Table 2-3) for 90 minutes in the dark. The sections were rinsed in 0.1 M PBS and mounted with Vectashield® Hard Set mounting medium for fluorescence as described in Section 2.6.5.

5.2.3 Biochemical techniques

To determine whether HDAC-Is penetrate the blood-brain barrier, mice were dosed with VPA (200 and 400 mg/kg; i.p) and SAHA (100 mg/kg; s.c). Post-injection, tissue was collected as

described in Section 5.2.3.2, and histone and nuclear extracts were collected for HDAC assay to determine HDAC activity, and Western blotting to determine levels of acetylated histones.

5.2.3.1 HDAC-I preparation

The HDAC-I, VPA (200 and 400 mg/kg) was freshly prepared as free base in 0.9 % saline on the day of the procedure. SAHA (100 mg/kg) was freshly dissolved in 5M HOP-β-CD.

5.2.3.2 Tissue preparation

Male mice were treated with single injection of VPA (200 and 400 mg/kg) or its vehicle (0.9 % saline; 10 ml/kg) intraperitoneally (i.p); or SAHA in HOP-β-CD (100 mg/kg) or its vehicle (5M HOP-β-CD; 5 ml/kg) subcutaneously (s.c). Two hours later, the animals were killed by decapitation using a guillotine. The brain was removed from the skull and dissected midsagitally, flash-frozen in liquid nitrogen and stored at -70^{o}C until needed for nuclear or histone extraction.

5.2.3.3 Nuclear extraction of brain tissue homogenates for HDAC assay

Nuclear extraction was performed using a nuclear extraction kit according to the manufacturer's instructions (Cayman Chemical supplied by Cambridge Bioscience Ltd, Cambridge). In summary, brain tissue was weighed, cut into small pieces, collected into an eppendorf and kept on ice. Tissue was homogenised in ice-cold hypotonic buffer supplemented with Dithiothreitol (DTT; 10 mM) and Nonidet P-40 (NP-40; 10 %) in a 1:4 w/v ratio, and incubated on ice for 15 minutes. The homogenate was centrifuged at 300 g for 10 minutes at 4^{o}C, and the supernatant was transferred into a pre-chilled eppendorf. The pellet was resuspended in hypotonic buffer (500 μl) and incubated on ice for 15 minutes. Subsequently NP-40 (10 %; 50 μl) was added to the homogenised pellet, centrifuged at 14,000 g for 30 seconds in a microcentrifuge. The two supernatants, containing the cytoplasmic fraction, were combined, aliquoted (100 μl) and stored at -70^{o}C.

The pellet was resuspended in ice-cold extraction buffer (50 μl) supplemented with protease and phosphatase inhibitors (Nuclear Extraction Kit, Cayman Chemical supplied by Cambridge Bioscience Ltd, Cambridge). The suspension was vortexed for 30 seconds at the highest setting and placed on ice for 10 minutes. The vortex and incubation on ice was repeated 5 more times to make a total of 6 cycles. After the last cycle, it was centrifuged at 14,000 g (Biofuge Fresco, Heraeus) for 10 minutes at 4^{o}C. The supernatant, containing the nuclear fraction was aliquoted into clean chilled eppendorfs, flash frozen in liquid nitrogen and stored at -70^{o}C until needed for HDAC assay (Section 5.2.3.4).

5.2.3.4 HDAC assay

The HDAC assay entails incubating an acetylated lysine substrate with samples containing HDAC protein. Deacetylation of the substrate releases a fluorescent product which is measured. The assay was performed in a black clear bottom 96 well microplate, and each sample and control was run in duplicate. Isolated nuclear extracts (10 µl) (Section 5.2.3.3) was added to assay buffer (140 µl; 25 mM Tris-HCl, pH 8.0, 137 mM NaCl, 2.7 mM KCl, 1 mM $MgCl_2$). This was followed by the HDAC inhibitor Trichostatin A (positive control) (TSA; 10 µl; 21 µM) supplied in kit, SAHA EC_{50} concentration (10 µl, 20 µM) and VPA EC_{50} concentration (10 µl; 60 µM), HOP-β-CD (10 µl; 5M), saline (10 µl) or assay buffer (10 µl) to vehicle. SAHA and VPA EC_{50} concentrations were obtained from concentration-response assays in Figure 5-1 using this protocol. The reaction was initiated with HDAC substrate Boc-Lys(Ac)-7-Amino-4-Methylcoumarin (MP Biomedicals, Cambridge, UK) (10 µl, final concentration 200 µM). The plate was covered and incubated in an orbital shaker (Aerotron, Bottmingen, Switzerland) for 30 minutes at 37°C. Subsequently, HDAC developer (40 µl) (Cambridge Bioscience, Cambridge, UK) was added to each well and incubated at room temperature for 15 minutes, to release the fluorescent product. Fluorescence was measured by spectrophotometer (Spectramax Gemini XS), and the fluorophore was analysed using an excitation wavelength of 350 nm and an emission wavelength of 455 nm (Figure 5-1).

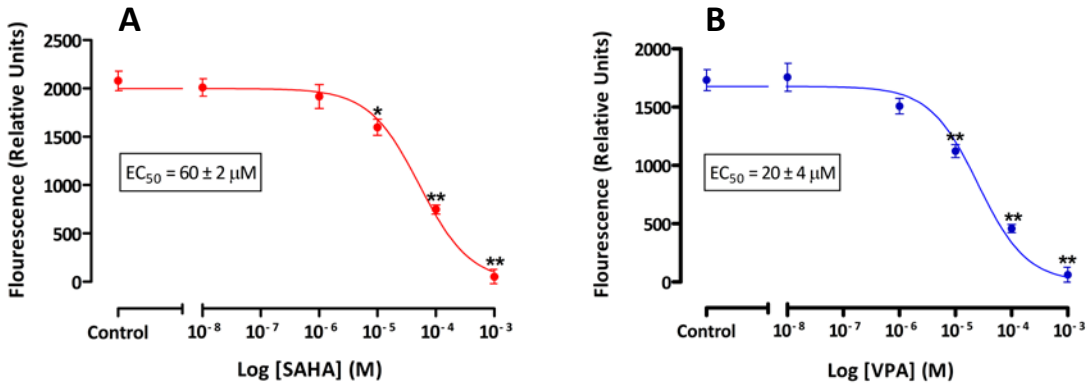

Figure 5-1 EC_{50} of VPA and SAHA following HDAC assay.
Nuclear extracts from brain tissue homogenates were treated with (A) SAHA (10^{-3} – 10^{-8} M) and (B) VPA (10^{-3} – 10^{-8} M). HDAC activity was assessed by HDAC assay. Non-linear regression curve was fitted to calculate EC_{50}. Data are expressed as mean ± SEM (n=3); *p<0.05, **p<0.01 compared to control cells (one-way ANOVA followed by Newman-Keuls test).

5.2.3.5 Histone extraction for western blotting

Brain tissue was homogenised (1:4 w/v) in cold buffer followed by centrifugation (Biofuge Fresco, Heraeus) at 800 g for 10 minutes at 4°C. The supernatant, containing the cytosolic fraction was discarded and the pelleted nuclei were resuspended in 0.2 M sulphuric acid (H_2SO_4) (500 µl) prior to 30 minutes incubation on ice. Centrifugation was repeated at 14000 g for 10 minutes at 4°C. The supernatant was collected and transferred into a fresh eppendorf and

proteins were precipitated on ice with precipitation buffer (250 µl). After 30 minutes incubation, the supernatant was centrifuged at 14000 g for 10 minutes at 4°C, and the protein pellet was washed by centrifugation at 14000 g for 5 minutes each with ice-cold acetone supplemented with HCl (0.1 %), followed by ice-cold acetone. The protein precipitates were collected between washes, and the resulting purified proteins were resuspended in Tris-HCl (10 mM; pH 8.0), and stored at -80°C.

Table 5-1 Buffers used for histone extraction.

Buffer	Components	Source
Lysis Buffer	10 mM Tris-HCl, pH 6.5	BDH, VWR International, Lutterworth, UK
	50 mM Sodium bisulfite	Sigma-Aldrich, Dorset, UK
	1 % Triton-X-100	Sigma-Aldrich, Dorset, UK
	10 mM $MgCl_2$	Sigma-Aldrich, Dorset, UK
	8.6 % Sucrose	Sigma-Aldrich, Dorset, UK
Homogenising Buffer	10 mM Tris-HCl	BDH, VWR International, Lutterworth, UK
	5 mM Sodium fluoride (NaF)	Sigma-Aldrich, Dorset, UK
	1 mM sodium orthovanadate (Na_3VO_4)	Sigma-Aldrich, Dorset, UK
	1 mM ethylenediamine tetraacetic acid (EDTA)	Sigma-Aldrich, Dorset, UK
	1 mM ethylene glycol tetraacetic acid (EGTA)	Sigma-Aldrich, Dorset, UK
	320 mM sucrose	Sigma-Aldrich, Dorset, UK
Precipitation Buffer	100% trichloroacetic acid	Sigma-Aldrich, Dorset, UK
	4 mg/ml deoxycholic acid	Sigma-Aldrich, Dorset, UK

5.2.3.6 Western blotting for histone acetylation

Western blot technique was used to detect the levels of histone H4 acetylation following HDAC-I treatment. The technique is described in detail in Section 2.4. Histone extracts prepared as described in Section 5.2.3.5, were resolved onto a SDS-PAGE gel (8-10 %) and transferred onto a PVDF membrane. The membrane was blocked with 5 % milk in TBS-T for 1 hour, and incubated with primary antibodies against Histone H4 (1:2000) overnight at 4°C. After incubation with anti-rabbit IgG-horseradish peroxidise (HRP)-conjugated secondary antibody (1:2000) for 1 hour, bands were visualised by the enhanced chemiluminescence system detailed in Section 2.4.4.

5.2.4 The HDAC-I preparation for neuroprotection study

5.2.4.1 VPA preparation

The HDAC-I, VPA (200 and 400 mg/kg) was freshly prepared as described in Section 5.2.3.1.

5.2.4.2 SAHA preparation

SAHA was administered in drinking water and prepared as previously described (Hockly *et al.*, 2003). To achieve this, SAHA was complexed in 5 molar equivalents of 2-hydroxypropyl-β-cyclodextrin (HOP-β-CD) in filtered, irradiated water at SAHA concentration of 0.67 g/l which resulted in an estimated dose of 160 mg/kg/day.

In order to solubilise the compound, the mixture was brought to a boil and kept boiling for two minutes before being cooled slowly to room temperature. The resultant solution was colourless.

The mice were housed individually and the drinking water containing SAHA was changed every 3 days. The stability of SAHA was confirmed by personal communication with Professor Gillian Bates (2011). Preliminary studies measuring the volumes of water, HOP-β-CD and SAHA consumed by the mice showed there was no difference between the volumes of water consumed. On average, 5.6 - 6 mls of liquid was drunk each day by a 25g mouse (Figure 5-2).

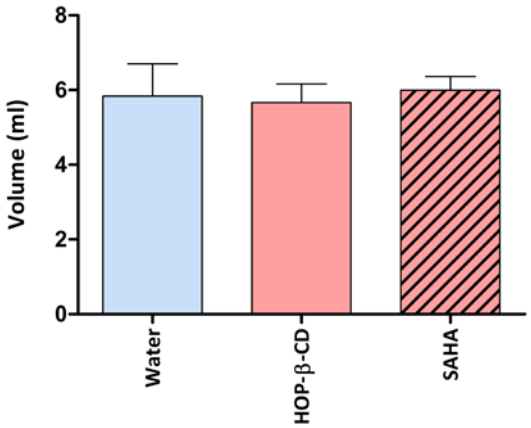

Figure 5-2 Volumes of water, HOP-β-CD and SAHA consumed by C57BL/6J in 24 hours.
Liquid intake of water, HOP-β-CD and SAHA of 25-30g mice were measured over 3 days. Data are mean ± SEM (n=3). Data was analysed by one way ANOVA.

5.2.5 6-Hydroxydopamine and LPS-induced destruction of the nigrostriatal pathway

5.2.5.1 6-Hydroxydopamine preparation

The dose of 6-OHDA-hydrochloride (7.5 μg in 4 μl; Sigma-Aldrich, Dorset, UK) was calculated as a free base and dissolved in 0.9 % saline containing 0.05 % L-ascorbic acid on ice on the day of

surgery. Aliquots (200 μl) were protected from light exposure and stored on ice until the surgical procedure.

5.2.5.2 Lipopolysaccharide preparation

Purchased Lipopolysaccharide, E. coli O55: B5 (Merck Chemicals Ltd, Nottingham, UK) was reconstituted in 0.9 % saline following manufacturer's instructions and stored at 4^{o}C. On the day of surgery, the stock was diluted to 7.5 μg/4 μl, aliquoted (200 μl), wrapped in foil to protect from light exposure, and stored on ice until the surgical procedure.

5.2.5.3 Intrastriatal administration of 6-OHDA and LPS

On the day of surgery, mice were anaesthetised with isofluorane (4 % in medical oxygen) in a chamber for 2 – 3 minutes then placed securely into a Kopf stereotaxic frame, with the ear bars positioned symmetrically, where the isofluorane was maintained at 1 – 2 % in medical oxygen. The temperature was maintained at 37^{o}C during the entire procedure using a homeothermic blanket. The mice head was shaved with excess hair cleaned first with isopropyl alcohol swabs and anaesthetised with 5 % EMLA^{TM} cream. An incision was made to expose the skull between the ears using a disposable scalpel. Scull was cleaned using a cotton bud, and hole was drilled above the site of injection using a sterilised hand drill (co-ordinates according to the mouse brain atlas of Paxinos and Watson (2004): Anterior = -0.02 mm, Lateral = +2.0 mm, and Ventral= -3.0 mm) (Figure 5-3). Toxin injection was performed using a 10 μl 70IRN Hamilton microsyringe fitted with a 26s gauge Hamilton needle (Essex scientific laboratory supplies ltd, Essex, UK). 6-OHDA and LPS (both 4 μl) or vehicle (sham, 4 μl; 0.9 % saline containing 0.05 % L-ascorbic acid; or 4 μl 0.9 % saline) were injected into the left striatum, at a flow rate of 1 μl per minute. The needle was left in the brain for an additional 4 minutes after administration and slowly withdrawn over a 4 minute period. All mice received a glucose saline solution (1 ml i.p. of 5 % glucose/ 0.9 % sodium chloride) to prevent dehydration. The skull was cleaned with isopropyl alcohol and the skin was sutured using 16 mm Ethicon-coated vicryl absorbable sutures (*Johnson's & Johnson's*, UK). The wound was treated with a few drops of Marcain Polyamp steripack (0.25 % bupivacaine hydrochloride; Astrazeneca UK Ltd) and the mice were allowed to recover in a warming chamber (Scanbur Technology, Denmark) before returning to their home cages. A bead steriliser (Steril-quartz, Satelec, Italy) was used to sterilise instruments in between procedures. Post surgery, the mice received mash (RM1 powder form; Special Diets Services, UK) daily until normal eating behaviour was observed. Body weight was also monitored daily until the mice had regained their original weight.

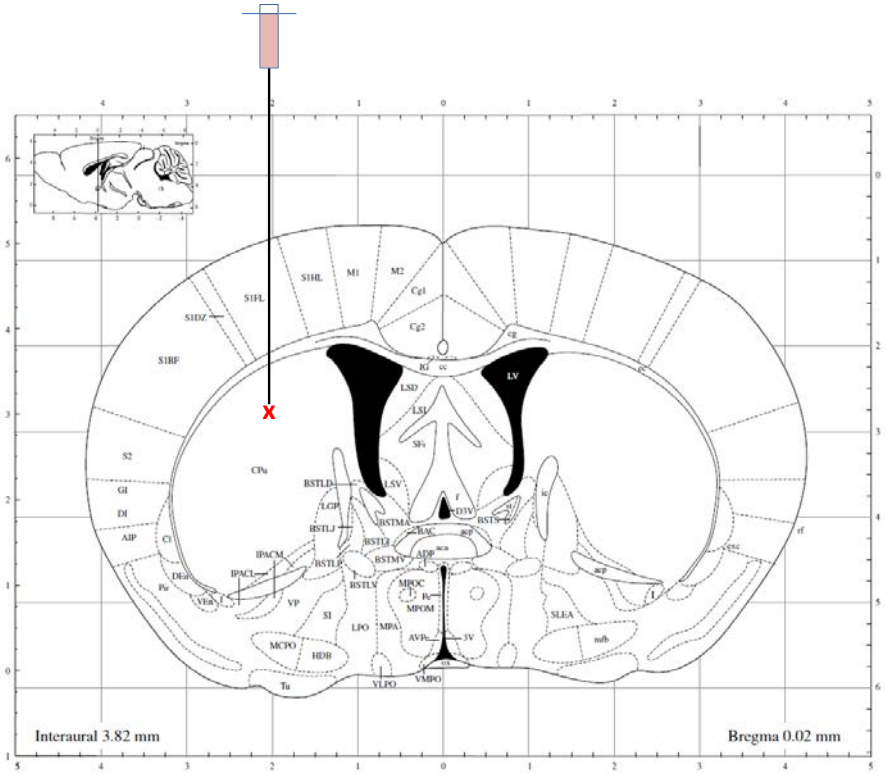

Figure 5-3 Site of 6-OHDA and LPS injection into the left striatum of mice.
6-OHDA and LPS were injected into the left striatum of mice at co-ordinates: A= -0.02 mm, L= +2.0 mm and V= -3.0 mm (Adapted from Paxinos and Watson, 2004). (**X**) depicts the site of injection in the striatum (Str).

5.2.6 Neuroprotection Study

Male C57BL/6J (n=8 per group; 25 -30 g) were treated with VPA and SAHA 2 days prior to 6-OHDA or LPS lesion and for ten days after surgery. VPA (200 and 400 mg/kg) and vehicle (1 ml/kg 0.9 % saline) were injected intraperitoneally (i.p), while SAHA (160 mg/kg/day) and vehicle (5 M HOP-β-CD) were administered in drinking water. The weights of all the mice were recorded daily. Twenty-four hours after last HDAC-I pre-treatment, the mice were lesioned with 6-OHDA (7.5 μg/ 4 μl) and LPS (7.5 μg/ 4 μl) or sham lesioned (vehicle) as described in Section 5.2.5. A detail of the experimental schedule is described in Figure 5-4.

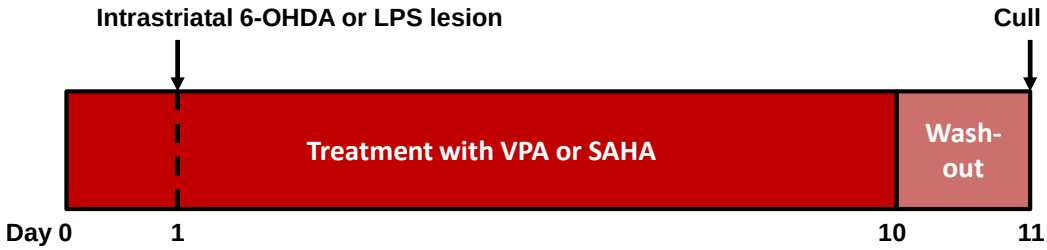

Figure 5-4 Overview of experimental timeline.
Mice were treated daily with VPA (200 and 400 mg /kg, i.p.) and SAHA (160 mg/kg/day, in drinking water) or vehicle for 10 days. Intrastriatal 6-OHDA and LPS-lesions (both 7.5 μg / 4 μl) or sham-lesions (vehicle) were performed 24 hours after the first drug administration. Following a 24 hour wash-out period, the mice were culled.

After 10 days of HDAC-I administration, treatment was withdrawn for 24 hours and mice were culled by transcardial perfusion with saline under general anaesthesia and the brains were dissected (Section 2.3.1) and processed for immunohistochemistry (Section 5.2.7).

5.2.7 Immunoperoxidase staining

Brains were cut into coronal sections at the level of the third nerve as described in Section 2.6.4, and assessed for immunoreactivity of TH, GFAP and OX-42 in the SN by immunoperoxidase staining, as described in detail in Section 2.6.6.2. In summary, the mouse sections (30 μm) were incubated in 24-well plates with primary antibodies against TH (1:500), GFAP (1:500) and OX-42 (1:100) (Table 2-2) overnight at room temperature. On the subsequent day, the sections were incubated with biotinylated secondary antibody (1:200) (Table 2-3) for 1 hour and further 45 minute incubation with the ABC kit at room temperature. The staining was visualised by exposing the sections to DAB (0.05 %; 500 μl) for 1 minute and the reaction was initiated on the addition of H_2O_2 (30 %; 1 μl). The sections were then mounted onto poly-D-lysine coated microscope slides, dehydrated, cover slipped and examined as described in Section 2.6.6.2.

5.2.8 Data analysis

Positive stained TH and OX-42 cells in the SN were counted bilaterally in three sections per mouse at X20 and X40 magnification respectively as detailed in Section 2.6.8. GFAP-positive staining in the SN was determined by measuring the optical density (OD) using Image J software (Schneider *et al.*, 2012).

5.2.9 Statistical analysis

Data are expressed as means ± SEM of experimental groups (n=4 – 8). GraphPad Prism software was used for statistical analysis. Difference between control and treatment groups was analysed with two-way or one-way ANOVA followed by Newman Keul's test where appropriate. $P<0.05$ was considered significant.

5.3 Results

5.3.1 Co-localisation of HDACs with dopaminergic and inflammatory cells in the substantia nigra

The expression of HDAC isoforms 3, 4, 5 and 11 was investigated in dopaminergic and glial cells, including astrocytes in the SN of naive mouse brain sections. Double-labelling by immunoflourescence with antibody against TH (Figure 5-5) showed that TH-positive cells expressed all four HDAC isoforms.

HDAC3 was located primarily in the nucleus of the dopaminergic neurones (Figure 5-5-A, E, I), but in some cells HDAC3 was found to have some diffused cytoplasmic staining. HDACs 4 and 5 were found to be in both the cytoplasm and nucleus of the cells (Figure 5-5-B, C, F, G, J, and K). However, HDAC4 did not co-localise with all TH-positive neurones. HDAC 11 was present in the perinuclear and cytoplasm of the dopaminergic cells (Figure 5-5-D, H, L).

Double staining with antibody against GFAP (Figure 5-6), also showed no co-localisation of any HDAC isoform with GFAP-positive cells.

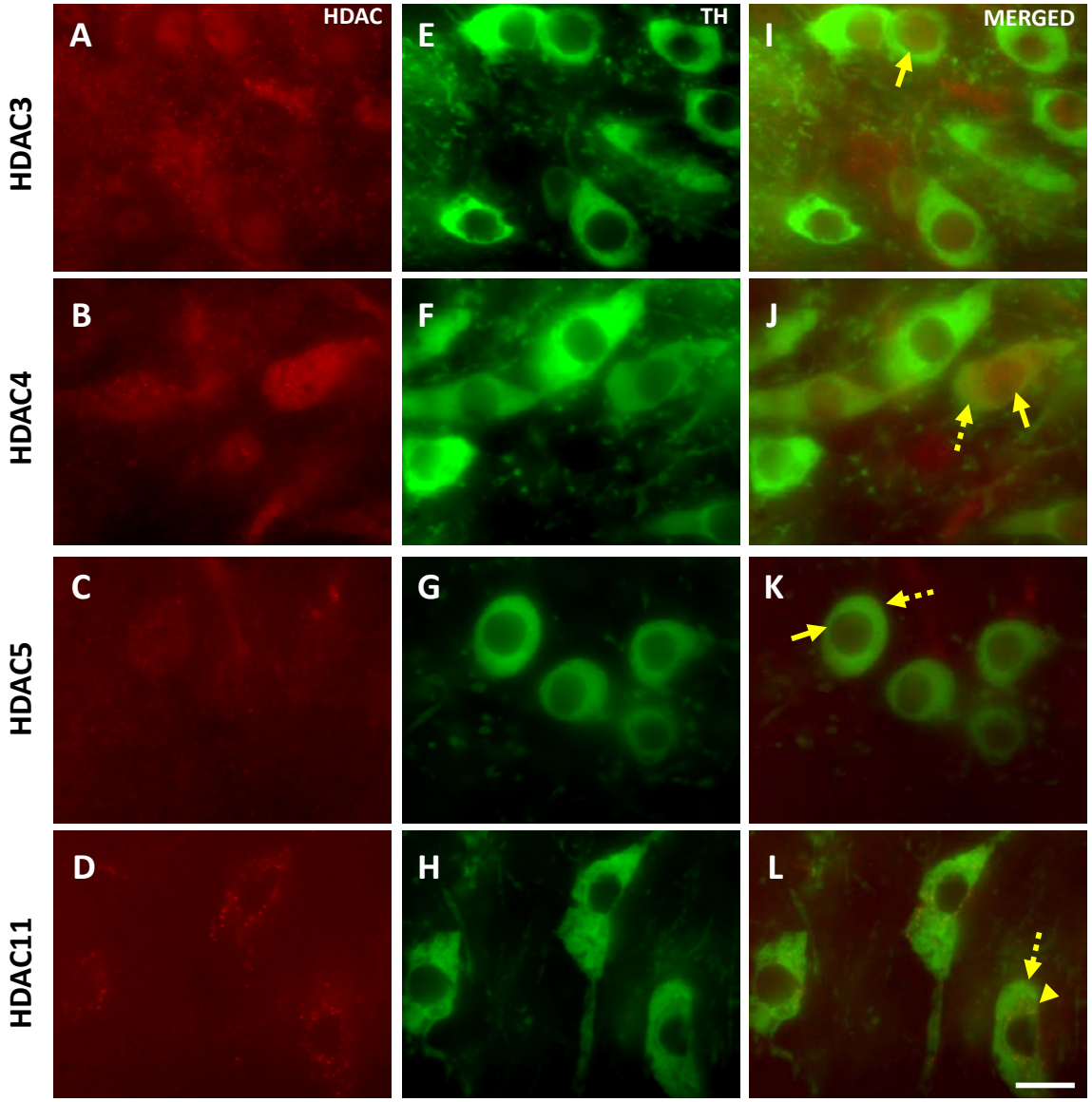

Figure 5-5 Double immunofluorescence staining in naive mouse brain SN showing co-localisation of TH-positive neurones with HDAC3, 4, 5 and 11.

Representative photomicrographs showing HDAC3, 4, 5 and 11 positive cells (red) and TH-positive cells (green) in the SN. Nuclear staining is indicated with solid yellow arrows, cytoplasmic staining with broken arrows and perinuclear staining with arrow head. Scale bar = 20μm is representative of all images.

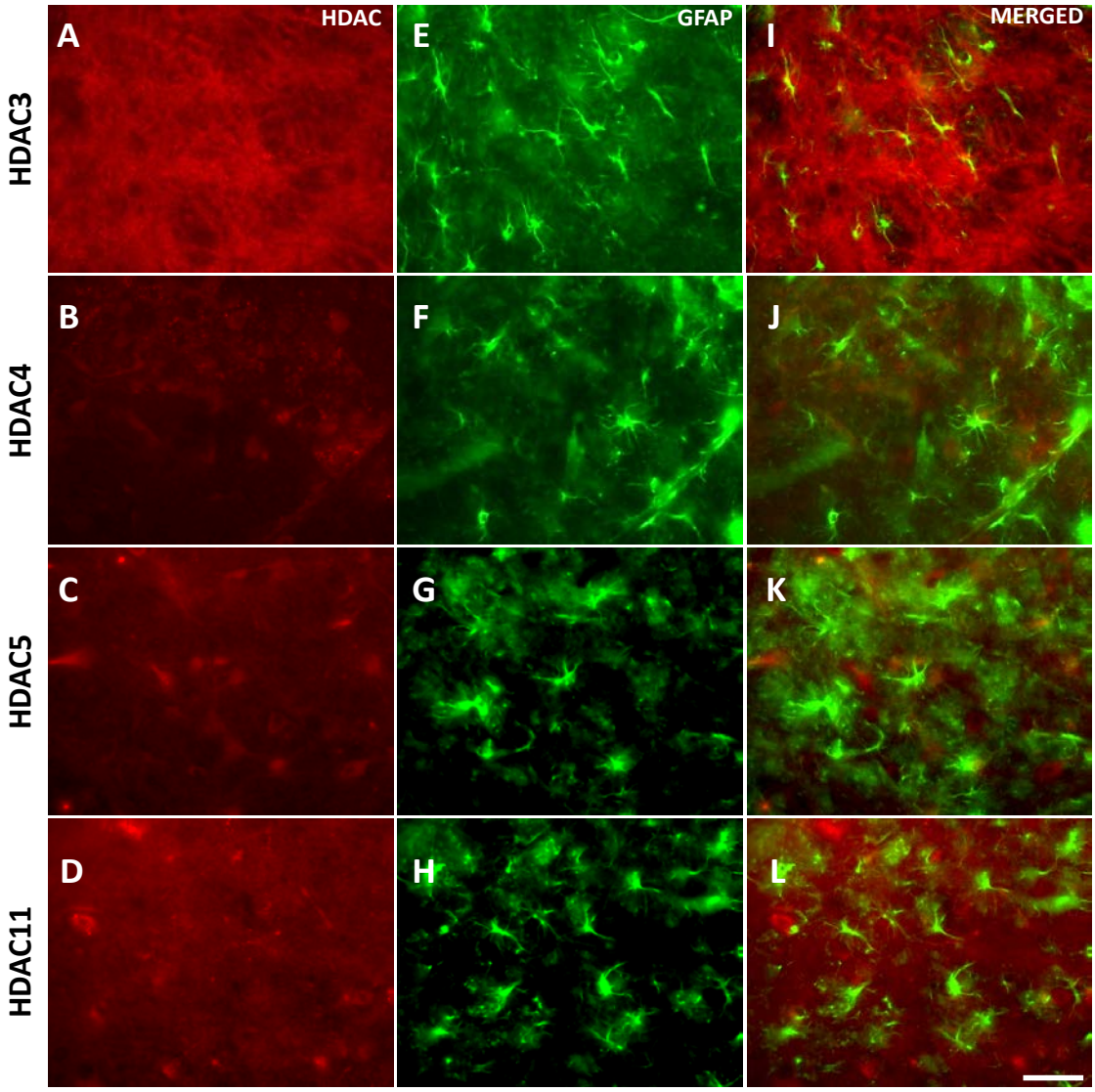

Figure 5-6 Double immunofluorescence showing no co-localisation between GFAP-positive cells with HDAC3, 4, 5 and 11 in naive mouse brain SN.
Representative photomicrographs showing HDAC3, 4, 5 and 11 (red) and GFAP-positive cells (green) in SN. Scale bar = 100 μm is representative of all images.

5.3.2 Confirmation of HDAC activity in mouse brain

Nuclear extracts of naive brain tissue were used to perform the assay to confirm the HDAC activity in the mouse brain. EC_{50} concentration of SAHA (20 μm) and VPA (60 μm) were used for the assay (Section 5.2.3.4).

In control nuclear extracts, high fluorescence readings of 10883 ± 1704 relative units (RU) was attained confirming the HDAC substrate was deactylated (Figure 5-7). Incubation with known HDAC inhibitor TSA (positive control) in the control well, significantly reduced the fluorescence reading by 63%, suggesting that the HDAC substrate deacetylation was inhibited. Similary to the control, high fluorescence readings of 10473 ± 927 RU and 10448 ± 1440 RU show that the

vehicles HOP-β-CD and saline, respectively, had no effect on HDAC activity. Incubation of brain tissue nuclear extracts with the vehicles, saline and HOP-β-CD had no effect on HDAC activity compared to control. As expected, SAHA and VPA significantly reduced HDAC activity by 48 % and 51 %, respectively, compared to their respective vehicles.

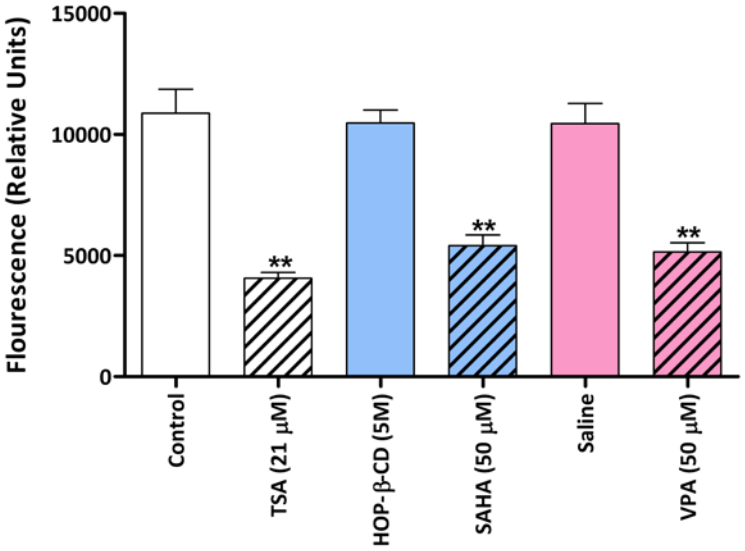

Figure 5-7 HDAC assay of mouse brain tissue.
Nuclear extracts from mouse brain tissue were treated with EC_{50} concentrations of VPA (60 μM), SAHA (20 μM), HOP-β-CD (5 M) and saline. Control wells were incubated with human recombinant HDAC1 and treated with assay buffer or known HDAC-I, TSA (21 μM). Data are expressed as mean ± SEM (n=4). **p<0.01 compared to vehicles. Analysis by one-way ANOVA followed by Newman Keul's post hoc.

5.3.3 Penetration of HDAC-Is across blood brain barrier

To determine whether SAHA and VPA penetrated through the blood brain barrier, mice were injected with saline (10 ml/kg, i.p) or VPA (200 mg/kg or 400 mg/kg, i.p), or treated orally in drinking water with HOP-β-CD (6 ml/kg/day, p.o) or SAHA (160 mg/kg/day, p.o in HOP-β-CD). VPA and saline-treated mice were killed after 2 hours while SAHA and HOP-β-CD-treated mice were culled after 24 hours of treatment. Brains were dissected and histone extractions were performed for Western blotting.

Western blotting was used to detect acetylated levels of histone H4 in the samples (Figure 5-8). Very low levels of acetylated histone H4 were detected in samples extracted from naive, saline (1 ml/kg) or HOP-β-CD (6 ml/kg/day) animals. Both SAHA (160 mg/kg/day) and VPA (200 and 400 mg/kg) induced a large increase in acetylated histone H4 levels of approximately 3-fold.

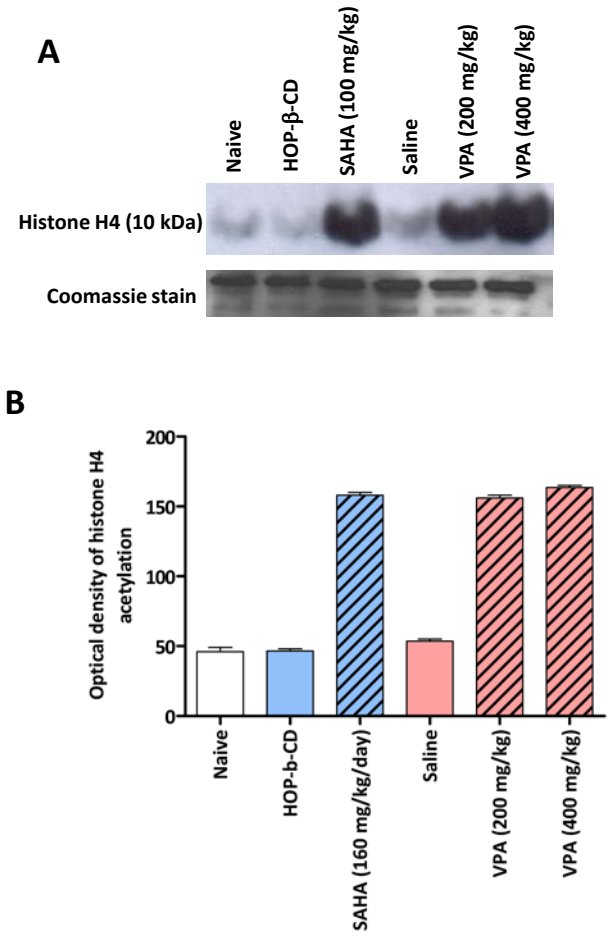

Figure 5-8 The effect of HDAC inhibition on histone H4 acetylation.
(A) Histones extracted from naive mice brain tissues (n=2) and those treated with HOP-β-CD, SAHA, saline, VPA were probed with histone H4 antibody to detect histone acetylation levels by Western blotting. *Bottom panel* shows Coomassie blue-stained poly-acrylamide gel of the total histones extracted from the tissue. (B) Bands quantified by Image J and expressed as optical density. Data are expressed as mean ± SEM of n=2 animals. Images are typical of n=2 animals.

5.3.4 The effect of HDAC inhibition on the number of TH-positive cells in the substantia nigra following 6-OHDA and LPS lesioning.

Sham lesion

There was no effect of the sham-lesioned + vehicle treatment on the number of TH-positive cells in the ipsilateral SN compared to the contralateral side (Figure 5-9). Similarly, treatment with VPA and SAHA alone had no significant effect on the number of TH-positive cells on the ipsilateral side in sham-lesioned mice compared to the contralateral side. The vehicle-treated (0.9 % saline containing 0.05 % L-ascorbic acid, and 0.9 % saline only) sham lesioned groups were combined after analysis showed there was no difference in the number of surviving TH-positive cells between the two groups.

6-OHDA lesion

Intrastriatal administration of 6-OHDA (7.5 μg) significantly reduced the number of TH-Positive cells in the ipsilateral SN by 40 % compared to the contralateral side (Figure 5-9). Treatment with VPA (200 mg/kg) had no effect on the 6-OHDA-induced cell loss in the ipsilateral side of the SN. However, the higher dose of VPA (400 mg/kg) reduced the 6-OHDA-induced loss of TH-positive cells, although the difference (21 %) was not significant. However, neither was there any difference from vehicle-treated sham controls. On the other hand, treatment with SAHA (160 mg/kg/day) significantly prevented 6-OHDA-induced loss of TH-positive cells whereby there was 22 % loss of TH-positive cells in the ipsilateral side compared to the contralateral side of the SN, compared to 40 % in the control.

LPS lesion

Intrastriatal injection of LPS (7.5 μg) significantly decreased the number of TH-positive cells by 40 % compared to the contralateral side (Figure 5-9). VPA protected against 6-OHDA toxicity in a dose-related manner such that although VPA (200 mg/kg) had no significant effect on the LPS-induced loss of TH-positive cells in SN, the higher dose of VPA (400 mg/kg) showed 18 % reduction. Similarly, SAHA (160 mg/kg/day) protected TH-positive cells from LPS-induced cell loss, exhibiting a reduction of 23 % in the ipsilateral side compared to the contralateral side of the SN.

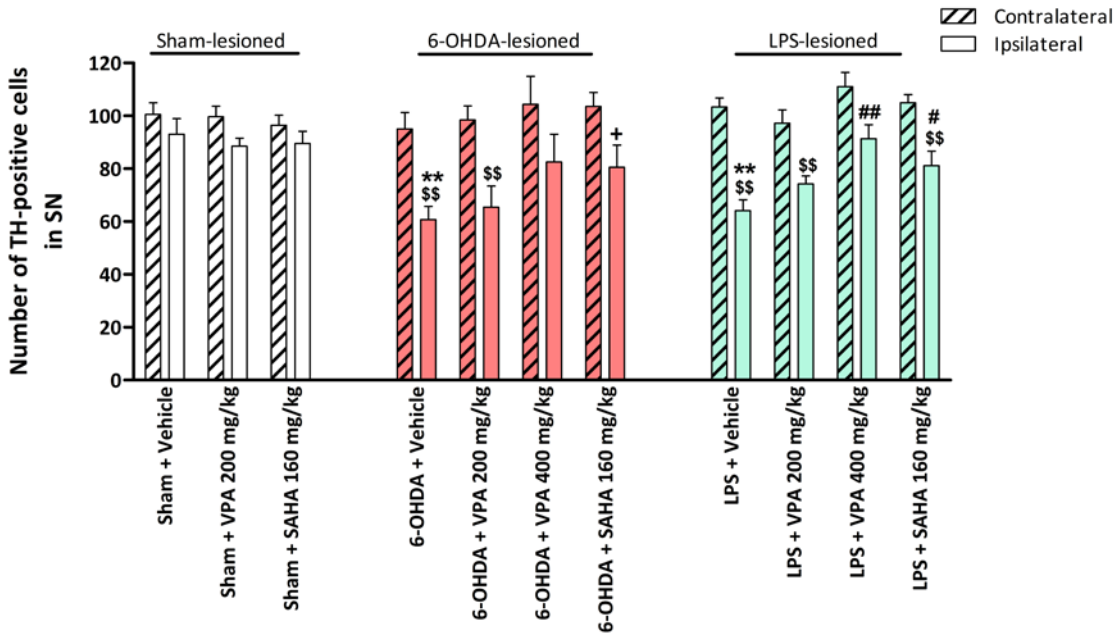

Figure 5-9 The effect of VPA and SAHA on the number of TH-positive cells in SN of sham-, 6-OHDA- and LPS-lesioned mice.

The number of TH-positive cells in the ipsilateral and contralateral sides of SN. Data are expressed as mean ± SEM (n= 4-8). $$p<0.01 compared to the contralateral side; **p<0.01 compared to sham-lesioned+vehicle ipsilateral; +p<0.05 compared 6-OHDA+vehicle ipsilateral; #p<0.05, ##p<0.01compared to LPS+vehicle ipsilateral SN. (Two-way ANOVA with Newman Keul's test)

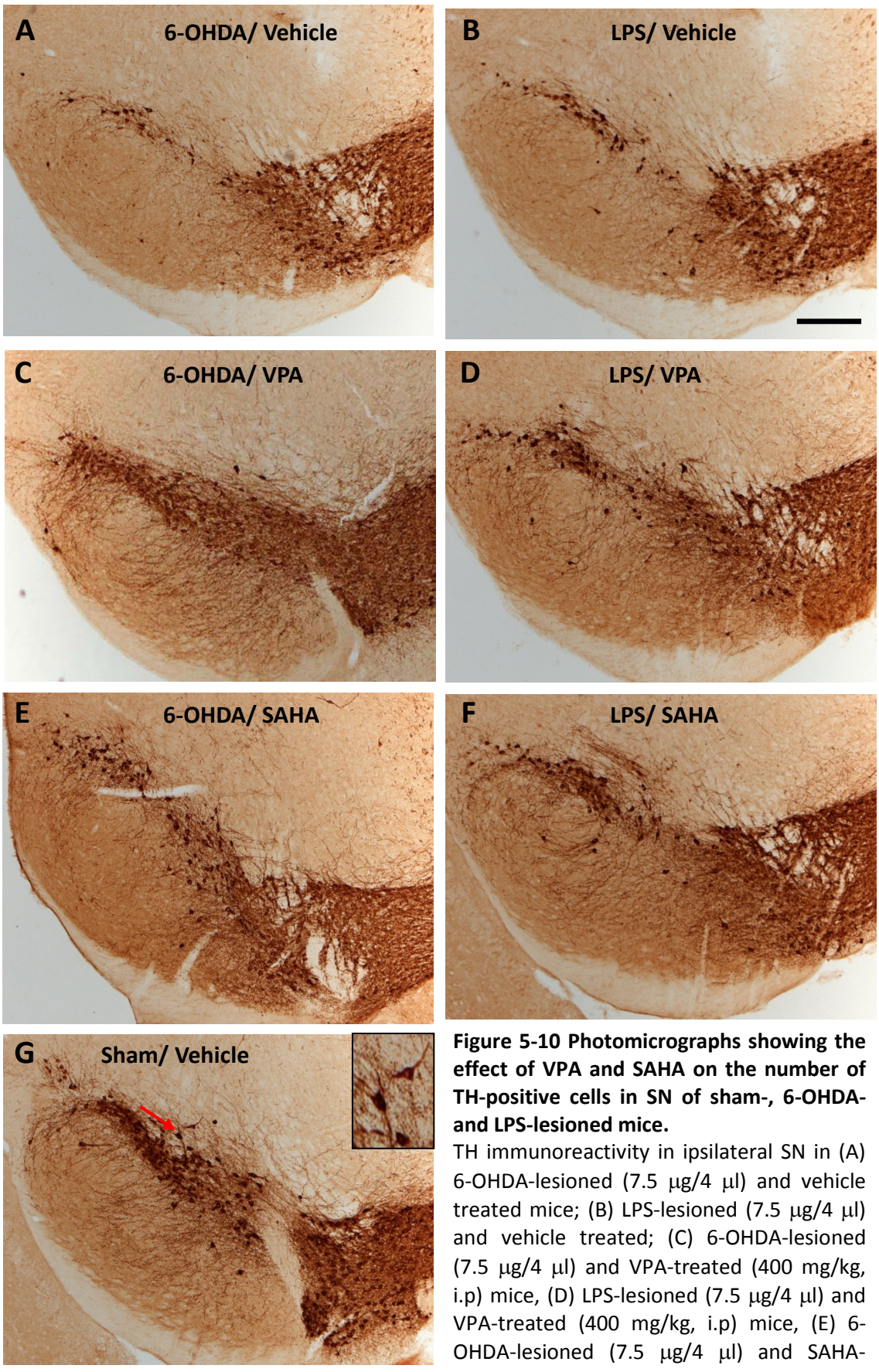

Figure 5-10 Photomicrographs showing the effect of VPA and SAHA on the number of TH-positive cells in SN of sham-, 6-OHDA- and LPS-lesioned mice.

TH immunoreactivity in ipsilateral SN in (A) 6-OHDA-lesioned (7.5 μg/4 μl) and vehicle treated mice; (B) LPS-lesioned (7.5 μg/4 μl) and vehicle treated; (C) 6-OHDA-lesioned (7.5 μg/4 μl) and VPA-treated (400 mg/kg, i.p) mice, (D) LPS-lesioned (7.5 μg/4 μl) and VPA-treated (400 mg/kg, i.p) mice, (E) 6-OHDA-lesioned (7.5 μg/4 μl) and SAHA-treated (160 mg/kg/day) mice; (F) LPS-lesioned (7.5 μg/4 μl) and SAHA-treated (160 mg/kg/day) mice; and (G) sham-lesioned and vehicle treated mice. A typical TH-positive cell is indicated with red arrow. Scale bar = 500 μm and inset scale bar = 50 μm are representative of all images.

5.3.5 The effect of HDAC inhibition on GFAP immunoreactivity in the substantia nigra following 6-OHDA and LPS lesioning.

Sham lesion

In the sham-lesioned vehicle-treated mice, there was no difference in the density of GFAP-positive cells between the ipsilateral and contralateral SN (Figure 5-11). Similarly, treatment with VPA (200 and 400 mg/kg) and SAHA (160 mg/kg/day) alone did not affect the GFAP-immunoreactivity between the ipsilateral and contralateral sides of the SN or compared to the vehicle treatment.

6-OHDA lesion

Intrastriatal injection of 6-OHDA increased GFAP-immunoreactivity in the ipsilateral SN compared to the contralateral side (Figure 5-11). Treatment with VPA (200 mg/kg) significantly reduced the 6-OHDA-induced increase in GFAP-immunoreactivity in the ipsilateral SN compared to the 6-OHDA alone. Similarly, the higher dose of VPA (400 mg/kg), and SAHA (160 mg/kg/day) reduced the 6-OHDA-induced increase in GFAP density in SN, although the differences were not significant. VPA (200 mg/kg) also reduced GFAP-immunoreactivity on the contralateral side of 6-OHDA lesioned mice.

LPS lesion

Intrastriatal administration of LPS increased the density of GFAP-immunoreactivity in the ipsilateral compared to the contralateral side of the SN (Figure 5-11). Treatment with VPA decreased the density of GFAP-immunoreactivity in a dose-dependent manner such that, VPA (400 mg/kg) significantly decreased GFAP-immunoractivity by 34 %. Similarly, SAHA (160 mg/kg/day) significantly decreased the GFAP-immunoreactivity density by 25 % respectively compared to the vehicle treated ipsilateral side of the SN.

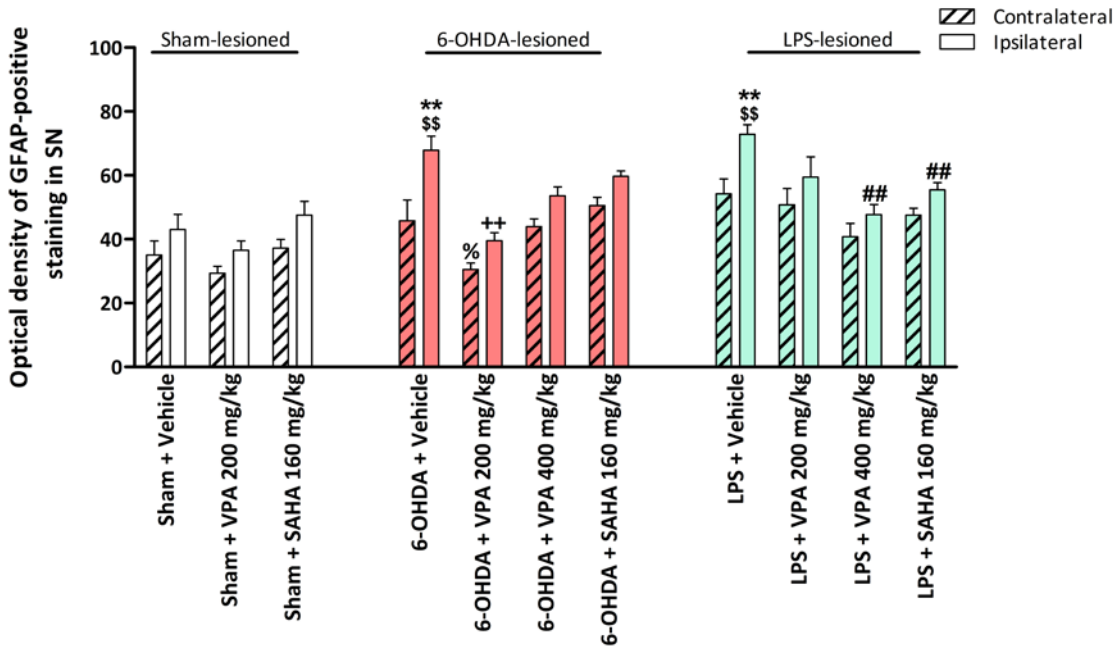

Figure 5-11 The effect of VPA and SAHA on GFAP-immunoreactivity in SN of sham-, 6-OHDA- and LPS-lesioned mice.

Data are optical density of GFAP-positive cells measured in the ipsilateral and contralateral side of SN expressed as mean ± SEM (n= 4-8). $$p<0.01 compared to the contralateral side; **p<0.01 compared to sham-lesioned+vehicle ipsilateral; ++p<0.01 compared 6-OHDA+vehicle ipsilateral; ##p<0.01 compared to LPS+vehicle ipsilateral; %p<0.05 compared to 6-OHDA+vehicle contralateral SN. (Two-way ANOVA with Newman Keul's test).

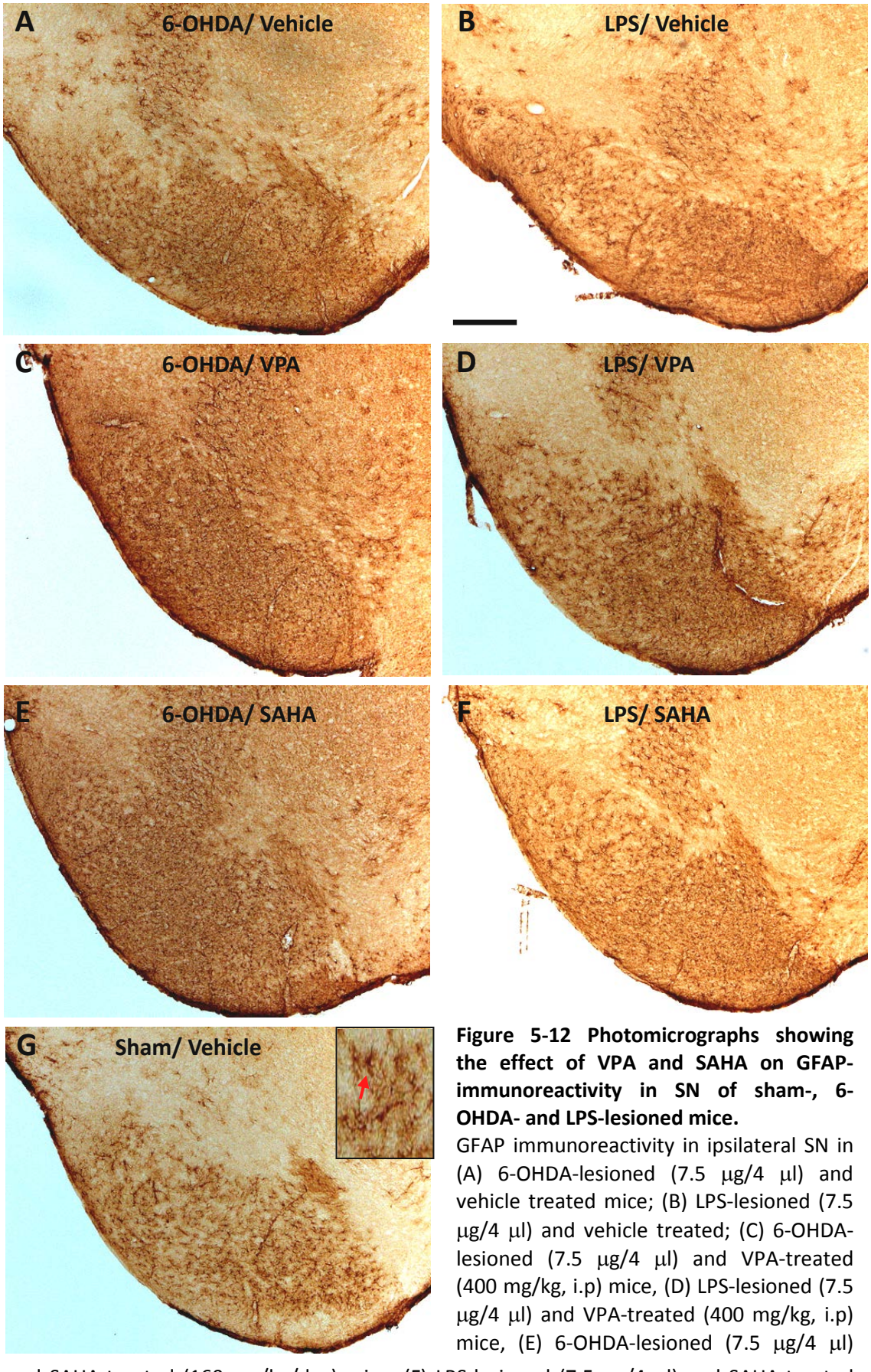

Figure 5-12 Photomicrographs showing the effect of VPA and SAHA on GFAP-immunoreactivity in SN of sham-, 6-OHDA- and LPS-lesioned mice.

GFAP immunoreactivity in ipsilateral SN in (A) 6-OHDA-lesioned (7.5 μg/4 μl) and vehicle treated mice; (B) LPS-lesioned (7.5 μg/4 μl) and vehicle treated; (C) 6-OHDA-lesioned (7.5 μg/4 μl) and VPA-treated (400 mg/kg, i.p) mice, (D) LPS-lesioned (7.5 μg/4 μl) and VPA-treated (400 mg/kg, i.p) mice, (E) 6-OHDA-lesioned (7.5 μg/4 μl) and SAHA-treated (160 mg/kg/day) mice; (F) LPS-lesioned (7.5 μg/4 μl) and SAHA-treated (160 mg/kg/day) mice; and (G) sham-lesioned and vehicle treated mice. A typical GFAP-positive cell is indicated with a red arrow (inset). Scale bar = 500 μm and inset scale bar = 50 μm are representative of all images.

5.3.6 The effect of HDAC inhibition on OX-42-positive cells in the substantia nigra following 6-OHDA and LPS Lesioning.

Sham lesion

Sham-lesioned mice had very few active OX-4-positive cells per section in the ipsilateral SN with no significant difference when compared to the contralateral side (Figure 5-13). Treatment with VPA (200 mg/kg) and SAHA (160 mg/kg/day) alone had no effect on the numbers of active OX-42 cells between the ipsilateral and contralateral sides.

6-OHDA lesion

There was no effect of 6-OHDA alone or combined with HDAC-I treatment in the number of active OX-42-positive cells in the SN contralateral to the lesion (Figure 5-13). Intrastriatal injection of 6-OHDA induced an increase in the number of OX-42-positive cells in the ipsilateral (84 ± 23) compared to the contralateral side (8 ± 6) of the SN. Treatment with VPA (200 mg/kg) or SAHA (160 mg/kg/day) had no effect on the 6-OHDA-induced increase in the number of active OX-42-positive cells in the ipsilateral SN compared to the 6-OHDA alone. However, there was some indication that VPA (400 mg/kg) decreased the number of active OX-42-positive cells in the ipsilateral side compared to the '6-OHDA + vehicle' ipsilateral side, however, this difference was not significant.

LPS lesion

There was no effect of LPS alone or combined HDAC-I treatment in the number of active OX-42-positive cells in the contralateral SN (Figure 5-13). Administration of LPS significantly increased the number of active OX-42-positive cells to 80 ± 25 in the ipsilateral SN compared to contralateral side and the ipsilateral side of sham/vehicle treated animals. Similarly to the 6-OHDA lesion, neither treatment with VPA (200 mg/kg) nor SAHA (160 mg/kg/day) had any effect on the LPS-induced increase on the number of OX-42-positive cells in the ipsilateral SN compared to the LPS alone. VPA (400 mg/kg) appeared to decrease the number of active OX-42-positive cells to 59 ± 19 in the ipsilateral SN compared to LPS alone, however the difference was not significant compared to the vehicle treated group.

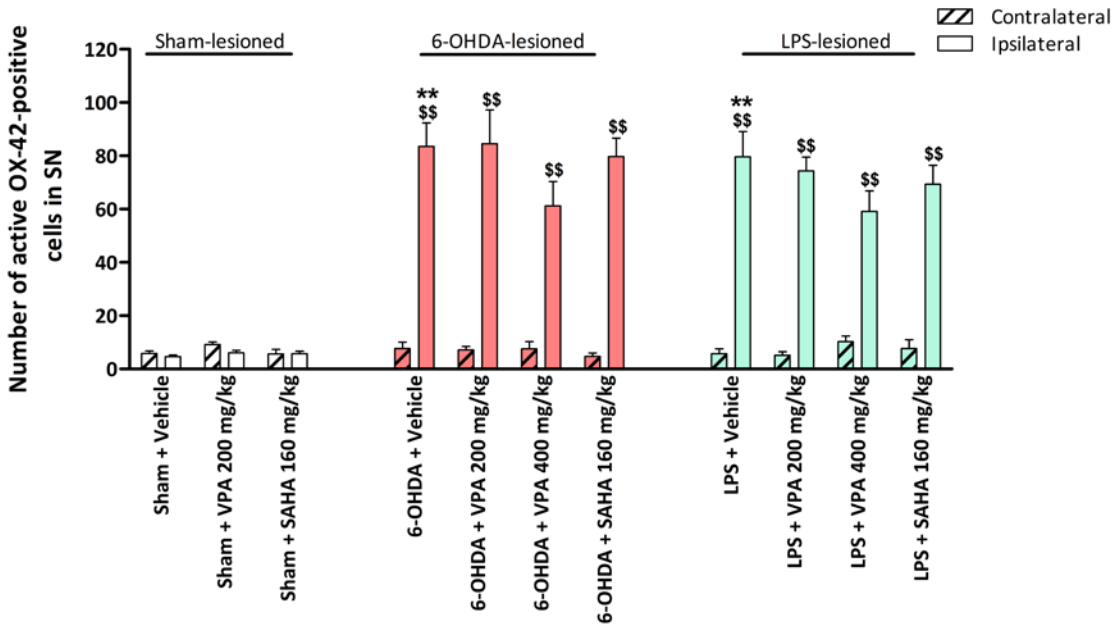

Figure 5-13 The effect of VPA and SAHA on the number active OX-42-positive cell in SN of sham-, 6-OHDA- and LPS-lesioned mice.

The number of active OX-42-positive cells in the ipsilateral and contralateral sides of SN. Data are expressed as mean ± SEM (n= 4-8). $$p<0.01 compared to the contralateral side; **p<0.01 compared to sham-lesioned+vehicle ipsilateral SN. (Two-way ANOVA with Newman Keul's test)

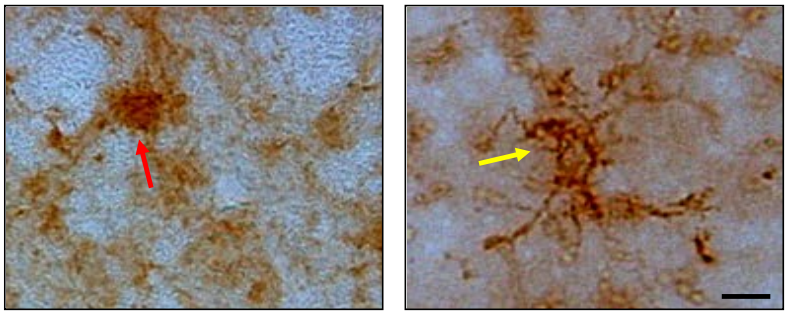

Figure 5-14 Images of resting and active OX-42-positive cells.

An example of a resting microglia is depicted with a yellow arrow, and an active microglia with a red arrow. Scale bar = 50 μm is representative of all images.

5.3.7 Co-localisation of HDACs with inflammatory cells in the substantia nigra following lesions

Double staining mouse brain sections following 6-OHDA and LPS lesions with antibodies against GFAP (Figure 5-15) and OX-42 (Figure 5-16) showed no co-localisation of any HDAC isoforms with GFAP- and OX-42-positive cells. Similar images were observed for both 6-OHDA and LPS-treated brain sections.

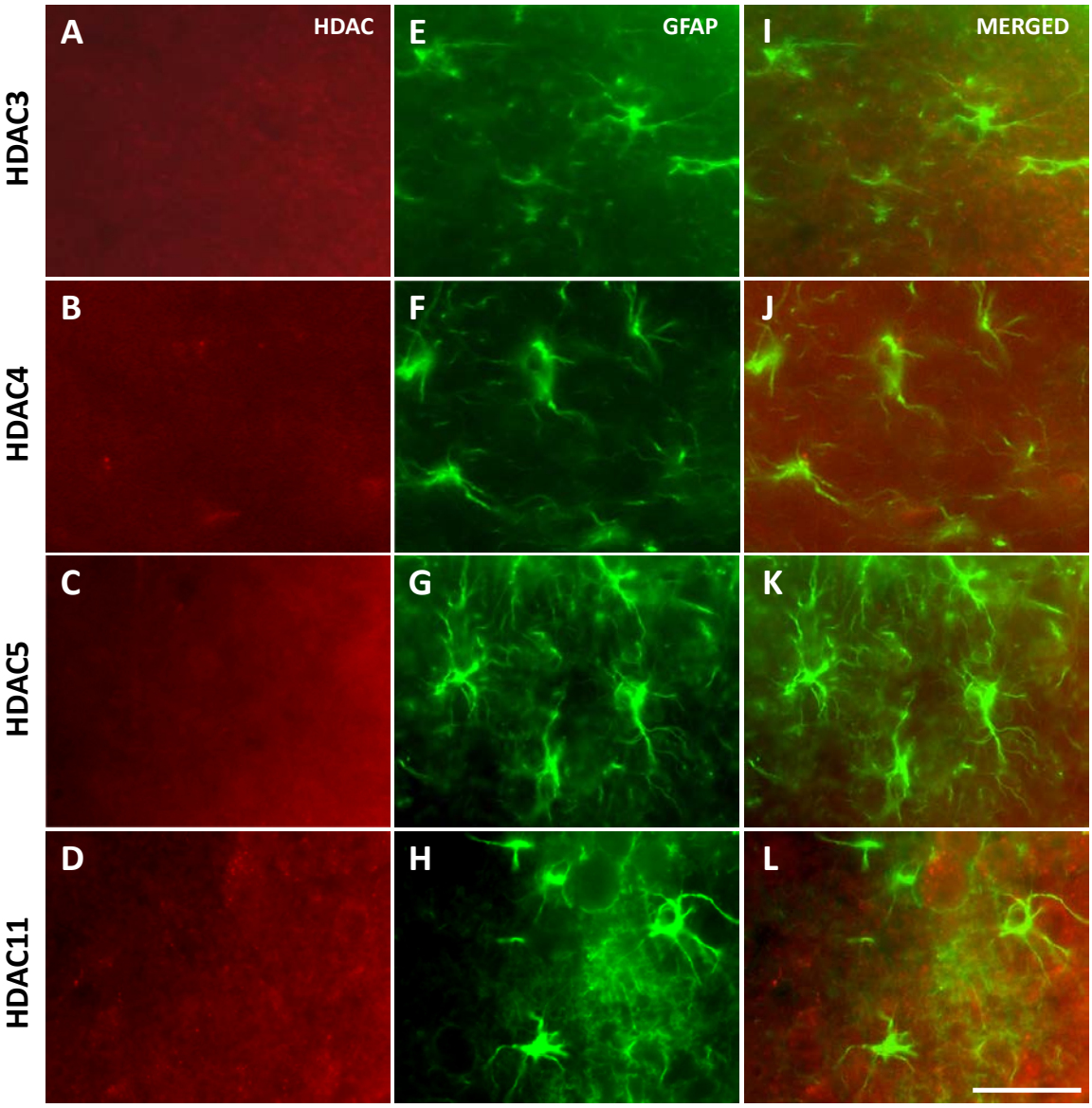

Figure 5-15 Double immunofluorescence showing no co-localisation between GFAP-positive cells with HDAC3, 4, 5 and 11 in treated mouse brain SN.
Representative photomicrographs showing HDAC3, 4, 5 and 11 (red) and GFAP-positive cells (green) in SN. Scale bar = 100 μm is representative of all images.

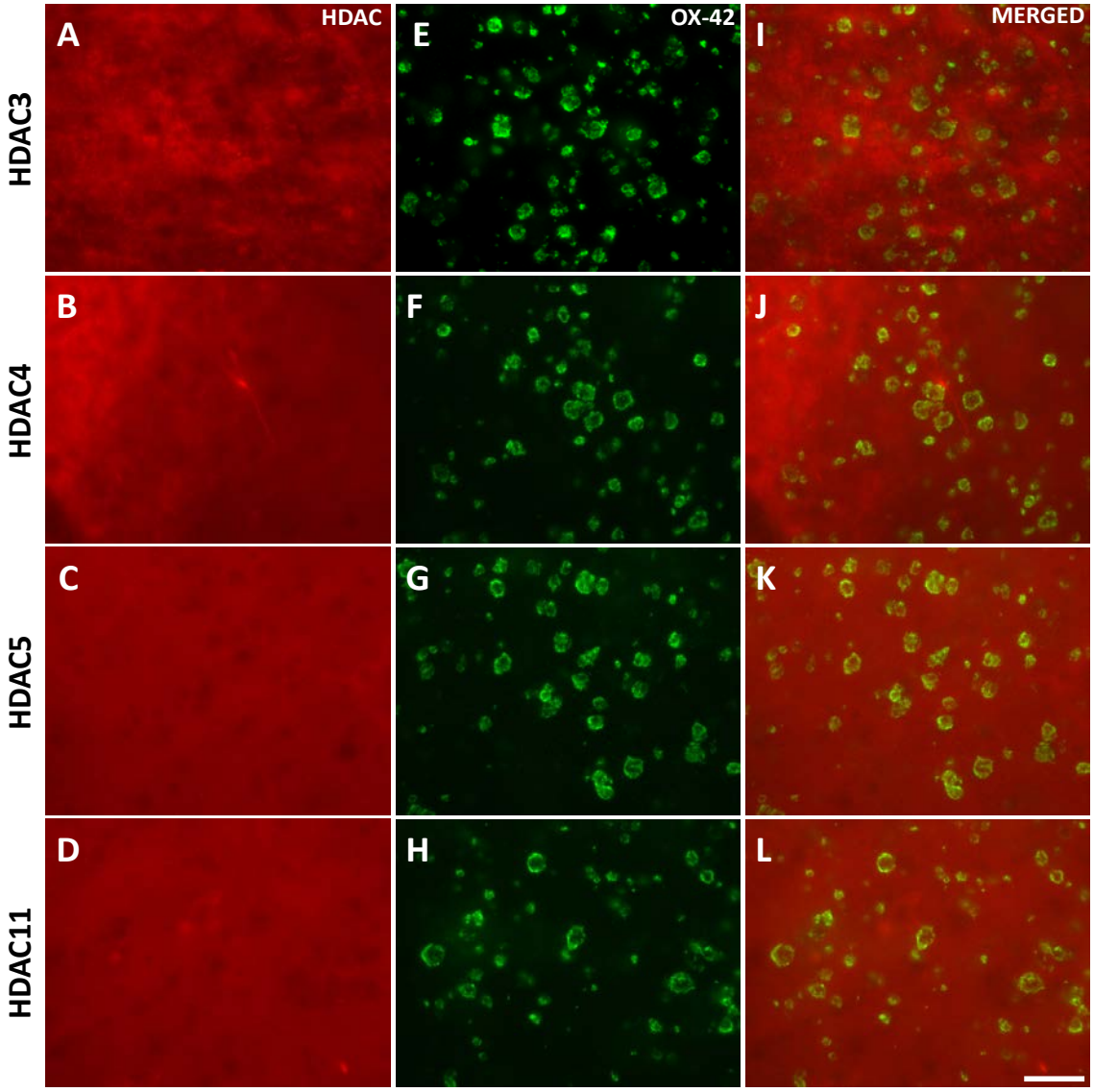

Figure 5-16 Double immunofluorescence showing no co-localisation between OX-42-positive cells with HDAC3, 4, 5 and 11 in treated mouse brain SN.

Representative photomicrographs showing HDAC3, 4, 5 and 11 (red) and OX-42-positive cells (green) in SN. Scale bar = 100 μm is representative of all images.

5.4 Discussion

The hypothesis of this study was that inhibition of HDACs protect against 6-OHDA- and LPS-induced degeneration of nigral dopaminergic neurones in the mouse *in vivo* through a reduction in glial cell activation and recruitment. This hypothesis was tested by investigating the effect of VPA and SAHA on 6-OHDA- and LPS-induced nigral cell loss in mice. First and importantly, it was established that HDACs 3, 4, 5 and 11 were expressed in the SN of the mouse brain. Second, it was established that VPA and SAHA could cross the BBB and could inhibit deacetylation of histones. Third, VPA and SAHA effects on dopaminergic cell loss in the SN of 6-OHDA and LPS-lesioned mice were determined to establish whether they exert a protective effect. Fourth, the effect of HDAC-Is on inflammatory cells following partial 6-OHDA and LPS lesioning was investigated in order to determine if the mechanism of neuroprotection was by a reduction in reactive gliosis.

5.4.1 Expression of HDACs in mouse SN

Immunocytochemistry studies revealed that HDAC3, 4, 5 and 11 were expressed in the SN of the mouse brain. These findings confirm previous reports of the ubiquitous expression of these proteins in the brain (Broide *et al.*, 2007; Lucio-Eterovic *et al.*, 2008). Cellular localisation of the HDACs was investigated by double immunofluorescence labelling, and showed all 4 HDACs were expressed on dopaminergic neurones in mouse brain, with HDAC3 mainly in the nucleus and HDAC4, 5 and 11 found in both nucleus and cytoplasm of the cells. This is the first time that the localisation of HDAC has been investigated in mouse SN, however, the findings are in agreement with the previous reports from Broide *et al.,* (2007) and Janssen *et al.,* (2010), who performed their studies in rat and human brain tissues, respectively.

Interestingly, mouse astrocytes did not express HDAC3, 4, 5 or 11. This is very surprising, as in primary rat mesencephalic cultures, these HDACs were shown to be localised to astrocytes (Chapter 4). This finding is, however, in agreement with reports by Broide *et al*. (2007) who claimed that only rat oligodendrocytes express HDACs, and not astrocytes or microglia. Thus it seems likely that this is also the case in adult mice. Even though double immunofluorescence staining of astrocytes performed in this thesis and previous evidence have shown no positive co-localisation with HDACs, there is a possibility that the HDAC isoforms may co-localise with microglial cells. This was tested, but due to the low sensitivity of the technique employed and differences in the antibodies used, resting microglial cells were not detected by immunofluorescence. In future studies, in-situ hybridisation might be used to label the HDAC isoforms mRNA followed by immunoperoxidase staining for the microglial cells.

Overall, these data suggest that HDAC3, 4, 5 and 11 are expressed on neurones, but not glial cells in normal naive mouse brain. The localisation of HDACs in glial cells was investigated in 6-OHDA- and LPS-treated mouse brain tissues. Surprisingly, there was no localisation of the HDACs within astrocytes or active microglia and this indicates that HDAC-Is do not exert their effects directly on these inflammatory cells.

5.4.2 Effect of 6-OHDA and LPS-lesioning in mice

Intrastriatal injection of 6-OHDA caused a partial 40 % loss of TH-positive neurones in the SN ipsilateral to the lesion 10 days following toxin injection. The extent of nigrostriatal degeneration at this time point is in agreement with previous reports which showed that the loss of TH-positive cells occurs within the first 7 days following toxin administration in mice (Alvarez-Fischer *et al.*, 2008). Similarly, intrastriatal injection of LPS also produced a 40 % loss of TH-positive dopaminergic neurones in the ipsilateral SN compared to sham-lesioned controls, in agreement with previous reports (Hunter *et al.*, 2007; Choi *et al.*, 2009).

The loss of TH-positive cells was most pronounced in the dorsal tier of the SNpc, which is in agreement with the topographical organisation of the mesostriatal DA projections confirming that the neurones of the dorsal SN project into the striatum (Bjorklund & Dunnett, 2007); and also confirming that intrastriatal 6-OHDA lesioning provides a selective destruction of DA axons and terminals within the striatum and a retrograde degeneration of DA neurones cell bodies in the SN (Debeir *et al.*, 2005).

This loss may reflect a down-regulation of TH, as death of dopaminergic neurones in the nigro-striatal pathway per se was not determined. However, previous studies by stereology in our labs and elsewhere have confirmed that both 6-OHDA and LPS induce dopaminergic degeneration rather than a down-regulation of the TH protein (Sauer & Oertel, 1994; Przedbroski *et al.*, 1995; Iravani *et al.*, 2002; Gao *et al.*, 2002a; Iczkiewicz *et al.*, 2010). This loss of dopaminergic cell bodies in the SN mimics the early stages of disease progression, but whether it is a suitable model for PD, is further discussed in Chapter 6.

5.4.3 Effect of HDAC-Is on dopaminergic cell death and inflammatory change in 6-OHDA and LPS-lesioned mice

This is the first report of the neuroprotective effects of HDAC-Is VPA and SAHA against 6-OHDA- and LPS-induced loss of dopaminergic neurones in the mouse SN *in vivo*. Eleven days administration of SAHA (160 mg/kg/day) and the highest dose of VPA (400 mg/kg) preserved TH-positive neurones from 6-OHDA and LPS intrastriatal lesions. This protective finding confirms

recent reports of HDAC-Is, sodium butyrate, phenylbutyrate and VPA respectively, to significantly protect dopaminergic neurones and striatal dopamine levels against MPTP toxicity in the same species (Gardian *et al.*, 2004; Kidd & Schneider, 2011; Zhou *et al.*, 2011), and against rotenone toxicity in rats (Monti *et al.*, 2010). The mechanism of this protective effect observed in the present study is not certain as it counteracts the results reported in Chapter 4 where there was no protection of TH-positive cells.

The loss of TH-positive cells in the SN was accompanied by an increase in astrocytes and microglia 10 days following intrastriatal injection with both 6-OHDA and LPS. This is in agreement with previous work where increased astroglia activation was observed 3 – 28 days post 6-OHDA injection, and 6 hours – 21 days post LPS lesioning in the striatum and SN (Liu, 2006). Whether this increase in inflammatory cells is the cause of dopaminergic neuronal loss following 6-OHDA and LPS injection remains unclear. However, treatment of rat mesencephalic cultures with the non-steroidal anti-inflammatory drug (NSAID) ibuprofen, protected dopaminergic neurones against 6-OHDA and MPP^+ toxicity (Carrasco *et al.*, 2005). Furthermore, the NSAID celecoxib (selective COX-2 inhibitor) protected rat dopaminergic cells against intrastriatal administration of 6-OHDA *in vivo* (Sanchez-Pernaute *et al.*, 2004), whereas treatment with ibuprofen also protected dopaminergic neurones against LPS administration *in vivo*, with a marked reduction of GFAP, OX-42, iNOS and 3-NT (Iravani, personal communication). Importantly, chronic NSAID users exhibited a decrease in PD incidence (Chen *et al.*, 2003; Chen *et al.*, 2005), suggesting that inflammation contributes to the degenerating process. By contrast, meta-analysis of NSAID observational studies concluded that NSAIDs on the whole do not modify PD risk, although users of COX-2 inhibitor ibuprofen showed some evidence of reduced PD incidence (Samii *et al.*, 2009). Overall, these studies suggest that the inflammatory response observed in PD brains does contribute to cell death and this is a target for neuroprotective therapy.

In the present study, HDAC inhibition by VPA and SAHA caused a small reduction in the number of 6-OHDA- and LPS-induced active microglia. In addition, VPA (200 mg/kg) significantly reduced the density of astrocytes in 6-OHDA-lesioned mice, and both VPA (400 mg/kg) and SAHA (160 mg/kg/po) reduced astrocytosis in LPS-lesioned mice. Surprisingly, an opposing effect of HDAC-Is on inflammatory cells were observed in primary cultures, where SAHA and VPA caused a significant reduction in both astrocytes and microglia numbers. These data, therefore suggest that HDAC-Is prevented TH-positive cell death by reducing some other aspect of cell death which thereby causes a reduction in the glial reaction, and in this case, a reduction in astrogliosis. This confirms pathological studies of PD brains and animal models (Chapter 1), which reports of

increases in the number of reactive astrocytes in the area associated with dopaminergic cell loss (Forno *et al.*, 1992).

Typically, glial cells have a number of protective properties, but the main question of how HDAC-Is decrease astrogliosis still remains unanswered. On the onset of injury and damage such as, following 6-OHDA and LPS administration, the inflammatory process is initiated with the activation of glial cells and the release of cytotoxic pro-inflammatory cytokines such as TNF-α, IFN-γ and IL-1β, which are also potent activators of iNOS in glial cells and induce their expression. This subsequently releases NO which diffuses to neighbouring neurones to react with superoxide to form peroxynitrite and contribute to the demise of dopaminergic neurones through nitrative stress (Chapter 1) (Teismann & Schulz, 2004). The cytokines also act directly on neurones to activate caspases which results in neuronal loss via apoptosis (Hartmann *et al.*, 2000; Hartmann *et al.*, 2001), and NF-κB which activates detrimental enzymes such as iNOS and COX-2, which contributes to ROS generation during COX-2 catalysis of prostaglandin G_2 (PGG_2) (Smith *et al.*, 1991; Teismann *et al.*, 2003b; Teismann & Schulz, 2004) and contribute to neuronal loss via oxidative stress. These dying neurones release toxic compounds which are scavenged by glial cells to protect neighbouring neurones (Rosenberg, 1991; Aloisi, 2001). But through a vicious cycle, the activation of the glial cells to remove these toxic compounds results in the initiation of the inflammatory process and results in further neuronal loss.

At the initial stages of inflammation, it is possible that HDAC-Is may exert their protective mechanisms by suppressing the release of the pro-inflammatory cytokines, as shown in acute arthritis by HDAC-I, ITF2357 (Joosten *et al.*, 2011). As the double immunofluorescence staining showed that the HDAC isoforms were not present in the inflammatory cells, namely astrocytes and microglia in both naive and toxin-treated mouse brain sections, it can be assumed that the HDAC-Is act indirectly on the inflammatory cells maybe by suppressing the release of these cytokines, which results in less deleterious effects on neurones by these cytokines and in turn, less activation of glia. Alternatively, the HDAC-Is may not have any effect on inflammation at all, and the reduction in glial cell number observed in the present study is a secondary effect. In Chapter 3, it was mentioned that HDAC-Is induce apoptosis in cancerous cells, but this is not the case for normal cells as HDAC-Is was shown to prevent p53-dependent and independent Bax-mediated neuronal apoptosis (Uo *et al.*, 2009). If this is the case, then it is plausible that the inflammatory process was initiated and progressed as expected after toxin lesions, but the HDAC-Is inhibited the neuronal death by apoptosis, which in the end resulted in less toxic compound release by the dying neurones and in turn less glia activation.

The exact mechanism of action of HDAC-Is on neuroprotection in the 6-OHDA and LPS model is not yet clear and prompts for further investigation, but it all seems to be related to an effect on glial cells. The staining results allow the assumption that HDAC-Is do not exert their effects directly on these inflammatory cells to protect dopaminergic neurones. It is possible they may act directly on dopaminergic neurones to result in protection. Even though HDAC-Is proved to be protective in lesioned mice, extensive research needs to be undertaken to establish their exact role in PD.

5.4.4 Conclusion

The hypothesis of this study is accepted as the data presented in this Chapter has shown that the multi-cellular populations of the animal models contributed to the protection of dopaminergic neurones in the 6-OHDA and LPS-unilateral lesioned mice during HDAC inhibition, in addition to reducing the numbers of astrocytes and microglia. But, the lack of HDACs in glial cells suggests that the reduction in glia was secondary to reduced neuronal damage. The precise mechanism of how HDAC-Is work is unknown due to the limited *in vivo* reports in PD models. A proposed mechanism will therefore be discussed further in Chapter 6.

Chapter 6 General Discussion

6.1 Summary of results

Neuroprotection is the gold standard for new treatment for PD, however, no drugs have shown unequivocal disease modifying effects in the clinic. As HDAC inhibitors have shown potential neuroprotective effects in other neurodegenerative diseases, it was hypothesised that they might protect dopaminergic neurones from cell death in PD. In this respect, the aim of this research was to establish whether HDAC inhibition was neuroprotective in experimental models of PD. Accordingly, the present study examined the effect of the HDAC-Is, VPA and SAHA, on toxin-induced cell death in cell lines, primary neuronal cultures and in mice. The following results were obtained in the individual studies:

1. Inhibition of HDACs with VPA and SAHA alone was toxic and enhanced the neurotoxicity of H_2O_2 and MPP^+ in neuroblastoma cell lines.
2. In primary mesencephalic cultures, inhibition of HDACs did not prevent dopaminergic neuronal death following MPP^+- and LPS-induced toxicity. However, toxin-induced gliosis was reduced following HDAC-I treatment.
3. In 6-OHDA-lesioned mice, high dose of VPA (400 mg/kg) and SAHA were effective in protecting dopaminergic neurones in the SN.
4. In LPS-lesioned mice, high dose of VPA and SAHA protected dopaminergic neurones from toxin-induced cell death.
5. In both 6-OHDA- and LPS-lesioned mice, VPA and SAHA administration induced a reduction in astrocytosis but not microgliosis.

Overall, these results support the hypothesis that HDAC inhibition would protect dopaminergic neurones against toxin-induced cell death in PD. Even though protection of dopaminergic neurones was not observed *in vitro*, it was observed *in vivo* in addition to a reduction in inflammation.

This protective effect of HDAC-Is observed in models of dopaminergic cell death adds to their neuroprotective potential. HDAC-Is have previously shown promise in animal models of other neurodegenerative disorders, such as HD where they decreased the neurodegenerative phenotype and improved the survival and motor performance of R6/2 transgenic mice (Ferrante *et al.*, 2003; Hockly *et al.*, 2003). In SMA, HDAC-I administration to transgenic mice increased their lifespan and improved motor symptoms (Chang *et al.*, 2001). In ALS combined treatment with phenylbutyrate and riluzole (FDA-approved ALS drug) increased survival and improved pathological phenotype (Del Signore *et al.*, 2009; Chuang *et al.*, 2009). Despite this only sodium phenylbutyrate has progressed to phase II clinical trials of HD and ALS (ClinicalTrials.gov). The delay may be partly due to the failed translation of positive *in vitro* effects into *in vivo* models,

and this questions the suitability of the models used. Indeed this was exemplified in the present study where the protective effects of HDAC inhibition were only seen *in vivo*.

6.2 Advantages and limitations of toxin-induced cell model

Despite promising pre-clinical data, the translation of the neuroprotective effects of most if not all of the potential agents, from cellular and animal studies have failed in clinical studies. The most recent example being Cogane (PYM50028), which failed phase II/III clinical trials despite its effect as a neuroprotective and neurorestorative agent as seen in experimental models of dopaminergic cell death (Visanji *et al.*, 2008); Phytopharm (2013)) (Table 1-2).

At the start of these studies, it was hypothesised that HDAC inhibitors would decrease dopaminergic cell death in models of nigro-striatal loss. Since there is no unifying proposed action of these inhibitors, the investigations looked at HDAC-Is potential neuroprotective action through two mechanisms: 1. oxidative stress, by using H_2O_2 and MPP^+ *in vitro*, and 6-OHDA *in vivo*; and 2. inflammation, by using LPS *in vitro* and *in vivo*. Interestingly, the HDAC-Is were only found to be effective *in vivo*, thereby questioning the usefulness of the *in vitro* studies.

6.2.1 Toxin-induced cell death *in vitro*

Cell lines

In the present studies, HDAC-Is had no effect on the survival of dopaminergic neurones in cell lines and primary cultures, but they did reduce the number of inflammatory cells in primary cultures. Similar findings have been reported for other potential neuroprotective agents that had no effect on SH-SY5Y cell line survival, but had positive effects *in vivo* (Presgraves *et al.*, 2004; Kou *et al.*, 2008), with a typical example being osteopontin (Ailane *et al*., in preparation, personal communication).

Cell culture systems are widely used to study the pathological mechanism involved in cell death in PD and to investigate the effects of potential neuroprotective agents (Gazdar *et al.*, 2010). Indeed, immortalised cell lines are widely used as they have several practical advantages. They are convenient, robust, grow and divide quickly and easily in culture, which allows the conduction of multiple experiments in a short period of time. Overall, experiments on cell lines are less expensive and less time consuming than testing compounds in primary cultures or in whole animals, and their functional and biochemical properties similar to dopaminergic neurones, makes them useful in PD research as they mimic aspects of the dopaminergic neuronal death observed in PD when treated by neurotoxins such as MPP^+ and 6-OHDA (Xie *et al.*, 2010).

Despite these advantages, there are limitations of cell lines that may have affected the results of the present study. Array-based comparative genomic hybridization studies have shown that the dopaminergic neurones of cell lines have significantly different characteristics from native dopaminergic neurones *in vivo* genetically and phenotypically (Skibinski & Finkbeiner, 2011). These differences start with the origins of the cell lines, where SH-SY5Y cell line is a thrice cloned subline of neuroblastoma cell line SK-N-SH, originally established from a bone marrow biopsy of a neuroblastoma patient with sympathetic adrenergic origin (Biedler *et al.*, 1978); and N1E-115 cell line, is derived from murine brain neuroblastoma also with cholinergic and adrenergic origin (Amano *et al.*, 1972; Biedler *et al.*, 1978; Richelson, 1973). The cancerous origin means these cells are continuously dividing, so their numbers increase during the course of an experiment, making it difficult to distinguish whether the compounds tested influence the proliferation or cell death rate (Datki *et al.*, 2003). SH-SY5Y cells, particularly expresses low levels of dopamine synthesising enzymes and DAT, which makes them respond differently to exogenous stimuli in comparison to mature neurones (Presgraves *et al.*, 2004). In addition, cell lines are also less sensitive to neurotoxins and neuroprotective agents (Storch *et al.*, 2000). This was evident in Chapter 3, where the EC_{50} of MPP^+ was 1000 fold greater in cell lines than in primary cultures. This is because in cell lines, DAT is required for MPP^+ toxicity *in vivo*, but in cell lines low DAT levels may mean that MPP^+ is either not taken into cell lines or it exerts effects via non-DAT mechanisms (Gainetdinov *et al.*, 1997; Xie *et al.*, 2010).

Another important aspect to consider is the lack of cell heterogeneity. The homogeneous cell population of SH-SY5Y and N1E-115 cell lines means they lack inflammatory cells, meaning that they do not represent a true physiological environment as occurs *in vivo* where neurones and glial cells co-exist. Cell cultures may therefore not truly reflect the actions of HDAC-Is as they would *in vivo*. However, in the absence of glial cells in this investigation, HDAC-Is had no effect on dopaminergic cell viability, suggesting that they do not act directly on neurones. Finally, the fact that cell lines originate from malignant cells makes them unsuitable candidates for HDAC inhibition studies, as the HDAC-Is have been shown to induce tumour-cell selective apoptosis in the cell cultures (Bolden *et al.*, 2013).

Primary culture

Primary cell culture in particular the VM cell cultures used in these studies, addresses some of the limitations of cell lines. They are good candidates as a source of dopaminergic neurones which have not been immortalised. Since they are derived from the brain and not tumours, they overcome the problem of HDAC-Is selectively inducing apoptosis in cancerous cells. The

dopaminergic neurones are cultured within a heterogeneous population with other neuronal and glial cells as in the SN, making a more physiological environment in which to examine the potential protective action of HDAC-Is.

Despite these advantages, there are also limitations. First, these cells are sensitive and immature, as they are derived from embryos. They are also slow in proliferation, have limited life-span, and it is difficult to produce optimal survival and growth in the primary cell cultures. This may be due to the stress of the isolation procedure and 'foreign environment' of the culture process which causes only 1 - 10 % of harvested cells to survive (Heyer, 1984; Halliwell, 2003). Dopaminergic neurones dissected from foetal rat VM make up ~5 % of the total culture (Chapter 4) compared to 50 % of cells harvested from mid-brain cultures derived from post-natal rodents (Rayport *et al.*, 1992). Furthermore, the environment in which the cells are grown, from the cell culture medium to the incubator, potentially increases cellular oxidative stress (Halliwell, 2003). The presence of high oxygen, free iron ions and the deficiency of antioxidants provide a pro-oxidant environment and force cells to adapt for survival by increasing their anti-oxidant defences. This is by down-regulating the expression of ROS-generating enzymes and altering cellular targets of oxidative damage to become more resistant to damage by ROS (Halliwell, 2003). These culture conditions cause the characteristics that the neurones display in culture to vary in comparison to how they would behave *in vivo*.

However, in the current investigation, important findings were obtained from the primary culture studies which gave insight into the actions of HDAC-Is. Even though the inhibitors did not promote cell survival in these heterogeneous cell cultures, they did reduce inflammatory cell proliferation and they did not exacerbate the effects of the toxins as found in cell lines. This suggests that glial cells do not control dopaminergic neuronal loss in these model systems. The fact that a reduction in astrocytes was also seen in the *in vivo* model as well as protection of dopaminergic neurones, shows that despite the limitations of primary cultures, they do mimic the brain in terms of the relevant cell types, and the difference in results may be due to the extensive cellular connections in the brain compared to the culture plate. However, cells dissected in an embryonic form and grown in culture are not optimal as a model for age-related changes in physiology or late-onset disease as they are not representative of the mature brain (Eide & McMurray, 2005). Neurones in developmental stages are still growing and maturing and therefore behave differently in terms of pharmacology, electrophysiology, development, and regenerative and pathological characteristics; whereas those of the mature brain are maintained in a homeostatic complex network for synaptic plasticity (Arenas *et al.*, 1995; Brewer & Torricelli, 2007). This could be the reason for the observation of HDAC expression on both neurones and

glia in primary culture, compared to their expression on neurones only in brain tissue sections. There might also be differences between the species, as the cultures were generated from rats whereas mice were used for the *in vivo* study. In addition, although primary cultures contain glia, their phenotype may be different to mature glia in the SN. This questions the validity of using immature cultures to mimic a disease which affects the middle to old age individuals, and therefore emphasises that experiments performed *in vitro* need to be validated in *in vivo* models of adult brain.

To conclude, cell lines and primary culture models provide a good starting point to investigate the properties of potential neuroprotective agents. Although caution needs to be taken when examining the effects of compounds in cell cultures, as neither cell lines nor primary cultures represent the true physiological conditions and neuronal behaviour that occur *in vivo*.

6.2.2 Toxin-induced cell death *in vivo*

Animal models are useful for modelling neurological disorders to study their pathology and for testing neuroprotective or neurorestorative therapeutic strategies. Animal models have offered insights into the understanding of the cell death process, aetiology, pathology as well as molecular mechanisms in PD (Blesa *et al.*, 2012). However, no model is perfect due to the complexity of the events occurring during neuronal loss which are still not fully understood. However, these models are important as they allow preclinical screening of potential new treatments. In this study, unilateral lesioning with neurotoxins 6-OHDA and LPS was used to produce models of nigro-striatal destruction.

Intrastriatal injection of 6-OHDA is widely used for investigating neuroprotective strategies (Kirik *et al.*, 1998) because it induces a lesion similar to early symptomatic stage in PD, where there is 50 – 60 % loss of dopaminergic neurones, and when neuroprotective therapy would be started. The intrastriatal 6-OHDA model is easily replicated, and it provides a more prolonged time frame for the neuroprotective agents to be effective due to the retrograde nature of cell death. This contrasts with SNpc and MFB lesioning where there is almost a complete loss of nigral cells (Emborg, 2004).

The bacterial endotoxin LPS has been a useful tool to investigate the role of neuro-inflammation in dopaminergic cell death (Liu & Bing, 2011). Intrastriatal LPS administration has not been well characterised, compared to its intranigral application. However, it produces a progressive degeneration of the nigrostriatal pathway similar to degeneration in PD which is driven by the toxic inflammatory factors released from the activated microglia and astrocytes. It also helps in

explaining the contribution of the various pro-inflammatory and neurotoxic factors to dopaminergic neurodegeneration and aid in the design of specific potential therapeutic agents and identifies early stage-diagnostic biomarkers (Dutta *et al.*, 2008; Hunter *et al.*, 2009). However, the degree of inflammation is several orders of magnitude greater than that seen in PD in man, and thus raises the question as to whether it truely reflects the pathology or pathogenic process.

Importantly, neither the 6-OHDA nor LPS model mimics all the pathological features of PD. For example, there is no real progression of cell death, non-dopaminergic areas are unaffected and no lewy bodies are observed. They do induce some of the pathogenic process such as, oxidative and nitrative stress, inflammation and mitochondrial impairment. The main difference between these 6-OHDA and LPS models is the mechanism by which neuronal cell death occurs. In the 6-OHDA model, the cell death mechanism involves accumulation of toxin in the dopaminergic neurones followed by oxygen radicals followed by semiquinone production which mediate cellular damage, and in turn induce activation of glial cells (Cicchetti *et al.*, 2002; McCoy *et al.*, 2006). LPS on the other hand is not directly toxic to neurones but causes their degeneration through activating glial cells to induce an inflammatory reaction leading to increased release of cytokines, iNOS induction, oxidative and nitrative stress, and decreased secretion of the neurotrophic factors BDNF and GDNF (McNaught & Jenner, 1999; McNaught & Jenner, 2000; MCNaught & Jenner, 2000; Dutta *et al.*, 2008).

The question as to whether these models truely reflect the pathology of PD needs to be considered as 6-OHDA induces destruction of the dopaminergic nigro-striatal tract, however, it has no effect on other brain regions affected in PD as it is injected focally into the striatum. Even though it provides a reproducible model of nigral cell death, there is still variability between animals in the extent of the lesion and this is overcome by using large groups of animals to average out these differences. Although the 6-OHDA-lesioned rodent remains a widely used model of PD, its success stems from its usefulness in the search for symptomatic agents, rather than neuroprotective therapies. While it mimics some of the mechanisms of cell death in PD, it fails to reflect the progressive nature or extensive pathology seen in PD. Maybe this is one reason why no neuroprotective agents have been successfully developed through its use.

LPS induces widespread inflammation in the brain and may therefore not be a model specific to PD (Qin *et al.*, 2007). It induces microgliosis, but also results in astrocytosis, which is not a major component of the glial reaction occurring in PD (Duty & Jenner, 2011). The main limitation of the LPS model is the method of application. Several models of LPS-induced nigral cell death have

been created via intranigral, intrastriatal, and systemic injection (Hunter *et al.*, 2009). However, there are disagreements on which route of LPS injection causes dopaminergic neurodegeneration. For example, a single i.p. administration of LPS has been shown to cause dopaminergic neuronal degeneration (Qin *et al.*, 2007) but is yet to be reproduced. The debate is mainly between intrastriatal used in this study and intranigral lesions. Recent characterisation of these routes concluded that intranigral LPS administration causes localised microgliosis in the SN accompanied by nigrostriatal degeneration and stable motor deficits, whereas intrastriatal administration only induced localised microgliosis in the striatum and no dopaminergic neuronal loss and transient motor dysfunction (Hoban *et al.*, 2013). The findings from the present study contradict this report, as intrastriatal LPS resulted in cell loss accompanied by localised microgliosis in the SN. The discrepancy between these reports is the species used, where evidence in favour of intranigral LPS administration used rats and that in favour of intrastriatal administration, like the present study, used mice. The size difference between the rat and mouse brain could be a factor, as LPS may diffuse a shorter distance to get to the SN of the mouse compared to the rat. An alternate explanation could be species difference in LPS sensitivity. A similar example is MPTP, which rats are resistant but causes neurodegeneration in mice (Chiueh *et al.*, 1984; Boyce *et al.*, 1984).

As mentioned earlier, LPS causes dopaminergic neuronal death through activation of glial cells. A decrease of this inflammatory response coupled with neuronal survival was achieved with ibuprofen and dexamethasone, where a marked reduction of GFAP, OX-42, iNOS and 3-NT was observed (Iravani, Personal communication). This report then supports the anti-inflammatory potential of HDAC-Is exhibited in vivo which was accompanied with dopaminergic neuronal survival. This however questions whether the VM culture may be too immature or may need a greater reduction in glial cells in order to get protection of dopaminergic cells. This is because a decrease of inflammatory cells without dopaminergic neuronal preservation was observed, and therefore emphasises the requirement of validating *in vitro* studies in *in vivo* models.

An alternative model to better predict the effect of HDAC-Is is the MPTP-treated mouse and primate model which is commonly utilised, as it causes selective loss of the nigro-striatal tract. This is because previous studies have already investigated the effects of HDAC-Is in MPTP-treated mice and observed the protection of dopaminergic neurones (Kidd & Schneider, 2011; Zhou *et al.*, 2011). MPTP is systemically active and readily crosses the BBB to be converted to the toxic moiety MPP^+ by MAO-B in glia and serotonergic neurones (Chiba *et al.*, 1985). Being systemically active means MPTP does not require the skilled stereotaxic surgery, as performed in this study; and it produces a bilateral degeneration of the nigro-striatal tract, more reflective of

that seen in PD, such as elevated acetylcholine (Hadjiconstantinou *et al.*, 1985), and extracellular glutamate levels associated with the induction of programmed cell death (Meredith *et al.*, 2009). However, as with every model, there are limitations. It would be ideal to investigate the effects of the inhibitors on MPTP-treated primates, as they are closely related to humans. But limitations of this model such as acute cell death processes induced by MPTP and lack of lewy body-like inclusions (Shimoji *et al.*, 2005), questions the validity of this model as a model of PD. Indeed, it too has been widely used to predict the efficacy of neuroprotective agents, but all have failed in human trials so far.

So to conclude, there is no perfect cell culture or animal model that completely models the pathology of PD. However, each *in vitro* and *in vivo* model used in the present study provided a key piece of the puzzle into the role of HDAC-Is in cell death processes, and this has enabled the mechanism of the inhibitors actions to be understood and deduced.

6.3 Proposed mechanism of HDAC-I's protection of dopaminergic neurones

The results from the studies described in this thesis showed that in the absence of inflammatory cells, there was no protection of dopaminergic neurones by HDAC-Is against toxic insults. Interestingly, when inflammatory cells were present in primary cultures, there was still no protection of dopaminergic neurones but there was a reduction in the number of astrocytes and microglia, suggesting that in primary culture these glial cells do not control cell death. By contrast, *in vivo* rodent models, there was protection of dopaminergic neurones in addition to a reduction in astrocytes number. However, since the data from primary cultures suggest that glial cells do not control cell death, the protection of dopaminergic neurones *in vivo* suggests that the HDAC-Is may be acting through other cell death pathways.

Studies from post mortem PD brains and animal models of the disease have shown an increase in the number of reactive astrocytes and microglia in areas associated with dopaminergic cell loss (McGeer *et al.*, 1988b; McGeer *et al.*, 2003; Forno *et al.*, 1992). This suggests that an inflammatory reaction may contribute to neuronal death via the release of pro-inflammatory cytokines, e.g. TNF-α, IL-1β and IL-6. They activate enzymes iNOS and COX-2 to contribute to nitrative and oxidative stress, and activate caspases, such as capase-1 and 3, to induce apoptosis of cells. This results in further activation of these glial cells to scavenge the toxic compounds released by the dying cells (Nagatsu *et al.*, 2000; Teismann & Schulz, 2004; Dutta *et al.*, 2008; Lima *et al.*, 2012) (Figure 6-1).

HDAC-Is can reduce the production of pro-inflammatory cytokines, thereby preventing the damaging effects of these cytokines on neurones and further activation of glial cells, thus preserving the surviving ones. Evidence for this comes from studies by Leoni *et al.* (2002) who demonstrated that SAHA pre-treatment suppressed LPS-induced cytokine release, such as TNF-α, IL-1β, IL-6, and IFN-γ by 50 % in mice (Leoni *et al.*, 2002), and this inhibited macrophage NO release stimulated by TNF-α and IFN-γ. This reduction in cytokine release was also observed with HDAC-I ITF2357 in peripheral blood mononuclear cells (Leoni *et al.*, 2005). In both studies, there was a marked reduction in LPS-induced increase of TNF-α and IFN-γ mRNA, but no change in IL-1β mRNA, however a reduction in the secretion of IL-1β was observed. This suggests that HDAC-Is may affect proteins, e.g. NLRP3 inflammasome, that are required for the activation of caspase-1, which cleaves pro-IL-1β to a mature, active and secretable form that binds to IL-1 receptor (Hoffman & Wanderer, 2010). Indeed, inhibition of caspase-1 has been shown to delay the onset of motor abnormalities in mouse models of HD (Ona *et al.*, 1999). However, the mechanism for the decrease in IL-1β secretion is unclear as ITF2357 did not inhibit the enzymatic activity of caspase-1 in LPS-stimulated monocytes (Leoni *et al.*, 2005). HDAC inhibition may prevent the secretion of IL-1β via a specialized secretory lysosomal pathway, where a subset of secretory lysosomes allows the cytokine to bind to lysosomal enzymes (Andrei *et al.*, 2004). This takes place through activation of phosphatidylcholine-specific phospholipase C and A_2, which facilitates the passage of caspase-1 to pro-IL-1β and, consequently, pro-IL-1β processing in these secretory lysosomes (Andrei *et al.*, 2004). This certainly is speculative with respect to PD pathology and will need to be explored further.

An alternative mode of action of HDAC-Is may be via oxidative stress and/or apoptosis pathways, which results in a decrease in inflammation and inflammatory cells as highlighted briefly in Chapter 5. The idea for this notion comes from numerous studies showing that HDAC-Is up-regulate the acetylation of transcription factors and expression of genes that confer resistance to oxidative stress, such as Sp1, Foxo3a and Mt2 (Ryu *et al.*, 2003; Shimazu *et al.*, 2013).

In contrast to the deleterious roles of microglia, astrocytes have a neuroprotective role via the release of the antioxidant glutathione. This protein acts as a defence against oxidative and nitrative stress by scavenging free radicals and reactive oxygen species including hydroxyl radical, lipid peroxyl radical, peroxynitrite, and H_2O_2 directly or through a series of enzymatic reactions (Wu *et al.*, 2004). Glutathione is present at higher concentrations in astrocytes (~3.8 mM) than in neurones (~2.5 mM), and once there is an increase in ROS levels, glutathione is released into the extracellular space to increase its availability to neurones, thereby making them less susceptible to the damaging species (Rappold & Tieu, 2010). Ryu and colleagues

(2003) showed that on glutathione depletion, Sp1, an apoptosis-associated transcription factor is activated. HDAC-Is were able to abrogate oxidative stress-induced death induced by glutathione depletion by augmenting Sp1 acetylation, Sp1 DNA binding and Sp1-dependent gene expression, which confer resistance to oxidative stress, thereby preventing neuronal loss *in vitro* and *in vivo* (Ryu *et al.*, 2003). Most recently, it has been reported that the transcription of two genes, namely Foxo3a and metallothionein 2 (Mt2), encoding oxidative stress resistance are increased in response to exogenous administration of an endogenous HDAC-I, β-Hydroxybutyrate (βOHB) to protect paraquat-treated mice against oxidative stress (Shimazu *et al.*, 2013). Examination of kidney tissue sections for oxidative stress markers: protein carbonyl and 4-Hydroxynonenal (4-HNE), found paraquat to significantly increase these markers, but this increase was suppressed in βOHB treated mice. An explanation for this result is that antioxidant enzymes, mitochondrial superoxide dismutase (MnSOD) and catalase are targets of Foxo3a. Once oxidative stress is triggered, Foxo3a activates the transcription of MnSOD and catalase, which scavenge superoxide and hydrogen peroxide respectively (Chiribau *et al.*, 2008) and contribute to the protective activity of Foxo3a against oxidative stress (Kops *et al.*, 2002; Shimazu *et al.*, 2013).

In addition to preventing oxidative stress, supporting evidence of HDAC-Is preventing apoptosis highlights another mechanism by which they may exert their neuroprotective properties. In postnatal cultured murine cortical neurones HDAC-Is were shown to protect neurones from p53-dependent and independent Bax-mediated neuronal apoptosis by selectively suppressing p53-dependent PUMA (p53 up-regulated modulator of apoptosis) expression, thereby preventing post-mitochondrial events including cleavage of caspase-9 and caspase-3 (Uo *et al.*, 2009). This effect was not observed in SH-SY5Y neuroblastoma cells, thus confirming that HDAC-Is selectively induce apoptosis in malignant cells and not in non-malignant cells such as the primary neurones (Shao *et al.*, 2004; Uo *et al.*, 2009). In addition, anti-apoptotic protein B cell lymphoma protein-2 (bcl-2) is markedly increased by HDAC-I VPA in the frontal cortex of rats (Chen *et al.*, 1999). Moreover, HDAC inhibition up-regulated heat-shock protein (HSP) 70 and attenuated the up-regulation of apoptotic-protease-activating factor-1 (apaf-1) and increased the binding between the two to block apoptosome formation and reduced the release of cytochrome c and activation of caspase-3, thereby inhibiting the apoptotic pathway (Zhang *et al.*, 2012).

Typically, astrocytes confer neuroprotection by releasing trophic factors, such as GDNF, BDNF and MANF (mesencephalic astrocytes-derived neurotrophic factor), that can support neuronal function. *In vitro* studies in rat midbrain neuron-glia cultures reported that HDAC inhibition increased the expression of GDNF and BDNF in astrocytes to protect dopaminergic neurones (Wu *et al.*, 2008). If this increased expression of the trophic factors also occurs *in vivo*, that

would contribute to the survival of dopaminergic neurones as intrastriatal injection of MANF in 6-OHDA lesioned mice was found to be neuroprotective (Voutilainen *et al.*, 2009).

Even though there is evidence reporting that HDAC-Is suppressing oxidative stress and apoptosis, this theory is not supported by the *in vitro* studies reported in this thesis. Particularly in cell lines where H_2O_2 and MPP^+ both act via increasing oxidative stress. This may have been primarily due to the origin of the cell lines being malignant. Numerous studies in cancer have found HDAC-Is to be ideal cancer therapeutic agents because they selectively induce apoptosis in tumours. The cell lines, SH-SY5Y and N1E-115 cell lines are both derived from neuroblastoma and this may have overcome the protective effects of the anti-apoptotic enzymes such as, glutathione, superoxide dismutase and catalase. In addition, the concentrations of the toxins H_2O_2 and MPP^+ used were extremely high and this toxicity may have enabled them to induce cell death by acting on pathways other than the mitochondria. This is especially the case for H_2O_2 as it is a non-selective mitochondrial toxin.

Similarly, the data from the primary culture studies do not support the theory of HDAC-Is suppressing oxidative stress and apoptosis, as inhibition of the mitochondria with MPP^+ also increases oxidative stress in cells. The HDAC-Is did not prevent MPP^+-induced cell death, but they did prevent exacerbation of MPP^+ toxic effect. However, the toxicity of the inhibitors may have played on the vulnerability and sensitivity of the primary cultures, and promoted the cell loss observed in the presence and absence of the toxin.

In summary, even though the data from the *in vitro* studies fail to support the mechanisms described, the data from the *in vivo* study best support the mechanism of HDAC-Is suppressing the secretion of pro-inflammatory cytokines, which initiates the vicious cycle of inflammation and cell death. How they do this is still very unclear, as immunostaining images in Chapter 5 showed that the HDACs are not found within these inflammatory cells and requires further investigation. The latter notion that HDAC-Is target another pathway and their effect on inflammatory cells is secondary seems very plausible as shown by the numerous evidence reported. Their ability to suppress oxidative stress and apoptosis means there would be less number of dopaminergic dying and releasing cell debris which would require the activation of glial cells to scavenge, and therefore impact the number of glial cells activated as observed in this thesis.

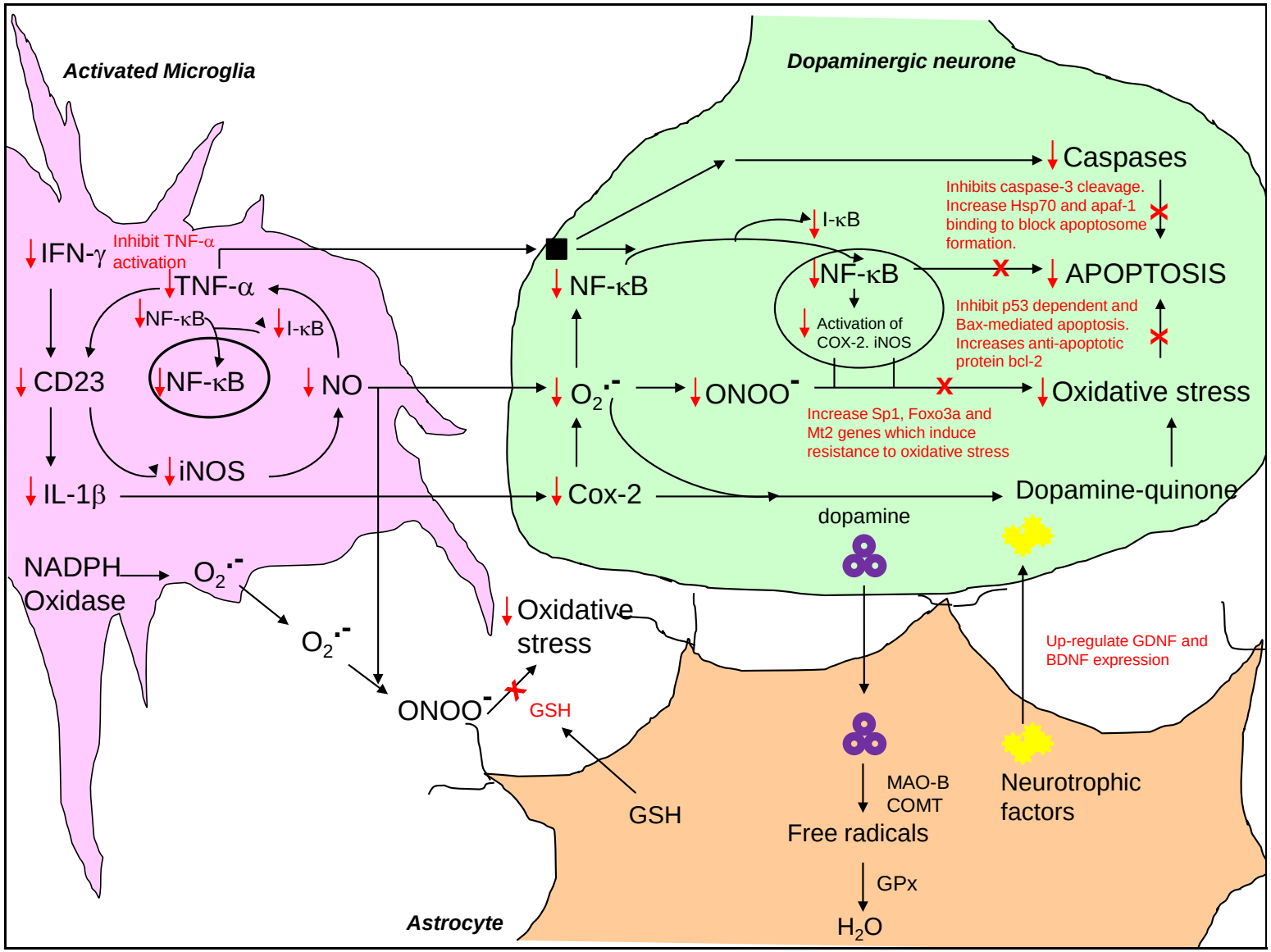

Figure 6-1 Mechanism of HDAC inhibition on inflammatory pathway.

HDAC-Is inhibit secretion of cytotoxic compounds such as cytokines (IFNγ, IL-1β) which decreases CD23 expression and subsequently reduces iNOS expression and NO release. HDAC-Is inhibit TNF-α activation and decreases TNF-α-induced NFκB activation. This affects the NFκB mediated transduction pathways and prevents the activation of deleterious enzymes (COX-2, iNOS) and ROS generation, which contribute to oxidative stress. This damaging stress is prevented by increased expression of oxidative stress resistance genes (Sp1, FOXO3A, MT2). HDAC inhibition also prevents apoptosis through caspase-3 cleavage and activation, increase binding of HSP 70 and apaf-1 to prevent apoptosome formation, and prevent p53 and Bax mediated apoptosis. Upregulation of neuroprotective proteins GSH and bcl-2 and neurotrohic factors (GDNF, BDNF) aid to protect the neurone. *Abbreviations: MAO-B, monoamine oxidase B; COMT, catechol-O-methyl transferase; GPx, glutathione peroxidise; GSH, glutathione; NAPDH nicotinamide adenine dinucleotide phosphate; NF-κb, nuclear factor-κb; TNF-α, tumour necrosis factor-α; IκB, Inhibitor of κB; iNOS, Inducible nitric oxide synthase; NO, nitric oxide; IFN-γ, interferon-γ; CD23, macrophage cell surface antigen Fc R11; apaf-1, apoptotic protease activating factor-1.* (Adapted and modified from Leoni *et al*., 2002; Ryu *et al*., 2003; Teismann & Schulz, 2004; Wu *et al*., 2008; Uo *et al*., 2009; Rappold & Tieu, 2010; Zhang *et al*., 2012; Shimazu *et al*., 2013).

6.4 Is HDAC inhibition the way forward for PD?

From the *in vivo* studies reported in this thesis, it was shown that inhibition of HDACs reduced inflammation and prevented toxin-induced dopamine cell loss. However, the *in vitro* studies suggest that these two effects are independent, and that HDAC inhibition can decrease glial cell number without protecting the neuronal cells.

Recently, there have been an increasing number of studies reporting the neuroprotective effects of HDAC-Is in both *in vitro* and *in vivo* models of dopaminergic cell death. For example, VPA protected rat nigro-striatal neurones from cell death initiated by the mitochondrial complex I inhibitor, rotenone, and reversed striatal dopamine depletion through hyperacetylation of histone H3 which correlated with a decrease in HDAC activity (Monti *et al.*, 2010). In addition, VPA prevented nuclear localisation of monoubiquitinated α-synuclein, where it has been described to induce histone acetylation inhibition (Monti *et al.*, 2010). Furthermore, DJ-1 protein, which acts as an antioxidant and its mutant form is associated with early-onset autosomal recessive PD (Chapter 1), was increased to approximately 260% following phenylbutyrate treatment as well as rescuing dopaminergic neurones from MPTP-induced cell death in mice (Zhou *et al.*, 2011). Additionally, phenylbutyrate and sodium butyrate increased DJ-1 transcription elevating protein levels to approximately 300% compared to control in N27 dopaminergic cell line, thereby rescuing cells from H_2O_2- and 6-OHDA-induced oxidative stress and A53T mutant α-synuclein toxicity (Zhou *et al.*, 2011). This evidence contributes to the theory that HDAC-Is suppress oxidative stress, as DJ-1 is a protective protein and HDAC-Is elevate its levels to increase cell survival from toxin-induced oxidative stress, even though neuronal protection was not seen in cell lines and primary culture following H_2O_2 and MPP^+ treatment in cell lines.

Despite these optimistic reports of HDAC-Is exhibiting neuroprotective effects, these inhibitors have a number of actions, including cell cycle arrest, apoptosis, angiogenesis, and immune modulation, which are potentially toxic (Bolden *et al.*, 2006). This is probably due to the selectivity of the individual inhibitors for HDAC classes rather than isoforms and/ or nonhistone substrates (Grayson *et al.*, 2010). For this reason, HDAC isoform-specific inhibitors need to be designed. This is because most of the inhibitors currently available are class- and not isoform-specific inhibitors. Not all HDACs need to be inhibited in order to observe a protective effect (as mentioned in Chapter 1). In some cases, inhibition of some HDACs can prove to have detrimental effects rather than protective ones. For example, inhibition of HDAC1 results in p25-induced DNA damage and aberrant cell cycle activity, and over-expression of HDAC1 rescues neurones from p25 toxicity (Kim *et al.*, 2008).

Besides, class-specificity, HDAC-Is have also been shown to exert cell-type- and region-specificity, which serves to be a problem (Svechnikova *et al.*, 2008). For example, HDAC-I MS-275 has been reported to be brain region-selective and up to 100 times more potent than VPA in increasing histone acetylation *in vivo*; but failed to increase acetylation in the striatum in doses up to 120 µmol/kg compared to VPA (Simonini *et al.*, 2006). MS-275, like VPA and SAHA, show beneficial properties for not only cancer treatment, but also psychiatric and neurodegenerative disorders, but their lack of specificity in different brain regions and organs are associated with non-specific cytotoxicity and significant *in vivo* side effects, including cognitive dysfunction, headaches, sedation, nausea and vomiting, thrombosis and a reduction in both blood cell count and blood electrolytes (Grayson *et al.*, 2010; Durham, 2012). Therefore, in order to overcome this issue, mRNA profiling studies of HDAC-Is effects in different brain regions including cortex, striatum, cerebellum, hippocampus, SN, etc in response to systemic drug administration needs to be compared to similar profiles obtained from organs including the kidney, liver, heart and pancreas of the same treated animals, to deduce the full effect of the candidate HDAC-I (Grayson *et al.*, 2010). Moreover, as HDAC-Is target a wide range of histone and nonhistone proteins such as transcription factors, identifying biomarkers and/ or specific mRNAs of proteins which are up- or down-regulated following HDAC inhibition could be used as indicators of drug inhibitor efficacy (Grayson *et al.*, 2010), and also improve the understanding of the mechanisms of these inhibitors and the pathophysiology of PD.

6.5 Other models for future studies

Recent positive reports of the neuroprotective effects of HDAC inhibition encourage the notion of these inhibitors to be investigated in other models of PD. In particular transgenic animal models based on gene defects in familial PD, as HDAC-Is are thought to work primarily at the level of transcription. These defects include α-synuclein, LRRK-2 and PINK1 among others (Chapter 1). For some reason the transgenic approach has failed to produce an effective animal model of PD in mice where the genetic defects exhibits the pathological changes with which they are associated in man (Duty & Jenner, 2011). However, this problem has been overcome by recombinant adeno-associated virus (rAAV) vector overexpression of α-synuclein in mice and primates which closely reproduce the pathology of the human condition, particularly the nigrostriatal tract degeneration (Kirik *et al.*, 2002). This model is of interest as increasing evidence confirms nigrostriatal degeneration initiates at the level of the axonal terminals in the putamen and cell loss is either caused or exacerbated by the presence of α-synuclein immunopositive neuronal inclusions (Chung *et al.*, 2009; Chu *et al.*, 2012). HDAC-I treatments

could slow down or potentially attenuate the degeneration of the nigrostriatal neurones as reported by Kontopoulos and group (2006) who showed that HDAC-Is were able to prevent α-synuclein neurotoxicity and prevent cell death (Kontopoulos *et al.*, 2006).

Furthermore, genetic models in multicellular model organisms are also emerging. These include the fruitfly *Drosophila melanogaster*, the nematode *Caenorhabditis elegans* model and the zebrafish *Danio rerio* as they have highly conserved homologues of the human genes associated with PD, such as parkin, UCH-L1, PINK1, DJ-1 and LRRK2 (Whitworth *et al.*, 2006; Duty & Jenner, 2011). These models would also be useful to test the neuroprotective properties of HDAC-Is.

6.6 Conclusion

As hypothesised, the data presented in this thesis coupled to previous studies on the effects of HDAC-I in PD models suggest that HDAC-Is are promising potential neuroprotective agents worthy of further investigation for future treatment of PD. The ability of these inhibitors to protect neurones from inflammation-mediated neurodegeneration, as in rheumatoid arthritis, and their beneficial properties observed in neurodegenerative disorders, particularly HD (Hockly *et al.*, 2003), makes them a potential candidates for neurodegenerative disorder treatments. However, a vast amount of further work needs to be completed to fully understand the mechanism of these inhibitors due to their multi-targets, and the fact that they have been proven to be useful in treating malignant conditions.

To take this field further, isoform-specific HDAC-Is need to be developed and tested as this would probably reduce the toxicity observed following the use of pan-inhibitors in the present study. In fact, HDAC1-specific HDAC-I, MS-275, is currently on the market but has not yet been tested in animal models of PD. Such investigations would provide better understanding of the role of the isoform and its potential neuroprotective role following inhibition. Second, the effects of the inhibitors need to be tested in genetic models such as the rAAV vector α-synuclein over-expressed mice and transgenic multicellular organisms, to determine and confirm the role of epigenetics in PD.

Chapter 7 Appendix

Table of statistics

Figure reference	Test	F value, (df), p value
Figure 3-7 Cell death in N1E-115 and SH-SY5Y cells following H_2O_2 and MPP^+ treatment.	One-way ANOVA	*H_2O_2* (A) N1E-115: F (2,6) = 3.24, p = 0.0748 (B) SH-SY5Y: F (2,7) = 18.60, p < 0.0001
		MPP^+ (C) N1E-115: F (2,7) = 5.60, p = 0.0163 (D) SH-SY5Y: F (2,7) = 16.41, p = 0.0002
Figure 3-8 Viable N1E-115 and SH-SY5Y cells following H_2O_2 treatment and MPP^+ treatment	One-way ANOVA	*H_2O_2* (A) N1E-115: F (2,5) = 2.70, p = 0.1156 (B) SH-SY5Y: F (2,5) = 2.67, p = 0.1179
		MPP^+ (C) N1E-115: F (2,5) = 0.85, p = 0.4566 (D) SH-SY5Y: F (2,5) = 1.23, p = 0.3344
Figure 3-9 Effect of H_2O_2 on cell survival following SAHA pre-treatment.	Two-way ANOVA	(A) *N1E-115: LDH assay* Interaction: F (7,32) = 4.60, p = 0.0012 SAHA: F (7,32) = 1.68, p = 0.1488 H_2O_2: F (1,32) = 74.24, p < 0.0001
		(B) *SH-SY5Y: LDH assay* Interaction: F (7,32) = 5.11, p = 0.0006 SAHA: F (7,32) = 15.98, p < 0.0001 H_2O_2: F (1,32) = 1236.68, p < 0.0001
		(C) *N1E-115: Trypan blue assay* Interaction: F (7,32) = 1.55, p = 0.1850 SAHA: F (7,32) = 6.65, p < 0.0001 H_2O_2: F (1,32) = 34.40, p < 0.0001
		(D) *SH-SY5Y: Trypan blue assay* Interaction: F (7,32) = 1.72, p = 0.1392 SAHA: F (7,32) = 2.46, p = 0.0391 H_2O_2: F (1,32) = 57.04, p < 0.0001
	One-way ANOVA	*LDH assay* (A) N1E-115: F (2,15) = 8.02, p = 0.0016 (B) SH-SY5Y: F (2,15) = 9.98, p = 0.0005
		Trypan blue assay (C) N1E-115: F (2,15) = 11.11, p = 0.0002 (D) SH-SY5Y: F (2,15) = 21.59, p < 0.0001

Figure 3-10 Effect of H_2O_2 on cell survival following VPA pre-treatment.	Two-way ANOVA	(A) *N1E-115: LDH assay* Interaction: F (7,32) = 0.51, p = 0.8219 VPA: F (1,32) = 1.19, p = 0.3368 H_2O_2: F (7,32) = 85.16, p < 0.0001
		(B) *SH-SY5Y: LDH assay* Interaction: F (7,32) = 1.20, p = 0.3312 VPA: F (7,32) = 0.75, p = 0.6317 H_2O_2: F (1,32) = 330.01, p < 0.0001
		(C) *N1E-115: Trypan blue assay* Interaction: F (7,32) = 0.82, p = 0.5752 VPA: F (7,32) = 2.13, p = 0.0682 H_2O_2: F (1,32) = 51.42, p < 0.0001
		(D) *SH-SY5Y: Trypan blue assay* Interaction: F (7,32) = 2.54, p = 0.0336 VPA: F (7,32) = 2.35, p = 0.0468 H_2O_2: F (1,32) = 49.65, p < 0.0001
	One-way ANOVA	*LDH assay* (A) N1E-115: F (2,15) = 40.15, p < 0.0001 (B) SH-SY5Y: F (2,15) = 3.37, p = 0.0479
		Trypan blue assay (C) N1E-115: F (2,13) = 2.35, p = 0.1158 (D) SH-SY5Y: F (2,15) = 21.40, p < 0.0001
Figure 3-11 Effect of MPP^+ on cell survival following SAHA pre-treatment.	Two-way ANOVA	(A) *N1E-115: LDH assay* Interaction: F (7,32) = 2.21, p = 0.0594 SAHA: F (7,32) = 3.49, p = 0.0068 MPP^+: F (1,32) = 24.41, p < 0.0001
		(B) *SH-SY5Y: LDH assay* Interaction: F (7,32) = 1.70, p = 0.1448 SAHA: F (7,32) = 48.53, p < 0.0001 MPP^+: F (1,32) = 306.68, p < 0.0001
		(C) *N1E-115: Trypan blue assay* Interaction: F (7,32) = 1.20, p = 0.3318 SAHA: F (7,32) = 4.53, p = 0.0013 MPP^+: F (1,32) = 50.37, p < 0.0001
		(D) *SH-SY5Y: Trypan blue assay*

		Interaction: F (7,32) = 0.79, p = 0.60 SAHA: F (7,32) = 3.73, p = 0.0047 MPP^+: F (1,32) = 86.39, p < 0.0001
	One-way ANOVA	*LDH assay* (A) N1E-115: F (2,15) = 11.31, p = 0.0002 (B) SH-SY5Y: F (2,15) = 0.88, p = 0.4248
		Trypan blue assay (C) N1E-115: F (2,15) = 5.75, p = 0.0077 (D) SH-SY5Y: F (2,15) = 21.59, p < 0.0001
Figure 3-12 Effect of MPP^+ on cell survival following VPA pre-treatment.	Two-way ANOVA	(A) *N1E-115: LDH assay* Interaction: F (7,32) = 0.64, p = 0.7189 VPA: F (7,32) = 0.44, p = 0.8718 MPP^+: F (1,32) = 60.20, p < 0.0001
		(B) *SH-SY5Y: LDH assay* Interaction: F (7,32) = 0.49, p = 0.8387 VPA: F (7,32) = 0.89, p = 0.5248 MPP^+: F (1,32) = 91.43, p < 0.0001
		(C) *N1E-115: Trypan blue assay* Interaction: F (7,32) = 1.28, p = 0.2895 VPA: F (7,32) = 2.24, p = 0.0565 MPP^+: F (1,32) = 50.30, p < 0.0001
		(D) *SH-SY5Y: Trypan blue assay* Interaction: F (7,32) = 0.11, p = 1.00 VPA: F (7,32) = 1.05, p = 0.4198 MPP^+: F (1,32) = 144.90, p < 0.0001
	One-way ANOVA	*LDH assay* (A) N1E-115: F (2,15) = 1.77, p = 0.1882 (B) SH-SY5Y: F (2,15) = 54.97, p < 0.0001
		Trypan blue assay (C) N1E-115: F (2,8) = 14.80, p = 0.0002 (D) SH-SY5Y: F (2,15) = 2.06, p = 0.1446
Figure 4-7 The effect of MPP+ and LPS on TH-positive cells in VM culture.	One-way ANOVA	(A) MPP^+: F (7,34) = 25.54, p < 0.0001
		(B) LPS: F (1,7) = 6.85, p = 0.0346
Figure 4-8 The effect of SAHA and	Two-way	(A) Interaction: F (3,16) = 3.60, p = 0.0370

VPA on the number of TH-positive cells following MPP^+ and LPS induced toxicity.	ANOVA	SAHA: F (3,16) = 6.07, p = 0.0058 MPP^+: F (1,16) = 7.72, p = 0.0134
		(B) Interaction: F (3,16) = 5.30, p = 0.0100 VPA: F (3,16) = 5.64, p = 0.0078 MPP^+: F (1,16) = 18.56, p = 0.0005
		(C) Interaction: F (3,16) = 5.85, p = 0.0068 SAHA: F (3,16) = 11.02, p = 0.0004 LPS: F (1,16) = 2.95, p = 0.1050
		(D) Interaction: F (3,16) = 11.97, p = 0.0002 VPA: F (3,16) = 13.77, p = 0.0001 LPS: F (1,16) = 37.55, p < 0.0001
	One-way ANOVA	(A) F (2,7) = 5.51, p = 0.0172
		(B) F (2,7) = 0.22, p = 0.8092
		(C) F (2,7) = 1.92, p = 0.1838
		(D) F (2,7) = 1.56, p = 0.2450
Figure 4-10 The effect of SAHA and VPA on the number of GFAP cells following MPP^+ and LPS exposure.	Two-way ANOVA	(A) Interaction: F (3,16) = 7.08, p = 0.0031 SAHA: F (3,16) = 0.38, p = 0.7653 MPP^+: F (1,16) = 7.39, p = 0.0152
		(B) Interaction: F (3,16) = 6.38, p = 0.0048 VPA: F (3,16) = 0.39, p = 0.7641 MPP^+: F (1,16) = 4.75, p = 0.0447
		(C) Interaction: F (3,16) = 3.51, p = 0.0398 SAHA: F (3,16) = 1.64, p = 0.2208 LPS: F (1,16) = 2.28, p = 0.1504
		(D) Interaction: F (3,16) = 13.46, p = 0.0001 VPA: F (3,16) = 6.61, p = 0.0041 LPS: F (1,16) = 13.87, p = 0.0018
	One-way ANOVA	(A) F (7,16) = 4.25, p = 0.0078
		(B) F (7,16) = 3.58, p = 0.0165
		(C) F (2,7) = 1.30, p = 0.3045
		(D) F (2,7) = 6.58, p = 0.0097
Figure 4-12 The effect of SAHA and VPA on the number of OX-42-positive cells following MPP^+ and LPS treatment.	Two -way ANOVA	(A) Interaction: F (6,24) = 6.58, p = 0.0003 Toxin: F (2,24) = 29.28, p < 0.0001 SAHA: F (3,24) = 2.71, p = 0.0677
		(B) Interaction: F (6,24) = 11.82, p < 0.0001

	One-way ANOVA	Toxin: F (2,24) = 14.98, p < 0.0001 VPA: F (3,24) = 8.46, p = 0.0005 (A) F (11,24) = 9.65, p < 0.0001 (B) F (11,24) = 11.48, p< 0.0001
Figure 5-1 EC_{50} of VPA and SAHA following HDAC assay	One-way ANOVA	(A) F (5,12) = 83.78, p<0.0001 (B) F (5,12) = 84.43, p<0.0001
Figure 5-2 Volumes of water, HOP-β-CD and SAHA consumed by C57BL/6J in 24 hours	One-way ANOVA	F (2,15) = 0.07, p =0.1627
Figure 5-7 HDAC assay of mouse brain tissue.	One-way ANOVA	F (2,18) = 25.73, p < 0.0001
Figure 5-9 The effect of VPA and SAHA on the number of TH-positive cells in SN of sham-, 6-OHDA- and LPS-lesioned mice.	Two-way ANOVA	*6-OHDA lesion* Interaction: F (6,74) = 1.52, p = 0.1826 Treatment: F (6,74) = 2.57, p = 0.0259 Lesioned side: F (1,74) = 27.10, p < 0.0001 *LPS lesion* Interaction: F (6,80) = 3.02, p = 0.0102 Treatment: F (6,80) = 3.73, p = 0.0025 Lesioned side: F (1,80) = 50.63, p < 0.0001
	One way ANOVA	6-OHDA lesion: F (13,76) = 4.61, p < 0.0001 LPS lesion: F (13,80) = 8.16, p < 0.0001
Figure 5-11 The effect of VPA and SAHA on GFAP-immunoreactivity in SN of sham-, 6-OHDA- and LPS-lesioned mice.	Two-way ANOVA	*6-OHDA lesion* Interaction: F (6,70) = 0.98, p = 0.4456 Treatment: F (6,70) = 12.10, p < 0.0001 Lesioned side: F (1,70) = 22.68, p < 0.0001 *LPS lesion* Interaction: F (6,76) = 0.85, p = 0.5388 Treatment: F (6,76) = 14.28, p < 0.0001 Lesioned side: F (1,76) = 23.02, p < 0.0001
	One way ANOVA	6-OHDA lesion: F (13,70) = 8.18, p < 0.0001 LPS lesion: F (13,76) = 9.04, p < 0.0001
Figure 5-13 The effect of VPA and SAHA on the number active OX-42-positive cell in SN of sham-, 6-OHDA- and LPS-lesioned mice.	Two-way ANOVA	*6-OHDA lesion* Interaction: F (6,72) = 20.08, p < 0.0001 Treatment: F (6,72) = 20.20, p < 0.0001 Lesioned side: F (1,72) = 128.49, p < 0.0001

		LPS lesion Interaction: F (6,78) = 25.19, p < 0.0001 Treatment: F (6,78) = 25.01, p < 0.0001 Lesioned side: F (1,78) = 171.69, p < 0.0001
	One way ANOVA	6-OHDA lesion: F (13,72) = 27.05, p < 0.0001
		LPS lesion: F (13,78) = 34.03, p < 0.0001

Negative staining controls

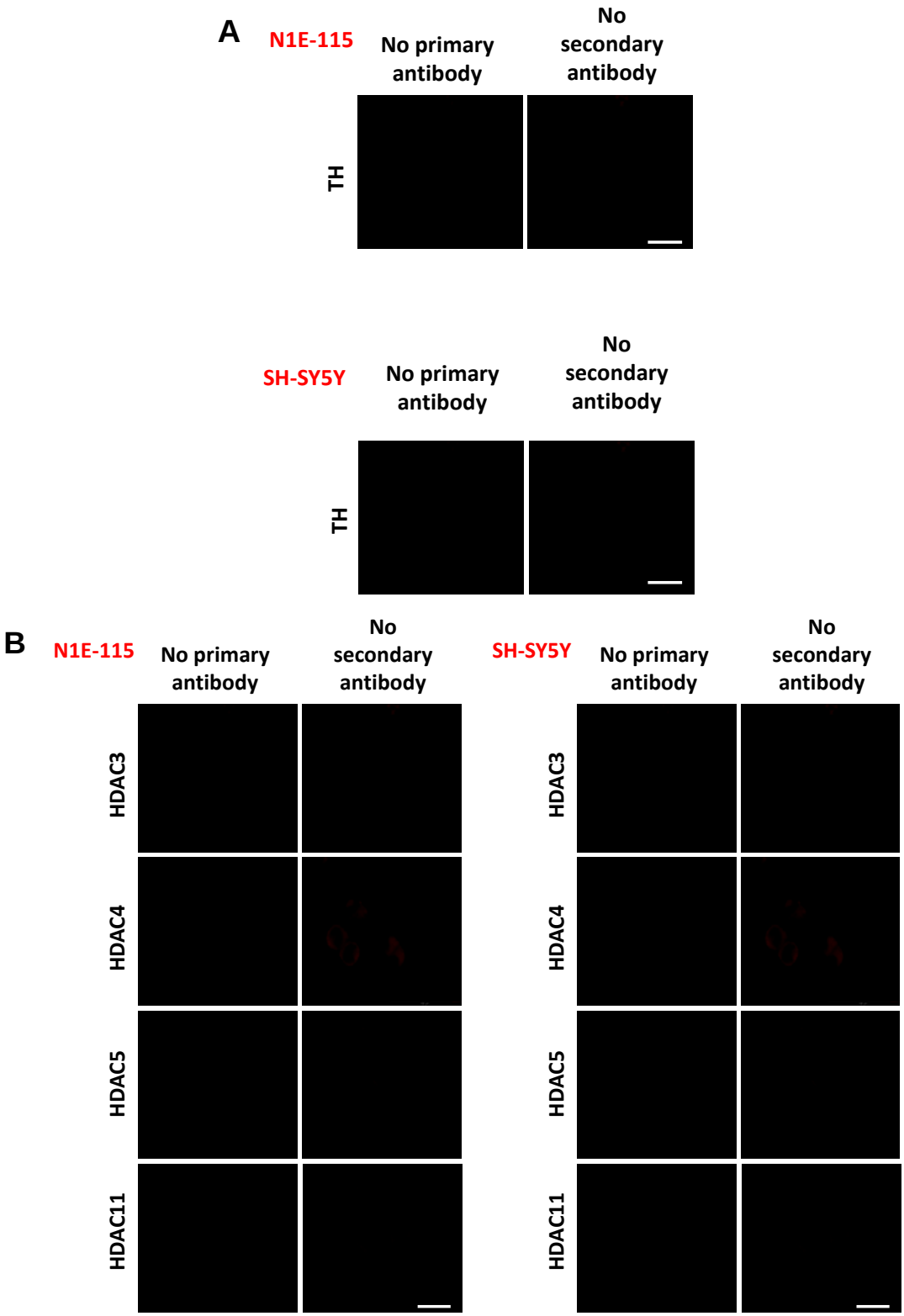

Figure 7-1 Negative staining images for immunofluorescence in cell lines.
(A) Primary antibody against TH and secondary antibody (Alexa fluor 594) omitted in N1E-115 and SH-SY5Y cell lines. (B) Primary antibodies against HDAC3, 4, 5 and 11, and secondary antibody (Alexa fluor 594) omitted in both cell lines. No immunoreactivity is visible. Scale bar = 100 μm is representative of all images.

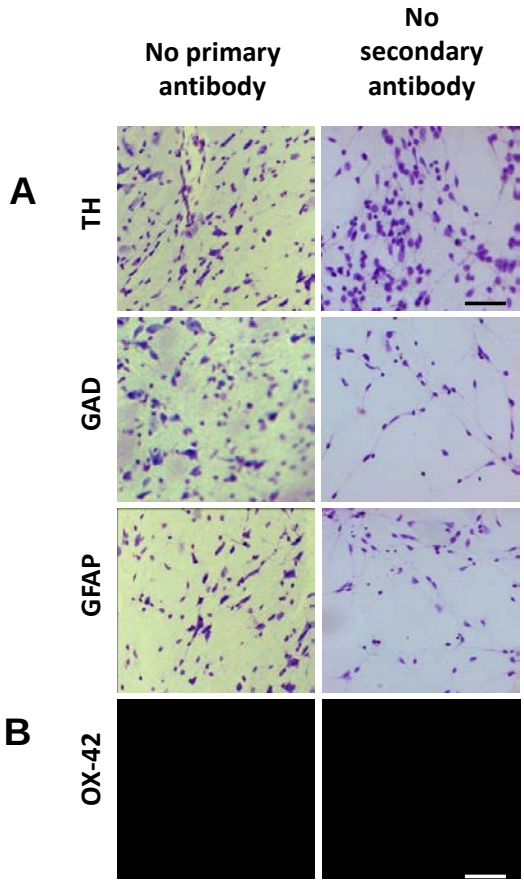

Figure 7-2 Immunoperoxidase and immunofluorescence negative control images for VM primary culture.

(A) Primary antibodies against TH, GAD and GFAP and biotinylated secondary antibody were omitted in VM cultures during immunoperoxidase staining. Cresyl violet was used to counterstain cells. (B) Primary antibody against OX-42 and secondary antibody (Alexa flour 488) omitted in immunofluorescence staining. (C) Primary antibodies against HDAC3, 4, 5, 11, TH and GFAP and secondary antibody (Alexa fluor 594 and Alexa flour 488) omitted in immunoflourescence staining. No immunoreactivity is visible in any image. Scale bar = 100 μm is representative of all images.

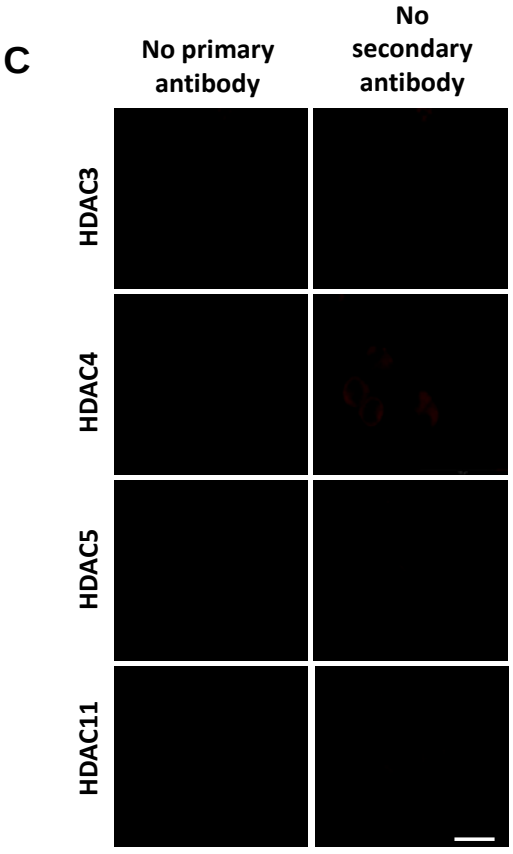

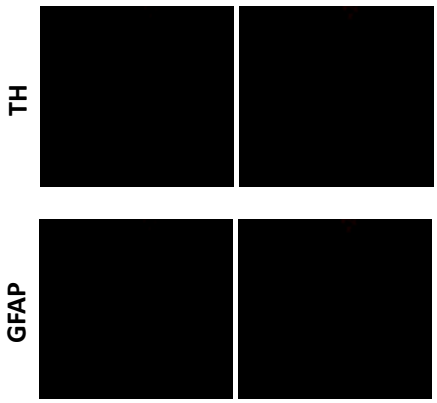

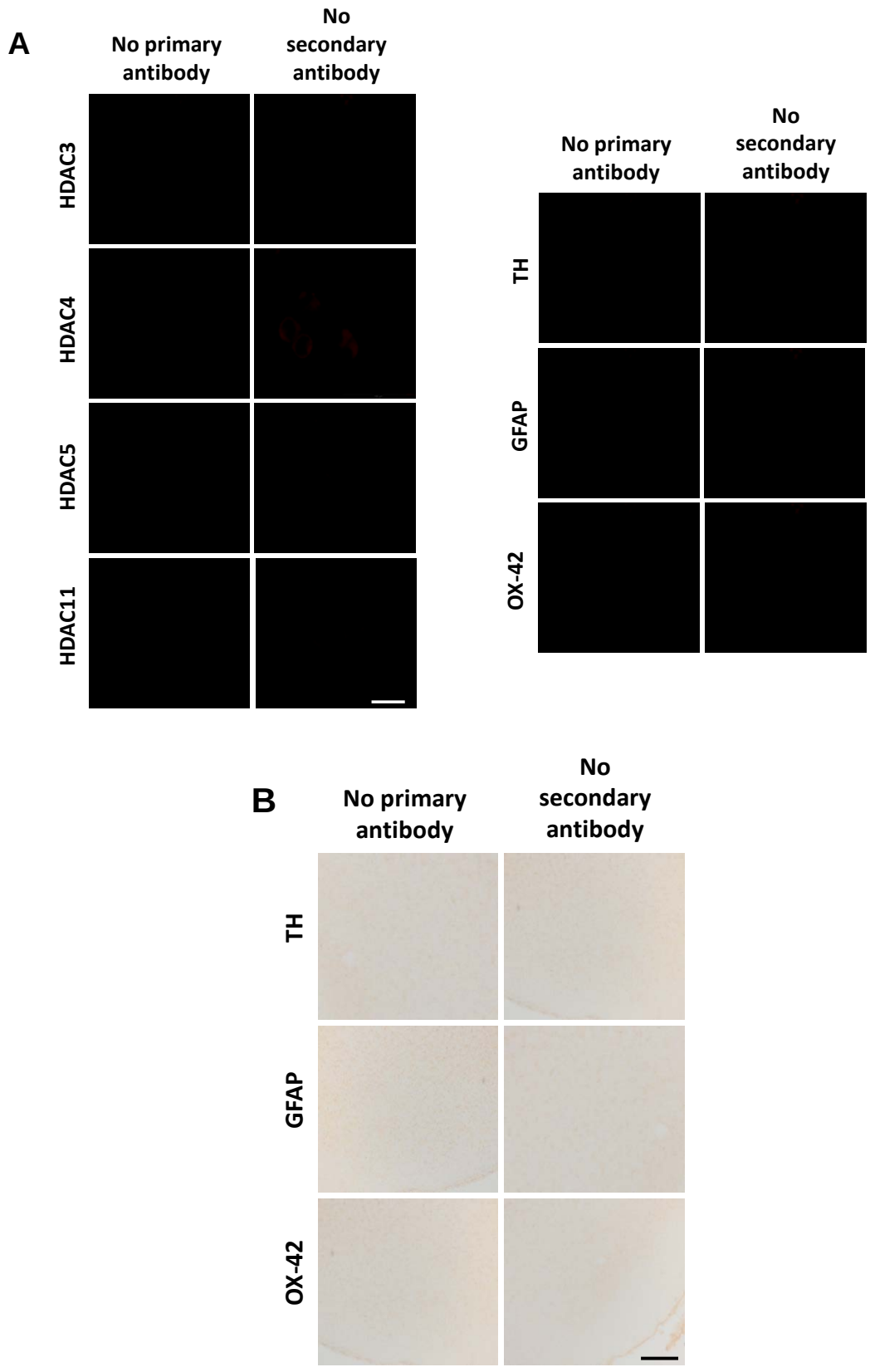

Figure 7-3 Negative staining images for mouse brain sections.
(A) Primary antibodies against HDAC3, 4, 5, 11, TH, GFAP and OX-42, and secondary antibodies Alexa fluor 594 and 488 were omitted in immunofluorescence staining. (B) Primary antibody against TH, GFAP and OX-42 and biotinylated secondary antibody omitted in mouse brain sections during immunoperoxidase staining. No visible immunoreactivity is seen. Scale bar = 100 μm (A), and 50 μm (B), is representative of the respective images.

Chapter 8 Reference

Abel, T & Zukin, RS. (2008). Epigenetic targets of HDAC inhibition in neurodegenerative and psychiatric disorders. *Current Opinion in Pharmacology*, **5**, 57-64.

Agid, Y. (1991). Parkinson's disease: pathophysiology. *Lancet*, **337**, 1321-1324.

Akhtar, MW, Raingo, J, Nelson, ED, Montgomery, RL, Olson, EN, Kavalali, ET & Monteggia, LM. (2009). Histone deacetylases 1 and 2 form a developmental switch that controls excitatory synapse maturation and function. *J Neurosci*, **29**, 8288-8297.

Akiyama, H & McGeer, PL. (1989). Microglial response to 6-hydroxydopamine-induced substantia nigra lesions. *Brain Res*, **489**, 247-253.

Alam, ZI, Daniel, SE, Lees, AJ, Marsden, DC, Jenner, P & Halliwell, B. (1997a). A generalised increase in protein carbonyls in the brain in Parkinson's but not incidental Lewy body disease. *J Neurochem*, **69**, 1326-1329.

Alam, ZI, Jenner, A, Daniel, SE, Lees, AJ, Cairns, N, Marsden, CD, Jenner, P & Halliwell, B. (1997b). Oxidative DNA Damage in the Parkinsonian Brain: An Apparent Selective Increase in 8-Hydroxyguanine Levels in Substantia Nigra. *Journal of Neurochemistry*, **69**, 1196-1203.

Albert, M & Helin, K. (2010). Histone methyltransferases in cancer. *Semin Cell Dev Biol*, **21**, 209-220.

Alegre-Abarrategui, J, Christian, H, Lufino, MM, Mutihac, R, Venda, LL, Ansorge, O & Wade-Martins, R. (2009). LRRK2 regulates autophagic activity and localizes to specific membrane microdomains in a novel human genomic reporter cellular model. *Hum Mol Genet*, **18**, 4022-4034.

Aloisi, F. (2001). Immune function of microglia. *Glia*, **36**, 165-179.

Alvarez-Erviti, L, Rodriguez-Oroz, MC, Cooper, JM, Caballero, C, Ferrer, I, Obeso, JA & Schapira, AH. (2010). Chaperone-mediated autophagy markers in Parkinson disease brains. *Arch Neurol*, **67**, 1464-1472.

Alvarez-Fischer, D, Henze, C, Strenzke, C, Westrich, J, Ferger, B, Hoglinger, GU, Oertel, WH & Hartmann, A. (2008). Characterization of the striatal 6-OHDA model of Parkinson's disease in wild type and alpha-synuclein-deleted mice. *Exp Neurol*, **210**, 182-193.

Amano, T, Richelson, E & Nirenberg, M. (1972). Neurotransmitter Synthesis by Neuroblastoma Clones. *Proc Natl Acad Sci USA*, **69**, 258-263.

Andrei, C, Margiocco, P, Poggi, A, Lotti, LV, Torrisi, MR & Rubartelli, A. (2004). Phospholipases C and A2 control lysosome-mediated IL-1 beta secretion: Implications for inflammatory processes. *Proc Natl Acad Sci U S A*, **101**, 9745-9750.

Anglade, P, Vyas, S, Javoy-Agid, F, Herrero, MT, Michel, PP, Marquez, J, Mouatt-Prigent, A, Ruberg, M, Hirsch, EC & Agid, Y. (1997). Apoptosis and autophagy in nigral neurons of patients with Parkinson's disease. *Histol Histopathol*, **12**, 25-31.

Ara, J, Przedborski, S, Naini, AB, Jackson-Lewis, V, Trifiletti, RR, Horwitz, J & Ischiropoulos, H. (1998). Inactivation of tyrosine hydroxylase by nitration following exposure to peroxynitrite and 1-methyl-4-phenyl-1,2,3,6-tetrahydropyridine (MPTP). *Proc Natl Acad Sci U S A*, **95**, 7659-7663.

Aranyi, T, Sarkis, C, Berrard, S, Sardin, K, Siron, V, Khalfallah, O & Mallet, J. (2007). Sodium butyrate modifies the stabilizing complexes of tyrosine hydroxylase mRNA. *Biochem Biophys Res Commun*, **359**, 15-19.

Arenas, E, Trupp, M, Akerud, P & Ibanez, CF. (1995). GDNF prevents degeneration and promotes the phenotype of brain noradrenergic neurons in vivo. *Neuron*, **15**, 1465-1473.

Arimoto, T & Bing, G. (2003). Up-regulation of inducible nitric oxide synthase in the substantia nigra by lipopolysaccharide causes microglial activation and neurodegeneration. *Neurobiol Dis*, **12**, 35-45.

Arrowsmith, CH, Bountra, C, Fish, PV, Lee, K & Schapira, M. (2012). Epigenetic protein families: a new frontier for drug discovery. *Nat Rev Drug Discov*, **11**, 384-400.

Aviles-Olmos, I, Dickson, J, Kefalopoulou, Z, Djamshidian, A, Ell, P, Soderlund, T, Whitton, P, Wyse, R, Isaacs, T, Lees, A, Limousin, P & Foltynie, T. (2013). Exenatide and the treatment of patients with Parkinson's disease. *J Clin Invest*, **123**, 2730-2736.

Banati, RB. (2003). Neuropathological imaging: in vivo detection of glial activation as a measure of disease and adaptive change in the brain. *Br Med Bull*, **65**, 121-131.

Bandopadhyay, R & de Belleroche J. (2010). Pathogenesis of Parkinson's disease: emerging role of molecular chaperones. *Trends Mol Med*, **16**, 27-36.

Banerjee, R, Beal, MF & Thomas, B. (2010). Autophagy in neurodegenerative disorders: pathogenic roles and therapeutic implications. *Trends Neurosci*, **33**, 541-549.

Bar-Am, O, Weinreb, O, Amit, T & Youdim, MBH. (2005). Regulation of Bcl-2 family proteins, neurotrophic factors, and APP processing in the neurorescue activity of propargylamine. *FASEB J*, **19**, 1899-1901.

Barcia, C, Sanchez, BA, Fernandez-Villalba, E, Bautista, V, Poza, YP, Fernandez-Barreiro, A, Hirsch, EC & Herrero, MT. (2004). Evidence of active microglia in substantia nigra pars compacta of parkinsonian monkeys 1 year after MPTP exposure. *Glia*, **46**, 402-409.

Bardai, FH & D'Mello, SR. (2011). Selective toxicity by HDAC3 in neurons: regulation by Akt and GSK3beta. *J Neurosci*, **31**, 1746-1751.

Beal, MF. (2003). Mitochondria, oxidative damage, and inflammation in Parkinson's disease. *Annals of the New York Academy of Sciences*, **991**, 120-131.

Bender, A, Koch, W, Elstner, M, Schombacher, Y, Bender, J, Moeschl, M, Gekeler, F, Muller-Myhsok, B, Gasser, T, Tatsch, K & Klopstock, T. (2006). Creatine supplementation in Parkinson disease: a placebo-controlled randomized pilot trial. *Neurology*, **67**, 1262-1264.

Bernstein, BE, Meissner, A & Lander, ES. (2007). The mammalian epigenome. *Cell*, **128**, 669-681.

Betarbet, R, Sherer, TB, MacKenzie, G, Garcia-Osuna, M, Panov, AV & Greenamyre, JT. (2000). Chronic systemic pesticide exposure reproduces features of Parkinson's disease. *Nat Neurosci*, **3**, 1301-1306.

Betteridge, DJ. (2000). What is oxidative stress? *Metabolism*, **49**, 3-8.

Bezard, E & Gross, CE. (1998). Compensatory mechanisms in experimental and human parkinsonism: towards a dynamic approach. *Prog Neurobiol*, **55**, 93-116.

Bezard, E, Gross, CE & Brotchie, JM. (2003). Presymptomatic compensation in Parkinson's disease is not dopamine-mediated. *Trends Neurosci*, **26**, 215-221.

Biedler, JL, Roffler-Tarlov, S, Schachner, M & Freedman, LS. (1978). Multiple Neurotransmitter Synthesis by Human Neuroblastoma Cell Lines and Clones. *Cancer Research*, **38**, 3751-3757.

Bieliauskas, AV & Pflum, MK. (2008). Isoform-selective histone deacetylase inhibitors. *Chem Soc Rev*, **37**, 1402-1413.

Bjorklund, A & Dunnett, SB. (2007). Dopamine neuron systems in the brain: an update. *Trends in Neurosciences*, **30**, 194-202.

Blanchard, F & Chipoy, C. (2005). Histone deacetylase inhibitors: new drugs for the treatment of inflammatory diseases? *Drug Discovery Today*, **10**, 197-204.

Blesa, J, Phani, S, Jackson-Lewis, V & Przedborski, S. (2012). Classic and new animal models of Parkinson's disease. *J Biomed Biotechnol*, **2012**, 845618.

Block, ML, Zecca, L & Hong, JS. (2007). Microglia-mediated neurotoxicity: uncovering the molecular mechanisms. *Nat Rev Neurosci*, **8**, 57-69.

Blum, D, Wu, Y, Nissou, MF, Arnaud, S, Alim, LB & Verna, JM. (1997). p53 and Bax activation in 6-hydroxydopamine-induced apoptosis in PC12 cells. *Brain Res*, **751**, 139-142.

Bolanos, JP, Heales, SJ, Peuchen, S, Barker, JE, Land, JM & Clark, JB. (1996). Nitric oxide-mediated mitochondrial damage: a potential neuroprotective role for glutathione. *Free Radic Biol Med*, **21**, 995-1001.

Bolden, JE, Shi, W, Jankowski, K, Kan, CY, Cluse, L, Martin, BP, MacKenzie, KL, Smyth, GK & Johnstone, RW. (2013). HDAC inhibitors induce tumor-cell-selective pro-apoptotic transcriptional responses. *Cell Death Dis*, **4**, e519.

Bolden, JE, Peart, MJ & Johnstone, RW. (2006). Anticancer activities of histone deacetylase inhibitors. *Nat Rev Drug Discov*, **5**, 769-784.

Bolger, TA & Yao, TP. (2005). Intracellular Trafficking of Histone Deacetylase 4 Regulates Neuronal Cell Death. *J Neurosci*, **25**, 9544-9553.

Bonifati, V, Rizzu, P, Squitieri, F, Krieger, E, Vanacore, N, van Swieten, JC, Brice, A, van Duijn, CM, Oostra, B, Meco, G & Heutink, P. (2003). DJ-1(PARK7), a novel gene for autosomal recessive, early onset parkinsonism. *Neurol Sci*, **24**, 159-160.

Bossy-Wetzel, E, Schwarzenbacher, R & Lipton, SA. (2004). Molecular pathways to neurodegenration. *Nature Medicine*, **10**, S2-S9.

Boutillier, AL, TRINH, EMMA & Loeffler, JP. (2002). Constitutive Repression of E2F1 Transcriptional Activity through HDAC Proteins Is Essential for Neuronal Survival. *Annals of the New York Academy of Sciences*, **973**, 438-442.

Boutillier, AL, TRINH, EMMA & Loeffler, JP. (2003). Selective E2F-dependent gene transcription is controlled by histone deacetylase activity during neuronal apoptosis. *Journal of Neurochemistry*, **84**, 814-828.

Boyce, S, Kelly, E, Reavill, C, Jenner, P & Marsden, CD. (1984). Repeated administration of N-methyl-4-phenyl 1,2,5,6-tetrahydropyridine to rats is not toxic to striatal dopamine neurones. *Biochem Pharmacol*, **33**, 1747-1752.

Braak, H, de Vos, RA, Bohl, J & Del, TK. (2006). Gastric alpha-synuclein immunoreactive inclusions in Meissner's and Auerbach's plexuses in cases staged for Parkinson's disease-related brain pathology. *Neurosci Lett*, **396**, 67-72.

Braak, H, Ghebremedhin, E, Rub, U, Bratzke, H & Del, TK. (2004). Stages in the development of Parkinson's disease-related pathology. *Cell Tissue Res*, **318**, 121-134.

Braak, H, Tredici, KD, Rnb, U, de Vos, RAI, Jansen Steur, ENH & Braak, E. (2003). Staging of brain pathology related to sporadic Parkinson's disease. *Neurobiology of Aging*, **24**, 197-211.

Breidert, T, Callebert, J, Heneka, MT, Landreth, G, Launay, JM & Hirsch, EC. (2002). Protective action of the peroxisome proliferator-activated receptor-gamma agonist pioglitazone in a mouse model of Parkinson's disease. *J Neurochem*, **82**, 615-624.

Brewer, GJ & Torricelli, JR. (2007). Isolation and culture of adult neurons and neurospheres. *Nat Protoc*, **2**, 1490-1498.

Brichta, L, Hofmann, Y, Hahnen, E, Siebzehnrubl, FA, Raschke, H, Blumcke, I, Eyupoglu, IY & Wirth, B. (2003). Valproic acid increases the SMN2 protein level: a well-known drug as a potential therapy for spinal muscular atrophy. *Hum Mol Genet*, **12**, 2481-2489.

Broide, RS, Redwine, JM, Aftahi, N, Young, W, Bloom, FE & Winrow, CJ. (2007). Distribution of histone deacetylases 1-11 in the rat brain. *J Mol Neurosci*, **31**, 47-58.

Bronstein, DM, Perez-Otano, I, Sun, V, Mullis Sawin, SB, Chan, J, Wu, GC, Hudson, PM, Kong, LY, Hong, JS & McMillian, MK. (1995). Glia-dependent neurotoxicity and neuroprotection in mesencephalic cultures. *Brain Research*, **704**, 112-116.

Bukhatwa, S, Iravani, MM, Zeng, BY, Cooper, JD, Rose, S & Jenner, P. (2009). An immunohistochemical and stereological analysis of PSI-induced nigral neuronal degeneration in the rat. *J Neurochem*, **109**, 52-59.

Bukhatwa, S, Zeng, BY, Rose, S & Jenner, P. (2010). A comparison of changes in proteasomal subunit expression in the substantia nigra in Parkinson's disease, multiple system atrophy and progressive supranuclear palsy. *Brain Res*, **1326**, 174-183.

Burke, RE, Dauer, WT & Vonsattel, JP. (2008a). A critical evaluation of the Braak staging scheme for Parkinson's disease. *Ann Neurol*, **64**, 485-491.

Burke, RE, Antonelli, M & Sulzer, D. (1998). Glial Cell Line-Derived Neurotrophic Growth Factor Inhibits Apoptotic Death of Postnatal Substantia Nigra Dopamine Neurons in Primary Culture. *Journal of Neurochemistry*, **71**, 517-525.

Burke, WJ, Kumar, VB, Pandey, N, Panneton, WM, Gan, Q, Franko, MW, O'Dell, M, Li, SW, Pan, Y, Chung, HD & Galvin, JE. (2008b). Aggregation of alpha-synuclein by DOPAL, the monoamine oxidase metabolite of dopamine. *Acta Neuropathol*, **115**, 193-203.

Camelo, S, Iglesias, AH, Hwang, D, Due, B, Ryu, H, Smith, K, Gray, SG, Imitola, J, Duran, G, Assaf, B, Langley, B, Khoury, SJ, Stephanopoulos, G, De Girolami, U, Ratan, RR, Ferrante, RJ & Dangond, F. (2005). Transcriptional therapy with the histone deacetylase inhibitor trichostatin A ameliorates experimental autoimmune encephalomyelitis. *Journal of Neuroimmunology*, **164**, 10-21.

Candido, EPM, Reeves, R & Davie, JR. (1978). Sodium butyrate inhibits histone deacetylation in cultured cells. *Cell*, **14**, 105-113.

Carlsson, A. (1959). The occurrence, distribution and physiological role of catecholamines in the nervous system. *Pharmacol Rev*, **11**, 490-493.

Carrasco, E, Casper, D & Werner, P. (2005). Dopaminergic neurotoxicity by 6-OHDA and MPP+: differential requirement for neuronal cyclooxygenase activity. *J Neurosci Res*, **81**, 121-131.

Cartier, AE, Djakovic, SN, Salehi, A, Wilson, SM, Masliah, E & Patrick, GN. (2009). Regulation of synaptic structure by ubiquitin C-terminal hydrolase L1. *J Neurosci*, **29**, 7857-7868.

Carvey, PM, Zhao, CH, Hendey, B, Lum, H, Trachtenberg, J, Desai, BS, Snyder, J, Zhu, YG & Ling, ZD. (2005). 6-Hydroxydopamine-induced alterations in blood-brain barrier permeability. *Eur J Neurosci*, **22**, 1158-1168.

Castano, A, Herrera, AJ, Cano, J & Machado, A. (1998). Lipopolysaccharide Intranigral Injection Induces Inflammatory Reaction and Damage in Nigrostriatal Dopaminergic System. *Journal of Neurochemistry*, **70**, 1584-1592.

Castellani, RJ, Perry, G, Siedlak, SL, Nunomura, A, Shimohama, S, Zhang, J, Montine, T, Sayre, LM & Smith, MA. (2002). Hydroxynonenal adducts indicate a role for lipid peroxidation in neocortical and brainstem Lewy bodies in humans. *Neurosci Lett*, **319**, 25-28.

Cedarbaum, JM. (1987). Clinical pharmacokinetics of anti-parkinsonian drugs. *Clin Pharmacokinet*, **13**, 141-178.

Celesia, GG & Wanamaker, WM. (1976). L-dopa-carbidopa: combined therapy for the treatment of Parkinson's disease. *Dis Nerv Syst*, **37**, 123-125.

Cersosimo, MG, Raina, GB, Pecci, C, Pellene, A, Calandra, CR, Gutierrez, C, Micheli, FE & Benarroch, EE. (2012). Gastrointestinal manifestations in Parkinson's disease: prevalence and occurrence before motor symptoms. *J Neurol*.

Chang, JG, Hsieh-Li, HM, Jong, YJ, Wang, NM, Tsai, CH & Li, H. (2001). Treatment of spinal muscular atrophy by sodium butyrate. *Proceedings of the National Academy of Sciences of the United States of America*, **98**, 9808-9813.

Chang, S, McKinsey, TA, Zhang, CL, Richardson, JA, Hill, JA & Olson, EN. (2004). Histone Deacetylases 5 and 9 Govern Responsiveness of the Heart to a Subset of Stress Signals and Play Redundant Roles in Heart Development. *Mol Cell Biol*, **24**, 8467-8476.

Chang, S, Young, BD, Li, S, Qi, X, Richardson, JA & Olson, EN. (2006). Histone Deacetylase 7 Maintains Vascular Integrity by Repressing Matrix Metalloproteinase 10. *Cell*, **126**, 321-334.

Chaudhuri, KR, Healy, DG & Schapira, AH. (2006). Non-motor symptoms of Parkinson's disease: diagnosis and management. *Lancet Neurol*, **5**, 235-245.

Chen, B & Cepko, CL. (2009). HDAC4 Regulates Neuronal Survival in Normal and Diseased Retinas. *Science*, **323**, 256-259.

Chen, G, Zeng, WZ, Yuan, PX, Huang, LD, Jiang, YM, Zhao, ZH & Manji, HK. (1999). The mood-stabilizing agents lithium and valproate robustly increase the levels of the neuroprotective protein bcl-2 in the CNS. *J Neurochem*, **72**, 879-882.

Chen, H, Jacobs, E, Schwarzschild, MA, McCullough, ML, Calle, EE, Thun, MJ & Ascherio, A. (2005). Nonsteroidal antiinflammatory drug use and the risk for Parkinson's disease. *Ann Neurol*, **58**, 963-967.

Chen, H, Zhang, SM, Hernan, MA, Schwarzschild, MA, Willett, WC, Colditz, GA, Speizer, FE & Ascherio, A. (2003). Nonsteroidal anti-inflammatory drugs and the risk of Parkinson disease. *Arch Neurol*, **60**, 1059-1064.

Chen, PS, Peng, GS, Li, G, Wu, X, Wang, CC, Wilson, B, Lu, RB, Gean, PW, Chuang, DM & Hong, JS. (2006). Valproate protects dopaminergic neurons in midbrain neuron/glia cultures by stimulating the release of neurotrophic factors from astrocytes. *Molecular Psychiatry*, **11**, 1116-1125.

Chen, SH, Wu, HM, Ossola, B, Schendzielorz, N, Wilson, BC, Chu, CH, Chen, SL, Wang, Q, Zhang, D, Qian, L, Li, X, Hong, JS & Lu, RB. (2012). Suberoylanilide hydroxamic acid, a histone deacetylase inhibitor, protects dopaminergic neurons from neurotoxin-induced damage. *British Journal of Pharmacology*, **165**, 494-505.

Cheung, NS, Hickling, YM & Beart, PM. (1997). Development and survival of rat embryonic mesencephalic dopaminergic neurones in serum-free, antioxidant-rich primary cultures. *Neuroscience Letters*, **233**, 13-16.

Chiba, K, Peterson, LA, Castagnoli, KP, Trevor, AJ & Castagnoli, N. (1985). Studies on the molecular mechanism of bioactivation of the selective nigrostriatal toxin 1-methyl-4-phenyl-1,2,3,6-tetrahydropyridine. *Drug Metabolism and Disposition*, **13**, 342-347.

Chiribau, CB, Cheng, L, Cucoranu, IC, Yu, YS, Clempus, RE & Sorescu, D. (2008). FOXO3A regulates peroxiredoxin III expression in human cardiac fibroblasts. *J Biol Chem*, **283**, 8211-8217.

Chiueh, CC, Markey, SP, Burns, RS, Johannessen, JN, Pert, A & Kopin, IJ. (1984). Neurochemical and behavioral effects of systemic and intranigral administration of N-methyl-4-phenyl-1,2,3,6-tetrahydropyridine in the rat. *Eur J Pharmacol*, **100**, 189-194.

Choi, DY, Liu, M, Hunter, RL, Cass, WA, Pandya, JD, Sullivan, PG, Shin, EJ, Kim, HC, Gash, DM & Bing, G. (2009). Striatal neuroinflammation promotes Parkinsonism in rats. *PLoS One*, **4**, e5482.

Choi, W-S, Yoon, S-Y, Oh, TH, Choi, E-J, O'Malley, KL & Oh, YJ. (1999). Two distinct mechanisms are involved in 6-hydroxydopamine- and MPP+-induced dopaminergic neuronal cell death: Role of caspases, ROS, and JNK. *J Neurosci Res*, **57**, 86-94.

Chu, Y, Morfini, GA, Langhamer, LB, He, Y, Brady, ST & Kordower, JH. (2012). Alterations in axonal transport motor proteins in sporadic and experimental Parkinson's disease. *Brain*, **135**, 2058-2073.

Chuang, DM, Leng, Y, Marinova, Z, Kim, HJ & Chiu, CT. (2009). Multiple roles of HDAC inhibition in neurodegenerative conditions. *Trends Neurosci*, **32**, 591-601.

Chung, CY, Koprich, JB, Siddiqi, H & Isacson, O. (2009). Dynamic changes in presynaptic and axonal transport proteins combined with striatal neuroinflammation precede dopaminergic neuronal loss in a rat model of AAV alpha-synucleinopathy. *J Neurosci*, **29**, 3365-3373.

Chung, CY, Seo, H, Sonntag, KC, Brooks, A, Lin, L & Isacson, O. (2005). Cell type-specific gene expression of midbrain dopaminergic neurons reveals molecules involved in their vulnerability and protection. *Human Molecular Genetics*, **14**, 1709-1725.

Chung, KK, Thomas, B, Li, X, Pletnikova, O, Troncoso, JC, Marsh, L, Dawson, VL & Dawson, TM. (2004). S-nitrosylation of parkin regulates ubiquitination and compromises parkin's protective function. *Science*, **304**, 1328-1331.

Cicchetti, F, Brownell, AL, Williams, K, Chen, YI, Livni, E & Isacson, O. (2002). Neuroinflammation of the nigrostriatal pathway during progressive 6-OHDA dopamine degeneration in rats monitored by immunohistochemistry and PET imaging. *Eur J Neurosci*, **15**, 991-998.

Ciechanover, A. (1998). The ubiquitin-proteasome pathway: on protein death and cell life. *EMBO J*, **17**, 7151-7160.

Clarke, PG. (1990). Developmental cell death: morphological diversity and multiple mechanisms. *Anat Embryol (Berl)*, **181**, 195-213.

Cohen, TJ, Barrientos, T, Hartman, ZC, Garvey, SM, Cox, GA & Yao, TP. (2009). The deacetylase HDAC4 controls myocyte enhancing factor-2-dependent structural gene expression in response to neural activity. *FASEB J*, **23**, 99-106.

Cohen, TJ, Waddell, DS, Barrientos, T, Lu, Z, Feng, G, Cox, GA, Bodine, SC & Yao, TP. (2007). The histone deacetylase HDAC4 connects neural activity to muscle transcriptional reprogramming. *J Biol Chem*, **282**, 33752-33759.

Cosi, C, Colpaert, F, Koek, W, Degryse, A & Marien, M. (1996). Poly(ADP-ribose) polymerase inhibitors protect against MPTP-induced depletions of striatal dopamine and cortical noradrenaline in C57B1/6 mice. *Brain Res*, **729**, 264-269.

Crotty, S, Fitzgerald, P, Tuohy, E, Harris, DM, Fisher, A, Mandel, A, Bolton, AE, Sullivan, AM & Nolan, Y. (2008). Neuroprotective effects of novel phosphatidylglycerol-based phospholipids in the 6-hydroxydopamine model of Parkinson's disease. *Eur J Neurosci*, **27**, 294-300.

Cuervo, AM, Stefanis, L, Fredenburg, R, Lansbury, PT & Sulzer, D. (2004). Impaired degradation of mutant alpha-synuclein by chaperone-mediated autophagy. *Science*, **305**, 1292-1295.

Cunliffe, VT. (2004). Histone deacetylase 1 is required to repress Notch target gene expression during zebrafish neurogenesis and to maintain the production of motoneurones in response to hedgehog signalling. *Development*, **131**, 2983-2995.

Cunliffe, VT & Casaccia-Bonnefil, P. (2006). Histone deacetylase 1 is essential for oligodendrocyte specification in the zebrafish CNS. *Mechanisms of Development*, **123**, 24-30.

Czlonkowska, A, Kurkowska-Jastrzebska, I, Czlonkowski, A, Peter, D & Stefano, GB. (2002). Immune processes in the pathogenesis of Parkinson's disease - a potential role for microglia and nitric oxide. *Med Sci Monit*, **8**, RA165-RA177.

Dagda, RK, Cherra, SJ, III, Kulich, SM, Tandon, A, Park, D & Chu, CT. (2009). Loss of PINK1 function promotes mitophagy through effects on oxidative stress and mitochondrial fission. *J Biol Chem*, **284**, 13843-13855.

Dagher, A & Robbins, TW. (2009). Personality, addiction, dopamine: insights from Parkinson's disease. *Neuron*, **61**, 502-510.

Damier, P, Hirsch, EC, Zhang, P, Agid, Y & Javoy-Agid, F. (1993). Glutathione peroxidase, glial cells and Parkinson's disease. *Neuroscience*, **52**, 1-6.

Datki, Z, Juhasz, A, Galfi, M, Soos, K, Papp, R, Zadori, D & Penke, B. (2003). Method for measuring neurotoxicity of aggregating polypeptides with the MTT assay on differentiated neuroblastoma cells. *Brain Res Bull*, **62**, 223-229.

Dauer, W & Przedborski, S. (2003). Parkinson's Disease: Mechanisms and models. *Neuron*, **39**, 889-909.

Davies, SW, Turmaine, M, Cozens, BA, DiFiglia, M, Sharp, AH, Ross, CA, Scherzinger, E, Wanker, EE, Mangiarini, L & Bates, GP. (1997). Formation of Neuronal Intranuclear Inclusions Underlies the Neurological Dysfunction in Mice Transgenic for the HD Mutation. *Cell*, **90**, 537-548.

Dawson, VL & Dawson, TM. (1996). Nitric oxide in neuronal degeneration. *Proc Soc Exp Biol Med*, **211**, 33-40.

de Ruijter, AJM, van Gennip, AH, Caron, HN, Kemp, S & Van Kuilenburg, ABP. (2003). Histone deacetylases (HDACs): characterization of the classical HDAC family. *Biochemical Journal*, **370**, 737-749.

Debeir, T, Ginestet, L, Fran+ºois, C, Laurens, Sp, Martel, JC, Chopin, P, Marien, M, Colpaert, F & Raisman-Vozari, R. (2005). Effect of intrastriatal 6-OHDA lesion on dopaminergic innervation of the rat cortex and globus pallidus. *Experimental Neurology*, **193**, 444-454.

Dehay, B, Martinez-Vicente, M, Ramirez, A, Perier, C, Klein, C, Vila, M & Bezard, E. (2012a). Lysosomal dysfunction in Parkinson disease: ATP13A2 gets into the groove. *Autophagy*, **8**, 1389-1391.

Dehay, B, Ramirez, A, Martinez-Vicente, M, Perier, C, Canron, MH, Doudnikoff, E, Vital, A, Vila, M, Klein, C & Bezard, E. (2012b). Loss of P-type ATPase ATP13A2/PARK9 function induces general lysosomal deficiency and leads to Parkinson disease neurodegeneration. *Proc Natl Acad Sci U S A*, **109**, 9611-9616.

Del Signore, SJ, Amante, DJ, Kim, J, Stack, EC, Goodrich, S, Cormier, K, Smith, K, Cudkowicz, ME & Ferrante, RJ. (2009). Combined riluzole and sodium phenylbutyrate therapy in transgenic amyotrophic lateral sclerosis mice. *Amyotroph Lateral Scler*, **10**, 85-94.

DelleDonne, A, Klos, KJ, Fujishiro, H, Ahmed, Z, Parisi, JE, Josephs, KA, Frigerio, R, Burnett, M, Wszolek, ZK, Uitti, RJ, Ahlskog, JE & Dickson, DW. (2008). Incidental Lewy body disease and preclinical Parkinson disease. *Arch Neurol*, **65**, 1074-1080.

Dennis, J & Bennett, JP. (2003). Interactions among nitric oxide and Bcl-family proteins after MPP+ exposure of SH-SY5Y neural cells I: MPP+ increases mitochondrial NO and Bax protein. *J Neurosci Res*, **72**, 76-88.

Devine, MJ, Plun-Favreau, H & Wood, NW. (2011a). Parkinson's disease and cancer: two wars, one front. *Nat Rev Cancer*, **11**, 812-823.

Devine, MJ, Ryten, M, Vodicka, P, Thomson, AJ, Burdon, T, Houlden, H, Cavaleri, F, Nagano, M, Drummond, NJ, Taanman, JW, Schapira, AH, Gwinn, K, Hardy, J, Lewis, PA & Kunath, T. (2011b). Parkinson's disease induced pluripotent stem cells with triplication of the alpha-synuclein locus. *Nat Commun*, **2**, 440.

Dexter, DT, CARAYON, A, Javoy-Agid, F, Agid, Y, Wells, FR, Daniel, SE, Lees, AJ, Jenner, P & Marsden, CD. (1991). ALTERATIONS IN THE LEVELS OF IRON, FERRITIN AND OTHER TRACE METALS IN PARKINSON'S DISEASE AND OTHER NEURODEGENERATIVE DISEASES AFFECTING THE BASAL GANGLIA. *Brain*, **114**, 1953-1975.

Dexter, DT, Carter, CJ, Wells, FR, Javoy-Agid, F, Agid, Y, Lees, A, Jenner, P & Marsden, CD. (1989a). Basal lipid peroxidation in substantia nigra is increased in Parkinson's disease. *J Neurochem*, **52**, 381-389.

Dexter, DT, Holley, AE, Flitter, WD, Slater, TF, Wells, FR, Daniel, SE, Lees, AJ, Jenner, P & Marsden, CD. (1994). Increased levels of lipid hydroperoxides in the parkinsonian substantia nigra: An HPLC and ESR study. *Movement Disorders*, **9**, 92-97.

Dexter, DT & Jenner, P. (2013). Parkinson disease: from pathology to molecular disease mechanisms. *Free Radic Biol Med*, **62**, 132-144.

Dexter, DT, Wells, FR, Lees, AJ, Agid, F, Agid, Y, Jenner, P & Marsden, CD. (1989b). Increased nigral iron content and alterations in other metal ions occurring in brain in Parkinson's disease. *J Neurochem*, **52**, 1830-1836.

Di Marcotullio, L, Canettieri, G, Infante, P, Greco, A & Gulino, A. (2011). Protected from the inside: Endogenous histone deacetylase inhibitors and the road to cancer. *Biochimica et Biophysica Acta (BBA) - Reviews on Cancer*, **1815**, 241-252.

Dietz, KC & Casaccia, P. (2010). HDAC inhibitors and neurodegeneration: At the edge between protection and damage. *Pharmacological Research*, **62**, 11-17.

Dobbs, RJ, Charlett, A, Purkiss, AG, Dobbs, SM, Weller, C & Peterson, DW. (1999). Association of circulating TNF-alpha and IL-6 with ageing and parkinsonism. *Acta Neurol Scand*, **100**, 34-41.

Dodel, RC, Du, Y, Bales, KR, Ling, ZD, Carvey, PM & Paul, SM. (1998). Peptide inhibitors of caspase-3-like proteases attenuate MPP+ -induced toxicity of cultured fetal rat mesencephalic dopamine neurons. *Neuroscience*, **86**, 701-707.

Dompierre, JP, Godin, JD, Charrin, BC, Cordelieres, FP, King, SJ, Humbert, S & Saudou, F. (2007). Histone Deacetylase 6 Inhibition Compensates for the Transport Deficit in Huntington's Disease by Increasing Tubulin Acetylation. *J Neurosci*, **27**, 3571-3583.

Ducray, A, Krebs, SH, Schaller, Bt, Seiler, RW, Meyer, M & Widmer, HR. (2006). GDNF family ligands display distinct action profiles on cultured GABAergic and serotonergic neurons of rat ventral mesencephalon. *Brain Research*, **1069**, 104-112.

Dunning, CJ, Reyes, JF, Steiner, JA & Brundin, P. (2012). Can Parkinson's disease pathology be propagated from one neuron to another? *Prog Neurobiol*, **97**, 205-219.

Durham, B. (2012). Novel histone deacetylase (HDAC) inhibitors with improved selectivity for HDAC2 and 3 protect against neural cell death. *Bioscience Horizons*, **5**.

Dutta, G, Zhang, P & Liu, B. (2008). The lipopolysaccharide Parkinson's disease animal model: mechanistic studies and drug discovery. *Fundam Clin Pharmacol*, **22**, 453-464.

Duty, S & Jenner, P. (2011). Animal models of Parkinson's disease: a source of novel treatments and clues to the cause of the disease. *Br J Pharmacol*, **164**, 1357-1391.

Ehringer, H & Hornykiewicz, O. (1998). Distribution of noradrenaline and dopamine (3-hydroxytyramine) in the human brain and their behavior in diseases of the extrapyramidal system. *Parkinsonism Relat Disord*, **4**, 53-57.

Ehrlich, M, Gama-Sosa, MA, Huang, LH, Midgett, RM, Kuo, KC, McCune, RA & Gehrke, C. (1982). Amount and distribution of 5-methylcytosine in human DNA from different types of tissues of cells. *Nucleic Acids Res*, **10**, 2709-2721.

Eide, L & McMurray, CT. (2005). Culture of adult mouse neurons. *Biotechniques*, **38**, 99-104.

Emborg, ME. (2004). Evaluation of animal models of Parkinson's disease for neuroprotective strategies. *J Neurosci Methods*, **139**, 121-143.

Engele, J & Bohn, MC. (1991). The neurotrophic effects of fibroblast growth factors on dopaminergic neurons in vitro are mediated by mesencephalic glia [published erratum appears in J Neurosci 1992 Mar;12(3):685]. *The Journal of Neuroscience*, **11**, 3070-3078.

Fahn, S, Oakes, D, Shoulson, I, Kieburtz, K, Rudolph, A, Lang, A, Olanow, CW, Tanner, C & Marek, K. (2004). Levodopa and the progression of Parkinson's disease. *N Engl J Med*, **351**, 2498-2508.

Fall, CP & Bennett, JP. (1999). Characterization and time course of MPP+-induced apoptosis in human SH-SY5Y neuroblastoma cells. *J Neurosci Res*, **55**, 620-628.

Faraco, G, Pancani, T, Formentini, L, Mascagni, P, Fossati, G, Leoni, F, Moroni, F & Chiarugi, A. (2006). Pharmacological Inhibition of Histone Deacetylases by Suberoylanilide Hydroxamic Acid Specifically Alters Gene Expression and Reduces Ischemic Injury in the Mouse Brain. *Molecular pharmacology*, **70**, 1876-1884.

Faraco, G, Pittelli, M, Cavone, L, Fossati, S, Porcu, M, Mascagni, P, Fossati, G, Moroni, F & Chiarugi, A. (2009). Histone deacetylase (HDAC) inhibitors reduce the glial inflammatory response in vitro and in vivo. *Neurobiology of Disease*, **36**, 269-279.

Farrer, M, Kachergus, J, Forno, L, Lincoln, S, Wang, DS, Hulihan, M, Maraganore, D, Gwinn-Hardy, K, Wszolek, Z, Dickson, D & Langston, JW. (2004). Comparison of kindreds with parkinsonism and alpha-synuclein genomic multiplications. *Ann Neurol*, **55**, 174-179.

Fearnley, JM & Lees, AJ. (1991). Ageing and Parkinson's disease: substantia nigra regional selectivity. *Brain*, **114 (Pt 5)**, 2283-2301.

Feinberg, AP. (2007). Phenotypic plasticity and the epigenetics of human disease. *Nature*, **447**, 433-440.

Ferrante, RJ, Hantraye, P, Brouillet, E & Beal, MF. (1999). Increased nitrotyrosine immunoreactivity in substantia nigra neurons in MPTP treated baboons is blocked by inhibition of neuronal nitric oxide synthase. *Brain Res*, **823**, 177-182.

Ferrante, RJ, Kubilus, JK, Lee, J, Ryu, H, Beesen, A, Zucker, B, Smith, K, Kowall, NW, Ratan, RR, Luthi-Carter, R & Hersch, SM. (2003). Histone Deacetylase Inhibition by Sodium Butyrate Chemotherapy Ameliorates the Neurodegenerative Phenotype in Huntington's Disease Mice. *J Neurosci*, **23**, 9418-9427.

Fischer, A, Sananbenesi, F, Mungenast, A & Tsai, LH. (2010). Targeting the correct HDAC(s) to treat cognitive disorders. *Trends Pharmacol Sci*, **31**, 605-617.

Forno, LS. (1996). Neuropathology of Parkinson's disease. *J Neuropathol Exp Neurol*, **55**, 259-272.

Forno, LS, DeLanney, LE, Irwin, I, Di, MD & Langston, JW. (1992). Astrocytes and Parkinson's disease. *Prog Brain Res*, **94**, 429-436.

Freese, JL, Pino, D & Pleasure, SJ. (2010). Wnt signaling in development and disease. *Neurobiol Dis*, **38**, 148-153.

Frye, RA. (1999). Characterization of Five Human cDNAs with Homology to the Yeast SIR2 Gene: Sir2-like Proteins (Sirtuins) Metabolize NAD and May Have Protein ADP-Ribosyltransferase Activity. *Biochemical and Biophysical Research Communications*, **260**, 273-279.

Fujiwara, H, Hasegawa, M, Dohmae, N, Kawashima, A, Masliah, E, Goldberg, MS, Shen, J, Takio, K & Iwatsubo, T. (2002). alpha-Synuclein is phosphorylated in synucleinopathy lesions. *Nat Cell Biol*, **4**, 160-164.

Furumai, R, Matsuyama, A, Kobashi, N, Lee, KH, Nishiyama, M, Nakajima, H, Tanaka, A, Komatsu, Y, Nishino, N, Yoshida, M & Horinouchi, S. (2002). FK228 (Depsipeptide) as a natural prodrug that inhibits Class I histone deacetylases. *Cancer Research*, **62**, 4916-4921.

Gainetdinov, RR, Fumagalli, F, Jones, SR & Caron, MG. (1997). Dopamine transporter is required for in vivo MPTP neurotoxicity: evidence from mice lacking the transporter. *J Neurochem*, **69**, 1322-1325.

Gainetdinov, RR, Fumagalli, F, Wang, YM, Jones, SR, Levey, AI, Miller, GW & Caron, MG. (1998). Increased MPTP neurotoxicity in vesicular monoamine transporter 2 heterozygote knockout mice. *J Neurochem*, **70**, 1973-1978.

Gandhi, S, Muqit, MM, Stanyer, L, Healy, DG, Abou-Sleiman, PM, Hargreaves, I, Heales, S, Ganguly, M, Parsons, L, Lees, AJ, Latchman, DS, Holton, JL, Wood, NW & Revesz, T. (2006). PINK1 protein in normal human brain and Parkinson's disease. *Brain*, **129**, 1720-1731.

Gao, HM, Jiang, J, Wilson, B, Zhang, W, Hong, JS & Liu, B. (2002a). Microglial activation-mediated delayed and progressive degeneration of rat nigral dopaminergic neurons: relevance to Parkinson's disease. *Journal of Neurochemistry*, **81**, 1285-1297.

Gao, HM, Liu, B, Zhang, W & Hong, JS. (2003). Synergistic dopaminergic neurotoxicity of MPTP and inflammogen lipopolysaccharide: relevance to the etiology of Parkinson's disease. *The FASEB Journal*.

Gao, J, Siddoway, B, Huang, Q & Xia, H. (2009). Inactivation of CREB mediated gene transcription by HDAC8 bound protein phosphatase. *Biochem Biophys Res Commun*, **379**, 1-5.

Gao, L, Cueto, MA, Asselbergs, F & Atadja, P. (2002b). Cloning and Functional Characterization of HDAC11, a Novel Member of the Human Histone Deacetylase Family. *J Biol Chem*, **277**, 25748-25755.

Gao, YS, Hubbert, CC, Lu, J, Lee, YS, Lee, JY & Yao, TP. (2007). Histone deacetylase 6 regulates growth factor-induced actin remodeling and endocytosis. *Mol Cell Biol*, **27**, 8637-8647.

Gardian, G, Browne, SE, Choi, DK, Klivenyi, P, Gregorio, J, Kubilus, JK, Ryu, H, Langley, B, Ratan, RR, Ferrante, RJ & Beal, MF. (2005). Neuroprotective Effects of Phenylbutyrate in the N171-82Q Transgenic Mouse Model of Huntington's Disease. *J Biol Chem*, **280**, 556-563.

Gardian, G, Yang, L, Cleren, C, Calingasan, N, Klivenyi, P & Beal, M. (2004). Neuroprotective effects of phenylbutyrate against MPTP neurotoxicity. *NeuroMolecular Medicine*, **5**, 235-241.

Gasser, T. (1998). Genetics of Parkinson's disease. *Clin Genet*, **54**, 259-265.

Gatto, EM, Riobo, NA, Carreras, MC, Chernavsky, A, Rubio, A, Satz, ML & Poderoso, JJ. (2000). Overexpression of neutrophil neuronal nitric oxide synthase in Parkinson's disease. *Nitric Oxide*, **4**, 534-539.

Gatto, NM, Cockburn, M, Bronstein, J, Manthripragada, AD & Ritz, B. (2009). Well-water consumption and Parkinson's disease in rural California. *Environ Health Perspect*, **117**, 1912-1918.

Gautier, CA, Kitada, T & Shen, J. (2008). Loss of PINK1 causes mitochondrial functional defects and increased sensitivity to oxidative stress. *Proc Natl Acad Sci U S A*, **105**, 11364-11369.

Gayle, DA, Ling, Z, Tong, C, Landers, T, Lipton, JW & Carvey, PM. (2002). Lipopolysaccharide (LPS)-induced dopamine cell loss in culture: roles of tumor necrosis factor-+¦, interleukin-1+¦, and nitric oxide. *Developmental Brain Research*, **133**, 27-35.

Gazdar, AF, Gao, B & Minna, JD. (2010). Lung cancer cell lines: Useless artifacts or invaluable tools for medical science? *Lung Cancer*, **68**, 309-318.

Geisler, S, Holmstrom, KM, Treis, A, Skujat, D, Weber, SS, Fiesel, FC, Kahle, PJ & Springer, W. (2010). The PINK1/Parkin-mediated mitophagy is compromised by PD-associated mutations. *Autophagy*, **6**, 871-878.

Giasson, BI, Duda, JE, Murray, IVJ, Chen, Q, Souza, J, Hurtig, HI, Ischiropoulos, H, Trojanowski, JQ & Lee, Y. (2000). Oxidative Damage Linked to Neurodegeneration by Selective alpha -Synuclein Nitration in Synucleinopathy Lesions. *Science*, **290**, 985-989.

Giasson, BI, Ischiropoulos, H, Lee, VM & Trojanowski, JQ. (2002). The relationship between oxidative/nitrative stress and pathological inclusions in Alzheimer's and Parkinson's diseases. *Free Radical Biology and Medicine*, **32**, 1264-1275.

Gilbert, EA, Edwards, RJ, Boobis, AR, Rose, S & Jenner, P. (2003). Differential expression of cytochrome P450 enzymes in cultured and intact foetal rat ventral mesencephalon. *Journal of Neural Transmission*, **110**, 1091-1101.

Gille, JJ & Joenje, H. (1992). Cell culture models for oxidative stress: superoxide and hydrogen peroxide versus normobaric hyperoxia. *Mutat Res*, **275**, 405-414.

Glickman, MH & Ciechanover, A. (2002). The ubiquitin-proteasome proteolytic pathway: destruction for the sake of construction. *Physiol Rev*, **82**, 373-428.

Glinka, Y, Gassen, M & Youdim, MB. (1997). Mechanism of 6-hydroxydopamine neurotoxicity. *J Neural Transm Suppl*, **50**, 55-66.

Glinka, YY & Youdim, MB. (1995). Inhibition of mitochondrial complexes I and IV by 6-hydroxydopamine. *Eur J Pharmacol*, **292**, 329-332.

Gloeckner, CJ, Kinkl, N, Schumacher, A, Braun, RJ, O'Neill, E, Meitinger, T, Kolch, W, Prokisch, H & Ueffing, M. (2006). The Parkinson disease causing LRRK2 mutation I2020T is associated with increased kinase activity. *Hum Mol Genet*, **15**, 223-232.

Goetz, CG, Poewe, W, Rascol, O & Sampaio, C. (2005). Evidence-based medical review update: pharmacological and surgical treatments of Parkinson's disease: 2001 to 2004. *Mov Disord*, **20**, 523-539.

Gomez, C, Reiriz, J, Piqu+®, M, Gil, J, Ferrer, I & Ambrosio, S. (2001). Low concentrations of 1-methyl-4-phenylpyridinium ion induce caspase-mediated apoptosis in human SH-SY5Y neuroblastoma cells. *J Neurosci Res*, **63**, 421-428.

Good, PF, Hsu, A, Werner, P, Perl, DP & Olanow, CW. (1998). Protein nitration in Parkinson's disease. *J Neuropathol Exp Neurol*, **57**, 338-342.

Grabiec, AM, Tak, PP & Reedquist, KA. (2008). Targeting histone deacetylase activity in rheumatoid arthritis and asthma as prototypes of inflammatory disease: should we keep our HATs on. *Arthritis Research & Therapy*, **10**, 226-239.

Graeber, MB & Kreutzberg, GW. (1994). Workshop 11: Microglia, Cell of the Brain Decade. *Brain Pathology*, **4**, 337-339.

Grant, S, Easley, C & Kirkpatrick, P. (2007). Vorinostat. *Nature Reviews Drug Discovery*, **6**, 21-22.

Gray, SG & Dangond, F. (2006). Rationale for the Use of Histone Deacetylase Inhibitors as a Dual Therapeutic Modality in Multiple Sclerosis. *Epigenetics*, **1**, 67-75.

Grayson, DR, Kundakovic, M & Sharma, RP. (2010). Is there a future for histone deacetylase inhibitors in the pharmacotherapy of psychiatric disorders? *Mol Pharmacol*, **77**, 126-135.

Greenacre, SA & Ischiropoulos, H. (2001). Tyrosine nitration: localisation, quantification, consequences for protein function and signal transduction. *Free Radic Res*, **34**, 541-581.

Greer, EL & Shi, Y. (2012). Histone methylation: a dynamic mark in health, disease and inheritance. *Nat Rev Genet*, **13**, 343-357.

Grozinger, CM & Schreiber, SL. (2000). Regulation of histone deacetylase 4 and 5 and transcriptional activity by 14-3- 3-dependent cellular localization. *Proceedings of the National Academy of Sciences of the United States of America*, **97**, 7835-7840.

Gu, M, Cooper, JM, Taanman, JW & Schapira, AH. (1998). Mitochondrial DNA transmission of the mitochondrial defect in Parkinson's disease. *Ann Neurol*, **44**, 177-186.

Guan, JS, Haggarty, SJ, Giacometti, E, Dannenberg, JH, Joseph, N, Gao, J, Nieland, TJF, Zhou, Y, Wang, X, Mazitschek, R, Bradner, JE, DePinho, RA, Jaenisch, R & Tsai, LH. (2009). HDAC2 negatively regulates memory formation and synaptic plasticity. *Nature*, **459**, 55-60.

Guardiola, AR & Yao, TP. (2002). Molecular cloning and characterization of a novel histone deactylase HDAC10. *The Journal of Biological Chemistry*, **277**, 3350-3356.

Hacker, G. (2000). The morphology of apoptosis. *Cell Tissue Res*, **301**, 5-17.

Hadjiconstantinou, M, Cavalla, D, Anthoupoulou, E, Laird, HE & Neff, NH. (1985). N-Methyl-4-phenyl-1,2,3,6-tetrahydropyridine increases acetylcholine and decreases dopamine in mouse striatum: both responses are blocked by anticholinergic drugs. *J Neurochem*, **45**, 1957-1959.

Halliwell, B. (2003). Oxidative stress in cell culture: an under-appreciated problem? *FEBS Lett*, **540**, 3-6.

Halliwell, B, Clement, MV, Ramalingam, J & Long, LH. (2000). Hydrogen peroxide. Ubiquitous in cell culture and in vivo? *IUBMB Life*, **50**, 251-257.

Halliwell, B & Aruoma, OI. (1991). DNA damage by oxygen-derived species Its mechanism and measurement in mammalian systems. *FEBS Letters*, **281**, 9-19.

Hanen, E, Hauke, J, Trankle, C, Eyupoglu, IY, Wirth, B & Blumcke, I. (2008). Histone deacetylase inhibitors: possible implications for neurodegenerative disorders. *EXPERT OPINION ON INVESTIGATIONAL DRUGS*, **17**, 169-184.

Hanrott, K, Gudmunsen, L, O'Neill, MJ & Wonnacott, S. (2006). 6-hydroxydopamine-induced apoptosis is mediated via extracellular auto-oxidation and caspase 3-dependent activation of protein kinase Cdelta. *J Biol Chem*, **281**, 5373-5382.

Hao, LY, Giasson, BI & Bonini, NM. (2010). DJ-1 is critical for mitochondrial function and rescues PINK1 loss of function. *Proc Natl Acad Sci U S A*, **107**, 9747-9752.

Haque, ME, Thomas, KJ, D'Souza, C, Callaghan, S, Kitada, T, Slack, RS, Fraser, P, Cookson, MR, Tandon, A & Park, DS. (2008). Cytoplasmic Pink1 activity protects neurons from dopaminergic neurotoxin MPTP. *Proc Natl Acad Sci U S A*, **105**, 1716-1721.

Hardy, J. (2010). Genetic analysis of pathways to Parkinson disease. *Neuron*, **68**, 201-206.

Hardy, J, Cai, H, Cookson, MR, Gwinn-Hardy, K & Singleton, A. (2006). Genetics of Parkinson's disease and parkinsonism. *Annals of Neurology*, **60**, 389-398.

Hartmann, A, Hunot, Sp, Michel, PP, Muriel, MP, Vyas, S, Faucheux, BA, Mouatt-Prigent, A, Turmel, H+, Srinivasan, A, Ruberg, M, Evan, GI, Agid, Y & Hirsch, EC. (2000). Caspase-3: A vulnerability factor and final effector in apoptotic death of dopaminergic neurons in Parkinson's disease. *Proceedings of the National Academy of Sciences of the United States of America*, **97**, 2875-2880.

Hartmann, A, Troadec, JD, Hunot, S, Kikly, K, Faucheux, BA, Mouatt-Prigent, A, Ruberg, M, Agid, Y & Hirsch, EC. (2001). Caspase-8 Is an Effector in Apoptotic Death of Dopaminergic Neurons in Parkinson's Disease, But Pathway Inhibition Results in Neuronal Necrosis. *J Neurosci*, **21**, 2247-2255.

Hashida, K, Sakakura, Y & Makino, N. (2002). Kinetic studies on the hydrogen peroxide elimination by cultured PC12 cells: rate limitation by glucose-6-phosphate dehydrogenase. *Biochim Biophys Acta*, **1572**, 85-90.

Hauser, RA. (2009). Levodopa: past, present, and future. *Eur Neurol*, **62**, 1-8.

Hayman, EG, Pierschbacher, MD, Suzuki, S & Ruoslahti, E. (1985). Vitronectin– A major cell attachment-promoting protein in fetal bovine serum. *Experimental Cell Research*, **160**, 245-258.

He, Y, Appel, S & Le, W. (2001). Minocycline inhibits microglial activation and protects nigral cells after 6-hydroxydopamine injection into mouse striatum. *Brain Res*, **909**, 187-193.

He, Y, Lee, T & Leong, SK. (2000). 6-Hydroxydopamine induced apoptosis of dopaminergic cells in the rat substantia nigra. *Brain Res*, **858**, 163-166.

Heales, SJ & Bolanos, JP. (2002). Impairment of brain mitochondrial function by reactive nitrogen species: the role of glutathione in dictating susceptibility. *Neurochem Int*, **40**, 469-474.

Herrera, AJ, Castano, A, Venero, JL, Cano, J & Machado, A. (2000). The single intranigral injection of LPS as a new model for studying the selective effects of inflammatory reactions on dopaminergic system. *Neurobiol Dis*, **7**, 429-447.

Heyer, EJ. (1984). Electrophysiological study of mammalian neurons from ventral mesencephalon grown in primary dissociated cell culture. *Brain Res*, **310**, 142-148.

Hinshaw, DB, Burger, JM, Delius, RE & Hyslop, PA. (1990). Mechanism of protection of oxidant-injured endothelial cells by glutamine. *Surgery*, **108**, 298-304.

Hirsch, EC & Hunot, S. (2009). Neuroinflammation in Parkinson's disease: a target for neuroprotection? *Lancet Neurol*, **8**, 382-397.

Hoban, DB, Connaughton, E, Connaughton, C, Hogan, G, Thornton, C, Mulcahy, P, Moloney, TC & Dowd, E. (2013). Further characterisation of the LPS model of Parkinson's disease: a comparison of intra-nigral and intra-striatal lipopolysaccharide administration on motor function, microgliosis and nigrostriatal neurodegeneration in the rat. *Brain Behav Immun*, **27**, 91-100.

Hockly, E, Richon, VM, Woodman, B, Smith, DL, Zhou, X, Rosa, E, Sathasivam, K, Ghazi-Noori, S, Mahal, A, Lowden, PAS, Steffan, JS, Marsh, JL, Thompson, LM, Marks, PA & Bates, GP. (2003). Suberoylanilide hydroxamic acid, a histone deacetylase inhibitor, ameliorates motor deficits in a mouse model of Huntington's disease. *Proceedings of the National Academy of Sciences*, **100**, 2041-2046.

Hoffman, HM & Wanderer, AA. (2010). Inflammasome and IL-1beta-mediated disorders. *Curr Allergy Asthma Rep*, **10**, 229-235.

Hornykiewicz, O. (2002). L-DOPA: from a biologically inactive amino acid to a successful therapeutic agent. *Amino Acids*, **23**, 65-70.

Hornykiewicz, O. (2008). Basic Research on Dopamine in Parkinson's Disease and the Discovery of the Nigrostriatal Dopamine Pathway: The View of an Eyewitness. *Neurodegenerative Dis*, **5**, 114-117.

Hou, JGG, Lin, LF & Mytilineou, C. (1996). Glial Cell Line-Derived Neurotrophic Factor Exerts Neurotrophic Effects on Dopaminergic Neurons In Vitro and Promotes Their Survival and Regrowth After Damage by 1-Methyl-4-Phenylpyridinium. *Journal of Neurochemistry*, **66**, 74-82.

Houlden, H & Singleton, AB. (2012). The genetics and neuropathology of Parkinson's disease. *Acta Neuropathol*, **124**, 325-338.

Hunter, RL, Cheng, B, Choi, DY, Liu, M, Liu, S, Cass, WA & Bing, G. (2009). Intrastriatal lipopolysaccharide injection induces parkinsonism in C57/B6 mice. *J Neurosci Res*, **87**, 1913-1921.

Hunter, RL, Dragicevic, N, Seifert, K, Choi, DY, Liu, M, Kim, HC, Cass, WA, Sullivan, PG & Bing, G. (2007). Inflammation induces mitochondrial dysfunction and dopaminergic neurodegeneration in the nigrostriatal system. *J Neurochem*, **100**, 1375-1386.

Hunter, RL, Liu, M, Choi, DY, Cass, WA & Bing, G. (2008). Inflammation and age-related iron accumulation in F344 rats. *Curr Aging Sci*, **1**, 112-121.

Iczkiewicz, J, Broom, L, Cooper, JD, Wong, AMS, Rose, S & Jenner, P. (2010). The RGD-containing peptide fragment of osteopontin protects tyrosine hydroxylase positive cells against toxic insult in primary ventral mesencephalic cultures and in the rat substantia nigra. *Journal of Neurochemistry*, **114**, 1792-1804.

Ikebe, S, Tanaka, M, Ohno, K, Sato, W, Hattori, K, Kondo, T, Mizuno, Y & Ozawa, T. (1990). Increase of deleted mitochondrial DNA in the striatum in Parkinson's disease and senescence. *Biochem Biophys Res Commun*, **170**, 1044-1048.

Imamura, K, Hishikawa, N, Sawada, M, Nagatsu, T, Yoshida, M & Hashizume, Y. (2003). Distribution of major histocompatibility complex class II-positive microglia and cytokine profile of Parkinson's disease brains. *Acta Neuropathol*, **106**, 518-526.

International Parkinson's Disease Genomic Consortium. (2011). A two-stage meta-analysis identifies several new loci for Parkinson's disease. *PLoS Genet*, **7**, e1002142.

Iravani, MM, Kashefi, K, Mander, P, Rose, S & Jenner, P. (2002). Involvement of inducible nitric oxide synthase in inflammation-induced dopaminergic neurodegeneration. *Neuroscience*, **110**, 49-58.

Iravani, MM, Leung, CCM, Sadeghian, M, Haddon, CO, Rose, S & Jenner, P. (2005). The acute and the long-term effects of nigral lipopolysaccharide administration on dopaminergic dysfunction and glial cell activation. *European Journal of Neuroscience*, **22**, 317-330.

Ishida, Y, Nagai, A, Kobayashi, S & Kim, SU. (2006). Upregulation of protease-activated receptor-1 in astrocytes in Parkinson disease: astrocyte-mediated neuroprotection through increased levels of glutathione peroxidase. *J Neuropathol Exp Neurol*, **65**, 66-77.

Ives, NJ, Stowe, RL, Marro, J, Counsell, C, Macleod, A, Clarke, CE, Gray, R & Wheatley, K. (2004). Monoamine oxidase type B inhibitors in early Parkinson's disease: meta-analysis of 17 randomised trials involving 3525 patients. *BMJ*, **329**, 593.

Iwata-Ichikawa, E, Kondo, Y, Miyazaki, I, Asanuma, M & Ogawa, N. (1999). Glial Cells Protect Neurons Against Oxidative Stress via Transcriptional Up-Regulation of the Glutathione Synthesis. *Journal of Neurochemistry*, **72**, 2334-2344.

Jakobsen, B, Gramsbergen, JB, Moller Dall, A, Rosenblad, C & Zimmer, J. (2005). Characterization of organotypic ventral mesencephalic cultures from embryonic mice and protection against MPP+ toxicity by GDNF. *European Journal of Neuroscience*, **21**, 2939-2948.

Jankovic, J. (2005). Searching for a relationship between manganese and welding and Parkinson's disease. *Neurology*, **64**, 2021-2028.

Jankovic, J. (2008). Parkinson's disease: clinical features and diagnosis. *J Neurol Neurosurg Psychiatry*, **79**, 368-376.

Janssen, CM, Schmalbach, SM, Boeselt, S, Sarlette, AM, Dengler, RM & Petri, SM. (2010). Differential Histone Deacetylase mRNA Expression Patterns in Amyotrophic Lateral Sclerosis. [Article]. *Journal of Neuropathology & Experimental Neurology*, **69**, 573-581.

Javitch, JA, D'Amato, RJ, Strittmatter, SM & Snyder, SH. (1985). Parkinsonism-inducing neurotoxin, N-methyl-4-phenyl-1,2,3,6 -tetrahydropyridine: uptake of the metabolite N-methyl-4-phenylpyridine by dopamine neurons explains selective toxicity. *Proc Natl Acad Sci U S A*, **82**, 2173-2177.

Javoy-Agid, F, Ruberg, M, Taquet, H, Bokobza, B, Agid, Y, Gaspar, P, Berger, B, N'Guyen-Legros, J, Alvarez, C, Gray, F & . (1984). Biochemical neuropathology of Parkinson's disease. *Adv Neurol*, **40**, 189-198.

Jellinger, KA. (2000). Cell death mechanisms in Parkinson's disease. *J Neural Transm*, **107**, 1-29.

Jenner, P. (2003a). Oxidative stress in Parkinson's disease. *Annals of Neurology*, **53**, S26-S38.

Jenner, P & Olanow, CW. (1996). Oxidative stress and the pathogenesis of Parkinson's disease. *Neurology*, **47**, 161S-170S.

Jenner, P, Rupniak, NM, Rose, S, Kelly, E, Kilpatrick, G, Lees, A & Marsden, CD. (1984). 1-Methyl-4-phenyl-1,2,3,6-tetrahydropyridine-induced parkinsonism in the common marmoset. *Neurosci Lett*, **50**, 85-90.

Jenner, P. (2002). Pharmacology of dopamine agonists in the treatment of Parkinson's disease. *Neurology*, **58**, 1S-8.

Jenner, P. (2003b). Oxidative stress in Parkinson's disease. *Ann Neurol*, **53**, S26-S38.

Jeon, BS, Kholodilov, NG, Oo, T, Tomaselli, KJ, Srinivasan, A, Stefanis, L & Burke, RE. (1999). Activation of caspase-3 in developmental models of programmed cell death in neurons of the substantia nigra. *Journal of Neurochemistry*, **73**, 322-333.

Jeong, MR, Hashimoto, R, Senatorov, VV, Fujimaki, K, Ren, M, Lee, MS & Chuang, DM. (2003). Valproic acid, a mood stabilizer and anticonvulsant, protects rat cerebral cortical neurons from spontaneous cell death: a role of histone deacetylase inhibition. *FEBS Letters*, **542**, 74-78.

Jha, N, Jurma, O, Lalli, G, Liu, Y, Pettus, EH, Greenamyre, JT, Liu, RM, Forman, HJ & Andersen, JK. (2000). Glutathione depletion in PC12 results in selective inhibition of mitochondrial complex I activity. Implications for Parkinson's disease. *J Biol Chem*, **275**, 26096-26101.

Jin, N, Kov+ícs, AD, Sui, Z, Dewhurst, S & Maggirwar, SB. (2005). Opposite effects of lithium and valproic acid on trophic factor deprivation-induced glycogen synthase kinase-3 activation, c-Jun expression and neuronal cell death. *Neuropharmacology*, **48**, 576-583.

Joosten, LA, Leoni, F, Meghji, S & Mascagni, P. (2011). Inhibition of HDAC activity by ITF2357 ameliorates joint inflammation and prevents cartilage and bone destruction in experimental arthritis. *Mol Med*, **17**, 391-396.

Kalaitzakis, ME, Graeber, MB, Gentleman, SM & Pearce, RK. (2008). The dorsal motor nucleus of the vagus is not an obligatory trigger site of Parkinson's disease: a critical analysis of alpha-synuclein staging. *Neuropathol Appl Neurobiol*, **34**, 284-295.

Karagiannis, TC & Ververis, K. (2012). Potential of chromatin modifying compounds for the treatment of Alzheimer's disease. *Pathobiol Aging Age Relat Dis*, **2**.

Karoum, F, Chrapusta, SJ, Egan, MF & Wyatt, RJ. (1993). Absence of 6-hydroxydopamine in the rat brain after treatment with stimulants and other dopaminergic agents: a mass fragmentographic study. *J Neurochem*, **61**, 1369-1375.

Karunakaran, S, Saeed, U, Mishra, M, Valli, RK, Joshi, SD, Meka, DP, Seth, P & Ravindranath, V. (2008). Selective activation of p38 mitogen-activated protein kinase in dopaminergic neurons of substantia nigra leads to nuclear translocation of p53 in 1-methyl-4-phenyl-1,2,3,6-tetrahydropyridine-treated mice. *J Neurosci*, **28**, 12500-12509.

Kawaguchi, Y, Kovacs, JJ, McLaurin, A, Vance, JM, Ito, A & Yao, TP. (2003). The deacetylase HDAC6 regulates aggresome formation and cell viability in response to misfolded protein stress. *Cell*, **115**, 727-738.

Kazantsev, AG & Thompson, LM. (2008). Therapeutic application of histone deacetylase inhibitors for central nervous system disorders. *Nature Reviews Drug Discovery*, **7**, 854-868.

Kazantsev, AG. (2007). Developing a neuroprotective therapy for Parkinson's and Huntington's diseases. *Expert Opinion on Therapeutic Patents*, **17**, 159-172.

Keane, PC, Kurzawa, M, Blain, PG & Morris, CM. (2011). Mitochondrial dysfunction in Parkinson's disease. *Parkinsons Dis*, **2011**, 716871.

Khan, N, Jeffers, M, Kumar, S, Hackett, C, Boldog, F, Khramtsov, N, Qian, X, Mills, E, Berghs, SC, Carey, N, Finn, PW, Collins, LS, Tumber, A, Ritchie, JW, Jensen, PB, Lichenstein, HS & Sehested, H. (2008). Determination of the class and isoform selectivity of small-molecule histone deacetylase inhibitors. *Biochemical Journal*, **409**, 581-589.

Kidd, SK & Schneider, JS. (2011). Protective effects of valproic acid on the nigrostriatal dopamine system in a 1-methyl-4-phenyl-1,2,3,6-tetrahydropyridine mouse model of Parkinson's disease. *Neuroscience*, **194**, 189-194.

Kidd, SK & Schneider, JS. (2010). Protection of dopaminergic cells from MPP+-mediated toxicity by histone deacetylase inhibition. *Brain Research*, **1354**, 172-178.

Kim, D, Frank, CL, Dobbin, MM, Tsunemoto, RK, Tu, W, Peng, PL, Guan, JS, Lee, BH, Moy, LY, Giusti, P, Broodie, N, Mazitschek, R, Delalle, I, Haggarty, SJ, Neve, RL, Lu, Y & Tsai, LH. (2008). Deregulation of HDAC1 by p25/Cdk5 in Neurotoxicity. *Neuron*, **60**, 803-817.

Kim, HJ, Leeds, P & Chuang, DM. (2009). The HDAC inhibitor, sodium butyrate, stimulates neurogenesis in the ischemic brain. *J Neurochem*, **110**, 1226-1240.

Kim, HJ, Rowe, M, Ren, M, Hong, JS, Chen, PS & Chuang, DM. (2007). Histone deacetylase inhibitors exhibit anti-inflammatory and neuroprotective effects in a rat permanent ischemic model of stroke: multiple mechanisms of action. *The Journal of Pharmacological and Experimental Therapeutics*, **321**, 892-901.

King, TD & Jope, RS. (2005). Inhibition of glycogen synthase kinase-3 protects cells from intrinsic but not extrinsic oxidative stress. *Neuroreport*, **16**, 597-601.

Kirik, D, Rosenblad, C & Bjorklund, A. (1998). Characterization of behavioral and neurodegenerative changes following partial lesions of the nigrostriatal dopamine system induced by intrastriatal 6-hydroxydopamine in the rat. *Exp Neurol*, **152**, 259-277.

Kirik, D, Rosenblad, C, Burger, C, Lundberg, C, Johansen, TE, Muzyczka, N, Mandel, RJ & Bjorklund, A. (2002). Parkinson-like neurodegeneration induced by targeted overexpression of alpha-synuclein in the nigrostriatal system. *J Neurosci*, **22**, 2780-2791.

Kitada, T, Pisani, A, Porter, DR, Yamaguchi, H, Tscherter, A, Martella, G, Bonsi, P, Zhang, C, Pothos, EN & Shen, J. (2007). Impaired dopamine release and synaptic plasticity in the striatum of PINK1-deficient mice. *Proc Natl Acad Sci U S A*, **104**, 11441-11446.

Kitada, T, Asakawa, S, Hattori, N, Matsumine, H, Yamamura, Y, Minoshima, S, Yokochi, M, Mizuno, Y & Shimizu, N. (1998). Mutations in the parkin gene cause autosomal recessive juvenile parkinsonism. *Nature*, **392**, 605-608.

Klein, C & Westenberger, A. (2012). Genetics of Parkinson's disease. *Cold Spring Harb Perspect Med*, **2**, a008888.

Knott, C, Stern, G, Kingsbury, A, Welcher, AA & Wilkin, GP. (2002). Elevated glial brain-derived neurotrophic factor in Parkinson's diseased nigra. *Parkinsonism Relat Disord*, **8**, 329-341.

Knott, C, Stern, G & Wilkin, GP. (2000). Inflammatory Regulators in Parkinson's Disease: iNOS, Lipocortin-1, and Cyclooxygenases-1 and -2. *Molecular and Cellular Neuroscience*, **16**, 724-739.

Kontopoulos, E, Parvin, JD & Feany, MB. (2006). {alpha}-synuclein acts in the nucleus to inhibit histone acetylation and promote neurotoxicity. *Hum Mol Genet*, **15**, 3012-3023.

Kops, GJ, Dansen, TB, Polderman, PE, Saarloos, I, Wirtz, KW, Coffer, PJ, Huang, TT, Bos, JL, Medema, RH & Burgering, BM. (2002). Forkhead transcription factor FOXO3a protects quiescent cells from oxidative stress. *Nature*, **419**, 316-321.

Kostrzewa, RM & Jacobowitz, DM. (1974). Pharmacological actions of 6-hydroxydopamine. *Pharmacol Rev*, **26**, 199-288.

Kou, W, Luchtman, D & Song, C. (2008). Eicosapentaenoic acid (EPA) increases cell viability and expression of neurotrophin receptors in retinoic acid and brain-derived neurotrophic factor differentiated SH-SY5Y cells. *Eur J Nutr*, **47**, 104-113.

Kouzarides, T. (2007). Chromatin Modifications and Their Function. *Cell*, **128**, 693-705.

Kovacs, JJ, Murphy, PJM, Gaillard, S, Zhao, X, Wu, JT, Nicchitta, CV, Yoshida, M, Toft, DO, Pratt, WB & Yao, TP. (2005). HDAC6 Regulates Hsp90 Acetylation and Chaperone-Dependent Activation of Glucocorticoid Receptor. *Molecular Cell*, **18**, 601-607.

Kreutzberg, GW. (1996). Microglia: a sensor for pathological events in the CNS. *Trends Neurosci*, **19**, 312-318.

Kues, WA, Anger, M, Carnwath, JW, Paul, D, Motlik, J & Niemann, H. (2000). Cell Cycle Synchronization of Porcine Fetal Fibroblasts: Effects of Serum Deprivation and Reversible Cell Cycle Inhibitors. *Biology of Reproduction*, **62**, 412-419.

Kumar, A. (2000). Rett and ICF syndromes: methylation moves into medicine. *J Biosci*, **25**, 213-214.

Kurth, MC, Adler, CH, Hilaire, MS, Singer, C, Waters, C, LeWitt, P, Chernik, DA, Dorflinger, EE & Yoo, K. (1997). Tolcapone improves motor function and reduces levodopa requirement in patients with Parkinson's disease experiencing motor fluctuations: a multicenter, double-blind, randomized, placebo-controlled trial. Tolcapone Fluctuator Study Group I. *Neurology*, **48**, 81-87.

Lagger, G, O'Carroll, D, Rembold, M, Khier, H, Tischler, J, Weitzer, G, Schuettengruber, B, Jenuwein, T & Seiser, C. (2002). Essential function of histone deacetylase 1 in prolferation control and CDK inhibitor repression. *EMBO Journal*, **21**, 2672-2681.

Lang, AE. (2007). The progression of Parkinson disease: a hypothesis. *Neurology*, **68**, 948-952.

Lang, AE, Gill, S, Patel, NK, Lozano, A, Nutt, JG, Penn, R, Brooks, DJ, Hotton, G, Moro, E, Heywood, P, Brodsky, MA, Burchiel, K, Kelly, P, Dalvi, A, Scott, B, Stacy, M, Turner, D, Wooten, VG, Elias, WJ, Laws, ER, Dhawan, V, Stoessl, AJ, Matcham, J, Coffey, RJ & Traub, M. (2006). Randomized controlled trial of intraputamenal glial cell line-derived neurotrophic factor infusion in Parkinson disease. *Ann Neurol*, **59**, 459-466.

Lang, AE & Lozano, AM. (1998). Parkinson's disease. First of two parts. *N Engl J Med*, **339**, 1044-1053.

Lang, AE, Melamed, E, Poewe, W & Rascol, O. (2013). Trial designs used to study neuroprotective therapy in Parkinson's disease. *Mov Disord*, **28**, 86-95.

Langley, B, D'Annibale, MA, Suh, K, Ayoub, I, Tolhurst, A, Bastan, B, Yang, L, Ko, B, Fisher, M, Cho, S, Beal, MF & Ratan, RR. (2008). Pulse Inhibition of Histone Deacetylases Induces Complete Resistance to Oxidative Death in Cortical Neurons without Toxicity and Reveals a Role for Cytoplasmic p21waf1/cip1 in Cell Cycle-Independent Neuroprotection. *J Neurosci*, **28**, 163-176.

Langston, JW. (2006). The Parkinson's complex: parkinsonism is just the tip of the iceberg. *Ann Neurol*, **59**, 591-596.

Langston, JW, Ballard, P, Tetrud, JW & Irwin, I. (1983a). Chronic Parkinsonism in humans due to a product of meperidine-analog synthesis. *Science*, **219**, 979-980.

Langston, JW, Ballard, P, Tetrud, JW & Irwin, I. (1983b). Chronic Parkinsonism in humans due to a product of meperidine-analog synthesis. *Science*, **219**, 979-980.

Langston, JW, Forno, LS, Tetrud, J, Reeves, AG, Kaplan, JA & Karluk, D. (1999). Evidence of active nerve cell degeneration in the substantia nigra of humans years after 1-methyl-4-phenyl-1,2,3,6-tetrahydropyridine exposure. *Ann Neurol*, **46**, 598-605.

Langston, JW, Langston, EB & Irwin, I. (1984). MPTP-induced parkinsonism in human and non-human primates--clinical and experimental aspects. *Acta Neurol Scand Suppl*, **100**, 49-54.

Lappalainen, K, J+ñ+ñskel+ñinen, I, Syrj+ñnen, K, Urtti, A & Syrj+ñnen, S. (1994). Comparison of Cell Proliferation and Toxicity Assays Using Two Cationic Liposomes. *Pharmaceutical Research*, **11**, 1127-1131.

Larsen, JP, Boas, J & Erdal, JE. (1999). Does selegiline modify the progression of early Parkinson's disease? Results from a five-year study. The Norwegian-Danish Study Group. *Eur J Neurol*, **6**, 539-547.

LaVoie, MJ & Hastings, TG. (1999). Dopamine quinone formation and protein modification associated with the striatal neurotoxicity of methamphetamine: evidence against a role for extracellular dopamine. *J Neurosci*, **19**, 1484-1491.

Le, Wd, Rowe, D, Xie, W, Ortiz, I, He, Y & Appel, SH. (2001). Microglial Activation and Dopaminergic Cell Injury: An In Vitro Model Relevant to Parkinson's Disease. *The Journal of Neuroscience*, **21**, 8447-8455.

Lee, JH, Jeong, EG, Choi, MC, Kim, SH, Park, JH, Song, SH, Park, J, Bang, YJ & Kim, TY. (2010a). Inhibition of histone deacetylase 10 induces thioredoxin-interacting protein and causes accumulation of reactive oxygen species in SNU-620 human gastric cancer cells. *Mol Cells*, **30**, 107-112.

Lee, JY, Nagano, Y, Taylor, JP, Lim, KL & Yao, TP. (2010b). Disease-causing mutations in parkin impair mitochondrial ubiquitination, aggregation, and HDAC6-dependent mitophagy. *J Cell Biol*, **189**, 671-679.

Lees, A. (2005). Alternatives to levodopa in the initial treatment of early Parkinson's disease. *Drugs Aging*, **22**, 731-740.

Lehnardt, S, Massillon, L, Follett, P, Jensen, FE, Ratan, R, Rosenberg, PA, Volpe, JJ & Vartanian, T. (2003). Activation of innate immunity in the CNS triggers neurodegeneration through a Toll-like receptor 4-dependent pathway. *Proc Natl Acad Sci U S A*, **100**, 8514-8519.

Leoni, F, Fossati, G, Lewis, EC, Lee, JK, Porro, G, Pagani, P, Modena, D, Moras, ML, Pozzi, P, Reznikov, LL, Siegmund, B, Fantuzzi, G, Dinarello, CA & Mascagni, P. (2005). The histone deacetylase inhibitor ITF2357 reduces production of pro-inflammatory cytokines in vitro and systemic inflammation in vivo. *Mol Med*, **11**, 1-15.

Leoni, F, Zaliani, A, Bertolini, G, Porro, G, Pagani, P, Pozzi, P, Don+á, G, Fossati, G, Sozzani, S, Azam, T, Bufler, P, Fantuzzi, G, Goncharov, I, Kim, SH, Pomerantz, BJ, Reznikov, LL, Siegmund, B, Dinarello, CA & Mascagni, P. (2002). The antitumor histone deacetylase inhibitor suberoylanilide hydroxamic acid exhibits antiinflammatory properties via suppression of cytokines. *Proceedings of the National Academy of Sciences*, **99**, 2995-3000.

Leroy, E, Boyer, R, Auburger, G, Leube, B, Ulm, G, Mezey, E, Harta, G, Brownstein, MJ, Jonnalagada, S, Chernova, T, Dehejia, A, Lavedan, C, Gasser, T, Steinbach, PJ, Wilkinson, KD & Polymeropoulos, MH. (1998). The ubiquitin pathway in Parkinson's disease. *Nature*, **395**, 451-452.

Lesage, S & Brice, A. (2009). Parkinson's disease: from monogenic forms to genetic susceptibility factors. *Hum Mol Genet*, **18**, R48-R59.

Li, P, Nijhawan, D, Budihardjo, I, Srinivasula, SM, Ahmad, M, Alnemri, ES & Wang, X. (1997). Cytochrome c and dATP-Dependent Formation of Apaf-1/Caspase-9 Complex Initiates an Apoptotic Protease Cascade. *Cell*, **91**, 479-489.

Liberatore, GT, Jackson-Lewis, V, Vukosavic, S, Mandir, AS, Vila, M, McAuliffe, WG, Dawson, VL, Dawson, TM & Przedborski, S. (1999). Inducible nitric oxide synthase stimulates dopaminergic neurodegeneration in the MPTP model of Parkinson disease. *Nat Med*, **5**, 1403-1409.

Lima, IV, Bastos, LF, Limborco-Filho, M, Fiebich, BL & de Oliveira, AC. (2012). Role of prostaglandins in neuroinflammatory and neurodegenerative diseases. *Mediators Inflamm*, **2012**, 946813.

Lin, HS, Hu, CY, Chan, HY, Liew, YY, Huang, HP, Lepescheux, L, Bastianelli, E, Baron, R, Rawadi, G & Cl+®ment-Lacroix, P. (2007). Anti-rheumatic activities of histone deacetylase (HDAC) inhibitors in vivo in collagen-induced arthritis in rodents. *British Journal of Pharmacology*, **150**, 862-872.

Liu, B. (2006). Modulation of microglial pro-inflammatory and neurotoxic activity for the treatment of Parkinson's disease. *AAPS J*, **8**, E606-E621.

Liu, B, Du, L & Hong, JS. (2000). Naloxone Protects Rat Dopaminergic Neurons against Inflammatory Damage through Inhibition of Microglia Activation and Superoxide Generation. *Journal of Pharmacology and Experimental Therapeutics*, **293**, 607-617.

Liu, H, Hu, Q, D'Ercole, AJ & Ye, P. (2009). Histone deacetylase 11 regulates oligodendrocyte-specific gene expression and cell development in OL-1 oligodendroglia cells. *Glia*, **57**, 1-12.

Liu, H, Hu, Q, Kaufman, A, D'Ercole, AJ & Ye, P. (2008). Developmental Expression of Histone Deacetylase 11 in the Murine Brain. *J Neurosci Res*, **86**, 537-543.

Liu, M & Bing, G. (2011). Lipopolysaccharide animal models for Parkinson's disease. *Parkinsons Dis*, **2011**, 327089.

Lobner, D. (2000). Comparison of the LDH and MTT assays for quantifying cell death: validity for neuronal apoptosis? *Journal of Neuroscience Methods*, **96**, 147-152.

Lohle, M & Reichmann, H. (2010). Clinical neuroprotection in Parkinson's disease -- Still waiting for the breakthrough. *Journal of the Neurological Sciences*, **289**, 104-114.

Long-Smith, CM, Sullivan, AM & Nolan, YM. (2009). The influence of microglia on the pathogenesis of Parkinson's disease. *Prog Neurobiol*, **89**, 277-287.

Longworth, MS & Laimins, LA. (2006). Histone deacetylase 3 localizes to the plasma membrane and is a substrate of Src. *Oncogene*, **25**, 4495-4500.

Lotharius, J, Dugan, LL & O'Malley, KL. (1999). Distinct mechanisms underlie neurotoxin-mediated cell death in cultured dopaminergic neurons. *J Neurosci*, **19**, 1284-1293.

Lu, Q, Qiu, X, Hu, N, Wen, H, Su, Y & Richardson, BC. (2006). Epigenetics, disease, and therapeutic interventions. *Ageing Research Reviews*, **5**, 449-467.

Lu, YC, Yeh, WC & Ohashi, PS. (2008). LPS/TLR4 signal transduction pathway. *Cytokine*, **42**, 145-151.

Lucio-Eterovic, A, Cortez, M, Valera, E, Motta, F, Queiroz, R, Machado, H, Carlotti, C, Neder, L, Scrideli, C & Tone, L. (2008). Differential expression of 12 histone deacetylase (HDAC) genes in astrocytomas and normal brain tissue: class II and IV are hypoexpressed in glioblastomas. *BMC Cancer*, **8**, 243.

Lynch-Day, MA, Mao, K, Wang, K, Zhao, M & Klionsky, DJ. (2012). The role of autophagy in Parkinson's disease. *Cold Spring Harb Perspect Med*, **2**, a009357.

MacDonald, JL & Roskams, AJ. (2008). Histone deacetylases 1 and 2 are expressed at distinct stages of neuro-glial development. *Dev Dyn*, **237**, 2256-2267.

Majno, G & Joris, I. (1995). Apoptosis, oncosis, and necrosis. An overview of cell death. *Am J Pathol*, **146**, 3-15.

Makino, N, Mochizuki, Y, Bannai, S & Sugita, Y. (1994). Kinetic studies on the removal of extracellular hydrogen peroxide by cultured fibroblasts. *J Biol Chem*, **269**, 1020-1025.

Mangiarini, L, Sathasivam, K, Seller, M, Cozens, B, Harper, A, Hetherington, C, Lawton, M, Trottier, Y, Lehrach, H, Davies, SW & Bates, GP. (1996). Exon 1 of the HD Gene with an Expanded CAG Repeat Is Sufficient to Cause a Progressive Neurological Phenotype in Transgenic Mice. *Cell*, **87**, 493-506.

Margariti, A, Zampetaki, A, Xiao, Q, Zhou, B, Karamariti, E, Martin, D, Yin, X, Mayr, M, Li, H, Zhang, Z, De, FE, Hu, Y, Cockerill, G, Xu, Q & Zeng, L. (2010). Histone deacetylase 7 controls endothelial cell growth through modulation of beta-catenin. *Circ Res*, **106**, 1202-1211.

Mariani, E, Polidori, MC, Cherubini, A & Mecocci, P. (2005). Oxidative stress in brain aging, neurodegenerative and vascular diseases: an overview. *J Chromatogr B Analyt Technol Biomed Life Sci*, **827**, 65-75.

Marks, PA, Richon, VM, Breslow, R & Rifkind, RA. (2001). Histone deacetylase inhibitors as new cancer drugs. *Curr Opin Oncol*, **13**, 477-483.

Marks, PA, Richon, VM, Miller, T & Kelly, WK. (2004). Histone deacetylase inhibitors. *Adv Cancer Res*, **91**, 137-168.

Marks, PA, Richon, VM & Rifkind, RA. (2000). Histone Deacetylase Inhibitors: Inducers of Differentiation or Apoptosis of Transformed Cells. *Journal of the National Cancer Institute*, **92**, 1210-1216.

Marletta, MA, Hurshman, AR & Rusche, KM. (1998). Catalysis by nitric oxide synthase. *Curr Opin Chem Biol*, **2**, 656-663.

Marsden, CD & Parkes, JD. (1977). Success and problems of long-term levodopa therapy in Parkinson's disease. *Lancet*, **1**, 345-349.

Marti, MJ, Saura, J, Burke, RE, Jackson-Lewis, V, Jimenez, A, Bonastre, M & Tolosa, E. (2002). Striatal 6-hydroxydopamine induces apoptosis of nigral neurons in the adult rat. *Brain Res*, **958**, 185-191.

Martinez-Vicente, M, Talloczy, Z, Kaushik, S, Massey, AC, Mazzulli, J, Mosharov, EV, Hodara, R, Fredenburg, R, Wu, DC, Follenzi, A, Dauer, W, Przedborski, S, Ischiropoulos, H, Lansbury, PT, Sulzer, D & Cuervo, AM. (2008). Dopamine-modified alpha-synuclein blocks chaperone-mediated autophagy. *J Clin Invest*, **118**, 777-788.

Marttila, RJ, Lorentz, H & Rinne, UK. (1988). Oxygen toxicity protecting enzymes in Parkinson's disease. Increase of superoxide dismutase-like activity in the substantia nigra and basal nucleus. *J Neurol Sci*, **86**, 321-331.

Mayer, B & Hemmens, B. (1997). Biosynthesis and action of nitric oxide in mammalian cells. *Trends Biochem Sci*, **22**, 477-481.

Mazzio, EA, Reams, RR & Soliman, KF. (2004). The role of oxidative stress, impaired glycolysis and mitochondrial respiratory redox failure in the cytotoxic effects of 6-hydroxydopamine in vitro. *Brain Res*, **1004**, 29-44.

McCoy, MK, Martinez, TN, Ruhn, KA, Szymkowski, DE, Smith, CG, Botterman, BR, Tansey, KE & Tansey, MG. (2006). Blocking soluble tumor necrosis factor signaling with dominant-negative tumor necrosis factor inhibitor attenuates loss of dopaminergic neurons in models of Parkinson's disease. *J Neurosci*, **26**, 9365-9375.

McGeer, PL, Itagaki, S, Akiyama, H & McGeer, EG. (1988a). Rate of cell death in parkinsonism indicates active neuropathological process. *Ann Neurol*, **24**, 574-576.

McGeer, PL, Itagaki, S, Boyes, BE & McGeer, EG. (1988b). Reactive microglia are positive for HLA-DR in the substantia nigra of Parkinson's and Alzheimer's disease brains. *Neurology*, **38**, 1285-1291.

McGeer, PL, Schwab, C, Parent, A & Doudet, D. (2003). Presence of reactive microglia in monkey substantia nigra years after 1-methyl-4-phenyl-1,2,3,6-tetrahydropyridine administration. *Ann Neurol*, **54**, 599-604.

McKinsey, TA, Zhang, CL & Olson, EN. (2002). Signaling chromatin to make muscle. *Current Opinion in Cell Biology*, **14**, 763-772.

McNaught, KS & Jenner, P. (1999). Altered glial function causes neuronal death and increases neuronal susceptibility to 1-methyl-4-phenylpyridinium- and 6-hydroxydopamine-induced toxicity in astrocytic/ventral mesencephalic co-cultures. *J Neurochem*, **73**, 2469-2476.

McNaught, KS & Jenner, P. (2000). Dysfunction of rat forebrain astrocytes in culture alters cytokine and neurotrophic factor release. *Neurosci Lett*, **285**, 61-65.

McNaught, KS, Mytilineou, C, Jnobaptiste, R, Yabut, J, Shashidharan, P, Jennert, P & Olanow, CW. (2002a). Impairment of the ubiquitin-proteasome system causes dopaminergic cell death and inclusion body formation in ventral mesencephalic cultures. *J Neurochem*, **81**, 301-306.

McNaught, KS, Perl, DP, Brownell, AL & Olanow, CW. (2004). Systemic exposure to proteasome inhibitors causes a progressive model of Parkinson's disease. *Ann Neurol*, **56**, 149-162.

McNaught, KS, Shashidharan, P, Perl, DP, Jenner, P & Olanow, CW. (2002b). Aggresome-related biogenesis of Lewy bodies. *Eur J Neurosci*, **16**, 2136-2148.

MCNaught, KS & Jenner, P. (1999). Altered Glial Function Causes Neuronal Death and Increases Neuronal Susceptibility to 1-Methyl-4-Phenylpyridinium- and 6-Hydroxydopamine-Induced Toxicity in Astrocytic/Ventral Mesencephalic Co-Cultures. *Journal of Neurochemistry*, **73**, 2469-2476.

MCNaught, KS & Jenner, P. (2000). Extracellular accumulation of nitric oxide, hydrogen peroxide, and glutamate in astrocytic cultures following glutathione depletion, complex I inhibition, and/or lipopolysaccharide-induced activation. *Biochemical Pharmacology*, **60**, 979-988.

McNaught, KS & Jenner, P. (2001). Proteasomal function is impaired in substantia nigra in Parkinson's disease. *Neuroscience Letters*, **297**, 191-194.

McNaught, P, Belizaire, R, Isacson, O, Jenner, P & Olanow, CW. (2003). Altered Proteasomal Function in Sporadic Parkinson's Disease. *Experimental Neurology*, **179**, 38-46.

McQuown, SC, Barrett, RM, Matheos, DP, Post, RJ, Rogge, GA, Alenghat, T, Mullican, SE, Jones, S, Rusche, JR, Lazar, MA & Wood, MA. (2011). HDAC3 is a critical negative regulator of long-term memory formation. *J Neurosci*, **31**, 764-774.

Meco, G, Bonifati, V, Vanacore, N & Fabrizio, E. (1994). Parkinsonism after chronic exposure to the fungicide maneb (manganese ethylene-bis-dithiocarbamate). *Scand J Work Environ Health*, **20**, 301-305.

Mello Filho, AC & Meneghini, R. (1984). In vivo formation of single-strand breaks in DNA by hydrogen peroxide is mediated by the Haber-Weiss reaction. *Biochim Biophys Acta*, **781**, 56-63.

Meredith, GE, Totterdell, S, Beales, M & Meshul, CK. (2009). Impaired glutamate homeostasis and programmed cell death in a chronic MPTP mouse model of Parkinson's disease. *Exp Neurol*, **219**, 334-340.

Michan, S & Sinclair, D. (2007). Sirtuins in mammals: insights into their biological function. *Biochemical Journal*, **404**, 1-13.

Michishita, E, Park, JY, Burneskis, JM, Barrett, JC & Horikawa, I. (2005). Evolutionarily Conserved and Nonconserved Cellular Localizations and Functions of Human SIRT Proteins. *Mol Biol Cell*, **16**, 4623-4635.

Miller, DW, Hague, SM, Clarimon, J, Baptista, M, Gwinn-Hardy, K, Cookson, MR & Singleton, AB. (2004). Alpha-synuclein in blood and brain from familial Parkinson disease with SNCA locus triplication. *Neurology*, **62**, 1835-1838.

Miller, GW. (2007). Paraquat: the red herring of Parkinson's disease research. *Toxicol Sci*, **100**, 1-2.

Miranda, TB & Jones, PA. (2007). DNA methylation: the nuts and bolts of repression. *J Cell Physiol*, **213**, 384-390.

Mizuno, Y, Sone, N & Saitoh, T. (1987). Effects of 1-Methyl-4-Phenyl-1,2,3,6-Tetrahydropyridine and 1-Methyl-4-Phenylpyridinium Ion on Activities of the Enzymes in the Electron Transport System in Mouse Brain. *Journal of Neurochemistry*, **48**, 1787-1793.

Mochizuki, H, Goto, K, Mori, H & Mizuno, Y. (1996). Histochemical detection of apoptosis in Parkinson's disease. *J Neurol Sci*, **137**, 120-123.

Mogi, M, Harada, M, Kondo, T, Mizuno, Y, Narabayashi, H, Riederer, P & Nagatsu, T. (1996). bcl-2 protein is increased in the brain from parkinsonian patients. *Neurosci Lett*, **215**, 137-139.

Mogi, M, Harada, M, Kondo, T, Riederer, P, Inagaki, H, Minami, M & Nagatsu, T. (1994a). Interleukin-1 beta, interleukin-6, epidermal growth factor and transforming growth factor-alpha are elevated in the brain from parkinsonian patients. *Neurosci Lett*, **180**, 147-150.

Mogi, M, Harada, M, Riederer, P, Narabayashi, H, Fujita, K & Nagatsu, T. (1994b). Tumor necrosis factor-alpha (TNF-alpha) increases both in the brain and in the cerebrospinal fluid from parkinsonian patients. *Neurosci Lett*, **165**, 208-210.

Moncada, S & Bolanos, JP. (2006). Nitric oxide, cell bioenergetics and neurodegeneration. *J Neurochem*, **97**, 1676-1689.

Monti, B, Gatta, V, Piretti, F, Raffaelli, SS, Virgili, M & Contestabile, A. (2010). Valproic acid is neuroprotective in the rotenone rat model of Parkinson's disease: involvement of alpha-synuclein. *Neurotox Res*, **17**, 130-141.

Morais, VA, Verstreken, P, Roethig, A, Smet, J, Snellinx, A, Vanbrabant, M, Haddad, D, Frezza, C, Mandemakers, W, Vogt-Weisenhorn, D, Van, CR, Wurst, W, Scorrano, L & De, SB. (2009). Parkinson's disease mutations in PINK1 result in decreased Complex I activity and deficient synaptic function. *EMBO Mol Med*, **1**, 99-111.

Morrison, BE, Majdzadeh, N & D'Mello, SR. (2007). Histone deacetylases: Focus on the nervous system. *Cellular and Molecular Life Sciences*, **64**, 2258-2269.

Nagakubo, D, Taira, T, Kitaura, H, Ikeda, M, Tamai, K, Iguchi-Ariga, SM & Ariga, H. (1997). DJ-1, a novel oncogene which transforms mouse NIH3T3 cells in cooperation with ras. *Biochem Biophys Res Commun*, **231**, 509-513.

Nagatsu, T, Mogi, M, Ichinose, H & Togari, A. (2000). Cytokines in Parkinson's disease. *J Neural Transm Suppl*, 143-151.

Nakamura, Y. (2002). Regulating factors for microglial activation. *Biol Pharm Bull*, **25**, 945-953.

Nalls, MA, Plagnol, V, Hernandez, DG, Sharma, M, Sheerin, UM, Saad, M, Simon-Sanchez, J, Schulte, C, Lesage, S, Sveinbjornsdottir, S, Stefansson, K, Martinez, M, Hardy, J, Heutink, P, Brice, A, Gasser, T, Singleton, AB & Wood, NW. (2011). Imputation of sequence variants for identification of genetic risks for Parkinson's disease: a meta-analysis of genome-wide association studies. *Lancet*, **377**, 641-649.

Narendra, D, Tanaka, A, Suen, DF & Youle, RJ. (2008). Parkin is recruited selectively to impaired mitochondria and promotes their autophagy. *J Cell Biol*, **183**, 795-803.

Nicklas, WJ, Youngster, SK, Kindt, MV & Heikkila, RE. (1987). MPTP, MPP+ and mitochondrial function. *Life Sci*, **40**, 721-729.

Nielsen, AL, Oulad-Abdelghani, M, Ortiz, JA, Remboutsika, E, Chambon, P & Losson, R. (2001). Heterochromatin formation in mammalian cells: interaction between histones and HP1 proteins. *Mol Cell*, **7**, 729-739.

NINDS NET-PD Investigators. (2006). A randomized, double-blind, futility clinical trial of creatine and minocycline in early Parkinson disease. *Neurology*, **66**, 664-671.

NINDS NET-PD Investigators. (2007). A randomized clinical trial of coenzyme Q10 and GPI-1485 in early Parkinson disease. *Neurology*, **68**, 20-28.

Nutt, JG, Burchiel, KJ, Comella, CL, Jankovic, J, Lang, AE, Laws, ER, Jr., Lozano, AM, Penn, RD, Simpson, RK, Jr., Stacy, M & Wooten, GF. (2003). Randomized, double-blind trial of glial cell line-derived neurotrophic factor (GDNF) in PD. *Neurology*, **60**, 69-73.

Oestreicher, E, Sengstock, GJ, Riederer, P, Olanow, CW, Dunn, AJ & Arendash, GW. (1994). Degeneration of nigrostriatal dopaminergic neurons increases iron within the substantia nigra: a histochemical and neurochemical study. *Brain Res*, **660**, 8-18.

Offen, D, Ziv, I, Panet, H, Wasserman, L, Stein, R, Melamed, E & Barzilai, A. (1997). Dopamine-induced apoptosis is inhibited in PC12 cells expressing Bcl-2. *Cell Mol Neurobiol*, **17**, 289-304.

Olanow, CW. (1990). Oxidation reactions in Parkinson's disease. *Neurology*, **40**, suppl-7.

Olanow, CW, Hauser, RA, Gauger, L, Malapira, T, Koller, W, Hubble, J, Bushenbark, K, Lilienfeld, D & Esterlitz, J. (1995). The effect of deprenyl and levodopa on the progression of Parkinson's disease. *Ann Neurol*, **38**, 771-777.

Olanow, CW, Perl, DP, DeMartino, GN & McNaught, KS. (2004). Lewy-body formation is an aggresome-related process: a hypothesis. *Lancet Neurol*, **3**, 496-503.

Olanow, CW, Rascol, O, Hauser, R, Feigin, PD, Jankovic, J, Lang, A, Langston, W, Melamed, E, Poewe, W, Stocchi, F & Tolosa, E. (2009). A double-blind, delayed-start trial of rasagiline in Parkinson's disease. *N Engl J Med*, **361**, 1268-1278.

Olanow, CW, Schapira, AH, LeWitt, PA, Kieburtz, K, Sauer, D, Olivieri, G, Pohlmann, H & Hubble, J. (2006). TCH346 as a neuroprotective drug in Parkinson's disease: a double-blind, randomised, controlled trial. *Lancet Neurol*, **5**, 1013-1020.

Olanow, CW. (2004). The Scientific Basis for the Current Treatment of Parkinson's Disease. *Annual Review of Medicine*, **55**, 41-60.

Ona, VO, Li, M, Vonsattel, JP, Andrews, LJ, Khan, SQ, Chung, WM, Frey, AS, Menon, AS, Li, XJ, Stieg, PE, Yuan, J, Penney, JB, Young, AB, Cha, JH & Friedlander, RM. (1999). Inhibition of caspase-1 slows disease progression in a mouse model of Huntington's disease. *Nature*, **399**, 263-267.

Ono, Y, Nakatani, T, Sakamoto, Y, Mizuhara, E, Minaki, Y, Kumai, M, Hamaguchi, A, Nishimura, M, Inoue, Y, Hayashi, H, Takahashi, J & Imai, T. (2007). Differences in neurogenic potential in floor plate cells along an anteroposterior location: midbrain dopaminergic neurons originate from mesencephalic floor plate cells. *Development*, **134**, 3213-3225.

Otto, D & Unsicker, K. (1993). FGF-2-mediated protection of cultured mesencephalic dopaminergic neurons against MPTP and MPP+: Specificity and impact of culture conditions, non-dopaminergic neurons, and astroglial cells. *J Neurosci Res*, **34**, 382-393.

Outeiro, TF, Kontopoulos, E, Altmann, SM, Kufareva, I, Strathearn, KE, Amore, AM, Volk, CB, Maxwell, MM, Rochet, JC, McLean, PJ, Young, AB, Abagyan, R, Feany, MB, Hyman, BT & Kazantsev, AG. (2007). Sirtuin 2 Inhibitors Rescue -Synuclein-Mediated Toxicity in Models of Parkinson's Disease. *Science*, **317**, 516-519.

Palacino, JJ, Sagi, D, Goldberg, MS, Krauss, S, Motz, C, Wacker, M, Klose, J & Shen, J. (2004). Mitochondrial dysfunction and oxidative damage in parkin-deficient mice. *J Biol Chem*, **279**, 18614-18622.

Palhagen, S, Heinonen, E, Hagglund, J, Kaugesaar, T, Maki-Ikola, O & Palm, R. (2006). Selegiline slows the progression of the symptoms of Parkinson disease. *Neurology*, **66**, 1200-1206.

Palhagen, S, Heinonen, EH, Hagglund, J, Kaugesaar, T, Kontants, H, Maki-Ikola, O, Palm, R & Turunen, J. (1998). Selegiline delays the onset of disability in de novo parkinsonian patients. Swedish Parkinson Study Group. *Neurology*, **51**, 520-525.

Palsson-McDermott, EM & O'Neill, LA. (2004). Signal transduction by the lipopolysaccharide receptor, Toll-like receptor-4. *Immunology*, **113**, 153-162.

Pandey, UB, Nie, Z, Batlevi, Y, McCray, BA, Ritson, GP, Nedelsky, NB, Schwartz, SL, DiProspero, NA, Knight, MA, Schuldiner, O, Padmanabhan, R, Hild, M, Berry, DL, Garza, D, Hubbert, CC, Yao,

TP, Baehrecke, EH & Taylor, JP. (2007). HDAC6 rescues neurodegeneration and provides an essential link between autophagy and the UPS. *Nature*, **447**, 860-864.

Panneton, WM, Kumar, VB, Gan, Q, Burke, WJ & Galvin, JE. (2010). The neurotoxicity of DOPAL: behavioral and stereological evidence for its role in Parkinson disease pathogenesis. *PLoS One*, **5**, e15251.

Pardo, B, Pa-¦¦üno, CL, Casarejos, MüJ & Mena, MüA. (1997). Neuronal-enriched cultures from embryonic rat ventral mesencephalon for pharmacological studies of dopamine neurons. *Brain Research Protocols*, **1**, 127-132.

Parker, WD, Jr., Boyson, SJ & Parks, JK. (1989). Abnormalities of the electron transport chain in idiopathic Parkinson's disease. *Ann Neurol*, **26**, 719-723.

Parker, WD, Jr., Parks, JK & Swerdlow, RH. (2008). Complex I deficiency in Parkinson's disease frontal cortex. *Brain Res*, **1189**, 215-218.

Parkinson Study Group PRECEPT Investigators. (2007). Mixed lineage kinase inhibitor CEP-1347 fails to delay disability in early Parkinson disease. *Neurology*, **69**, 1480-1490.

Parkinson Study Group. (2000). Pramipexole vs levodopa as initial treatment for Parkinson disease: A randomized controlled trial. Parkinson Study Group. *JAMA*, **284**, 1931-1938.

Parkkinen, L, Kauppinen, T, Pirttila, T, Autere, JM & Alafuzoff, I. (2005). Alpha-synuclein pathology does not predict extrapyramidal symptoms or dementia. *Ann Neurol*, **57**, 82-91.

Parmigiani, RB, Xu, WS, Venta-Perez, G, Erdjument-Bromage, H, Yaneva, M, Tempst, P & Marks, PA. (2008). HDAC6 is a specific deacetylase of peroxiredoxins and is involved in redox regulation. *Proc Natl Acad Sci U S A*, **105**, 9633-9638.

Paxinos G. & Franklin F. (2004). The mouse brain in stereotaxic coordinates. California: Elsevier.

Peng, GS, Li, G, Tzeng, NS, Chen, PS, Chuang, DM, Hsu, YD, Yang, S & Hong, JS. (2005). Valproate pretreatment protects dopaminergic neurons from LPS-induced neurotoxicity in rat primary midbrain cultures: role of microglia. *Molecular Brain Research*, **134**, 162-169.

Pennathur, S, Jackson-Lewis, V, Przedborski, S & Heinecke, JW. (1999). Mass spectrometric quantification of 3-nitrotyrosine, ortho-tyrosine, and o,o'-dityrosine in brain tissue of 1-methyl-4-phenyl-1,2,3, 6-tetrahydropyridine-treated mice, a model of oxidative stress in Parkinson's disease. *J Biol Chem*, **274**, 34621-34628.

Perry, TL & Yong, VW. (1986). Idiopathic Parkinson's disease, progressive supranuclear palsy and glutathione metabolism in the substantia nigra of patients. *Neurosci Lett*, **67**, 269-274.

Perumal, AS, Gopal, VB, Tordzro, WK, Cooper, TB & Cadet, JL. (1992). Vitamin E attenuates the toxic effects of 6-hydroxydopamine on free radical scavenging systems in rat brain. *Brain Res Bull*, **29**, 699-701.

Peterson, CL & Laniel, MA. (2004). Histones and histone modifications. *Current Biology*, **14**, R546-R551.

Phiel, CJ, Zhang, F, Huang, EY, Guenther, MG, Lazar, MA & Klein, PS. (2001). Histone Deacetylase Is a Direct Target of Valproic Acid, a Potent Anticonvulsant, Mood Stabilizer, and Teratogen. *The Journal of Biological Chemistry*, **276**, 36734-36741.

Pitkanen, S & Robinson, BH. (1996). Mitochondrial complex I deficiency leads to increased production of superoxide radicals and induction of superoxide dismutase. *J Clin Invest*, **98**, 345-351.

Polymeropoulos, MH, Lavedan, C, Leroy, E, Ide, SE, Dehejia, A, Dutra, A, Pike, B, Root, H, Rubenstein, J, Boyer, R, Stenroos, ES, Chandrasekharappa, S, Athanassiadou, A, Papapetropoulos, T, Johnson, WG, Lazzarini, AM, Duvoisin, RC, Di, IG, Golbe, LI & Nussbaum, RL. (1997). Mutation in the alpha-synuclein gene identified in families with Parkinson's disease. *Science*, **276**, 2045-2047.

Poole, AC, Thomas, RE, Yu, S, Vincow, ES & Pallanck, L. (2010). The mitochondrial fusion-promoting factor mitofusin is a substrate of the PINK1/parkin pathway. *PLoS One*, **5**, e10054.

Popperl, G, Tatsch, K, Ruzicka, E, Storch, A, Gasser, T & Schwarz, J. (2004). Comparison of alpha-dihydroergocryptine and levodopa monotherapy in Parkinson's disease: assessment of changes in DAT binding with [123I]IPT SPECT. *J Neural Transm*, **111**, 1041-1052.

Portela, A & Esteller, M. (2010). Epigenetic modifications and human disease. *Nat Biotechnol*, **28**, 1057-1068.

Presgraves, SP, Ahmed, T, Borwege, S & Joyce, JN. (2004). Terminally differentiated SH-SY5Y cells provide a model system for studying neuroprotective effects of dopamine agonists. *Neurotox Res*, **5**, 579-598.

Priyadarshi, A, Khuder, SA, Schaub, EA & Priyadarshi, SS. (2001). Environmental risk factors and Parkinson's disease: a metaanalysis. *Environ Res*, **86**, 122-127.

Priyadarshi, A, Khuder, SA, Schaub, EA & Shrivastava, S. (2000). A meta-analysis of Parkinson's disease and exposure to pesticides. *Neurotoxicology*, **21**, 435-440.

Pruszak, J, Just, L, Isacson, O & Nikkhah, G. (2009). Isolation and culture of ventral mesencephalic precursor cells and dopaminergic neurons from rodent brains. *Curr Protoc Stem Cell Biol*, **Chapter 2**, Unit.

Przedbroski, S, Leviver, M, Jiang, H, Ferreira, M, Jackson-Lewis, V, Donaldson, D & Togasaki, DM. (1995). Dose-dependent lesions of the dopaminergic nigrostriatal pathway induced by instrastriatal injection of 6-hydroxydopamine. *Neuroscience*, **67**, 631-647.

Qian, L, Block, ML, Wei, SJ, Lin, Cf, Reece, J, Pang, H, Wilson, B, Hong, JS & Flood, PM. (2006). Interleukin-10 Protects Lipopolysaccharide-Induced Neurotoxicity in Primary Midbrain Cultures by Inhibiting the Function of NADPH Oxidase. *Journal of Pharmacology and Experimental Therapeutics*, **319**, 44-52.

Qin, L, Wu, X, Block, ML, Liu, Y, Breese, GR, Hong, JS, Knapp, DJ & Crews, FT. (2007). Systemic LPS causes chronic neuroinflammation and progressive neurodegeneration. *Glia*, **55**, 453-462.

Qin, L, Liu, Y, Cooper, C, Liu, B, Wilson, B & Hong, JS. (2002). Microglia enhance +¦-amyloid peptide-induced toxicity in cortical and mesencephalic neurons by producing reactive oxygen species. *Journal of Neurochemistry*, **83**, 973-983.

Rappold, PM & Tieu, K. (2010). Astrocytes and therapeutics for Parkinson's disease. *Neurotherapeutics*, **7**, 413-423.

Rascol, O, Brooks, DJ, Korczyn, AD, De Deyn, PP, Clarke, CE & Lang, AE. (2000). A five-year study of the incidence of dyskinesia in patients with early Parkinson's disease who were treated with ropinirole or levodopa. 056 Study Group. *N Engl J Med*, **342**, 1484-1491.

Rascol, O, Olanow, W, Brooks, D, Koch, G, Truffinet, P & Beijut, R. (2002). A 2-year, multicenter, placebo-controlled, double-blind, parallel group study of the effect of riluzole on Parkinson's disease progression. p. S39.

Rayport, S. (2001). Glutamate is a cotransmitter in ventral midbrain dopamine neurons. *Parkinsonism & Related Disorders*, **7**, 261-264.

Rayport, S, Sulzer, D, Shi, WX, Sawasdikosol, S, Monaco, J, Batson, D & Rajendran, G. (1992). Identified postnatal mesolimbic dopamine neurons in culture: morphology and electrophysiology. *J Neurosci*, **12**, 4264-4280.

Remy, P, Doder, M, Lees, A, Turjanski, N & Brooks, D. (2005). Depression in Parkinson's disease: loss of dopamine and noradrenaline innervation in the limbic system. *Brain*, **128**, 1314-1322.

Renthal, W, Maze, I, Krishnan, V, Covington, HE, III, Xiao, G, Kumar, A, Russo, SJ, Graham, A, Tsankova, N, Kippin, TE, Kerstetter, KA, Neve, RL, Haggarty, SJ, McKinsey, TA, Bassel-Duby, R, Olson, EN & Nestler, EJ. (2007). Histone deacetylase 5 epigenetically controls behavioral adaptations to chronic emotional stimuli. *Neuron*, **56**, 517-529.

Rentzos, M, Nikolaou, C, Andreadou, E, Paraskevas, GP, Rombos, A, Zoga, M, Tsoutsou, A, Boufidou, F, Kapaki, E & Vassilopoulos, D. (2007). Circulating interleukin-15 and RANTES chemokine in Parkinson's disease. *Acta Neurol Scand*, **116**, 374-379.

Richardson, JR, Quan, Y, Sherer, TB, Greenamyre, JT & Miller, GW. (2005). Paraquat neurotoxicity is distinct from that of MPTP and rotenone. *Toxicol Sci*, **88**, 193-201.

Richelson, E. (1973). REGULATION OF TYROSINE HYDROXYLASE ACTIVITY IN MOUSE NEUROBLASTOMA CLONE N1E-115. *Journal of Neurochemistry*, **21**, 1139-1145.

Rinne, UK, Larsen, JP, Siden, A & Worm-Petersen, J. (1998). Entacapone enhances the response to levodopa in parkinsonian patients with motor fluctuations. Nomecomt Study Group. *Neurology*, **51**, 1309-1314.

Riobo, NA, Clementi, E, Melani, M, Boveris, A, Cadenas, E, Moncada, S & Poderoso, JJ. (2001). Nitric oxide inhibits mitochondrial NADH:ubiquinone reductase activity through peroxynitrite formation. *Biochem J*, **359**, 139-145.

Rockwell, P, Yuan, H, Magnusson, R & Figueiredo-Pereira, ME. (2000). Proteasome Inhibition in Neuronal Cells Induces a Proinflammatory Response Manifested by Upregulation of Cyclooxygenase-2, Its Accumulation as Ubiquitin Conjugates, and Production of the Prostaglandin PGE2. *Archives of Biochemistry and Biophysics*, **374**, 325-333.

Rosenberg, PA. (1991). Accumulation of extracellular glutamate and neuronal death in astrocyte-poor cortical cultures exposed to glutamine. *Glia*, **4**, 91-100.

Rott, R, Szargel, R, Haskin, J, Shani, V, Shainskaya, A, Manov, I, Liani, E, Avraham, E & Engelender, S. (2008). Monoubiquitylation of alpha-synuclein by seven in absentia homolog (SIAH) promotes its aggregation in dopaminergic cells. *J Biol Chem*, **283**, 3316-3328.

Rottach, A, Leonhardt, H & Spada, F. (2009). DNA methylation-mediated epigenetic control. *J Cell Biochem*, **108**, 43-51.

Rouaux, C, Jokic, N, Mbebi, C, Boutillier, S, Loeffler, JP & Boutillier, AL. (2003). Critical loss of CBP/p300 histone acetylase activity by caspase-6 during neurodegeneration. *EMBO J*, **22**, 6537-6549.

Rouaux, C, Panteleeva, I, Rene, F, Gonzalez de Aguilar, J-L, Echaniz-Laguna, A, Dupuis, L, Menger, Y, Boutillier, AL & Loeffler, JP. (2007). Sodium Valproate Exerts Neuroprotective Effects In Vivo through CREB-Binding Protein-Dependent Mechanisms But Does Not Improve Survival in an Amyotrophic Lateral Sclerosis Mouse Model. *J Neurosci*, **27**, 5535-5545.

Ryu, H, Lee, J, Olofsson, BA, Mwidau, A, Deodoglu, A, Escudero, M, Flemington, E, Azizkhan-Clifford, J, Ferrante, RJ & Ratan, RR. (2003). Histone deacetylase inhibitors prevent oxidative neuronal death independent of expanded polyglutamine repeats via an Sp1-dependent pathway. *Proceedings of the National Academy of Sciences*, **100**, 4281-4286.

Ryu, H, Smith, K, Camelo, SI, Carreras, I, Lee, J, Iglesias, AH, Dangond, F, Cormier, KA, Cudkowicz, ME, Brown Jr, RH & Ferrante, RJ. (2005). Sodium phenylbutyrate prolongs survival and regulates expression of anti-apoptotic genes in transgenic amyotrophic lateral sclerosis mice. *Journal of Neurochemistry*, **93**, 1087.

Saggu, H, Cooksey, J, Dexter, D, Wells, FR, Lees, A, Jenner, P & Marsden, CD. (1989). A selective increase in particulate superoxide dismutase activity in parkinsonian substantia nigra. *J Neurochem*, **53**, 692-697.

Saha, RN & Pahan, K. (2006). HATs and HDACs in neurodegeneration: a tale of disconcerted acetylation homeostasis. *Cell death and differentiation*, **13**, 539-550.

Saigoh, K, Wang, YL, Suh, JG, Yamanishi, T, Sakai, Y, Kiyosawa, H, Harada, T, Ichihara, N, Wakana, S, Kikuchi, T & Wada, K. (1999). Intragenic deletion in the gene encoding ubiquitin carboxy-terminal hydrolase in gad mice. *Nat Genet*, **23**, 47-51.

Samii, A, Etminan, M, Wiens, MO & Jafari, S. (2009). NSAID use and the risk of Parkinson's disease: systematic review and meta-analysis of observational studies. *Drugs Aging*, **26**, 769-779.

Sanchez-Pernaute, R, Ferree, A, Cooper, O, Yu, M, Brownell, AL & Isacson, O. (2004). Selective COX-2 inhibition prevents progressive dopamine neuron degeneration in a rat model of Parkinson's disease. *J Neuroinflammation*, **1**, 6.

Sanchez-Ramos, J, Overvik, E & Ames, BN. (1994). A marker of oxyradical-mediated DNA damage (8-hydroxy-2'deoxyguanosine) is increased in nigro-striatum of Parkinson's disease brain. pp. 197-204.

Saner, A & Thoenen, H. (1971). Model experiments on the molecular mechanism of action of 6-hydroxydopamine. *Mol Pharmacol*, **7**, 147-154.

Saporito, MS, Thomas, BA & Scott, RW. (2000). MPTP activates c-Jun NH(2)-terminal kinase (JNK) and its upstream regulatory kinase MKK4 in nigrostriatal neurons in vivo. *J Neurochem*, **75**, 1200-1208.

Sauer, H & Oertel, WH. (1994). Progressive degeneration of nigrostriatal dopamine neurons following intrastriatal terminal lesions with 6-hydroxydopamine: A combined retrograde tracing and immunocytochemical study in the rat. *Neuroscience*, **59**, 401-415.

Sawada, M, Imamura, K & Nagatsu, T. (2006). Role of cytokines in inflammatory process in Parkinson's disease. *J Neural Transm Suppl*, 373-381.

Schapira, AH. (2008). Mitochondria in the aetiology and pathogenesis of Parkinson's disease. *Lancet Neurol*, **7**, 97-109.

Schapira, AH. (2009). Neurobiology and treatment of Parkinson's disease. *Trends Pharmacol Sci*, **30**, 41-47.

Schapira, AH, Albrecht, S, Barone, P, Comella, CL, McDermott, MP, Mizuno, Y, Poewe, W, Rascol, O & Marek, K. (2010). Rationale for delayed-start study of pramipexole in Parkinson's disease: the PROUD study. *Mov Disord*, **25**, 1627-1632.

Schapira, AH, Cooper, JM, Dexter, D, Clark, JB, Jenner, P & Marsden, CD. (1990). Mitochondrial complex I deficiency in Parkinson's disease. *J Neurochem*, **54**, 823-827.

Schapira, AHV, Bezard, E, Brotchie, J, Calon, F, Collingridge, GL, Ferger, B, Hengerer, B, Hirsch, E, Jenner, P, Novere, NL, Obeso, JA, Schwarzschild, MA, Spampinato, U & Davidai, G. (2006). Novel pharmacological targets for the treatment of Parkinson's disease. *Nat Rev Drug Discov*, **5**, 845-854.

Schlissel, MS. (2003). Regulating antigen-receptor gene assembly. *Nat Rev Immunol*, **3**, 890-899.

Schneider, CA, Rasband, WS & Eliceiri, KW. (2012). NIH Image to ImageJ: 25 years of image analysis. *Nat Methods*, **9**, 671-675.

Schneider, JS, Sendek, S, Daskalakis, C & Cambi, F. (2010). GM1 ganglioside in Parkinson's disease: Results of a five year open study. *J Neurol Sci*, **292**, 45-51.

Schraufstatter, IU, Hinshaw, DB, Hyslop, PA, Spragg, RG & Cochrane, CG. (1986). Oxidant injury of cells. DNA strand-breaks activate polyadenosine diphosphate-ribose polymerase and lead to depletion of nicotinamide adenine dinucleotide. *J Clin Invest*, **77**, 1312-1320.

Schroeder, FA, Lin, CL, Crusio, WE & Akbarian, S. (2007). Antidepressant-like effects of the histone deacetylase inhibitor, sodium butyrate, in the mouse. *Biol Psychiatry*, **62**, 55-64.

Sengupta, N & Seto, E. (2004). Regulation of histone deacetylase activities. *Journal of Cellular Biochemistry*, **93**, 57-67.

Shannon, KM, Keshavarzian, A, Mutlu, E, Dodiya, HB, Daian, D, Jaglin, JA & Kordower, JH. (2012). Alpha-synuclein in colonic submucosa in early untreated Parkinson's disease. *Mov Disord*, **27**, 709-715.

Shao, Y, Gao, Z, Marks, PA & Jiang, X. (2004). Apoptotic and autophagic cell death induced by histone deacetylase inhibitors. *Proceedings of the National Academy of Sciences*, **101**, 18030-18035.

Sheehan, JP, Palmer, PE, Helm, GA & Tuttle, JB. (1997). MPP+ induced apoptotic cell death in SH-SY5Y neuroblastoma cells: An electron microscope study. *J Neurosci Res*, **48**, 226-237.

Shen, S, Li, J & Casaccia-Bonnefil, P. (2005). Histone modifications affect timing of oligodendrocyte progenitor differentiation in the developing rat brain. *J Cell Biol*, **169**, 577-589.

Shen, S, Sandoval, J, Swiss, VA, Li, J, Dupree, J, Franklin, RJM & Casaccia-Bonnefil, P. (2008). Age-dependent epigenetic control of differentiation inhibitors is critical for remyelination efficiency. *Nat Neurosci*, **11**, 1024-1034.

Shimazu, T, Hirschey, MD, Newman, J, He, W, Shirakawa, K, Le, MN, Grueter, CA, Lim, H, Saunders, LR, Stevens, RD, Newgard, CB, Farese, RV, Jr., de, CR, Ulrich, S, Akassoglou, K & Verdin, E. (2013). Suppression of oxidative stress by beta-hydroxybutyrate, an endogenous histone deacetylase inhibitor. *Science*, **339**, 211-214.

Shimoda, K, Sauve, Y, Marini, A, Schwartz, JP & Commissiong, JW. (1992). A high percentage yield of tyrosine hydroxylase-positive cells from rat E14 mesencephalic cell culture. *Brain Research*, **586**, 319-331.

Shimoji, M, Zhang, L, Mandir, AS, Dawson, VL & Dawson, TM. (2005). Absence of inclusion body formation in the MPTP mouse model of Parkinson's disease. *Brain Res Mol Brain Res*, **134**, 103-108.

Shults, CW, Oakes, D, Kieburtz, K, Beal, MF, Haas, R, Plumb, S, Juncos, JL, Nutt, J, Shoulson, I, Carter, J, Kompoliti, K, Perlmutter, JS, Reich, S, Stern, M, Watts, RL, Kurlan, R, Molho, E, Harrison, M & Lew, M. (2002). Effects of coenzyme Q10 in early Parkinson disease: evidence of slowing of the functional decline. *Arch Neurol*, **59**, 1541-1550.

Sian, J, Dexter, DT, Lees, AJ, Daniel, S, Agid, Y, Javoy-Agid, F, Jenner, P & Marsden, CD. (1994). Alterations in glutathione levels in Parkinson's disease and other neurodegenerative disorders affecting basal ganglia. *Ann Neurol*, **36**, 348-355.

Simonini, MV, Camargo, LM, Dong, E, Maloku, E, Veldic, M, Costa, E & Guidotti, A. (2006). The benzamide MS-275 is a potent, long-lasting brain region-selective inhibitor of histone deacetylases. *Proceedings of the National Academy of Sciences of the United States of America*, **103**, 1587-1592.

Singleton, AB, Farrer, M, Johnson, J, Singleton, A, Hague, S, Kachergus, J, Hulihan, M, Peuralinna, T, Dutra, A, Nussbaum, R, Lincoln, S, Crawley, A, Hanson, M, Maraganore, D, Adler, C, Cookson, MR, Muenter, M, Baptista, M, Miller, D, Blancato, J, Hardy, J & Gwinn-Hardy, K. (2003). {alpha}-Synuclein Locus Triplication Causes Parkinson's Disease. *Science*, **302**, 841.

Skibinski, G & Finkbeiner, S. (2011). Drug discovery in Parkinson's disease-Update and developments in the use of cellular models. *Int J High Throughput Screen*, **2011**, 15-25.

Smith, WL, Marnett, LJ & DeWitt, DL. (1991). Prostaglandin and thromboxane biosynthesis. *Pharmacol Ther*, **49**, 153-179.

Snow, BJ, Rolfe, FL, Lockhart, MM, Frampton, CM, O'Sullivan, JD, Fung, V, Smith, RA, Murphy, MP & Taylor, KM. (2010). A double-blind, placebo-controlled study to assess the mitochondria-targeted antioxidant MitoQ as a disease-modifying therapy in Parkinson's disease. *Mov Disord*, **25**, 1670-1674.

Sofic, E, Lange, KW, Jellinger, K & Riederer, P. (1992). Reduced and oxidized glutathione in the substantia nigra of patients with Parkinson's disease. *Neurosci Lett*, **142**, 128-130.

Sofic, E, Paulus, W, Jellinger, K, Riederer, P & Youdim, MB. (1991). Selective increase of iron in substantia nigra zona compacta of parkinsonian brains. *J Neurochem*, **56**, 978-982.

Sofroniew, MV. (2009). Molecular dissection of reactive astrogliosis and glial scar formation. *Trends in Neurosciences*, **32**, 638-647.

Spencer, C, Hyman, C, Studer, L, Egli, M, Evtouchenko, L, Jackson, C, Dahl-J+©rgensen, A, Lindsay, RM & Seiler, RW. (1995). Effect of BDNF on Dopaminergic, Serotonergic, and GABAergic Neurons in Cultures of Human Fetal Ventral Mesencephalon. *Experimental Neurology*, **133**, 50-63.

Spillantini, MG, Schmidt, ML, Lee, VM, Trojanowski, JQ, Jakes, R & Goedert, M. (1997). Alpha-synuclein in Lewy bodies. *Nature*, **388**, 839-840.

Starke, PE & Farber, JL. (1985). Ferric iron and superoxide ions are required for the killing of cultured hepatocytes by hydrogen peroxide. Evidence for the participation of hydroxyl radicals formed by an iron-catalyzed Haber-Weiss reaction. *J Biol Chem*, **260**, 10099-10104.

Steffan, JS, Bodai, L, Pallos, J, Poelman, M, McCampbell, A, Apostol, BL, Kazantsev, A, Schmidt, E, Zhu, YZ, Greenwald, M, Kurokawa, R, Housman, DE, Jackson, GR, Marsh, JL & Thompson, LM. (2001). Histone deacetylase inhibitors arrest polyglutamine-dependent neurodegeneration in Drosophila. *Nature*, **413**, 739-743.

Steiger-Barraissoul, S & Rami, A. (2009). Serum deprivation induced autophagy and predominantly an AIF-dependent apoptosis in hippocampal HT22 neurons. *Apoptosis*, **14**, 1274-1288.

Stein, A. (1980). DNA wrapping in nucleosomes. The linking number problem re-examined. *Nucleic Acids Res*, **8**, 4803-4820.

Storch, A, Burkhardt, K, Ludolph, AC & Schwarz, J. (2000). Protective effects of riluzole on dopamine neurons: involvement of oxidative stress and cellular energy metabolism. *J Neurochem*, **75**, 2259-2269.

Studer, L. (2001). Culture of substantia nigra neurons. *Curr Protoc Neurosci*, **Chapter 3**, Unit.

Subramanian, C, Opipari, AW, Castle, VP & Kwok, RPS. (2005a). Histone Deacetylase Inhibition Induces Apoptosis in Neuroblastoma. *Cell Cycle*, **4**, 1741-1743.

Subramanian, C, Opipari, AW, Bian, X, Castle, VP & Kwok, RPS. (2005b). Ku70 acetylation mediates neuroblastoma cell death induced by histone deacetylase inhibitors. *Proceedings of the National Academy of Sciences of the United States of America*, **102**, 4842-4847.

Sugo, N, Oshiro, H, Takemura, M, Kobayashi, T, Kohno, Y, Uesaka, N, Song, WJ & Yamamoto, N. (2010). Nucleocytoplasmic translocation of HDAC9 regulates gene expression and dendritic growth in developing cortical neurons. *Eur J Neurosci*, **31**, 1521-1532.

Svechnikova, I, Almqvist, PM & Ekstrom, TJ. (2008). HDAC inhibitors effectively induce cell type-specific differentiation in human glioblastoma cell lines of different origin. *Int J Oncol*, **32**, 821-827.

Swerdlow, RH, Parks, JK, Miller, SW, Tuttle, JB, Trimmer, PA, Sheehan, JP, Bennett, JP, Jr., Davis, RE & Parker, WD, Jr. (1996). Origin and functional consequences of the complex I defect in Parkinson's disease. *Ann Neurol*, **40**, 663-671.

Szabo, C, Ischiropoulos, H & Radi, R. (2007). Peroxynitrite: biochemistry, pathophysiology and development of therapeutics. *Nat Rev Drug Discov*, **6**, 662-680.

Takahashi-Niki, K, Niki, T, Taira, T, Iguchi-Ariga, SM & Ariga, H. (2004). Reduced anti-oxidative stress activities of DJ-1 mutants found in Parkinson's disease patients. *Biochem Biophys Res Commun*, **320**, 389-397.

Takai, N, Nakanishi, H, Tanabe, K, Nishioku, T, Sugiyama, T, Fujiwara, M & Yamamoto, K. (1998). Involvement of caspase-like proteinases in apoptosis of neuronal PC12 cells and primary cultured microglia induced by 6-hydroxydopamine. *J Neurosci Res*, **54**, 214-222.

Takeshima, T, Johnston, JM & Commissiong, JW. (1994a). Mesencephalic type 1 astrocytes rescue dopaminergic neurons from death induced by serum deprivation. *J Neurosci*, **14**, 4769-4779.

Takeshima, T, Shimoda, K, Sauve, Y & Commissiong, JW. (1994b). Astrocyte-dependent and -independent phases of the development and survival of rat embryonic day 14 mesencephalic, dopaminergic neurons in culture. *Neuroscience*, **60**, 809-823.

Tanji, K, Mori, F, Kakita, A, Takahashi, H & Wakabayashi, K. (2011). Alteration of autophagosomal proteins (LC3, GABARAP and GATE-16) in Lewy body disease. *Neurobiol Dis*, **43**, 690-697.

Tanner, CM, Kamel, F, Ross, GW, Hoppin, JA, Goldman, SM, Korell, M, Marras, C, Bhudhikanok, GS, Kasten, M, Chade, AR, Comyns, K, Richards, MB, Meng, C, Priestley, B, Fernandez, HH, Cambi, F, Umbach, DM, Blair, A, Sandler, DP & Langston, JW. (2011). Rotenone, paraquat, and Parkinson's disease. *Environ Health Perspect*, **119**, 866-872.

Tatton, NA. (2000). Increased caspase 3 and Bax immunoreactivity accompany nuclear GAPDH translocation and neuronal apoptosis in Parkinson's disease. *Exp Neurol*, **166**, 29-43.

Tatton, NA & Kish, SJ. (1997). In situ detection of apoptotic nuclei in the substantia nigra compacta of 1-methyl-4-phenyl-1,2,3,6-tetrahydropyridine-treated mice using terminal deoxynucleotidyl transferase labelling and acridine orange staining. *Neuroscience*, **77**, 1037-1048.

Tatton, NA, Maclean-Fraser, A, Tatton, WG, Perl, DP & Olanow, CW. (1998). A fluorescent double-labeling method to detect and confirm apoptotic nuclei in Parkinson's disease. *Ann Neurol*, **44**, S142-S148.

Teismann, P & Schulz, JB. (2004). Cellular pathology of Parkinson's disease: astrocytes, microglia and inflammation. *Cell Tissue Res*, **318**, 149-161.

Teismann, P, Tieu, K, Cohen, O, Choi, DK, Wu, DC, Marks, D, Vila, M, Jackson-Lewis, V & Przedborski, S. (2003a). Pathogenic role of glial cells in Parkinson's disease. *Mov Disord*, **18**, 121-129.

Teismann, P, Vila, M, Choi, DK, Tieu, K, Wu, DC, Jackson-Lewis, V & Przedborski, S. (2003b). COX-2 and neurodegeneration in Parkinson's disease. *Ann N Y Acad Sci*, **991**, 272-277.

Thanvi, BR & Lo, TC. (2004). Long term motor complications of levodopa: clinical features, mechanisms, and management strategies. *Postgrad Med J*, **80**, 452-458.

Thomas, GD, O'Hagan, KP & Zambraski, EJ. (1991). Chemical sympathectomy alters the development of hypertension in miniature swine. *Hypertension*, **17**, 357-362.

Tong, Y, Yamaguchi, H, Giaime, E, Boyle, S, Kopan, R, Kelleher, RJ, III & Shen, J. (2010). Loss of leucine-rich repeat kinase 2 causes impairment of protein degradation pathways, accumulation of alpha-synuclein, and apoptotic cell death in aged mice. *Proc Natl Acad Sci U S A*, **107**, 9879-9884.

Tremblay, ME, Stevens, B, Sierra, A, Wake, H, Bessis, A & Nimmerjahn, A. (2011). The role of microglia in the healthy brain. *J Neurosci*, **31**, 16064-16069.

Trojer, P, Li, G, Sims, RJ, III, Vaquero, A, Kalakonda, N, Boccuni, P, Lee, D, Erdjument-Bromage, H, Tempst, P, Nimer, SD, Wang, YH & Reinberg, D. (2007). L3MBTL1, a histone-methylation-dependent chromatin lock. *Cell*, **129**, 915-928.

Tsai, LK, Tsai, MS, Ting, CH & Li, H. (2008). Multiple therapeutic effects of valproic acid in spinal muscular atrophy model mice. *J Mol Med (Berl)*, **86**, 1243-1254.

Tsang, AH & Chung, KK. (2009). Oxidative and nitrosative stress in Parkinson's disease. *Biochim Biophys Acta*, **1792**, 643-650.

Tsankova, NM, Berton, O, Renthal, W, Kumar, A, Neve, RL & Nestler, EJ. (2006). Sustained hippocampal chromatin regulation in a mouse model of depression and antidepressant action. *Nat Neurosci*, **9**, 519-525.

Turrens, JF. (2003). Mitochondrial formation of reactive oxygen species. *The Journal of Physiology*, **552**, 335-344.

Uberti, D, Piccioni, L, Colzi, A, Bravi, D, Canonico, PL & Memo, M. (2002). Pergolide protects SH-SY5Y cells against neurodegeneration induced by H2O2. *European Journal of Pharmacology*, **434**, 17-20.

Ulevitch, RJ & Tobias, PS. (1995). Receptor-dependent mechanisms of cell stimulation by bacterial endotoxin. *Annu Rev Immunol*, **13**, 437-457.

Ungerstedt, U. (1968). 6-Hydroxy-dopamine induced degeneration of central monoamine neurons. *Eur J Pharmacol*, **5**, 107-110.

Uo, T, Veenstra, TD & Morrison, RS. (2009). Histone Deacetylase inhibitors prevent p53-Dependent and p53-Independent Bax-mediated neuronal apoptosis through two distinct mechanisms. *J Neurosci*, **29**, 2824-2832.

Valente, EM, Abou-Sleiman, PM, Caputo, V, Muqit, MM, Harvey, K, Gispert, S, Ali, Z, Del, TD, Bentivoglio, AR, Healy, DG, Albanese, A, Nussbaum, R, Gonzalez-Maldonado, R, Deller, T, Salvi, S, Cortelli, P, Gilks, WP, Latchman, DS, Harvey, RJ, Dallapiccola, B, Auburger, G & Wood, NW. (2004). Hereditary early-onset Parkinson's disease caused by mutations in PINK1. *Science*, **304**, 1158-1160.

VanderMolen, KM, McCulloch, W, Pearce, CJ & Oberlies, NH. (2011). Romidepsin (Istodax, NSC 630176, FR901228, FK228, depsipeptide): a natural product recently approved for cutaneous T-cell lymphoma. *J Antibiot (Tokyo)*, **64**, 525-531.

Velayati, A, Yu, WH & Sidransky, E. (2010). The role of glucocerebrosidase mutations in Parkinson disease and Lewy body disorders. *Curr Neurol Neurosci Rep*, **10**, 190-198.

Verdin, E, Dequiedt, F & Kasler, HG. (2003). Class II histone deacetylases: versatile regulators. *Trends in Genetics*, **19**, 286-293.

Vila, M, Jackson-Lewis, V, Vukosavic, S, Djaldetti, R, Liberatore, G, Offen, D, Korsmeyer, SJ & Przedborski, S. (2001). Bax ablation prevents dopaminergic neurodegeneration in the 1-methyl-4-phenyl-1,2,3,6-tetrahydropyridine mouse model of Parkinson's disease. *Proc Natl Acad Sci U S A*, **98**, 2837-2842.

Villagra, A, Cheng, F, Wang, HW, Suarez, I, Glozak, M, Maurin, M, Nguyen, D, Wright, KL, Atadja, PW, Bhalla, K, Pinilla-Ibarz, J, Seto, E & Sotomayor, EM. (2009). The histone deacetylase HDAC11 regulates the expression of interleukin 10 and immune tolerance. *Nat Immunol*, **10**, 92-100.

Vincow, ES, Merrihew, G, Thomas, RE, Shulman, NJ, Beyer, RP, Maccoss, MJ & Pallanck, LJ. (2013). The PINK1-Parkin pathway promotes both mitophagy and selective respiratory chain turnover in vivo. *Proc Natl Acad Sci U S A*, **110**, 6400-6405.

Visanji, NP, Orsi, A, Johnston, TH, Howson, PA, Dixon, K, Callizot, N, Brotchie, JM & Rees, DD. (2008). PYM50028, a novel, orally active, nonpeptide neurotrophic factor inducer, prevents and reverses neuronal damage induced by MPP+ in mesencephalic neurons and by MPTP in a mouse model of Parkinson's disease. *FASEB J*, **22**, 2488-2497.

Viswanath, V, Wu, Y, Boonplueang, R, Chen, S, Stevenson, FF, Yantiri, F, Yang, L, Beal, MF & Andersen, JK. (2001). Caspase-9 activation results in downstream caspase-8 activation and bid cleavage in 1-methyl-4-phenyl-1,2,3,6-tetrahydropyridine-induced Parkinson's disease. *J Neurosci*, **21**, 9519-9528.

Voges, D, Zwickl, P & Baumeister, W. (1999). The 26S proteasome: a molecular machine designed for controlled proteolysis. *Annu Rev Biochem*, **68**, 1015-1068.

Voutilainen, MH, B+ñck, S, P+Ârsti, E, Toppinen, L, Lindgren, L, Lindholm, P+, Per+ñnen, J, Saarma, M & Tuominen, RK. (2009). Mesencephalic Astrocyte-Derived Neurotrophic Factor Is Neurorestorative in Rat Model of Parkinson's Disease. *The Journal of Neuroscience*, **29**, 9651-9659.

Wagner, JM, Hackanson, B, Lubbert, M & Jung, M. (2010). Histone deacetylase (HDAC) inhibitors in recent clinical trials for cancer therapy. *Clin Epigenetics*, **1**, 117-136.

Walkinshaw, G & Waters, CM. (1994). Neurotoxin-induced cell death in neuronal PC12 cells is mediated by induction of apoptosis. *Neuroscience*, **63**, 975-987.

Walsh, E, Ueda, Y, Nakanishi, H & Yoshida, K. (1992). Neuronal survival and neurite extension supported by astrocytes co-cultured in transwells. *Neuroscience Letters*, **138**, 103-106.

Wang, AH & Yang, XJ. (2001). Histone Deacetylase 4 Possesses Intrinsic Nuclear Import and Export Signals. *Mol Cell Biol*, **21**, 5992-6005.

Wang, J & Maldonado, MA. (2006). The Ubiquitin-Proteasome System and its role in inflammatory and anutoimmune diseases. *Cellular and Molecular Immunology*, **3**, 255-261.

Wang, WH, Cheng, LC, Pan, FY, Xue, B, Wang, DY, Chen, Z & Li, CJ. (2011). Intracellular trafficking of histone deacetylase 4 regulates long-term memory formation. *Anat Rec (Hoboken)*, **294**, 1025-1034.

Wang, W, Sun, F, An, Y, Ai, H, Zhang, L, Huang, W & Li, L. (2009a). Morroniside protects human neuroblastoma SH-SY5Y cells against hydrogen peroxide-induced cytotoxicity. *European Journal of Pharmacology*, **613**, 19-23.

Wang, X, Petrie, TG, Liu, Y, Liu, J, Fujioka, H & Zhu, X. (2012). Parkinson's disease-associated DJ-1 mutations impair mitochondrial dynamics and cause mitochondrial dysfunction. *J Neurochem*, **121**, 830-839.

Wang, Y, Wang, X, Liu, L & Wang, X. (2009b). HDAC inhibitor trichostatin A-inhibited survival of dopaminergic neuronal cells. *Neuroscience Letters*, **467**, 212-216.

Whittemore, ER, Loo, DT, Watt, JA & Cotman, CW. (1995). A detailed analysis of hydrogen peroxide-induced cell death in primary neuronal culture. *Neuroscience*, **67**, 921-932.

Whitworth, AJ, Wes, PD & Pallanck, LJ. (2006). Drosophila models pioneer a new approach to drug discovery for Parkinson's disease. *Drug Discov Today*, **11**, 119-126.

Whone, AL, Watts, RL, Stoessl, AJ, Davis, M, Reske, S, Nahmias, C, Lang, AE, Rascol, O, Ribeiro, MJ, Remy, P, Poewe, WH, Hauser, RA & Brooks, DJ. (2003). Slower progression of Parkinson's disease with ropinirole versus levodopa: The REAL-PET study. *Ann Neurol*, **54**, 93-101.

Wirdefeldt, K, Adami, HO, Cole, P, Trichopoulos, D & Mandel, J. (2011). Epidemiology and etiology of Parkinson's disease: a review of the evidence. *Eur J Epidemiol*, **26 Suppl 1**, S1-58.

Witt, O, Deubzer, HE, Milde, T & Oehme, I. (2008). HDAC family: What are the cancer relevant targets? *Cancer letters*, **Epub ahead of print**.

Wu, G, Fang, YZ, Yang, S, Lupton, JR & Turner, ND. (2004). Glutathione metabolism and its implications for health. *J Nutr*, **134**, 489-492.

Wu, X, Chen, PS, Dallas, S, Wilson, B, Block, ML, Wang, CC, Kinyamu, H, Lu, N, Gao, X, Leng, Y, Chuang, DM, Zhang, W, Lu, RB & Hong, JS. (2008). Histone deacetylase inhibitors up-regulate astrocyte GDNF and BDNF gene transcription and protect dopaminergic neurons. *The International Journal of Neuropsychopharmacology*, **11**, 1123-1134.

Xiang, Z, Chen, M, Ping, J, Dunn, P, Lv, J, Jiao, B & Burnstock, G. (2006). Microglial morphology and its transformation after challenge by extracellular ATP in vitro. *J Neurosci Res*, **83**, 91-101.

Xie, HR, Hu, LS & Li, GY. (2010). SH-SY5Y human neuroblastoma cell line: in vitro cell model of dopaminergic neurons in Parkinson's disease. *Chin Med J (Engl)*, **123**, 1086-1092.

Xu, WS & Marks, PA. (2007). Histone deacetylase inhibitors: molecular mechanisms of action. *Oncogene*, **26**, 5541-5552.

Yamaguchi, M, Tonou-Fujimori, N, Komori, A, Maeda, R, Nojima, Y, Li, H, Okamoto, H & Masai, I. (2005). Histone deacetylase 1 regulates retinal neurogenesis in zebrafish by suppressing Wnt and Notch signaling pathways. *Development*, **132**, 3027-3043.

Yang, L, Matthews, RT, Schulz, JB, Klockgether, T, Liao, AW, Martinou, JC, Penney, JB, Jr., Hyman, BT & Beal, MF. (1998). 1-Methyl-4-phenyl-1,2,3,6-tetrahydropyride neurotoxicity is attenuated in mice overexpressing Bcl-2. *J Neurosci*, **18**, 8145-8152.

Yang, XJ & Seto, E. (2007). HATs and HDACs: from structure, function and regulation to novel strategies for therapy and prevention. *Oncogene*, **26**, 5310-5318.

Yang, Z & Klionsky, DJ. (2010). Eaten alive: a history of macroautophagy. *Nat Cell Biol*, **12**, 814-822.

Yao, Z & Wood, NW. (2009). Cell death pathways in Parkinson's disease: role of mitochondria. *Antioxid Redox Signal*, **11**, 2135-2149.

Yoritaka, A, Hattori, N, Uchida, K, Tanaka, M, Stadtman, ER & Mizuno, Y. (1996). Immunohistochemical detection of 4-hydroxynonenal protein adducts in Parkinson disease. *Proceedings of the National Academy of Sciences of the United States of America*, **93**, 2696-2701.

Young, TH, Huang, JH, Hung, SH & Hsu, JP. (2000). The role of cell density in the survival of cultured cerebellar granule neurons. *J Biomed Mater Res*, **52**, 748-753.

Zeng, BY, Bukhatwa, S, Hikima, A, Rose, S & Jenner, P. (2006). Reproducible nigral cell loss after systemic proteasomal inhibitor administration to rats. *Ann Neurol*, **60**, 248-252.

Zhang, B, West, EJ, Van, KC, Gurkoff, GG, Zhou, J, Zhang, XM, Kozikowski, AP & Lyeth, BG. (2008). HDAC inhibitor increases histone H3 acetylation and reduces microglia inflammatory response following traumatic brain injury in rats. *Brain Research*, **1226**, 181-191.

Zhang, W, Wang, T, Pei, Z, Miller, DS, Wu, X, Block, ML, Wilson, B, Zhang, W, Zhou, Y, Hong, JS & Zhang, J. (2005). Aggregated {alpha}-synuclein activates microglia: a process leading to disease progression in Parkinson's disease. *FASEB J*, **19**, 533-542.

Zhang, Z, Qin, X, Tong, N, Zhao, X, Gong, Y, Shi, Y & Wu, X. (2012). Valproic acid-mediated neuroprotection in retinal ischemia injury via histone deacetylase inhibition and transcriptional activation. *Exp Eye Res*, **94**, 98-108.

Zhou, W, Bercury, K, Cummiskey, J, Luong, N, Lebin, J & Freed, CR. (2011). Phenylbutyrate up-regulates the DJ-1 protein and protects neurons in cell culture and in animal models of Parkinson disease. *J Biol Chem*, **286**, 14941-14951.

Ziegler, U & Groscurth, P. (2004). Morphological features of cell death. *News Physiol Sci*, **19**, 124-128.

Zimprich, A, Biskup, S, Leitner, P, Lichtner, P, Farrer, M, Lincoln, S, Kachergus, J, Hulihan, M, Uitti, RJ, Calne, DB, Stoessl, AJ, Pfeiffer, RF, Patenge, N, Carbajal, IC, Vieregge, P, Asmus, F, Muller-Myhsok, B, Dickson, DW, Meitinger, T, Strom, TM, Wszolek, ZK & Gasser, T. (2004). Mutations in LRRK2 cause autosomal-dominant parkinsonism with pleomorphic pathology. *Neuron*, **44**, 601-607.

Zurn, AD & Werren, F. (1994). Development of CNS Cholinergic Neurons in Vitro: Selective Effects of CNTF and LIF on Neurons from Mesencephalic Cranial Motor Nuclei. *Developmental Biology*, **163**, 309-315.

ClincalTrials.gov (2013) Sodium Phenylbuyrate [Online] Available at: http://www.clinicaltrials.gov/ct2/results?term=sodium+phenylbutyrate (Accessed 24/06/2013).

Phytopham (2013) Results From Cogane™ in Parkinson's Disease Clinical Trial [Online] Available at: http://phytopharm.com/images/stories/Rel_190_Final_130117.pdf (Accessed 24/06/2013).